HAL
open science

Origine, âge et processus physico-chimiques des circulations de fluides dans les fractures : exemple de socle sous couverture (Vienne) et de formations riches en argiles (Gard, Est)

Stéphane Buschaert

▶ **To cite this version:**

Stéphane Buschaert. Origine, âge et processus physico-chimiques des circulations de fluides dans les fractures : exemple de socle sous couverture (Vienne) et de formations riches en argiles (Gard, Est). Sciences de la Terre. Université Henri Poincaré - Nancy 1, 2001. Français. NNT : 2001NAN10233 . tel-01748372

HAL Id: tel-01748372

https://hal.univ-lorraine.fr/tel-01748372v1

Submitted on 29 Mar 2018

HAL is a multi-disciplinary open access archive for the deposit and dissemination of scientific research documents, whether they are published or not. The documents may come from teaching and research institutions in France or abroad, or from public or private research centers.

L'archive ouverte pluridisciplinaire **HAL**, est destinée au dépôt et à la diffusion de documents scientifiques de niveau recherche, publiés ou non, émanant des établissements d'enseignement et de recherche français ou étrangers, des laboratoires publics ou privés.

UNIVERSITÉ DE LORRAINE

AVERTISSEMENT

Ce document est le fruit d'un long travail approuvé par le jury de soutenance et mis à disposition de l'ensemble de la communauté universitaire élargie.

Il est soumis à la propriété intellectuelle de l'auteur. Ceci implique une obligation de citation et de référencement lors de l'utilisation de ce document.

D'autre part, toute contrefaçon, plagiat, reproduction illicite encourt une poursuite pénale.

Contact : ddoc-theses-contact@univ-lorraine.fr

LIENS

Code de la Propriété Intellectuelle. articles L 122. 4
Code de la Propriété Intellectuelle. articles L 335.2- L 335.10
http://www.cfcopies.com/V2/leg/leg_droi.php
http://www.culture.gouv.fr/culture/infos-pratiques/droits/protection.htm

SC N2001 233B

S.C.D. - U.H.P. NANCY 1
BIBLIOTHÈQUE DES SCIENCES
Rue du Jardin Botanique - BP 11
54601 VILLERS-LES-NANCY Cédex

Collection Les Rapports

Thèse

par **Stéphane BUSCHAERT**

Présentée pour l'obtention du titre de
Docteur de l'Université
Henri Poincaré, Nancy-I

Spécialité :
Science de l'Univers

Origine, âge et processus physico-chimiques des circulations de fluides dans les fractures :

Exemple de socle sous couverture (Vienne) et de formations riches en argiles (Gard, Est)

Soutenue publiquement le 3 octobre 2001
devant la commission d'examen :

Membres du jury :

Président :
J. Leroy
Professeur Université Henri Poincaré - Nancy

Rapporteurs :
P. Muchez
Professeur - Université de Louvain - Belgique
J. Lancelot
Professeur - Université de Montpellier

Directeurs de thèse :
M. Cathelineau
Directeur de Recherches - G2R-CREGU - Nancy
S. Fourcade
Professeur - Université de Rennes

Examinateurs :
C. France-Lanord
ecteur de Recherches - CRPG - Nancy
M. Steinberg
'rofesseur émérite - Université d'Orsay
S. Altmann
Ingénieur - Andra - Châtenay-Malabry

BIBLIOTHEQUE SCIENCES NANCY 1
D 095 152704 9

CENTRE NATIONAL DE LA RECHERCHE SCIENTIFIQUE
Université HENRI POINCARÉ NANCY I
G2R
ANDRA
Agence nationale pour la gestion des déchets radioactifs
GdR FORPRO
CNRS-ANDRA G0788

S.C.D. - U.H.P. NANCY 1
BIBLIOTHÈQUE DES SCIENCES
Rue du Jardin Botanique - BP 11
54601 VILLERS-LES-NANCY Cédex

POSITIONNEMENT DE LA THESE DANS LE PROGRAMME SCIENTIFIQUE DE L'ANDRA ET APPORTS SCIENTIFIQUES DES TRAVAUX DE RECHERCHE

Scott ALTMANN (Andra)

L'étude des cristallisations dans les fractures et les discontinuités des roches peu perméables, en tant qu'indicateurs de la paléo-hydrologie d'un système géologique, s'est largement développée depuis plusieurs années, notamment dans le cadre de la caractérisation des sites potentiels de stockage des déchets nucléaires (Canada, Suède, Suisse...).

Le développement de ce type d'études est lié d'une part à l'intérêt évident des interprétations portant sur les capacités de confinement des roches déduites de l'histoire des circulations fluides passées et récentes à l'intérieur des milieux considérés et d'autre part à l'amélioration constante des performances analytiques.

Compte tenu de l'histoire en général complexe (souvent multiphasée) des remplissages de fractures et de la relative jeunesse de la méthodologie employée, il n'existe pas de méthode standard à appliquer pour ce type d'étude. L'intérêt scientifique de ce travail de thèse est principalement constitué par l'aspect multi-techniques, reposant principalement sur des traçages isotopiques et mettant également en œuvre les techniques les plus modernes actuellement disponibles, telles que l'analyse par microsonde ionique des néoformations cristallines et des remplissages de fractures.

L'ANDRA a mis en œuvre depuis 1993 un programme d'étude des cristallisations de fractures en milieu granitique impliquant de nombreux centres de recherches, dont l'UMR G2R-CREGU, au sein de laquelle ce travail a été réalisé en collaboration avec d'autres laboratoires, dont l'UMR Géosciences-Rennes. En effet, la thèse de Stéphane Buschaert a été réalisée dans le cadre du thème "systèmes eaux/fractures passés à actuels" du GDR FORPRO, relevant de l'action 98-III de recherche animée par Michel Cathelineau et Serge Fourcade, également co-directeurs de la thèse.

Les études préliminaires sur le site de la Vienne avaient permis de parvenir à la reconnaissance des paragénèses successives de remplissage de fractures. L'étude des remplissages de fractures de la couche silteuse de Marcoule avait également déjà en partie débuté avant ce travail. Cependant, un certain nombre de points, dont celui des calages chronologiques plus précis et de l'origine précise de certains fluides piégés, restait à préciser pour ces deux sites. Par contre, la paléo-hydrologie au niveau du site de l'Est demandait encore à être décrite.

Ce travail de thèse, débuté en octobre 1998 par Stéphane Buschaert, a donc porté sur les trois sites étudiés par l'Andra à cette date, soit le massif granitique de la Vienne, les siltites du Gard et les argilites de l'Est du bassin de Paris. L'un des intérêts et originalités de ce travail pour l'Andra, hormis la compréhension de la paléo-hydrologie globale et de la caractérisation des capacités de confinement des formations géologiques, était d'appliquer pour la première fois les mêmes techniques

sur les trois sites d'étude afin de pouvoir comparer les informations recueillies dans ces différents milieux géologiques.

Cette recherche constituait donc un complément aux études préliminaires mentionnées sur la Vienne et le Gard en proposant de répondre à certaines questions restées en suspens, mais constituait aussi l'une des premières tentatives de ce type sur le site de l'Est. Bien que l'effort de comparaison entre les trois sites ait été maintenu, l'étude a été recentrée sur le site de l'Est après la décision gouvernementale fin 98 de ne retenir que ce dernier pour l'implantation d'un laboratoire souterrain

Pour conclure cette présentation et synthétiser les acquis de cette thèse, on peut retenir que l'étude des colmatages minéraux précipités dans les discontinuités lors du passage de fluides anciens et récents, est la seule possibilité de reconstituer les comportements paléo-hydrologique et -hydrogéochimique des milieux géologiques.
Ce travail a démontré que le traçage isotopique des minéraux de discontinuités, constitue un outil robuste pour la reconstitution des conditions paléo-hydrogéologiques, quel que soit le milieu géologique. Cependant, seul le couplage du traçage isotopique avec des outils pétrographiques, minéralogiques et géochimiques peut permettre de déterminer précisément l'origine des fluides et les conditions physico-chimiques prévalant lors du colmatage.

S.C.D. - U.H.P. NANCY 1
BIBLIOTHÈQUE DES SCIENCES
Rue du Jardin Botanique - BP 11
54601 VILLERS-LES-NANCY Cédex

Faculté des Sciences

UMR 7566

U.F.R. S.T.M.P.
Ecole Doctorale :
RP²E (Ressources, Produits, Procédés et Environnement)

Thèse

présentée pour l'obtention du titre de

Docteur de l'Université Henri Poincaré, Nancy I

en Sciences de l'Univers

par

Stéphane BUSCHAERT

Origine, âge et processus physico-chimiques des circulations de fluides dans les fractures : Exemple de socle sous couverture (Vienne) et de formations riches en argiles (Gard, Est)

Soutenue publiquement le 3 octobre 2001

Membres du jury :

Président	M. J. Leroy	Professeur, Université Henri Poincaré, Nancy
Rapporteurs	M. P. Muchez	Professeur, Université de Louvain, Belgique
	M. J. Lancelot	Professeur, Université de Montpellier
Directeurs de thèse	M. M. Cathelineau	Directeur de Recherches, G2R-CREGU, Nancy
	M. S. Fourcade	Professeur, Université de Rennes
Examinateurs	M. C. France-Lanord	Directeur de Recherches, CRPG, Nancy
	M. M. Steinberg	Professeur émérite, Université d'Orsay
	M. S. Altmann	Ingénieur ANDRA, Châtenay Malabry

AVANT-PROPOS

Contexte général du sujet

Le programme de reconnaissance géologique, entrepris dès 1994 par l'Andra, a permis l'établissement en 1996 des demandes d'autorisation d'installation et d'exploitation (DAIE) d'un laboratoire souterrain d'expérimentation dans la Vienne, dans le Gard Rhodanien et dans l'Est du bassin parisien. La loi du 30 décembre 1991, relative à la gestion des déchets radioactifs de haute activité et à vie longue en France, a en effet défini différentes voies de recherches, dont la possibilité de leur stockage dans les formations géologiques profondes. Cette voie de recherche a été confiée à l'Agence Nationale pour la gestion des Déchets Radioactifs (Andra).

Par ailleurs, le CNRS a créé en 1997 un Programme sur l'Aval du Cycle Electronucléaire (PACE), en association avec l'Andra, représenté par le Groupement de Recherches FORPRO sous la conduite du Pr Joël Lancelot. Ce travail de Doctorat, dont ce mémoire ponctue 3 années de recherches au sein de l'UMR G2R – CREGU, a été entrepris dès octobre 1998 à Nancy sur les trois sites avec l'aide du système d'allocation de bourse de thèse Andra et dans le cadre de nombreuses collaborations nationales au sein de l'action 98-III du GdR FORPRO, sous la thématique 'Fractures' animée par Michel Cathelineau et Serge Fourcade, par ailleurs aussi directeurs de ma thèse.

Le 9 décembre 1998, le gouvernement annonce par communiqué sa décision de ne retenir parmi les trois propositions précédentes que le site de l'Est du bassin parisien pour la création d'un laboratoire souterrain autorisé par le décret du 3 août 1999 et actuellement en cours de réalisation. Cette étude a alors été recentrée sur le site de l'Est, à la demande de l'Andra, tout en poursuivant les comparaisons avec les deux autres sites. En effet, une seconde cible restant à définir en milieu granitique, l'activité de caractérisation du site de la Vienne a été maintenue, en tant que potentiel analogue au nouveau site qui sera choisi. D'autre part, l'étude comparée des sites du Gard et de l'Est va nous permettre une confrontation des résultats et interprétations.

Remerciements

Avec la fin de la rédaction de ce mémoire, voici les remerciements toujours écrits en dernier, presque à la hâte, pour finalement les placer au début du mémoire.

Je tiens donc à remercier toutes les personnes et unités qui ont rendu possible ce travail :

Tout d'abord, l'UMR G2R – CREGU dans son ensemble, pour m'avoir accueilli, il y a 4 ans à Nancy, afin d'effectuer mon DEA sous la direction de Jean Dubessy et de Jacques Pironon, que je tiens tous deux à remercier.

Ensuite, mes remerciements vont à mes directeurs de thèse, MM. Michel Cathelineau et Serge Fourcade, qui ont encadré ces travaux. La majorité des analyses isotopiques a été réalisée dans le laboratoire de géochimie isotopique de S. Fourcade à Géosciences Rennes avec l'aimable participation de François Martineau.

Ce travail a été possible grâce à la participation financière du GdR Forpro et de l'Andra qui m'a salariée pendant ces 3 années de thèse. Je remercie également l'Andra pour la publication du mémoire.

Je remercie les membres du jury d'avoir accepté d'y participer et de juger ce travail, MM. Philippe Muchez, Joël Lancelot, Christian France-Lanord, Michel Steinberg, Scott Altmann et Jacques Leroy.

Ce travail a bénéficié de nombreuses collaborations, aussi bien dans le cadre du GdR FORPRO et de l'Andra, représenté notamment par MM. Norbert Clauer et Davy Rousset du CGS Strasbourg, Jean Luc Michelot d'Orsay, Melle Véronique Lavastre de l'IPGP, et par l'équipe de Joël Lancelot de Montpellier, qu'au sein de l'UMR G2R, avec Yacouba Coulibaly, Régina Freiberger, Marie-Christine Boiron, Christian Hibsch, Grégoire André et Bernard Lathuillière. D'autres laboratoires et personnes ont participé aux travaux, tels que David Banks de Leeds, Adrian Boyce de Glasgow, Etienne Deloule du CRPG. Ce travail a été suivi à l'Andra, d'abord par J.F. Aranyossy, puis par Roger Njitchoua et Scott Altmann.

La bonne humeur des personnes qui m'ont entouré pendant la thèse a fortement contribué à la réalisation de ce travail. Tout d'abord, Cess (Cécile Fabre), pour qui la vie ne vaut le coup que si elle est compliquée, qui m'a beaucoup aidé dans les finitions de ce mémoire, Damien Guillaume (l'*), ambassadeur du Lyonnais et des vins du Beaujolais, Delphine Charpentier, qui m'a fait réaliser qu'il y avait beaucoup plus anxieux que moi, Teintur' (Stéphane Teinturier), master of the virtual worlds, à qui j'ai toujours refusé de jouer en réseaux de 23h à 5h du mat', et tous les autres compagnons et 'anciens', Régis, Bocar, Jean, Philippe, Guillaume, Dona, Jow, Régine, Jean Louis, tout le personnel et aussi l'équipe de foot du G2R... Merci aussi à mes parents et à Olivier.

A Karine, mon épouse

S.C.D. - U.H.P. NANCY 1
BIBLIOTHÈQUE DES SCIENCES
Rue du Jardin Botanique - BP 11
54601 VILLERS-LES-NANCY Cédex

RESUME

L'étude des colmatages minéraux déposés dans les discontinuités et porosités lors des circulations de fluides, anciennes à récentes, est l'unique moyen de reconstituer les comportements paléo-hydrologique et -hydrogéochimique des milieux granitiques ou sédimentaires. Le couplage d'outils pétrographiques, minéralogiques, isotopiques (C, O, H), et géochimiques (K/Ar) a permis de déterminer la source et la nature des fluides à l'origine des colmatages (carbonates et silicates), ainsi que les processus physico-chimiques mis en jeu. Cette étude a été ciblée sur trois contextes distincts dans le cadre des recherches menées par l'Andra pour l'implantation d'un laboratoire géologique souterrain :

- Dans les plutonites sous couverture sédimentaire de Charroux-Civray (Vienne), trois événements principaux de percolations fluides (fluides hercyniens, saumures mésozoïques et eaux diagénétiques) ont été identifiés au cours de l'histoire du massif. Les carbonates déposés dans les fractures ou disséminés dans les plutonites lors des épisodes de circulations se sont formés à partir d'une source unique en C ($\delta^{13}C$ entre -9 et -14 ‰) introduite précocement lors du métamorphisme rétrograde hercynien, et remobilisée par les différents fluides successifs, donnant à ces plutonites riches en Ca une capacité d'auto-colmatage efficace face aux circulations fluides.

- Dans les siltites et les encaissants gréso-calcaires Crétacés de Marcoule (Gard Rhodanien), le colmatage calcitique des fractures, elles-mêmes créées lors de compressions éocènes et/ou lors des extensions oligocènes a lieu sous gradient thermique modéré (T<50-55°C). Les sources en C et O des calcites des fractures diffèrent en fonction du niveau stratigraphique, et leur colmatage a lieu : i) en système clos avec redistribution locale de matière, répercutant ainsi, dans les fractures, l'identité des carbonates diagénétiques plus précoces de la porosité, ou ii) dans les niveaux initialement plus poreux, en système ouvert avec participation d'eaux météoriques et introduction de C et O d'origine externe. Ces processus tardifs ont globalement contribué aux faibles perméabilités actuelles du site par le colmatage du réseau de fractures.

- Dans l'Est du bassin de Paris, durant le Tertiaire, des circulations de fluides météoriques ont été identifiées à l'échelle régionale dans les fractures ainsi que dans la porosité des ensembles calcaires Bathoniens et Kimméridgiens encadrant les argilites Callovo-Oxfordiennes. Les valeurs isotopiques en C des calcites déposées montrent que ces fluides ont circulé de façon ascendante le long des accidents distensifs régionaux. La précipitation des calcites dans la porosité des calcaires a été induite par l'infiltration de ces fluides latéralement aux failles. Ceci explique les faibles valeurs de perméabilités actuelles des calcaires. Cependant, ces fluides ne semblent pas avoir eu d'influence notable sur les caractéristiques isotopiques des ciments des argilites.

D'un point de vue méthodologique, la composition isotopique en C doit être employée avec précaution pour le traçage des fluides dans l'éventualité d'une (re)cristallisation polyphasée de carbonates, car le carbone des minéraux initiaux peut être remobilisé lors de circulations fluides plus tardives. Ce travail a montré que le traçage isotopique en C et O des minéraux remplissant les discontinuités ou porosités, couplé aux études pétrographiques, minéralogiques, et thermiques obtenues sur les inclusions fluides, sur les matières organiques et sur les argiles, constitue un outil puissant pour reconstituer les conditions paléo-hydrogéologiques, quel que soit le contexte.

Mots clefs : Fracture, Colmatage, Isotopes stables, Paleo-circulation, Interaction fluide-roche, Redistribution du carbone, Plutonites de la Vienne, Séries Mesozoïques, Est du bassin Parisien, basin du Sud-Est.

ABSTRACT

The study of minerals sealing the discontinuities and the cavities by past to recent fluid circulations is the only method to assess the paleo -hydrological and –hydrogeochemical behavior of both sedimentary or granitic systems. Petrographic, mineralogic, isotopic (C, O, H) and geochemical (K/Ar) tools provide the opportunity: i) to identify the source and the nature of sealing (carbonates and quartz) -forming waters and ii) to precise the physical and chemical mechanisms occurring during fluid circulations. This study is focused on 3 sites selected in the framework of a survey managed by Andra for the feasibility of an underground laboratory:

- In the covered plutonites of Charroux Civray (Vienne), 3 major fluid circulations (Hercynian fluids, Mesozoic brines, diagenetic waters) have been identified. The carbonates deposited in discontinuities or pervasively inside the granitic rocks have been formed from an unique C source ($\delta^{13}C$ ranging from -9 and -14 ‰). C stock has been early introduced during retrograde metamorphism, and afterwards, remobilized by successive fluid inputs. This confers on the Ca-rich plutonic rocks an efficient self-sealing capacity during later fracturing and fluid flow.

- In Cretaceous siltites and surrounding limestones and sandstones of Marcoule (South-eastern Basin), calcites from fracture formed during Eocene compression and/or Oligocene extension have been deposited under low temperature conditions (T<50-55°C). C and O sources of fracture calcites differ as a function of stratigraphical levels. Fracture sealing occurs: i) either in close system, by redistribution of the nearby host-rock cements, or ii) in open system with introduction of C and O from external sources. These late events have contributed to reduce the global permeability of the rocks trough the sealing of the fractures.

- In the Eastern part of the Paris basin, circulations of meteoric fluids have occurred at a regional scale during Tertiary, both in the fractures, cavities and in the porosity of the Bathonian and Oxfordian limestone series surrounding the Callovian-Oxfordian argillites. Carbon isotopic values of deposited calcites indicate that fluid circulations occurred upwards along the distensive regional faults. Fluids have also infiltrated limestones and sealed the porosity by crystallizing late sparite, resulting in the low present-day permeability values. However, these fluids have not influenced the isotopic characteristics of argillites cements.

The carbon isotopic composition must be exercised with caution to unravel the fluid origins in the event of poly-cyclic carbonate redistribution, as carbon of early minerals could be easily redistributed by the later fluid flows. Our methodology, based on the combined use of C-O isotopic tracers, petrographic, mineralogical and thermal (fluid inclusion, organic matter, clay typology) studies, is a promising powerful tool to assess the paleo-hydrogeologic behavior in geological systems.

Keywords: Discontinuity sealing, Stable isotopes, Paleo-circulation, Fluid-rock interaction, Carbon remobilization, Vienne plutonites, Mesozoic series, Eastern Paris basin, South Eastern basin.

S.C.D. - U.H.P. NANCY 1
BIBLIOTHÈQUE DES SCIENCES
Rue du Jardin Botanique - BP 11
54601 VILLERS-LES-NANCY Cédex

Tables des matières

RESUME *1*
ABSTRACT *3*
INTRODUCTION GENERALE *11*
A. LE MASSIF GRANITIQUE DE CHARROUX-CIVRAY *15*

INTRODUCTION *17*

RÉSULTATS SYNTHÉTIQUES *17*
a. Synthèse des connaissances sur les circulations fluides 17
b. Problématiques abordées 18
- Les altérations hydrothermales tardi-magmatiques hercyniennes 18
- Origine des circulations de saumures mésozoïques 19
- Etude des circulations fluides polyphasées dans les fractures argileuses 20
- Historique des circulations fluides de la Vienne et source du carbone 21

1 RETROGRADE P-T EVOLUTION AND HIGH TEMPERATURE – LOW PRESSURE FLUID CIRCULATION IN RELATION TO LATE-HERCYNIAN INTRUSIONS: A MINERALOGICAL AND FLUID INCLUSION STUDY OF THE CHARROUX-CIVRAY PLUTONIC COMPLEX (NW MASSIF CENTRAL, FRANCE) *1-23*
Figure captions 1-24
Table captions 1-24
Abstract 1-25
1.1 Introduction 1-27
1.2 Studied material 1-28
1.3 Petrography and succession of alteration types 1-29
1.4 Fluid inclusion data 1-33
1.5 Oxygen isotope data 1-39
1.6 Reconstruction of the P-T-X evolution 1-40
1.7 Discussion and concluding remarks 1-43
Acknowledgments 1-47
References 1-48

2 PENETRATION OF BRINES INTO A CRYSTALLINE BASEMENT DURING EXTENSIONAL TECTONICS: IMPLICATIONS ON FRACTURE SEALING *2-53*
Figure captions 2-54
Table captions 2-54
Abstract 2-55
2.1 Introduction 2-57
2.2 Geological setting 2-57
2.3 Mineral sequences and studied material 2-58
2.4 Fluid characterisation 2-59
2.5 Stable isotope data on quartz and carbonates 2-67
2.6 Discussion 2-70
2.7 Conclusions 2-72
Acknowledgements 2-74
References 2-75

3 MULTISTAGE PALEOFLUID PERCOLATIONS IN GRANITES: A STABLE ISOTOPE AND K-AR STUDY OF FRACTURE ILLITE FROM THE VIENNE PLUTONITES (N.W. OF THE FRENCH MASSIF CENTRAL) ***3-81***

Figure captions 3-82
Table captions 3-82
Abstract 3-83
3.1 Introduction 3-85
3.2 Sample description 3-87
3.3 Analytical methods and results 3-90
3.4 Discussion 3-100
3.5 Conclusions 3-103
Acknowledgements 3-104
References 3-105

4 MULTISTAGE FLUID CIRCULATION WITH EARLY INTRODUCTION AND RECURRING REMOBILIZATIONS OF CARBON DURING SUBSURFACE FLUID-ROCK INTERACTIONS: THE CASE STUDY OF THE VIENNE GRANITOIDS (FRANCE) ***4-111***

Figure captions 4-112
Table captions 4-112
Abstract 4-113
4.1 Introduction 4-115
4.2 Geology and description of the studied material 4-116
4.3 C and O isotopes on bulk altered rocks and veins 4-121
4.4 Discussion 4-130
4.5 Concluding remarks 4-134
Acknowledgments 4-136
References 4-137

B. LES ENSEMBLES SEDIMENTAIRES DU GARD RHODANIEN ET DE L'EST DU BASSIN DE PARIS 143

INTRODUCTION ***145***

RÉSULTATS SYNTHÉTIQUES ***145***

a. Origine des circulations fluides dans les formations de Marcoule 145
b. Origine des circulations fluides dans les formations de l'Est 147

5 LOCAL PALEO-FLUID INFILTRATION AND FRACTURE SEALING IN LOW PERMEABILITY CRETACEOUS SILTITES (SOUTH-EASTERN BASIN, FRANCE): AN ISOTOPIC AND DIAGENETIC STUDY OF FRACTURE AND ROCK CEMENTS ***5-151***

Figure captions 5-152
Table captions 5-152
Abstract 5-153
5.1 Introduction 5-155
5.2 Geological backgound and sampling 5-157
5.3 Analytical techniques 5-161
5.4 Results 5-162
5.5 Interpretation of the fluid origin 5-169
5.6 Concluding remarks 5-171
Acknowledgements 5-172
References 5-173

6 WIDESPREAD CEMENTATION INDUCED BY INFLOW OF CONTINENTAL WATER IN THE EASTERN PART OF THE PARIS BASIN: O AND C ISOTOPIC STUDY OF CARBONATE CEMENTS ***6-179***

Figure captions 6-180
Table captions 6-180
Abstract 6-181
6.1 Introduction 6-183
6.2 Geological background of the eastern flank of the Paris Basin 6-184
6.3 Late sparite crystallisation stage 6-185
6.4 Analytical methods 6-188
6.5 Results 6-189
6.6 Interpretation of the fluid source 6-197
6.7 Concluding remarks 6-200
Acknowledgements 6-202
References 6-203

7 FRACTURE SEALING IN MESOZOIC LIMESTONES (EASTERN PARIS BASIN, FRANCE): CONTINENTAL WATERS DRAINAGE IN THE VICINITY OF FAULT ZONES ***7-209***

Figure captions 7-210
Table captions 7-210
Abstract 7-211
7.1 Introduction 7-213
7.2 Geological background of the eastern flank of the Paris Basin 7-213
7.3 Sample collection 7-215
7.4 Analytical techniques 7-218
7.5 Isotopic results 7-220
7.6 Interpretation of fluid origin 7-221
7.7 Summary and conclusions 7-224
Acknowledgements 7-226
References 7-227

CONCLUSIONS GENERALES 233
REFERENCES GENERALES 247

S.C.D. - U.H.P. NANCY 1
BIBLIOTHÈQUE DES SCIENCES
Rue du Jardin Botanique - BP 11
54601 VILLERS-LES-NANCY Cédex

INTRODUCTION GENERALE

S.C.D. - U.H.P. NANCY 1
BIBLIOTHÈQUE DES SCIENCES
Rue du Jardin Botanique - BP 11
54601 VILLERS-LES-NANCY Cédex

INTRODUCTION GENERALE

Objectifs de l'étude

La compréhension des *circulations et des transferts massiques anciens à actuels* dans les milieux granitiques et sédimentaires est essentielle à la caractérisation et à la modélisation du comportement hydrogéologique des formations semi-perméables cibles et des aquifères fracturés. L'évolution dans le temps et l'espace des principaux événements de percolation et l'origine de la circulation des fluides anciens à récents constituent donc un enjeu important dans la compréhension des systèmes hydrologiques et hydrogéochimiques actuels. C'est pourquoi, cette étude est axée sur la caractérisation des remplissages minéraux formés au cours du temps, dans les fractures et les cavités recoupées lors des forages Andra, afin d'appréhender le fonctionnement des processus de colmatage.

Pour leur grande majorité, les remplissages de fissures ou de la porosité semblent relativement anciens (> 1 Ma) dans le cas des trois sites étudiés. Cependant, il est important de savoir comment s'est formé le réseau de discontinuités minéralisées, susceptible d'être percolé actuellement ou dans le futur. En particulier, il est capital de pouvoir associer à chaque stade de fracturation, un épisode de circulation de fluides et d'interaction entre fluides et roches (dissolution ou cristallisation). Il faut cependant noter que les événements de fracturation n'impliquent pas nécessairement une circulation significative de fluides, et que les fluides peuvent circuler dans des fractures postérieurement à la formation de celles-ci, sans y déposer de matériaux solides ou provoquer leur colmatage.

Les seuls témoins de paléo-circulations, disponibles actuellement, sont donc des échantillonnages discrets et discontinus des événements de percolation, à savoir :

1. les paragenèses d'altération et les colmatages de fissures et cavités résultant de la sursaturation passagère d'un fluide vis à vis d'une espèce minérale, suite à l'interaction de ce fluide avec les minéraux de la roche ou à une variation des paramètres externes comme la pression et la température. Ces minéraux formés lors de phases de circulation d'eaux intra-formationnelles (diagenèse des sédiments) ou allochtones (hydrothermaux s.l., fluides de bassin dans les granites, fluides provenant éventuellement d'aquifères distincts dans les séries sédimentaires) régissent une grande partie des caractéristiques chimiques des eaux préservées dans la porosité (zone de drainage) des roches ou des eaux percolantes.

2. les microvolumes de fluides piégés sous forme d'inclusions, soit lors de la cicatrisation de microfissures, soit lors de la néoformation des minéraux. Par ailleurs, des micropiégeages de fluides (microcavités et pores mal connectés) préservent les fluides anciens, et peuvent être à l'origine d'hétérogénéités spatiales de la composition des fluides actuels, par exemple, à travers les processus de la distribution du stock " chlore ancien", dans le cas de la Vienne.

Cette étude est focalisée sur les trois sites lors de l'initialisation de ce travail de thèse, dont le massif granitique de Charroux-Civray dans la Vienne et deux sites

sédimentaires, l'un dans les siltites de Marcoule dans le Gard Rhodanien, l'autre dans les argilites de l'Est du bassin parisien à la limite entre les départements de la Haute-Marne et de la Meuse près de Bure, soit des contextes géologiques assez variés.

La problématique majeure, et cela quel que soit le site, est donc la détermination de l'origine des éléments chimiques constitutifs des minéraux ou se trouvant dans les solutions piégées sous forme d'inclusions fluides.

Dans le cas de la Vienne, par exemple, se pose le problème de l'origine de certains éléments allochtones tels que le carbone des carbonates ou encore le chlore préservé dans les inclusions fluides des minéraux des paragenèses à saumures. En effet, les carbonates des différentes générations de colmatage dans la Vienne possèdent une signature isotopique particulière en carbone (-9 à -10 ‰ PDB), mais relativement constante. Le carbone semble avoir été introduit précocement lors de l'histoire hercynienne du granite de la Vienne, puis aurait été remobilisé par la suite au cours des événements successifs de circulations identifiés par l'étude pétrographique des colmatages. Le chlore aurait été introduit au mésozoïque lors des circulations de saumures à grande échelle, reconnues par ailleurs dans le massif central. La circulation des saumures constitue l'événement principal dans la Vienne par la quantité de remplissages minéraux déposés. Ce stock chlore a également été remobilisé, car des gradients de salinités allant de 1 $g.l^{-1}$ à 150 m de profondeur (au toit du granite, sous la couverture sédimentaire) jusqu'à 10 $g.l^{-1}$ à des profondeurs de 400 à 600 m ont été observés dans les eaux actuelles. Bien qu'ils aient déjà été décrits auparavant, l'âge des processus et des circulations, relatif ou absolu, reste à préciser, ainsi que l'origine des fluides et des phénomènes physico-chimiques mis en jeu. Ils pourront être contraints par l'étude du rapport isotopique de l'oxygène et du carbone des remplissages et par l'étude microthermométrique et chimique des inclusions fluides. Par ailleurs, les fractures colmatées par des remplissages argileux fourniront assurément un matériel de choix pour les datations des phénomènes afin de reconstituer l'historique des circulations fluides dans la Vienne et de préciser la paleo - hydrologie générale du site au cours du temps.

Les sites du Gard et de l'Est sont deux sites sédimentaires assez analogues recoupés dans les niveaux les plus compétents par des fractures (et cavités), tapissées ou parfois remplies de carbonates. Cependant, l'histoire des circulations y semble assez différente. Un événement particulier a été identifié dans l'Est et bien que les signatures isotopiques en carbone des calcites sparitiques déposées reflètent celles de l'encaissant calcaire qui a tamponné le fluide percolant, les valeurs en oxygène des calcites tardives situées aussi bien dans les géodes que les fractures diffèrent nettement de celles des calcaires. Il était nécessaire d'identifier l'origine de ce fluide tardif et de tester son impact sur l'encaissant et sa porosité. Enfin, on s'intéressera à l'extension régionale et à l'âge des circulations dans l'Est du bassin de Paris. Quant au Gard, la précipitation de carbonates dans les pores et dans les fractures des siltites et des encaissants gréseux à calcaires est produite par la circulation de fluides à tendance marine, lors d'une diagenèse de basse température, mais elle aboutit à une histoire assez complexe, et d'intensité variable en fonction des niveaux stratigraphique. Il sera utile de comprendre quels sont les processus à l'origine de cette spécificité, assez inattendue pour une série sédimentaire en contexte thermique faible et aux caractéristiques géochimiques et organiques assez immatures.

Méthodologie

Les objectifs de cette étude (réalisée dans le cadre de collaborations au sein du GdR FORPRO) vise donc à évaluer le fonctionnement des réseaux de discontinuités au cours du temps et leur influence sur les capacités de confinement passées, présentes et futures des barrières géologiques. Bien que des travaux analytiques préliminaires aient déjà été réalisés sur certains aspects, notamment en pétrographie avant 1998 dans le cas de la Vienne, il apparaissait par conséquent nécessaire :

1. *d'améliorer la compréhension des percolations et la formation des colmatages* (quartz, carbonates, argiles) dans les fractures et les cavités à des périodes passées à récentes et de *définir parfaitement le système eau ancienne-fracture/cavité*, en déterminant *la source et la nature des fluides mis en jeu*, par le couplage de la pétrographie et du traçage des *sources isotopiques (C/O/H)*, pour que le même type d'information géochimique soit disponible sur le maximum d'événements de percolation identifiés au niveau des trois sites,

2. *de caractériser et de comprendre les processus d'altération au sein et au voisinage des fractures/cavités,* notamment au niveau de la porosité, afin de tester l'impact des fluides provenant éventuellement d'autres formations, par exemple, de la couverture sédimentaire vers le socle dans la Vienne, des aquifères vers les argilites (Est) ou siltites (Gard),

3. *de préciser l'extension verticale et latérale (géographique) des paléo-circulations fluides*,

4. *de contraindre l'âge des percolations*, si possible par datation des processus géochimiques (par ex. par méthode K-Ar pour les argiles), sinon de manière relative.

Ce mémoire s'organisera en deux parties principales. En raison du grand nombre d'intervenants sur ce programme et de la quantité de données analytiques acquises, il a été décidé en accord avec les responsables du programme de structurer et de présenter les données sous forme de publications ou de projets de publications. La première partie traitera des circulations ayant affecté le massif cristallin de Charroux-Civray. La problématique posée pour la Vienne profitera fortement des résultats des travaux de thèse réalisés par R. Freiberger (2000) et Y. Coulibaly (1998), et d'études contractuelles réalisées avant 1998. La seconde partie de ce travail portera respectivement sur les résultats obtenus dans le cas des formations sédimentaires du Gard et de l'Est. Pour le site de l'Est, l'étude des remplissages dans les forages Andra sera renforcée dans un deuxième temps par l'extension de la caractérisation des cristallisations des fractures à l'échelle régionale.

A. LE MASSIF GRANITIQUE DE CHARROUX-CIVRAY

INTRODUCTION

Le massif granitique étudié est situé dans le sud du département de la Vienne sur la bordure Nord-Ouest du Massif Central à proximité des localités de Charroux et de Civray. Il constitue le passage entre les domaines vendéen et limousin et est localisé sous une couverture sédimentaire mésozoïque (essentiellement du Lias au Dogger) d'une épaisseur allant de 120 à 160 m. Deux types de corps plutoniques ont été reconnus dans la Vienne, le premier étant méso-varisque à associations calco-alcalines à sub-alcalines généralement regroupées sous l'appellation générale de "ligne tonalitique du limousin" (Didier et Lameyre, 1971), l'autre tardi-varisque est de type leucogranitique peralumineux.

Les travaux de reconnaissance entrepris par l'Andra dès 1994, dont la synthèse est réalisée par Mouroux (1999) et Virlogeux et al. (1999), ont permis la réalisation de nombreux forages carottés. Ils ont été échantillonnés dans le cadre d'études antérieures, notamment celles de : i) Cuney et al. (1999) et Freiberger (2000) pour l'étude des conditions P-T-X de l'histoire magmatique à tardi-magmatique des plutonites de la Vienne et ii) Cathelineau et al. (1999) et Coulibaly (1998) lors d'un projet intitulé 'Etude des cristallisations dans les fractures' ciblant l'histoire des circulations post-magmatiques, basé notamment sur les caractéristiques minéralogiques et thermo-barométriques des différentes générations de remplissages et des paléofluides piégés. Ces études ont permis d'identifier les principaux épisodes de circulation de fluides et de colmatage de fractures.

RESULTATS SYNTHETIQUES

Ce chapitre étant présenté sous forme d'articles, il a été choisi de synthétiser les problématiques et les principaux résultats ci-après.

a. Synthèse des connaissances sur les circulations fluides

Deux stades principaux attribuables à deux événements géodynamiques majeurs ont été reconnus :

Stade 1 : les multiples fluides du métamorphisme rétrograde tardi-Hercynien et associés aux flux de chaleur magmatiques ont produit des altérations à épidote / prehnite / quartz / chlorite / hématite ± carbonates (dolomite, calcite) ± adulaire ± laumontite et des veines à (quartz) / chlorite / phengite / muscovite / quartz / sulfures / illite. Ces fluides appartiennent aux systèmes CO_2-N_2, H_2O-CO_2, et H_2O-sels, et sont piégés dans une gamme P-T étendue : 130° à 450°C, 0,5 à 3,5 kb.

Stade 2 : des saumures (plusieurs centaines de g/l de sels) ont colmaté les fractures du socle par une association à hématite / adulaire / dolomite / quartz / fluorite / barytine ± sulfures (Cu,Zn) / calcite. Ces veines sont prédominantes dans les plutonites, et montrent une séquence paragénétique très constante. Elles ont circulé à des températures de 110°C maximum.

Enfin, des remplissages fissuraux beaucoup moins abondants et plus tardifs (stade 3) à (kaolinite) / calcite / oxy-hydroxydes de fer, se sont formés à partir de

fluides de basse température (<50°C), en relation avec des épisodes mineurs de circulation. Des calcites de même type ont aussi été identifiées dans des géodes dans la couverture.

b. Problématiques abordées

La problématique principale de ce travail est d'appréhender les paléo-circulations ayant affecté le massif cristallin de Charroux-Civray afin d'en reconstituer l'historique et ainsi la paléo- hydrologie globale du site au cours du temps. Cette étude consistera à parachever les caractérisations des remplissages cristallins en complétant l'acquisition de données isotopiques parfois manquantes, notamment sur les silicates de fractures dans le socle (quartz et argiles), sur les carbonates interstitiels disséminés dans les plutonites, et par des compléments analytiques sur des carbonates de fractures/ cavités notamment situés dans la couverture sédimentaire. Les données nouvelles de ce travail et les acquis antérieurs pétrographiques et isotopiques (sur les carbonates) ont été synthétisés sous forme de publications.

L'étude des colmatages a soulevé plusieurs questions majeures sous-jacentes, notamment sur l'origine des éléments allochtones tels que le carbone des carbonates ou le chlore préservé dans les inclusions fluides des minéraux des paragenèses à saumures. En effet, les carbonates des différentes générations de colmatage dans la Vienne possèdent une signature isotopique particulière et assez constante en carbone (-9 à -14 ‰ PDB). Il était important d'identifier la source en carbone introduit apparemment précocement lors de l'histoire hercynienne du granite de la Vienne, puis remobilisé au cours des événements successifs de circulations. L'origine du chlore, probablement introduit lors des circulations de saumures à grande échelle doit être spécifiée. La circulation des saumures constitue l'événement principal dans la Vienne par la quantité de remplissages minéraux déposés. Bien qu'ils aient déjà été avancés auparavant, l'âge des processus et des circulations reste à préciser, ainsi que les phénomènes physico-chimiques mis en jeu lors des circulations. Par ailleurs, les fractures colmatées par des remplissages argileux pourront fournir un matériel adapté aux datations.

Ce chapitre est articulé autour de quatre articles synthétiques, dont un aperçu des problématiques et une synthèse des réponses apportées sont données ci après.

- **Les altérations hydrothermales tardi-magmatiques hercyniennes**

Objectifs et moyens

Les multiples altérations hydrothermales tardi-magmatiques hercyniennes qui se sont déroulées au niveau du granite de la Vienne constituent les premiers événements de circulations fluides ayant conduit à des modifications minéralogiques et géochimiques importantes du complexe plutonique calco-alcalin de Charroux-Civray daté de 350 à 360 Ma (Bertrand et al., 2000). En effet, une intrusion leucogranitique daté à 309 Ma (Alexandrov et al, 2000) dans le massif calco-alcalin a

été mise en évidence à la fois par les anomalies gravimétriques et par les forages. Le complexe plutonique, qui subissait jusque là une évolution P-T rétrograde, est affecté par des circulations pervasives sous un régime haute température – basse pression lors de l'intrusion.

La caractérisation de l'histoire magmatique à tardi-magmatique du massif de la Vienne a permis de préciser les processus mis en jeu afin d'établir un modèle des conditions P-T-x-t (pression - température - chimie – temps) des altérations pervasives.

L'étude détaillée des fluides piégés dans les micro-fissures des quartz sera utilisée comme marqueur des altérations. Les inclusions fluides constituent en effet un des meilleurs outils pour cela, car elles enregistrent la nature des fluides et permettront à la fois d'étudier l'évolution pression-temperature rétrograde et les circulations fluides reliées aux intrusions tardi-magmatiques.

Principaux résultats

Les résultats sont présentés dans l'article *'Retrograde P-T evolution and high temperature – low pressure fluid circulation in relation to late-hercynian intrusions: a mineralogical and fluid inclusion study of the Charroux-Civray plutonic complex (NW massif central, France)'.* Il est montré par le couplage du domaine de stabilité de l'épidote avec la barométrie de l'hornblende et les données des inclusions fluides que le refroidissement du complexe plutonique débute à environ 4 kbar. Il se poursuit durant l'uplift du massif jusqu'à des températures de 200 à 280°C et sous des pressions de 2 à 3 kbar jusqu'à l'assemblage prehnite-pumpellyite. Ensuite, les circulations hydrothermales de haute température (HT, 400-450°C) associées à l'intrusion du leucogranite induisent la formation de minéralisations de type greisen. Cependant, l'uplift se poursuivant, les greisens sont altérés en un assemblage à chlorite-phengite- dolomite associé aux circulations à des fluides de HT contenant de l'azote. Plus tardivement, la diminution de la température aux environs de 130° à 250°C et de la pression à une valeur proche de 0.5 kbar produit une nouvelle altération à dolomite-illite-chlorite.

- **Origine des circulations de saumures mésozoïques**

Objectifs et moyens

Le but de ce travail est de déterminer l'origine et la nature des saumures percolant le socle et de préciser leur rôle dans les transferts massiques des bassins vers les socles. L'extension régionale des circulations vers le Nord-Limousin sera étudiée par l'échantillonnage d'autres localités présentant des fractures avec le même type de paragenèse. Cet épisode mésozoïque, qui représente la grande majorité des colmatages reconnus dans les fractures, fait l'objet du dernier article portant notamment sur la chimie détaillée des fluides piégés et l'isotopie de la paragenèse correspondante (Fluorite, Quartz, Dolomite, Barytine, Calcite) afin de préciser l'origine et l'extension de la circulation des saumures mésozoïques.

Principaux résultats

Les résultats sont présentés dans l'article *'Penetration of brines into a crystalline basement during extensional tectonics: Implications on fracture sealing'.* Dans la Vienne, la séquence paragenétique laissée par l'événement à saumures à la fois dans le socle et dans la partie inférieure de la couverture (Infra-Toarcien) est systématiquement la suivante : hématite - adulaire/ quartz / dolomite (±fluorite ±barytine ± sulfates de Cu, Zn, Fe)/ calcite. Les analyses des fluides piégés dans les inclusions de cette paragenèse montrent une saumure à H_2O-NaCl-KCl-$CaCl_2$-($MgCl_2$) de salinité de l'ordre de 16 à 23 eq. wt. % NaCl. Les fluides, qui présentent des rapports Na/K de 5 à 40, Na/Li de 20 à 350 et Cl/Br de 200 à 1000, sont typiques donc des eaux de bassins profonds. Les températures de circulations du fluide sont autour de 90 ±25°C et ont pour composition isotopique reconstituée un $\delta^{18}O$ de 6 ± 2 SMOW et un δD de -30 ± 10‰. Ces fluides sont interprétés comme des saumures chaudes de type bassin sédimentaire profond, circulant à l'interface socle/couverture, et pénétrant profondément le socle. Celles ci sont probablement expulsées lors du maximum de subsidence du bassin Aquitain pendant l'ouverture de l'océan Atlantique et du golfe de Gascogne.

- **Etude des circulations fluides polyphasées dans les fractures argileuses**

Objectifs et moyens

Le troisième article est à la fois une étude méthodologique basée sur le couplage des données minéralogiques et isotopiques (O et H) et sur une approche originale de datations en K/Ar des fractures à remplissage argileux (ou gouges). En effet, la détermination de l'âge des percolations nécessite la présence d'un matériel minéral adapté, tel que les argiles. En effet, il n'est pas possible de dater les autres remplissages, tels que les carbonates et quartz. En sachant que les gouges argileuses sont encore actuellement le lieu de percolations et que ces fractures sont interprétées comme créées de façon précoce dans l'histoire du massif, on peut penser qu'elles ont vu circuler la plupart des fluides et qu'elles ont enregistré les principaux événements de percolations. L'objectif de cette étude est de déterminer, au niveau des gouges, les âges des épisodes de percolations fluides aussi reconnus dans les fractures à carbonates et quartz.

Principaux résultats

Les résultats sont présentés dans l'article *'Multistage paleofluid percolations in granites: a stable isotope and K-Ar study of fracture illite from the vienne plutonites (n.w. of the french massif central)'.* Les argiles des gouges sont essentiellement dominées par la présence d'illite et d'interstratifiés à prépondérance illitique. Les argiles analysées (<2 µm) et les sous-fractions granulométriques réalisées entre 0 et 2 µm présentent des $\delta^{18}O$ compris entre 8 et 18‰ SMOW corrélés respectivement

avec les âges K/Ar qui vont de 290 à 188 ± 5 Ma. On observe ainsi un rééquilibrage des fractions fines (<0.2 μm) des argiles lors d'un événement de circulation d'âge inférieur à 188 Ma. La partie néorfomée cristallise à partir d'un fluide recalculé ayant pour $\delta^{18}O$ une valeur de l'ordre de 5 ± 2 ‰ SMOW, donnée en accord avec celles obtenues sur les autres remplissages (carbonates et quartz) de cette même génération. Cependant, cet âge n'est certainement pas le pôle représentant strictement l'enregistrement des circulations mésozoïques, car cette fraction est aussi en partie un mélange entre argiles hercyniennes et mésozoïques. L'événement mésozoïque majeur, interprété comme lié aux épisodes distensifs associés au rifting de l'océan Atlantique et du golfe de Gascogne, est estimé avoir eu lieu entre 180 et 110 Ma.

- **Historique des circulations fluides de la Vienne et source du carbone**

Objectifs et moyens

Le principal objectif de cette étude est de reconstituer les différentes percolations fluides ayant circulé pendant l'histoire post-magmatique et de préciser leurs conditions de circulation. La reconstitution isotopique et thermo-barométrique des différents fluides (stades hercyniens, saumures mésozoïques, fluides diagenétiques dilués) ayant percolé le massif granitique, en y laissant pour empreinte des remplissages cristallins, est indispensable à la compréhension de paléo- hydrologie du site. Un problème directement sous-jacent à cette étude est le traçage de la source en carbone et sa remobilisation successive au cours du temps.

Principaux résultats

Les résultats sont présentés dans l'article *'Multistage fluid circulation with early introduction and recurring remobilizations of carbon during subsurface fluid-rock interactions: the case study of the Vienne granitoids (France)'.* Trois épisodes majeurs ont été identifiés par l'étude pétrographique, minéralogique et isotopique en oxygène des remplissages de carbonates et de quartz. D'abord, des circulations fluides (post-magmatiques) à des températures relativement élevées ont lieu durant l'Hercynien dans les fractures. Ensuite, des saumures diagénétiques sont expulsées latéralement le long de l'interface socle/couverture. Elles pénètrent et percolent ainsi le socle durant des épisodes distensifs liés à l'évolution du bassin. Enfin, des eaux marines plus tardives, légèrement modifiées par la diagenèse ont été reconnues à l'intérieur du socle. Cependant, les valeurs isotopiques en carbone sont très constantes (-9 à -14 ‰ PDB) alors que les valeurs en oxygène sont très variables (+3 à +30 ‰ SMOW) entre les 3 générations. Les analyses isotopiques des carbonates diffus disséminés dans les roches plutoniques se distribuent en deux groupes, le premier groupe présente des valeurs comparables aux carbonates de fractures hercyniens, et le second aux carbonates de fractures mésozoïques. Le carbone aurait alors été introduit durant le métamorphisme rétrograde et systématiquement réutilisé par les stades ultérieurs de circulations, conférant aux roches plutoniques riches en calcium cette capacité d'auto-colmatage face aux circulations fluides.

1 RETROGRADE P-T EVOLUTION AND HIGH TEMPERATURE – LOW PRESSURE FLUID CIRCULATION IN RELATION TO LATE-HERCYNIAN INTRUSIONS: A MINERALOGICAL AND FLUID INCLUSION STUDY OF THE CHARROUX-CIVRAY PLUTONIC COMPLEX (NW MASSIF CENTRAL, FRANCE)

R. Freiberger[a,b], M. C. Boiron[b], M. Cathelineau[b], M. Cuney[b], S. Buschaert[b,c]

[a] *Institut für Mineralogie, Petrologie und Geochemie, Albert-Ludwigs-Universität Freiburg, Albertstr. 23b, 79104 Freiburg, Germany*
[b] *UMR G2R 7566 - CREGU, BP 23, 54501 Vandoeuvre-lès-Nancy Cedex, FRANCE*
[c] *Andra, French Agency for Nuclear Waste Management, 92298 Châtenay-Malabry*

In press, Geofluids, 2002

Figure captions ***1-24***
Table captions ***1-24***
Abstract ***1-25***

1.1 INTRODUCTION ***1-27***

1.2 STUDIED MATERIAL ***1-28***

1.3 PETROGRAPHY AND SUCCESSION OF ALTERATION TYPES ***1-29***
1.3.1 Stage 1: Ca-Al silicate assemblage 1-29
1.3.2 Stage 2: Greisen assemblage 1-30
1.3.3 Stage 3: Chlorite-phengite-dolomite±adularia assemblage 1-31
1.3.4 Stage 4: Dolomite-illite-chlorite assemblage 1-31
1.3.5 Later stages 1-31

1.4 FLUID INCLUSION DATA ***1-33***
1.4.1 Analytical methods 1-33
1.4.2 Location and typology of fluid inclusions 1-33
1.4.3 Relationships with alteration types 1-36
1.4.4 Aqueous-carbonic fluid inclusions Lc(-w) and Lc-w 1-36
1.4.5 Aqueous-carbonic fluid inclusions Lw-c 1-37
1.4.6 Nitrogen vapor inclusions Vn 1-38
1.4.7 Water-nitrogen liquid inclusions Lw-n 1-38
1.4.8 Aqueous fluids Lw 1-38

1.5 OXYGEN ISOTOPE DATA ***1-39***

1.6 RECONSTRUCTION OF THE P-T-X EVOLUTION ***1-40***
1.6.1 Stage 1: Aqueous fluids Lw_I 1-41
1.6.2 Stage 2: Carbonic fluids Lc(-w), Lc-w and Lw-c 1-42
1.6.3 Stage 3: Nitrogen and aqueous fluids Lw-n, Vn and Lw 1-42
- Nitrogen fluids Lw-n and Vn 1-42
- Aqueous fluids LwII 1-43

1.6.4 Stage 4: Aqueous fluids Lw_{III} 1-43

1.7 DISCUSSION AND CONCLUDING REMARKS ***1-43***
Acknowledgments ***1-47***
References ***1-48***

FIGURE CAPTIONS

Fig. 1.1. Map of the Charroux-Civray area with the northwestern part of the Massif Central. At the drilling locations, the basement is covered by about 150 m thick sedimentary rocks of Jurassic age. The basement beneath Charroux-Civray mainly consists of medium-K and high-K calcalkaline plutonic associations of which the contours have been derived from geophysical and petrologic investigations. *1-28*

Fig. 1.2. Relative crystallization sequence of post-magmatic alteration stages 1 to 4, deduced from petrographic observations. *1-30*

Fig. 1.3. Photomicrographs of typical alteration assemblages within the calc-alkaline plutonic rocks from Charroux-Civray. A: subsolidus epidote associated with quartz and biotite (stage 1); B: paragenesis of secondary prehnite and pumpellyite as replacement of biotite (stage 1); C,D: greisen assemblage including white mica sheets, tourmaline, chlorite and quartz (stage 2); E: chloritisation of biotite associated with K-feldspar lenses parallel to the former biotite cleavage (stage 3); F: pervasive alteration of feldspar to mainly illite (stage 4). *1-32*

Fig. 1.4. Ternary diagram H_2O–CO_2–$10(CH_4+N_2)$ showing the bulk composition of all investigated fluid inclusion types. Note the two distinct correlation trends between carbonic and aqueous and nitrogen and aqueous inclusions, respectively. *1-36*

Fig. 1.5. Typical examples of the different types of studied fluid inclusions. Carbonic fluids occur as 3- or 2-phase inclusions (a, b, c), nitrogen-bearing fluids as 2- and 1-phase inclusions (d, e) and aqueous fluids as 2-phase inclusions (f). *1-39*

Fig. 1.6. P-T diagrams showing calculated isochores of the investigated fluid inclusions. Grey fields indicate the assumed P-T ranges during fluid trapping. a) primary aqueous FI in epidote and secondary aqueous FI in quartz of stage 1, b) secondary carbonic FI of different densities in quartz (stage 2), c) nitrogen-bearing liquid and vapor FI (stage 3), d) secondary aqueous FI of stage 4 in quartz. *1-41*

Fig. 1.7. P-T diagram showing the stability ranges of the different alteration assemblages, determined through fluid inclusion studies and paragenetical implications. Dark grey fields show the assumed P-T ranges during trapping of the different fluids as revealed in Fig. 1.6. Light grey arrows indicate the deduced P-T evolution within the calc-alkaline plutonic complex during post-magmatic stages. Stippled horizontal lines indicate pressure within the calc-alkaline complex: 1) during leucogranite intrusion, 2) during later fluid convection, derived from fluid inclusion isochores (see Fig. 1.6.c, d). The cooling path from the subsolidus stage at around 600°C down to about 250°C is taken from Freiberger et al. (in press), the P-T field of prehnite–pumpellyite paragenesis is from Frey et al. (1991). *1-44*

Fig. 1.8. Summary of possible T-t paths for the post-magmatic evolution of the Charroux-Civray area, based on the constraints issued from fluid inclusion studies and the consideration of two main magmatic stages. The grey line marks one probable T-t path. Indicated depths are assumed with crustal temperatures of 25 to 30°C/km. T1 to T3 are temperatures within the unaffected basement during calc-alkaline intrusions (T1), during post-magmatic times of prehnite–pumpellyite formation (T2), and during late hydrothermal circulation (T3). *1-46*

TABLE CAPTIONS

Table 1.1. Investigated samples for fluid inclusion and stable isotope studies. Indicated are host rock type, predominant alteration type and petrographic characteristics of fluid inclusion and oxygen isotope samples. *1-29*

Table 1.2. Ranges of microthermometric parameters of the fluids of alteration stages 1 to 4. ..... *1-34*

Table 1.3. Summary of microthermometry and Raman microspectroscopy data with calculated global composition (in mol.%) of different fluid inclusion types. *1-35*

Table 1.4. Oxygen isotope data of quartz fracture samples and calculated $\delta^{18}O$ of the associated fluid. $\delta^{18}O_{fluid}$ values were calculated considering quartz-water isotopic fractionation factors of Zheng (1993) and using estimated temperature of formation of quartz as indicated. *1-40*

ABSTRACT

The calc-alkaline plutonic complex from Charroux-Civray (North-Western part of the French Massif Central) display multiphase hydrothermal alteration. Plutonic rocks as well as early retrograde Ca-Al silicate assemblages, which have crystallized during cooling and uplifting of the plutonic series, are affected by multiphase chlorite–phengite–illite–carbonate alteration linked to intense pervasive fluid circulation through micro-fractures. The petrographic study of alteration sequences and their associated fluid inclusions in microfissures of the plutonic rocks as well as in mineral fillings of the veins, yield to a reconstruction of the P-T-X evolution of the Hercynian basement since the crystallization of the main calc-alkaline plutonic bodies. This reconstruction covers the uplift of the basement up to its outcropping and the subsequent burial by Mesozoic sediments.

Cooling of the calc-alkaline plutonic series starts at solidus temperatures at about 4 kbar as indicated by magmatic epidote stability, hornblende barometry and fluid inclusion data. Then cooling continues under slightly decreasing pressure during uplift down to 2 to 3 kbar at 200 to 280°C (prehnite–pumpellyite paragenesis). Thus, after cooling down to about 250°C, a hot geothermal circulation within the calc-alkaline rocks was induced and leads to the formation of greisen-like mineralizations. During this stage, temperatures around 400–450°C are still rather high for the inferred depths (~ 2 kbar) and imply abnormal heat flows and thermal gradients of about 60 to 80°C/km. The hypotheses of the existence of one large or a succession of smaller peraluminous plutons at depth, based on geophysical considerations, leads to the assumption that localized heat flows are linked to concealed leucogranite intrusions. As uplift continues, greisen mineralization is subsequently affected by the chlorite–phengite–dolomite assemblage correlated with aqueous and nitrogen-bearing fluid circulations in the temperature range of 400 to 450°C. In a later stage continuously decrease of temperature with nearly constant pressure (~ 0.5 kbar) leads to alteration of the dolomite–illite–chlorite type in the temperature range of 130 up to 250°C.

Keywords : fluid inclusion, multiphase hydrothermal alteration, retrograde evolution, Hercynian, intrusion, microthermometry, Raman spectroscopy.

1.1 Introduction

The recent study of the Hercynian basement covered by about 150 m of Mesozoic sediments (limestones and clays) has provided exceptional sections and unweathered material of Hercynian plutonic suites over an area of about 125 km^2, in between the Armorican Massif and the Massif Central in France (Fig. 1.1). 17 continuously cored and oriented boreholes, 200 m to 1000 m deep, have shown that the major plutonic bodies can be grouped in two calc-alkaline rock suites, which consist of medium- and high-K calc-alkaline rocks. All these plutonic bodies are emplaced during the same magmatic event dated between 350 and 360 (± 5) Ma (Bertrand et al. 2000). After this early magmatic stage, calc-alkaline suites are intruded by a peraluminous granite. This leucogranite is a younger intrusion with an age at least older than 309 Ma (on the basis of K-Ar considerations, Alexandrov 2000) like other leucogranites from Massif Central, which have ages generally around 325 Ma (e.g. Duthou et al. 1984). The main evidence of peraluminous leucogranite intrusion within the calc-alkaline plutonites, is the intersection of a granite body along almost 200 m of one drill hole (CHA 109, Fig. 1.1). Inferred from major negative gravimetric anomalies, this intrusive body is supposed to represent a small part of a large peraluminous body at depth of more than 7 km width and about 20 km long (Virlogeux et al. 1999).

In post-magmatic times the plutonic complex is affected by multiphase pervasive alteration that displays heterogeneous distribution, probably in response to heterogeneous paleofluid flows. Preliminary fluid inclusion studies trapped in healed micro-cracks in quartz from altered calc-alkaline suites have shown that the density and trapping P-T conditions for most fluids were incompatible with an ordinary anti-clockwise retrograde P-T path. This has encouraged a detailed study of the fluids and their relationships with the pervasive alteration observed petrographically. Several fluid inclusion types were recognized within the Charroux-Civray plutonic complex, and investigated in the present study in view of their probable origin in the alteration history. Samples for fluid inclusion studies were thus selected in order to i) characterize the fluids corresponding to the different alteration stages affecting the plutonites, ii) reconstruct the alteration P-T path and iii) determine the causes of fluid convection in the plutonites. Fluid inclusion planes (FIP) in basement rocks are used in the present study as markers of the thermal effects produced by the late intrusions, and provide a rather good record of the nature of fluids percolating in a pervasive manner within the basement. An interpretative framework for the formation conditions of the extended pervasive alterations, affecting the granitoids in this region, is thus proposed at the light of a P-T path.

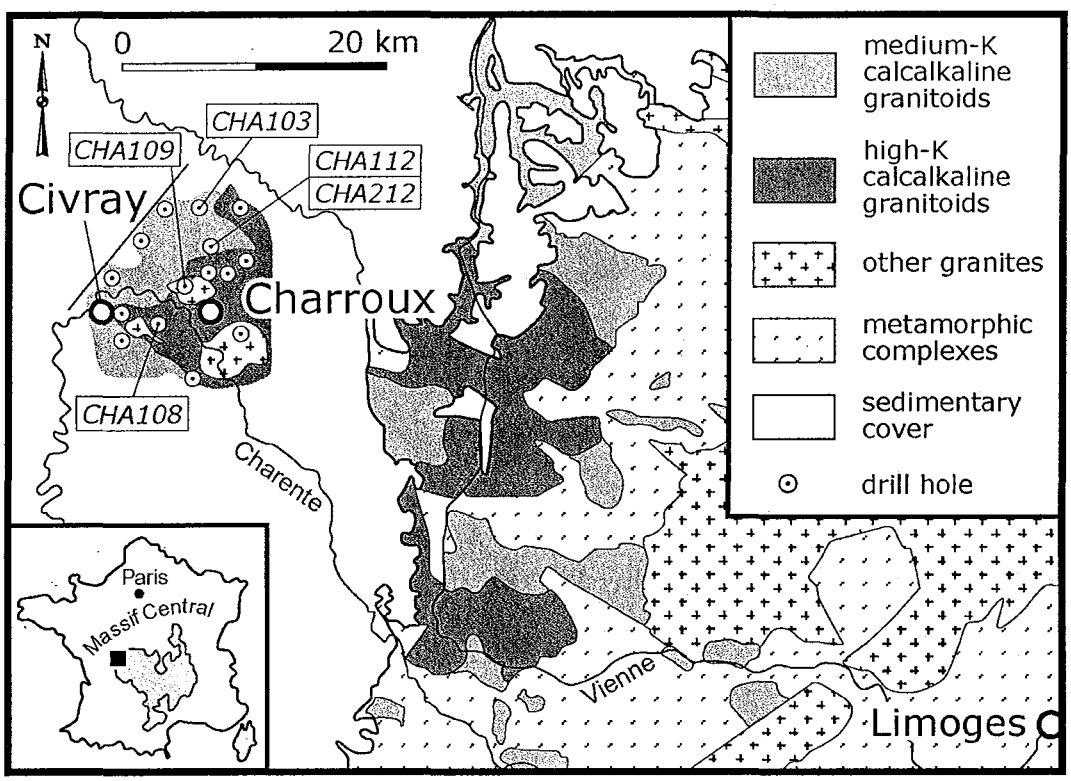

Fig. 1.1. Map of the Charroux-Civray area with the northwestern part of the Massif Central. At the drilling locations, the basement is covered by about 150 m thick sedimentary rocks of Jurassic age. The basement beneath Charroux-Civray mainly consists of medium-K and high-K calcalkaline plutonic associations of which the contours have been derived from geophysical and petrologic investigations. The studied samples come from marked drillings.

1.2 Studied material

The plutonic complex of Charroux-Civray is composed of multiple magmatic intrusions presenting a large variation of composition. The rocks can be grouped in three major associations: a medium-K calc-alkaline, a high-K (monzonitic) calc-alkaline associations and a peraluminous leucogranite intrusion (Cuney et al. 1999). Most drill holes show predominantly the two calc-alkaline series which cover a large range of composition, including gabbros, monzogabbros, diorites, monzodiorites, tonalites, leucotonalites, monzonites, monzogranites, and granodiorites. One drilling is represented by a two-mica leucogranite. The calc-alkaline rocks contain abundantly diorite and monzogabbro-diorite enclaves. Aplite and aplo-pegmatites veins are observed locally. Beside the ordinary rock forming minerals (mainly plagioclase (An_{25-45}), biotite, hornblende, and quartz) the common occurrence of magmatic as well as early post-magmatic epidote with pistacite contents of around 28 % is particularly characteristic (Freiberger 2000). One special feature of the calc-alkaline plutonites is the occurrence of magmatic anhydrite (Freiberger & Cuney 1999).

Studied samples were selected within an extended set of samples mainly from 2 major deep drillings, so-called CHA 112 drill hole (vertical, 579 m deep) and CHA 212 (drilled at the same place but with a 60° dip towards the east, down to 996 m). Complementary samples were taken from CHA 103 drill hole at 218 and 254 m below

surface, from CHA 108 at 242 m depth and from the leucogranite in drilling CHA 109 at 177 m depth (Fig. 1.1, Table 1.1).

Drilling	Sample	Depth (m)	Rock type	Alteration type	FI petrography
CHA 103	103A	218	gd	few chlorite+phengite	FIP in quartz
CHA 103	1984	254.04	to	Ca-Al silicates, chlorite+phengite	FIP in quartz
CHA 108	2420	242.6	mzd	illite+chlorite, carbonate	FIP in quartz from fracture
CHA 109	1610	177.5	lgr	quartz-filled fracture	FIP in quartz from fracture
CHA 112	4394	540.32	to + d	ductile epidote zone, Ca-Al silicates	FIP in quartz and primary FI in epidote of ductile shear zone
CHA 112	5094	535.47	to	greisen (quartz+tourmaline +muscovite), chlorite+phengite	FIP in quartz of fracture zone with tourmaline
CHA 212	5096	254.85	to	greisen (tourmaline+muscovite +carbonate+pyrite)	FIP in quartz
CHA 212	8649	695.64	to	Ca-Al silicates, chlorite+phengite	FIP in quartz
CHA 212	8650	710.77	to	Ca-Al silicates, chlorite+phengite	FIP in quartz
CHA 212	8653	766.55	lto	chlorite+phengite, carbonate (calcite, dolomite)	FIP in quartz
CHA 212	6880	968.67	to + ep	epidote zone, chlorite+phengite	FIP in quartz of epidote zone
CHA 212	6871	673.5	to	quartz- and dolomite-filled fracture	Primary FI in quartz and dolomite
CHA 212	8709	982.1	lto	quartz-filled fracture	FIP in quartz from fracture

Table 1.1. Investigated samples for fluid inclusion and stable isotope studies. Indicated are host rock type, predominant alteration type and petrographic characteristics of fluid inclusion and oxygen isotope samples.
gd – granodiorite, lto – leucotonalite, lgr– leucogranite, to – tonalite, d – diorite, mzd – monzodiorite, ep – massive epidote zone, FI – fluid inclusion, FIP – fluid inclusion plane

1.3 Petrography and succession of alteration types

Several episodes of post-magmatic hydrothermal alteration have been recognized in the batholith. Pervasive alteration affects the granitoid rocks of Charroux-Civray with variable intensities, depending on the degree of microfracturing and proximity to fractures, where alteration is generally more significantly developed. Overall, early post-magmatic alteration of the Charroux-Civray plutonic complex can be grouped into four main alteration stages (Fig. 1.2).

1.3.1 Stage 1: Ca-Al silicate assemblage

A very early post-magmatic alteration stage includes pervasive formation of several Ca-Al silicates in the course of plutonite cooling (Freiberger et al. in press). First subsolidus alteration comprises formation of sub-euhedral epidote in millimeter long patches, locally associated with incipient ductile deformation (Fig. 1.3.A). Further Ca-Al silicates include hydrogarnet, post-dated by prehnite and pumpellyite (partly in textural paragenesis, Fig. 1.3.B), Fe-rich epidote (pistacite) and later laumontite (predominately in small fractures). The Ca-Al silicates – except laumontite – occur almost exclusively as lenses parallel to the cleavage of magmatic biotite, frequently in

totally fresh rock samples. The formation of Ca-Al silicates represents a penetrative alteration that seems to be independent of (later) fracturing.

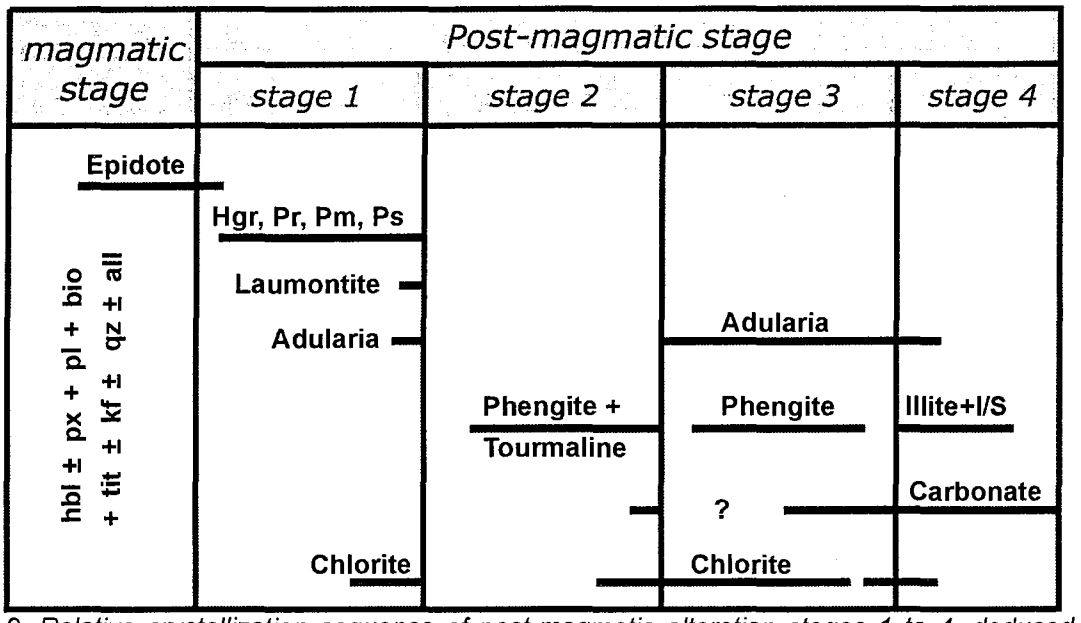

Fig. 1.2. Relative crystallization sequence of post-magmatic alteration stages 1 to 4, deduced from petrographic observations.
hbl – hornblende, px – pyroxene, pl – plagioclase, bio – biotite, tit – titanite, kf – K-feldspar, qz – quartz, all – allanite, hgr – hydrogarnet, pr – prehnite, pm – pumpellyite, ps – Fe-epidote.

1.3.2 Stage 2: Greisen assemblage

Some occurrences of greisen-like assemblages were found within the wall rock of quartz fractures. In general, the greisen zones are limited to about ten centimeters each side of the associated fracture. Greisen alteration is developed within the calc-alkaline plutonites, but also within the leucogranite. In the present study, chiefly greisen zones within the calc-alkaline rocks were treated for fluid inclusion studies.

The so-called greisen assemblage in the plutonic rocks is characterized by an almost complete pervasive replacement of the main rock forming minerals (feldspars, Fe-Mg silicates) by bulky sheets of white mica (mainly muscovite to phengite composition, Fig. 1.3.C). Always associated with white mica, newly formed quartz crystals mainly occur within fracture zones. Small needles of tourmaline are rarely found in some greisen samples, generally occurring in fracture zones associated with either quartz or white mica (Fig. 1.3.D). Euhedral pyrite may grow pervasively in white mica (± quartz) zones. Anhedral to sub-euhedral carbonate crystallized afterwards, both in fractures and pervasively. Rarely in some fractures, fluorite, cassiterite or molybdenite were observed. Chlorite is found in some instances in close association with muscovite, but can be considered as crystallized later on, as it frequently fills grain boundaries and vugs within the greisen.

1.3.3 Stage 3: Chlorite-phengite-dolomite±adularia assemblage

Intense pervasive alteration, post-dating the two first stages is by far predominant and concerns the most widespread occurrences of alteration phenomena. It is characterized by the following association: chlorite, phengite, dolomite, calcite, pyrite (or hematite). Alteration minerals are mostly found in close association with the primary minerals: i) hornblende is frequently altered to chlorite, calcite and hematite; ii) biotite is partially or totally replaced by chlorite (± K-feldspar (adularia), Fig. 1.3.E), which is frequently associated with anatase and hematite, carbonate may also occur locally parallel to the biotite cleavage; iii) Ca-plagioclase is replaced by calcite and phengite, K-feldspar is better preserved but display phengite patches; iv) titanite is replaced by anatase and carbonate. The whole mineral association can also be found in thin microfractures (less than 200 µm thick).

1.3.4 Stage 4: Dolomite-illite-chlorite assemblage

Locally, an illite (or ordered mixed layered illite/smectite with a high content in illite)–chlorite–dolomite mineral assemblage occurs. This kind of mineral association presents similarities with that of stage 3. But locally it is very well developed and replaces or invades all earlier alteration minerals (Fig. 1.3.F). Such minerals are locally found in macroscopic veins filled by the succession: chlorite–euhedral quartz–dolomite. This dolomite–illite–chlorite assemblage is indicative of lower temperature (association between low temperature epithermal type quartz combs and illite) as also reflected by the fluid inclusion data (see below).

1.3.5 Later stages

The Charroux-Civray area is subsequently affected by several fluid percolation stages, which are all characterized by low temperatures. On the basis of their fluid nature (basinal brines, Cathelineau et al. 1999, Boiron et al, submitted; diagenetic fluids), and K-Ar ages (on adularia, Cheilletz et al. 1997; on illites, Cathelineau et al., submitted), these later fluid circulations are considered as post-dating the uplift and Permian-Triassic erosion. These processes did not affect the studied samples and correspond to: i) a surficial alteration linked to erosion/oxidation and are localized at the top of the basement, around a few tens of meters below the palaeo-surface; ii) the filling of opened fractures by a quartz ±carbonate ±sulfates ±fluorite association due to basinal brines, during a stage at less posterior to Hettangian; or iii) the filling of a small number of microfractures by late calcite and kaolinite probably in relation with the latest fluid circulation during or after the Mesozoic marine sedimentary cover deposit.

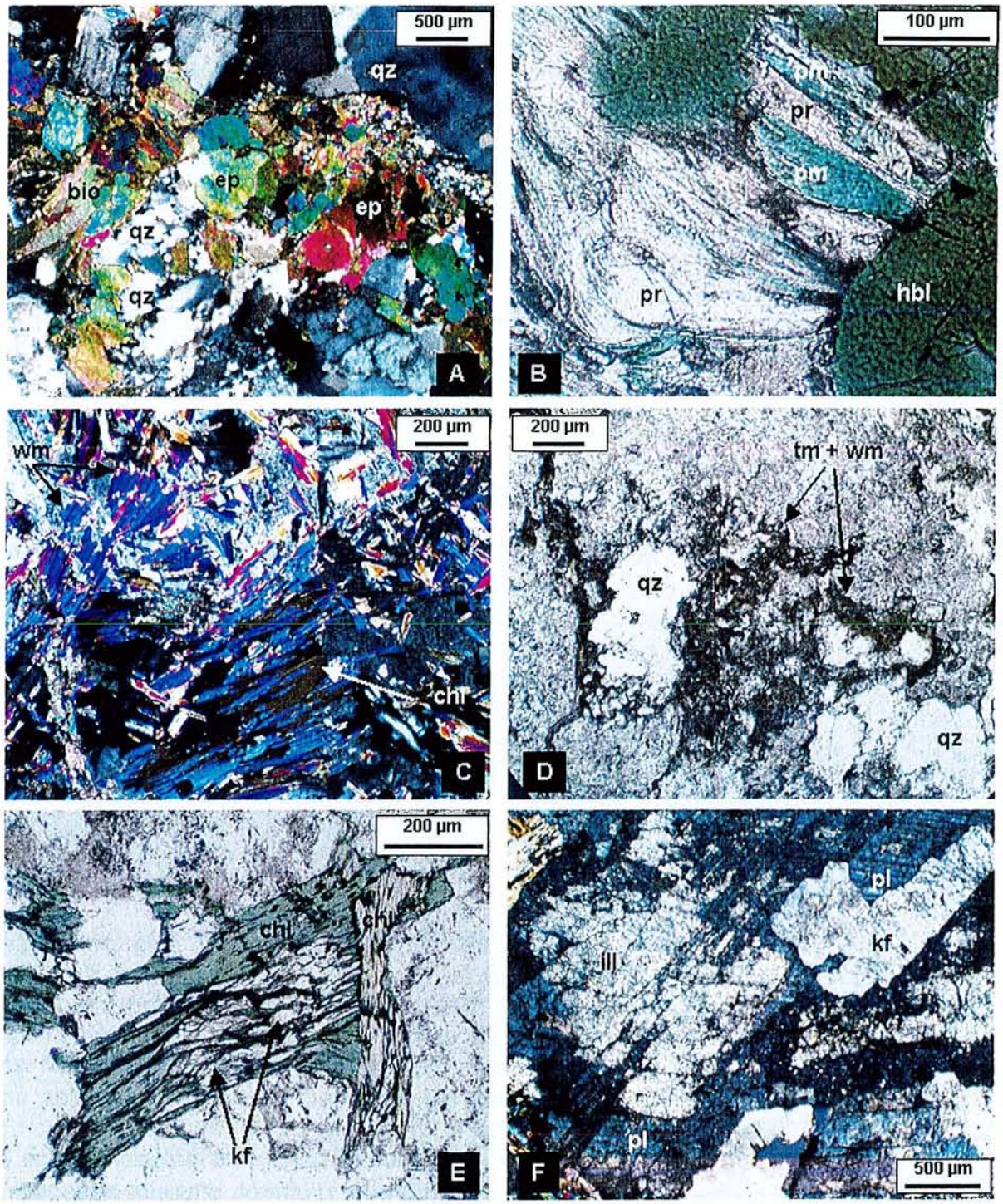

Fig. 1.3. Photomicrographs of typical alteration assemblages within the calc-alkaline plutonic rocks from Charroux-Civray. A: subsolidus epidote associated with quartz and biotite (stage 1); B: paragenesis of secondary prehnite and pumpellyite as replacement of biotite (stage 1); C,D: greisen assemblage including white mica sheets, tourmaline, chlorite and quartz (stage 2); E: chloritisation of biotite associated with K-feldspar lenses parallel to the former biotite cleavage (stage 3); F: pervasive alteration of feldspar to mainly illite (stage 4).
ep – epidote, bio – biotite, qz – quartz, pr – prehnite, pm – pumpellyite, hbl – hornblende, tm – tourmaline, wm – white mica, chl – chlorite, kf – K-feldspar, pl – plagioclase, ill – illite.

1.4 Fluid inclusion data

1.4.1 Analytical methods

P-T-V-X characterization of percolating fluids was obtained through a multidisciplinary study of fluid inclusions by techniques that included microthermometry and quantitative in-situ analysis of gases by Raman spectroscopy. Nomenclature of fluid inclusions follows the convention of Boiron et al. (1992) and is based on the type of total homogenization Th (L-V to the vapor noted V, L-V to the liquid noted L) and the presence of C-H-O-(N-S) species detectable by Raman spectroscopy (subscript c, when C-H-O-S species are dominant; c-w and w-c-n, when both water and CO_2 and/or N_2 species are present; and w when C-H-O-(N-S) species are not detected by any method).

Microthermometric studies of fluid inclusions were performed on wafers using a Chaixmeca heating-freezing stage (Poty et al. 1976). The stage was calibrated with melting-point standards at T > 25°C and with natural and synthetic fluid inclusions at T < 0°C. The rate of heating was monitored in order to obtain an accuracy of ± 0.2°C during freezing, ± 1°C when heating over the 25-400°C range and ± 4°C over the 400-600°C range.

Salinity, expressed as wt. % eq. NaCl, was calculated from microthermometric data using equations from Bodnar (1993). In volatile-bearing fluid inclusions, CO_2 was identified by melting of a solid below -56.6°C. The volumetric fraction of the aqueous liquid (flw) and the volumetric fraction of the volatile-rich liquid (CO_2 dominated liquid) in the volatile-rich phase (flc) have been estimated at room temperature by reference to the volumetric chart of Roedder (1984). Molar fractions of CO_2, CH_4, H_2S and N_2 were determined in individual fluid inclusions by micro-Raman analysis performed on a DILOR LABRAM Raman spectrometer at CREGU, Nancy. Bulk composition and molar volume were computed from P-T-V-X properties of individual inclusions in the C-O-H-S system (Dubessy 1984; Dubessy et al. 1989; Thiery et al. 1994, Bakker 1997).

The P-T properties were modelled using the V-X data and the equation of state from Bowers and Helgeson (1983) revised by Bakker (1999) for aqueous-carbonic fluid inclusions, and the data from Zhang and Frantz (1987) for aqueous fluids.

1.4.2 Location and typology of fluid inclusions

The calc-alkaline plutonic rocks from Charroux-Civray were repeatedly affected by pervasive fluid percolation as shown by the superimposed sets of FIP containing distinct fluid types, and the alteration of older alteration assemblages. Microfractures in quartz grains from calc-alkaline plutonic rocks appear as healed FIP and may bear all fluid types, even when alterations are not developed. This attests that fluids may have percolated within rocks with no significant effects on bulk mineralogy. In strongly altered zones, the abundance of FIP is such that the fluid inclusions can be related with a rather good confidence to the alteration facies.

The fluid inclusion study was carried out on primary inclusions in epidote, on secondary inclusions as FIP in quartz from the granitoids and on primary fluid inclusions within quartz and dolomite from fracture zones (Table 1.1). Eight types of fluids have been recognized from both petrographic observations and microthermometric measurements, of which the microthermometric results, including ranges and modes, are summarized in Table 1.2. Raman analyses carried out on representative fluid inclusions are given in Table 1.3.

Fluid inclusion type		Alteration mineralogy	Fluid composition	Sample no	Tm_{CO2}	$Th_{vol.\ phase}$	Tm_{cl}	Tm_{ice}	Th
stage 1									
Lw_I	primary FI in epidote FIP in quartz	Ca-Al silicates	H_2O-NaCl	4394				-6.6/-3.8	269/285(L)
Stage 2									
Lc(-w)	FIP in quartz	no alteration	CO_2-N_2	103A	-58.0/-57.0	-11.1/29.9 (L)			
Lc-w	FIP in quartz	muscovite chlorite	CO_2-N_2-H_2O-NaCl	1984, 6880, 8653, 8709	-58.6/-56.6	22.7/30.6 (L/C)	3.5/5	-12.2/-6.1	230/430(L)
Lw-c	FIP in quartz	muscovite chlorite	H_2O-CO_2-N_2-NaCl	5094, 5096, 8650	-58.5/-57.2		2.6/8.3	-7.6/-1.2	258/352(L)
Stage 3									
Lw-n	FIP in quartz	phengite chlorite	H_2O-N_2-CH_4-NaCl	1984, 8653				-5.1/-0.9	312/385(L)
Vn	FIP in quartz	phengite chlorite,	N_2-CH_4	4394, 8653		-149.2 /-145.1(V)			
Lw_{II}	FIP in quartz	phengite chlorite,	H_2O-NaCl	1984, 4394, 8649, 8650				-3.4/-0.5	368/393(L)/448(V)
Stage 4									
Lw_{III}	FIP in quartz	Illite chlorite carbonate	H_2O-NaCl	2420, 1610				-3.0/-0.5	170/340(L)
	primary FI in quartz and dolomite	chlorite quartz dolomite	H_2O-NaCl	6871				-3.2/-0.3	150/196(L)

Table 1.2. Ranges of microthermometric parameters of the fluids of alteration stages 1 to 4.

Tm_{CO2} – melting temperature of CO_2
$Th_{vol.\ phase}$ – homogenization temperature of the volatile phase
Tm_{cl} – melting temperature of clathrate
Tm_{ice} – melting temperature of ice
Th – total homogenization temperature
L – liquid, V – vapor, C – critic
all temperatures in °C

Type	Sample	Incl.	Microthermometry						Raman data			Calculated bulk composition				
			Tm_{CO2}	$Th_{vol.\ phase}$		Tm_{cl}	Tm_{ice}	Th	CO_2	CH_4	N_2	H_2O	CO_2	CH_4	N_2	NaCl
Lc-(w)	103A	16	-57.9	25.5	L				97.7	n.d.	2.3	15.6	82.5	0	1.9	
Lc-(w)	103A	1	-58.0	15.4	L				96.9	n.d.	3.1	13.7	83.5	0	2.8	
Lc-(w)	103A	8	-58.0	-11.2	L				97.7	n.d.	2.3	11.5	86.5	0	2.0	
Lc-(w)	103A	5	-57.1	27.7	L				100	n.d.	n.d.	15.4	84.6	0	0	
Lc-(w)	103A	10	-57.0	29.9	L				100	n.d.	n.d.	16.2	83.8	0	0	
Lc-w	8653	4b	-57.8	29.5	L	2.2	-8.6	>430	96.9	n.d.	3.1	41.0	55.4	0	1.7	1.9
Lc-w	8653	2cc	-57.3	22.7	L	2.0	-12.0		100	n.d.	n.d.	23.6	75.4	0	0	1.0
Lc-w	8653	2aa	-57.5	26.6	L	2.0	-12.2		100	n.d.	n.d.	24.8	74.1	0	0	1.1
Lc-w	1984	2d	-57.8	29.6	L	3.6	-6.1	>420	97.0	n.d.	3.0	55.3	41.6	0	0.8	2.3
Lc-w	6880	14	-58.6	25.7	L	-1.1		decr.	96.7	n.d.	3.3	81.5	13.2	0	0.4	4.9
Lc-w	6880	16	-58.6	25.5	L	-3.5		385	96.2	0.3	2.5	75.0	19.1	0.1	0.4	5.4
Lc-w	6880	12	-58.6	25.9	L	-2.3		362	93.4	n.d.	6.6	81.1	12.7	0	0.8	5.4
Lc-w	6880	19	-58.2	24.9	L	-1.5		decr.	95.1	0.2	4.7	80.3	14.0	0.05	0.6	5.05
Lc-w	8709	2	-56.6	29.4	C	0.3		296	97.8	n.d.	2.2	85.8	9.0	0	0.2	5.0
Lc-w	8709	3a		29.5	C	0.4		346	97.7	n.d.	2.3	79.3	16.2	0	0.3	4.2
Lc-w	8709	3b		29.4	C	0.5			97.0	n.d.	3.0	83.6	11.7	0	0.3	4.4
Lw-c	5096	3-1a	-58.1			8.1	-4.1	282	100	n.d.	n.d.	94.2	4.8	0	0	1.0
Lw-c	5096	3-2a				7.7	-4.5	263	79.0	n.d.	21.0	93.7	4.6	0	0.6	1.1
Lw-c	5096	2a	-58.5			8.0	-4.9	336	100	n.d.	n.d.	92.9	5.9	0	0	1.2
Lw-c	5094	4c	-58.3			7.3	-3.6	348	94.0	n.d.	6.0	94.0	5.0	0	0.2	0.8
Lw-c	5094	2j	-57.7			7.8	-4.6		92.7	n.d.	7.3	91.9	6.9	0	0.3	0.9
Lw-c	8650	1a	-58.0			5.4	-7.6	346.5	96.3	n.d.	3.7	93.2	4.3	0	0.1	2.4
Vn	8653	5c		-149.0	V				n.d.	0.8	99.2	25.8	0	0.6	73.6	
Vn	8653	3b-b		-145.1	V				n.d.	2.7	97.3	26.0	0	2.0	72.0	
Vn	4394	3c		-149.2	V				n.d.	n.d.	100	25.8	0	0	74.2	
Lw-n	8653	1b					-0.9	380	n.d.	n.d.	100	86.9	0	0	13.1	
Lw-n	1984	1a					-5.1	318	n.d.	n.d.	100	93.9	0	0	6.1	

Table 1.3. Summary of microthermometry and Raman microspectroscopy data with calculated global composition (in mol.%) of different fluid inclusion types.
Tm_{CO2} – melting temperature of CO_2
$Th_{vol.\ phase}$ – homogenization temperature of the volatile phase
Tm_{cl} – melting temperature of clathrate
Tm_{ice} – melting temperature of ice
Th – total homogenization temperature
(>430 = decrepitated at 430°C)
n.d. – not detected
decr. – decrepitated
L – liquid, V – vapor, C – critic
all temperatures in °C

Based on microthermometric data and Raman microspectroscopy, the fluids from the Charroux-Civray samples may be classified into three compositional groups: (i) carbonic (L+L+V and L+V) fluids, (ii) aqueous (L+V) fluids, and (iii) nitrogen-bearing (L+V and V) fluids. Raman spectroscopy shows that the vapor composition varies between H_2O and CO_2 and H_2O and N_2 end-members. Almost no methane was detected. Bulk compositions of the different fluids have been plotted in a ternary diagram H_2O–CO_2–10(CH_4+N_2) (Fig. 1.4), in which the two compositional trends are observable.

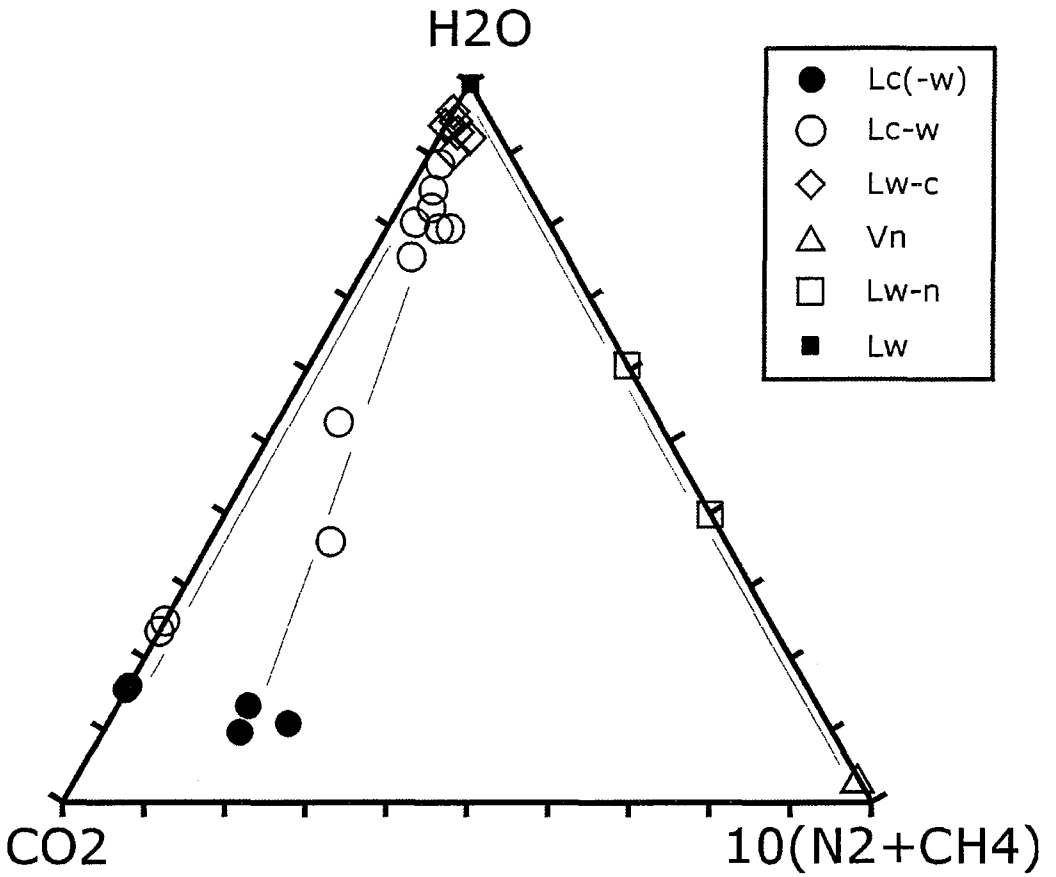

Fig. 1.4. Ternary diagram H_2O–CO_2–$10(CH_4+N_2)$ showing the bulk composition of all investigated fluid inclusion types. Note the two distinct correlation trends between carbonic and aqueous and nitrogen and aqueous inclusions, respectively.

1.4.3 Relationships with alteration types

Some relationships between alteration type and fluid composition might be considered. In exceptional cases, fluids are strictly related to the alteration facies. They are found i) in primary inclusions in epidote (Lw_I), ii) in primary or pseudo-primary inclusions in quartz of fractures with associated greisen type alteration (sample 5094 and 5096), which contain dominantly carbonic fluids (Lc(-w), Lc-w, Lw-c), and iii) in dolomite-quartz from stage 4 veins in primary inclusions(Lw_{III}).

Secondary carbonic fluid inclusions are most frequent in samples showing greisen type alteration. Aqueous fluid inclusions (Lw_I) are more common in the FIP from the almost unaltered samples 1984 and 4394, which show only Ca-Al silicate new formation. Lw_{II} and Lw_{III}, Lw-n and Vn inclusions were mainly found in samples presenting late pervasive alteration features (stage 3).

1.4.4 Aqueous-carbonic fluid inclusions Lc(-w) and Lc-w

Aqueous-carbonic fluid inclusions occur as secondary fluid inclusions in quartz from the granite (healed microfissures). The Lc-w type inclusions occur mostly in groups of

several similar inclusions, only rarely in better-defined FIP. Aqueous carbonic inclusions are abundant in some samples (mainly greisen samples), but are not homogeneously distributed. The inclusions vary in size from a few micrometers up to 15 µm. At room temperature, two groups of carbonic inclusions could be distinguished on the basis of the volumetric fraction of the aqueous liquid (flw). In Lc-w inclusions water content varies in a range of 50 to 70 % (Fig. 1.5.B). Although liquid water may be present as a thin film wetting the walls of the Lc(-w) inclusions, it is almost invisible at ambient conditions due to insufficient separation power of microscope. However, as a volume of about 5 % of liquid water film could be observable at room temperature in rather large inclusions (above 10 µm), the maximum range of water content of these inclusions should be comprised between 10 to 20 mole %, this constraining the bulk fluid composition (Table 1.3). However, microthermometric parameters are very similar for the two groups of inclusions (Table 1.3). The melting temperature of CO_2 (Tm_{CO2}) ranges from -58.6°C to -56.6°C. The homogenization of the volatile phase (Th_{CO2}) occurs to the liquid (or to the critic) phase from -11.2°C to +30.6°C, but most of the data are within +15°C to +30°C temperature range. The highest density could reflect the highest pressure recorded by Lc-w inclusions as non geological processes can easily form high density fluids by post-trapping changes. The clathrate melting temperature (Tm_{cl}) is observed between +3.5°C and +5°C. The ice melting temperature (Tm_{ice}) ranges from -12.2°C to -6.1 °C. Minimum trapping temperatures (Th) have been recorded in the large range of 230°C to 430°C (Fig. 1.5.A). The Raman analyses show that CO_2 is always higher than 93 mol.% up to 100 mol.% in the volatile phase. The CH_4 content, when measured, is very low and ranges from 0.2 to 0.3 mol.%. N_2 ranges from 2.2 to 6.6 mol.%. Lc-w aqueous-carbonic fluids are characterized by a H_2O content in the range of 12 to 86 mol.%, a CO_2 content between 9 and 86 mol.% and a very low content of CH_4 and N_2(<0.1 and 2.8 mol.% respectively) (Table 1.3).

1.4.5 Aqueous-carbonic fluid inclusions Lw-c

H_2O-CO_2-N_2-NaCl fluid inclusions are observed as FIP in quartz grains from the granite. These aqueous-carbonic inclusions are the most abundant type of inclusions within the studied samples. This Lw-c fluid (Fig. 1.5.C) generally occurs in distinct FIP and only very rarely as isolated groups. Inclusions show 20 to 50 vol.% vapor phase and contain partly small, elongated solids (mica?) within their aqueous phase.

These fluid inclusions vary in size from smaller than 1 µm up to 8 µm. Tm_{CO2} ranges from -58.5°C to -57.2°C, Tm_{cl} varies from +2.6°C to +8.1°C, Tm_{ice} from -7.6°C to -1.2°C, and Th is in the range of 258°C to 352°C (Table 1.2). The volatile phase is dominated by CO_2 (79 to 100 mol.%), and N_2 (0 to 21 mol.%). CH_4 has not been detected. Lw-c fluids are thus dominated by H_2O, whose content ranges from 92 to 94 mol.%, whereas CO_2 varies from 4 to 7 mol.%. N_2 content is low, less than 0.5 mol.%. Vn inclusions are dominated by N_2 (72 to 75 mol.%) and water content is around 25 mol.%. CH_4 content could reach 2 mol.%.

1.4.6 Nitrogen vapor inclusions Vn

Vapor inclusions are observed as planes of FIP in granite and have a size up to 15 µm. In such inclusions, water is not visible under the microscope (Fig. 1.5.E). An assumption of 5 % in volume in water has been taken into account for the calculation of bulk composition. Only homogenization of the volatile phase could be observed and ranges from -145.1° to -149.2°C (to the vapor phase, Table 1.2). Raman analyses show that N_2 ranges from 97 to 100 mol.%. In some inclusions, CH_4 has been detected and could reach 2.7 mol.%.

1.4.7 Water-nitrogen liquid inclusions Lw-n

H_2O-N_2-NaCl inclusions have been observed as FIP in granite. Inclusions of this type are not very abundant and mostly small (< 10 µm; Fig. 1.5.D), they reach only rarely a size up to 15 µm. Tm_{ice} ranges from -5.1°C to -0.9°C, and Th varies from 312°C to 385°C (Table 1.2). N_2 has been detected by Raman spectroscopy and is the only gas in the vapor phase. Lw-n inclusions are dominated by H_2O (87 to 94 mol.%) and N_2 remains in the range of 6 to 13 mol.%.

1.4.8 Aqueous fluids Lw

Earliest aqueous fluids Lw_I and Lw_{II} occur as isolated primary fluid inclusions in epidote, and secondary inclusions in quartz respectively. They are generally small and do not exceed 10 µm (Fig. 1.5.F), flw varies from 0.7 to 0.9. Aqueous inclusions in epidote (Lw_I) are characterized by Tm_{ice} ranging from -6.6°C to -3.9°C corresponding to salinities of 6.3 to 10 wt.% NaCl eq. Th(L) is ranging from 269°C to 285°C. Aqueous inclusions Lw_{II} are characterized by Tm_{ice} ranging from -4°C to -0.5°C corresponding to salinities of 1 to 6.4 wt.% NaCl eq. Th(L) is in the range of 368°C to 393°C (Table 1.2).

Lw_{III} fluids were mostly studied in FIP, with the exception of one sample of a fracture filled by quartz and dolomite (stage 4). All fluid inclusions display Tm_{ice} ranging from -3.2° to -0.3°C, corresponding to salinities of 0.5 to 5.3 wt.% NaCl eq. Th (L) is in the range of 170°C to 340°C (Table 1.2) in FIP and 150°C to 196°C in quartz and dolomite of the fracture.

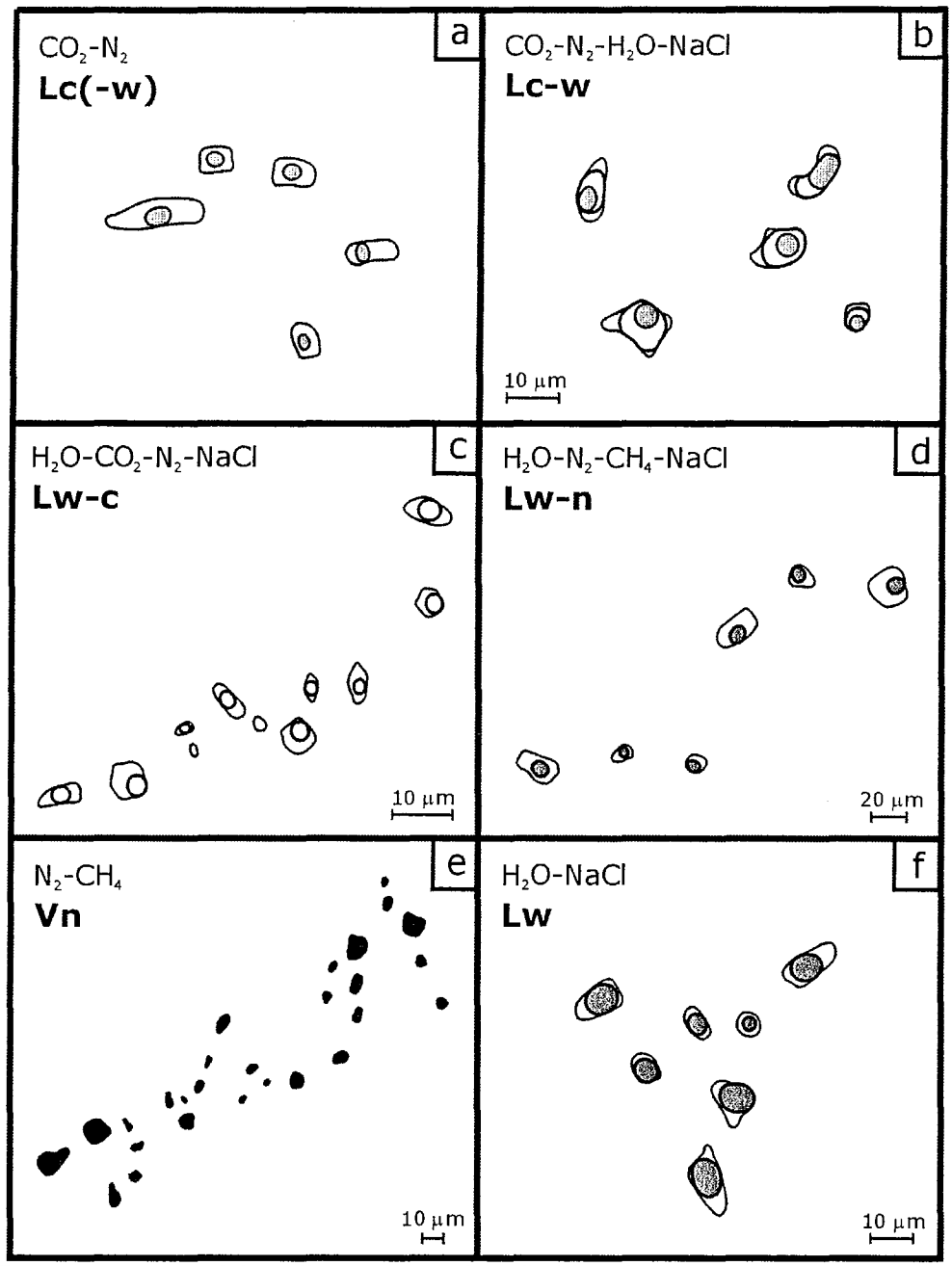

Fig. 1.5. Typical examples of the different types of studied fluid inclusions. Carbonic fluids occur as 3- or 2-phase inclusions (a, b, c), nitrogen-bearing fluids as 2- and 1-phase inclusions (d, e) and aqueous fluids as 2-phase inclusions (f).

1.5 Oxygen isotope data

Oxygen isotope analyses on quartz samples from fracture zones were carried out at the department of Geoscience at Rennes University. Conventional measurement technique based on improved method of fluorination developed by Clayton & Mayeda (1963) has been used for oxygen isotope analysis. Quartz samples have been separated using dental drill when it was necessary, either from whole rocks or directly sampled on polished wafers used for fluid inclusion studies. Quartz samples were finely crushed and then about 6 or 7 mg of quartz powder were reacted with BrF_5 during 12 hours at 650°C. After reaction, oxygen produced is combined with carbon from heated graphite bar to produce CO_2 gas analyzable using a VG SIRA 10 mass

spectrometer. Results are expressed using internal silicate standards and NBS28 reference material with the conventional $\delta^{18}O$ notation vs. SMOW. The precision established on duplication of samples is generally better than 0.10 ‰.

Oxygen isotopes values of quartz range from 8.4 to 12.5 ‰ $\delta^{18}O$ (Table 1.4). Analysed quartz either hosts Lc-w inclusions or is affected by later Lw FIP. $\delta^{18}O$ values of quartz are not typical of a particular stage of the P-T-X fluid evolution, because all studied quartz crystallized early at temperatures around 400 – 450°C (except for sample 6871, which corresponds to a low temperature hydrothermal quartz, see below) and are crosscut by Lc-w fluids and by all later Lw FIP.

Sample no	$\delta^{18}O$	±	T (°C)	$\delta^{18}O_{fluid}$
6880	9.52	0.08	450	5.4
8709	8.40	0.10	450	4.3
2420	8.36	0.03	450	4.2
1610	11.56	0.07	450	7.5
6871	12.49	0.11	200/250	0.2/2.9

Table 1.4. Oxygen isotope data of quartz fracture samples and calculated $\delta^{18}O$ of the associated fluid. $\delta^{18}O_{fluid}$ values were calculated considering quartz-water isotopic fractionation factors of Zheng (1993) and using estimated temperature of formation of quartz as indicated.
For further sample description see Table 1.1.

Water isotopic composition is calculated considering quartz-water isotopic fractionation factors of Zheng (1993) and using estimated temperature of formation of quartz. $\delta^{18}O$ values for fluids are thus in the order of 4 to 7.5 ‰ (Table 1.4). These $\delta^{18}O_{fluid}$ values are typical of primary igneous and/or metamorphic waters defined by Sheppard (1986), or fluids having deeply interacted with the crystalline basement at high temperature.

The late quartz 6871 is an exception, as it crystallized at much lower temperature (200-250°C, if a reasonable, not higher pressure than of the preceding stages is used for P-correction of the measured Th). Related fluids are probably more superficial waters with $\delta^{18}O_{fluid}$ = 0.2 to 3 ‰ (at 200-250°C). This may indicate the invading of fluids from the previous deep reservoir, when the structural level is sufficiently shallow to allow fluid circulation at significantly decreased temperatures.

1.6 Reconstruction of the P-T-X evolution

A reconstruction of the P-T changes has been carried out based on calculated fluid inclusion isochores for each fluid inclusion generation and on the consideration of the mineral assemblages. Calculated isochores of the investigated fluids from different stages are shown in Fig. 1.6. The proposed P-T path for the early post-magmatic evolution is presented in Fig. 1.7.

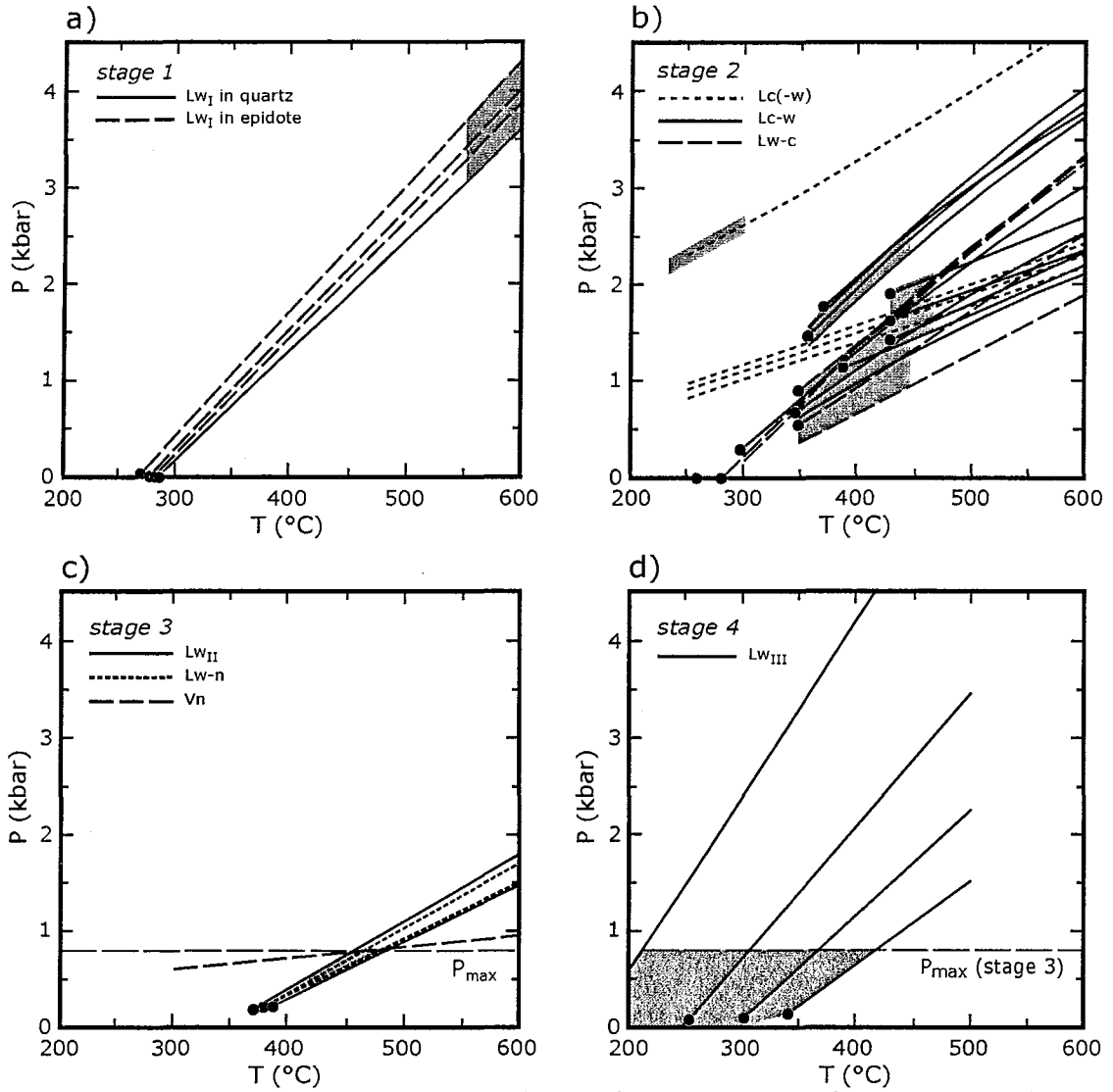

Fig. 1.6. P-T diagrams showing calculated isochores of the investigated fluid inclusions. Grey fields indicate the assumed P-T ranges during fluid trapping. a) primary aqueous FI in epidote and secondary aqueous FI in quartz of stage 1, b) secondary carbonic FI of different densities in quartz (stage 2), c) nitrogen-bearing liquid and vapor FI (stage 3), d) secondary aqueous FI of stage 4 in quartz

1.6.1 Stage 1: Aqueous fluids Lw_I

The late-Hercynian post-magmatic evolution starts with subsolidus epidote, whose primary fluid inclusions show homogenization temperatures around 270 to 280°C (Th (L)), the calculated isochores (Fig. 1.6.a) have a steep slope and reach up to 4 kbar at 600°C. This indicates relatively high pressure during the subsolidus stage (Fig. 1.7). Some aqueous inclusions of FIP within quartz present similar characteristics as the inclusions in epidote. These aqueous inclusions are presumably also correlated with the formation of Ca-Al silicates during a very early post-magmatic step (stage 1). This early subsolidus P-T range is in good accordance with the occurrence of magmatic epidote and the results of hornblende barometry for the late-magmatic stage in the Charroux-Civray area (Cuney et al. 1999).

The following period of the early postmagmatic stage is characterized by the retrograde crystallization of Ca-Al silicates like hydrogarnet, prehnite, pumpellyite, pistacite and laumontite during progressive cooling of the plutonic complex (Freiberger et al. in press). They occur as lenses within unaltered to partly altered biotite. The development of the common paragenesis prehnite + pumpellyite indicates a rather narrow temperature range of 200 to 280°C and pressures of 2 to 3 kbar (Frey et al. 1991, Fig. 1.7).

1.6.2 Stage 2: Carbonic fluids Lc(-w), Lc-w and Lw-c

Postdating the Ca-Al silicate formation, a greisen type alteration (white mica, chlorite, pyrite, tourmaline, etc.) within the calc-alkaline plutonites is restricted to very well defined zones, exclusively in the vicinity of fractures. Associated CO_2-bearing fluids can be divided into almost pure CO_2 inclusions Lc(-w), 3-phase carbonic inclusions Lc-w with relatively high density and less dense 2-phase aqueous-carbonic inclusions Lw-c (Fig. 1.6.b). They all show Th of more than 250°C up to more than 400°C and show isochores that are concentrated within the 1 to 2 kbar pressure range. Only one Lc(-w) inclusion shows a higher density that is more compatible with high pressure (above 2 kbar). The temperature was at least around 350 to 400°C (around or slightly above the maximal Th) and maximal around 450°C (Fig. 1.7), as no biotite but chlorite is stable in the vicinity. These temperatures are in good accordance with those generally assumed for greisen mineralisation (e.g. Lehmann, 1990). Petrographic chronology in addition to the generally higher homogenization temperatures of Lc-w type inclusions argue for Lc-w inclusions possibly predating Lw-c trapping. Starting with circulation of fluids of the Lc-w type, with decreasing temperature and decreasing pressure, the fluids get less dense and richer in water. In this later stage Lw-c inclusions are formed (Fig. 1.7). Some isolated very dense Lc(-w) inclusions were probably formed at the beginning of carbonic fluid circulation under still lower temperature but slightly higher pressure than later Lc-w inclusions.

1.6.3 Stage 3: Nitrogen and aqueous fluids Lw-n, Vn and Lw

Pervasive multiphase hydrothermal alteration occurred after greisen formation. Aqueous and vapor N_2-bearing fluid inclusions may be correlated with this alteration stage 3.

- Nitrogen fluids Lw-n and Vn

Nitrogen fluids occur either as 2-phase aqueous inclusions with relatively low salinity and with high homogenization temperature around 380°C or as monophase vapor inclusions (Fig. 1.6.c). Assuming that all N_2-bearing inclusion types (liquid or vapor) are nearly coeval, the pressure range can be restricted to be <1 kbar at 450 to 500°C (intersection of isochores). Because of their high homogenization temperature, but at rather flat isochores at low pressure, these fluid inclusions may indicate a relatively fast pressure decrease after the greisen alteration stage (Fig. 1.7). Therefore, the Lw-n and Vn inclusions are probably related to high-temperature hydrothermal alteration, postdating the carbonic fluid event under already lower pressure. These fluids may

be associated with the alteration of primary rock forming minerals as well as the alteration of Ca-Al silicates (stage 3). Results of chlorite thermometry (Cathelineau 1988) show a large range from ~ 400 to 220°C, which may reflect the progressive temperature decrease in the course of the pervasive alteration stage.

- Aqueous fluids LwII

Secondary aqueous fluid inclusions within quartz (Lw_{II}) (Fig. 1.6.c) present higher homogenization temperatures (around 380°C), but distinctly less steep isochores than Lw_I inclusions attributed to Ca-Al silicate formation. Furthermore, aqueous Lw_{II} inclusions have distinctly lower salinities than Lw_I inclusions. Both, different Th and salinity indicate the dissimilar origin of Lw_I and Lw_{II}. The inclusions of Lw_{II} type may be correlated with inclusions containing N_2 in their vapor phase (Lw-n, Vn, Fig. 1.7) and therefore they are attributed to the alteration stage 3.

1.6.4 Stage 4: Aqueous fluids Lw_{III}

Pervasive carbonatisation and argilitisation of the whole rock is associated with formation of dolomite-quartz veins. Aqueous fluids found in FIP or as primary inclusions from macroscopic dolomite-quartz veins show rather low homogenization temperatures from 130 up to 250°C (Fig. 1.6.d). At the pressure range that is constrained by the estimated pressures for the preceding stages, trapping temperatures must be at most 30°C higher than Th. This implies a significant cooling of the plutonites, down to 200°C after stage 3 (Fig. 1.7). The P-T path intersects then the thermal gradients typical of the upper crust, indicative of the progressive decrease of the thermal effects linked to the late magmatism.

1.7 Discussion and concluding remarks

The petrographic study of alteration sequences and their associated fluid inclusions in microfissures of the plutonic rocks as well as in the mineral fillings of the veins, yield to a reconstruction of the P-T-X evolution of the Charroux-Civray Hercynian basement since the crystallization of the main calc-alkaline plutonic bodies. This reconstruction covers the uplift of the basement up to its outcropping and the subsequent burial by Mesozoic sediments. Fluid inclusions can be considered as the most sensitive markers of the fluid migration at several scales, and they are much more discriminative than mineral assemblages by themselves.

Cooling of the calc-alkaline plutonic series starts at solidus temperatures at about 4 kbar as indicated by magmatic epidote stability, hornblende barometry and fluid inclusion data. Cooling continues under slightly decreasing pressure during uplift down to 2 to 3 kbar at 200 to 280°C (prehnite – pumpellyite paragenesis, Fig. 1.7).

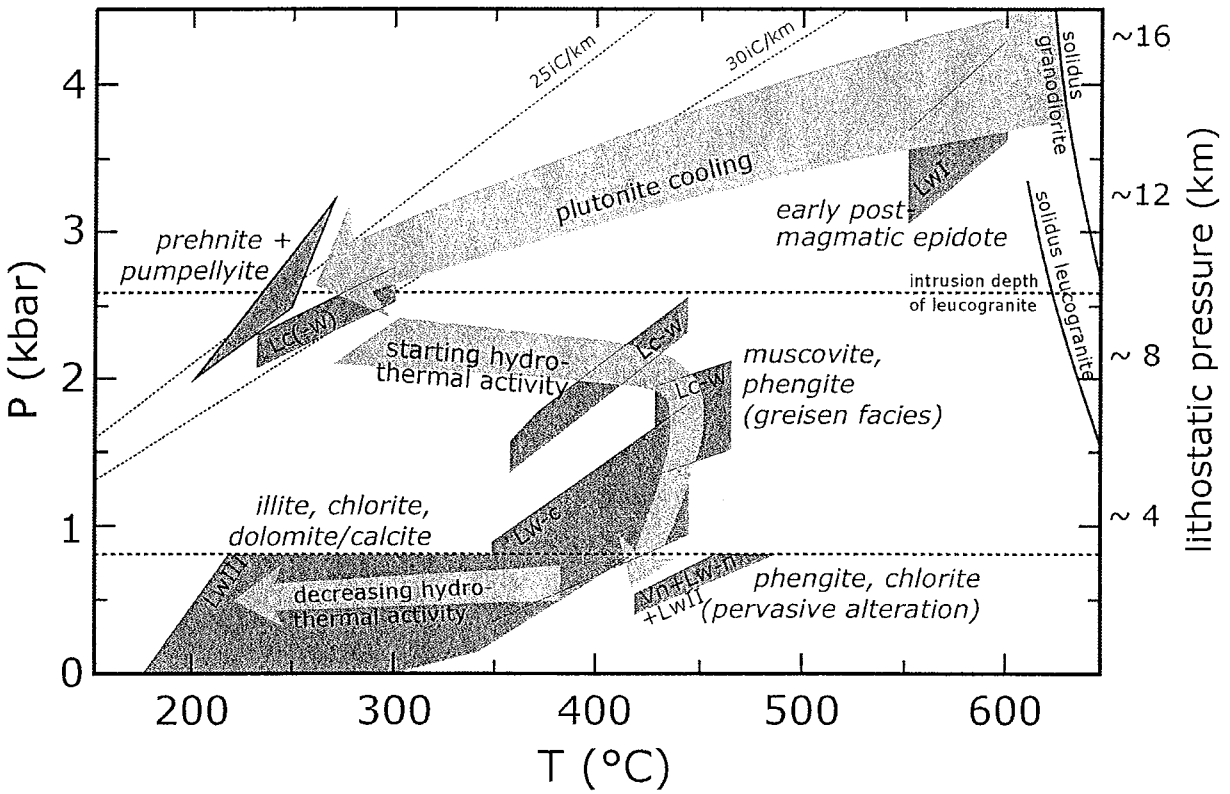

Fig. 1.7. P-T diagram showing the stability ranges of the different alteration assemblages, determined through fluid inclusion studies and paragenetical implications. Dark grey fields show the assumed P-T ranges during trapping of the different fluids as revealed in Fig. 1.6. Light grey arrows indicate the deduced P-T evolution within the calc-alkaline plutonic complex during post-magmatic stages. Stippled horizontal lines indicate pressure within the calc-alkaline complex: 1) during leucogranite intrusion, 2) during later fluid convection, derived from fluid inclusion isochores (see Fig. 1.6.c, d). The cooling path from the subsolidus stage at around 600°C down to about 250°C is taken from Freiberger et al. (in press), the P-T field of prehnite–pumpellyite paragenesis is from Frey et al. (1991).

Thus, after cooling down to about 250°C, a hot geothermal circulation within the calc-alkaline rocks was induced and leads to the formation of greisen-like mineralizations in the vicinity of fractures. When greisen-forming fluid circulation starts, some very dense Lc(-w) inclusions were trapped around 300°C and 2.5 kbar (Fig. 1.7). However, the main stage of greisen formation is marked by the percolation of hotter aqueous carbonic fluids, characterized by high temperatures at a relatively high structural level. During this stage, temperatures around 400 to 450°C are rather high for the inferred depths (1 to 2 kbar). This implies abnormal heat flows and thermal gradients of around 60 to 80°C/km, if fluid temperatures are considered to be representative of the temperature within the host formations. Different possibilities for such abnormal hot fluid flows have to be considered: i) quick uplift may cause the exhumation of large crustal blocks at a speed sufficient to keep high temperatures adiabatic uplift at shallow levels (2-5 km), ii) delamination of the crust and production of deep seated water in anatectic zones, ascending and yielding to subsequent heating of fractured blocks, or iii) localized heat flows linked to series of intrusions. The latter process being likely to occur in the northern Limousin granite, as shown by the St. Sylvestre episyenite alteration (305 Ma, Scaillet et al. 1996) at about 350°C and pressures below 0.5 kbar (Lespinasse & Cathelineau 1990, André et al. 1999).

As most fluids were trapped in thin micro-fissures in rocks, fluids are likely to be in thermal equilibrium with their host rocks. This means that, either extended rock

S.C.D. - U.H.P. NANCY 1
BIBLIOTHÈQUE DES SCIENCES
Rue du Jardin Botanique - BP 11
54601 VILLERS-LES-NANCY Cédex

volumes were percolated by hot fluids in the vicinity of open fracture systems, or the whole mass of the plutonic complex was at the same temperature as the circulating fluids. Such conditions are typically those observed to the proximity of some geothermal field (e.g. Larderello, Cathelineau et al. 1994, or Geyser) related to concealed granite intrusions. Therefore, the hot fluid circulation in the Charroux-Civray area may be attributed to the intrusion of a slightly younger leucogranite body (or a set of small leucogranite intrusions), which is known from the CHA 109 drilling and is inferred in its concealed dimensions from geophysical investigations (Virlogeux et al. 1999). In northern Limousin, most peraluminous granites emplaced around 325 ± 10 Ma (Turpin et al. 1990), a part of them at a shallower structural level than the calc-alkaline suites.

As uplift continues, greisen mineralization is subsequently affected by the chlorite–phengite/illite assemblage correlated with aqueous and nitrogen-bearing fluid circulations in the P-T range of <1 kbar and 400 to 450°C. Several possible scenarios may account for this decreasing pressure at almost constant temperature, of which two extremes are outlined here: i) rapidly decreasing pressure is caused by fast uplift during only very slight cooling of the plutonic complex, or ii) a persistent hot fluid percolation with progressive changing fluid composition (from aqueous-carbonic to aqueous-nitrogen fluids) during continuing uplift with rates similar to the previous stages. $\delta^{18}O$ values for fluids of this alteration stage are close to those of metamorphic waters defined by Sheppard (1986), or close to fluids having deeply interacted with the crystalline basement at high temperature.

In a later stage continuously decrease of temperature with nearly constant pressure leads to alterations of the illite–chlorite–dolomite type in the temperature range of 250°C down to 130°C. O-isotope data imply circulation of more superficial waters ($\delta^{18}O_{fluid}$ = 0.2 – 3 ‰) during these later alteration stages.

No evidence of fluids related to post-Triassic stages was found from fluid inclusion studies of rocks and early fracture fillings. Since no late fluids are trapped as fluid inclusions in microfractures, this may indicate the lack of significant pervasive fluid circulation since the Mesozoic.

The duration of each observed thermal (alteration) stage is difficult to evaluate, but our study confirms the relative space-time relationships between the main fluid percolation stages and late Hercynian heat flows. The hypotheses of the existence of large peraluminous plutons at depth based on geophysical considerations, or the existence of a succession of smaller pluton intrusions leads to the assumption that localized heat flows linked to concealed leucogranite intrusion(s) is likely to occur in the Charroux-Civray area.

Possible temperature–time relation is sketched in Fig. 1.8. Considered are intrusions of the calc-alkaline plutonic complex, followed by the intrusion of a peraluminous leucogranite causing hydrothermal fluid circulation within the calc-alkaline plutonic complex. The thermal effect of a magmatic intrusion is generally short in time as a pluton cool down to the thermal equilibrium with its environment in less than a few million years. However, abnormal heat flows or further thermal processes may characterize the upper crust during its uplift.

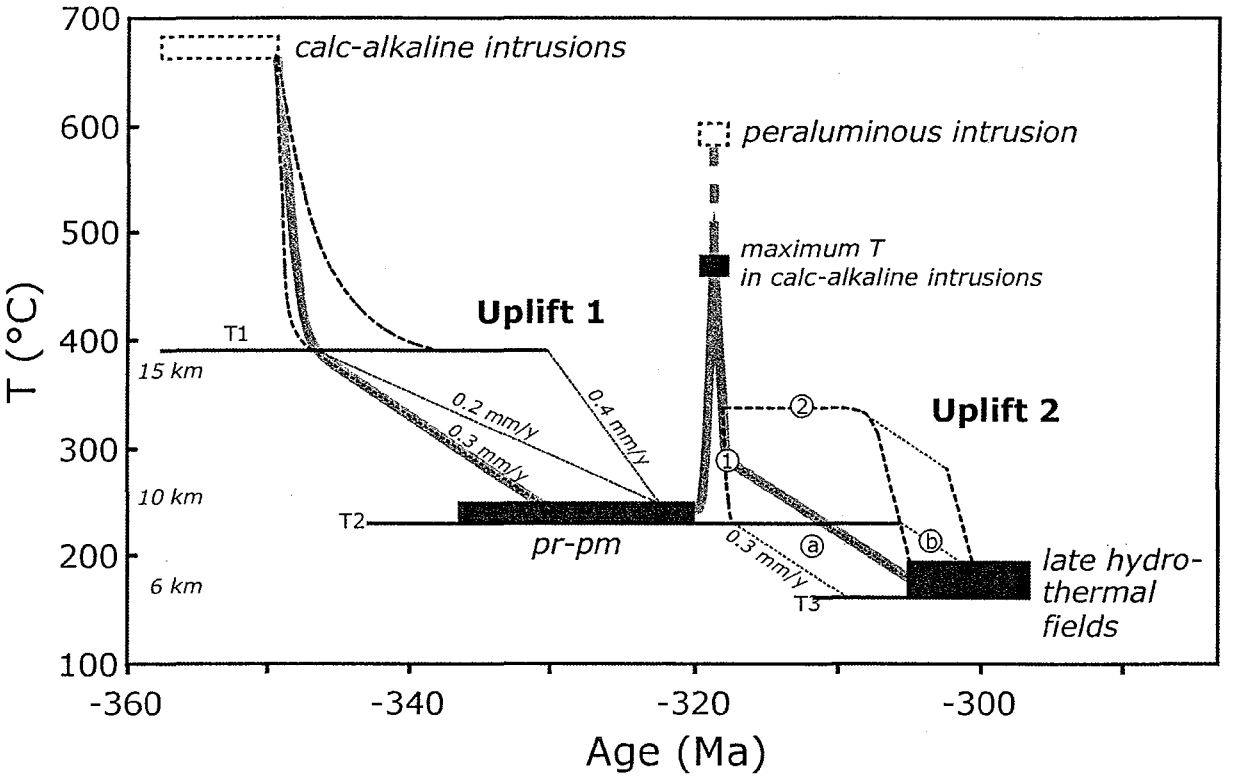

Fig. 1.8. Summary of possible T-t paths for the post-magmatic evolution of the Charroux-Civray area, based on the constraints issued from fluid inclusion studies and the consideration of two main magmatic stages. The grey line marks one probable T-t path. Indicated depths are assumed with crustal temperatures of 25 to 30°C/km. T1 to T3 are temperatures within the unaffected basement during calc-alkaline intrusions (T1), during post-magmatic times of prehnite–pumpellyite formation (T2), and during late hydrothermal circulation (T3).
For detailed discussion see text.

The T-t evolution may be outlined as follows (Fig. 1.8). After intrusion of the calc-alkaline plutonites at around 350 Ma, the complex cools down rapidly, until it reaches thermal equilibrium with its metamorphic environment (~ 380°C, according to geothermal gradients). Then, T continues to decrease according to the uplift of the chain (0.2, 0.3 or 0.4 mm per year) down to about 250°C (prehnite–pumpellyite). At around 320 Ma leucogranite intrusion and associated hot fluid percolation leads to a drastic T increase (up to at least 450°C), followed by rapid T decrease during cooling of the peraluminous mass. Post-leucogranite evolution may best described with two extremes (labelled 1 and 2 in Fig. 1.8). Path 1 represents continuing cooling of the leucogranite down to the temperature of the environment (~ 250–300°C, path 1a, Fig. 1.8), followed by decreasing T according to an uplift rate of ~ 0.3 mm per year. Another possible path (1b) is the fast cooling of the leucogranite down to 250°C, then holding T at this temperature for some million years before continuing the uplift. Path 2 considers a persistent hot fluid circulation (~ 350°C) some million years after the leucogranite intrusion. With expiring hydrothermal activity T decreases rapidly with a rate that results of a combination of uplift and dying heat flow during subsequently cooling of the plutonic mass. Reflecting all mineralogical and fluid inclusion evidences of this study, the preferred T-t path for the Charroux-Civray retrograde evolution may be outlined as marked by the grey line in Fig. 1.8.

ACKNOWLEDGMENTS

This work has been initiated within the framework of contracts commissioned by Andra (Agence Nationale pour la Gestion des Déchets Radioactifs). The study has been then supported by GdR FORPRO – Action 98-III (contribution paper FORPRO No 2001/08 A), a National Research Program between CNRS and Andra (French Nuclear Waste Management Company). Andra is acknowledged for the facilities and permission of sampling the drill cores. R. Freiberger's stay in Nancy was supported by a grant from DAAD. S. Buschaert benefits of a grant from Andra for completion of his PhD.

REFERENCES

Alexandrov P, 2000. Geochronologie U-Pb et 40Ar/39Ar de deux segments de la chaine varisque: le Haut Limousin et les Pyrénées orientales. Unpubl. PhD thesis, Nancy, 186p.

André AS, Lespinasse M, Cathelineau M, Boiron MC, Cuney M, Leroy JL, 1999. Percolation de fluides tardi-hercyniens dans le granite de Saint Sylvestre (Nord-Ouest du Massif Central Français): données des inclusions fluides sur un profil Razès-Saint-Pardoux. C. R. Ac. Sc., Paris, 329, 23-30.

Bakker RJ, 1997. Clathrates: Computer programs to calculate fluid inclusion V-X properties using clathrate melting temperatures. Computers & Geosciences, 23, 1-18.

Bakker RJ, 1999. Adaptation of the Bowers and Helgeson, 1983. equation of state to the H2O-CO2-CH4-N2-NaCl system. Chemical Geology, 154, 225-236.

Bertrand JM, Leterrier J, Delaperrière E, Brouand M, Cuney M, Stussi JM, Virlogeux D (in press) Géochronologie U-Pb sur zircon de granitoides du Confolentais, du massif de Charroux-Civray (seuil du Poitou) et de Vendée. Géologie de la France.

Bodnar RJ, 1993. Revised equation and table for determining the freezing point depression of H2O-NaCl solutions. Geochimica Cosmochimica Acta, 57, 683-684.

Boiron MC, Essarraj S, Sellier E, Cathelineau M, Lespinasse M, Poty B, 1992. Identification of fluid inclusions in relation with their host microstructural domains in quartz by cathodoluminescence. Geochimica Cosmochimica Acta, 56, 175-185.

Boiron, M.C., Cathelineau, M., Banks, D., Buschaert, S., Fourcade, S., Coulibaly, Y., Boyce, A., and Michelot, J.L. (submitted). Penetration of brines into a crystalline basement during extensional tectonics: role on fracture sealing and mass transfer.

Bowers TS, Helgeson HC, 1983. Calculation of the thermodynamic and geochimical consequences of non-ideal mixing in the system H_2O-CO_2–NaCl on phase relations in geologic system: metamorphic equilibria at high pressures and temperatures. American Mineralogist, 68, 1059-1075.

Cathelineau M, 1988. Cation site occupancy in chlorites and illites as a function of temperature. Clay Minerals, 23, 471-485.

Cathelineau M, Cuney M, Boiron MC, Coulibaly Y, Ayt Ougougdal M, 1999. Paléo-percolations et paléointeractions fluides/roches dans les plutonites de Charroux-Civray. Etude du Massif de Charroux-Civray - Actes des Journées Scientifiques CNRS/Andra, Poitiers 13 et 14 octobre 1997, 159-179.

Cathelineau, M., Fourcade, S., Clauer, N., Buschaert, S., Rousset, D., Boiron, M.C., Martineau, F., Meunier, A., Javoy, M., Nitjchoua, R., 2001. Multistage paleofluid percolations in granites: A stable isotope and K-Ar study of fracture illite from Vienne plutonites (N.W. of the french Massif Central). Clay Min., submitted.

Cathelineau M, Marignac C, Boiron MC, Gianelli G, Puxeddu M, 1994. Evidence of Li-rich brines and early magmatic water-rock interaction in a geothermal field: the fluid inclusion data from the Larderello field. Geochimica Cosmochimica Acta, 58, 1083-1099.

Cheilletz A, Cuney M, Coulibaly Y, Brouand M, Cathelineau M, Stussi JM, 1997. L'adularisation à l'interface socle/couverture dans la région de Charroux - Civray. Journées. Scientifiques Andra, Poitiers, p 16.

Clayton RN, Mayeda TK, 1963. The use of bromine pentafluoride in the extraction of oxygen from oxides and silicates for isotopic analyses. Geochimica Cosmochimica Acta, 27, 2075-2092.

Cuney M, Brouand M, Stussi JM, Gagny C, 1999. Le massif de Charroux-Civray (Vienne): un exemple caractéristique des premières manifestations plutoniques de la chaîne hercynienne. Etude du Massif de Charroux-Civray - Actes des Journées Scientifiques CNRS/Andra, Poitiers 13 et 14 octobre 1997, 63-104.

Dubessy, J, 1984. Simulation des équilibres chimiques dans le système C-O-H. Conséquences méthodologiques pour les inclusions fluides. Bulletin Mineralogique, 107, 155-168.

Dubessy J, Poty B, Ramboz C, 1989. Advances in the C-O-H-N-S fluid geochemistry based on micro-Raman spectroscopic analysis of fluid inclusions. European Journal of Mineralogy, 1, 517-534.

Duthou JL, Cantagrel JM, Didier J, Vialette Y, 1984. Paleozoic granitoids from the French Massif Central: age and origin studied by 87Rb-87Sr system. Physical Earth and Planetary Sciences International, 35, 131-144.

Fourcade, S., Michelot J.L., Buschaert S., Cathelineau M., Freiberger R., Coulibaly Y., Aranyossy J. F., 2001, Multi-stage fluid circulation with early introduction and recurring remobilizations of carbon during subsurface fluid-rock interactions: the case study of the vienne granitoids (france), submitted.

Freiberger R, Cuney M, 1999. Magmatic anhydrite in plutonic rocks: Occurrence from the Hercynian calcalkaline batholith of Charroux-Civray (NW' Massif Central, France). In: The origin of granites and related rocks - Fourth Hutton Symposium, Clermont-Ferrand (ed Barbarin B). Editions BRGM, 290, 209.

Freiberger R, 2000. P-T-X conditions of the late magmatic to early postmagmatic crystallization history of intermediate to basic plutonites: The Hercynian granitoid complex of Charroux-Civray, NW border of the Massif Central, France. Unpubl. PhD thesis, Lehrstuhl für Angewandte Mineralogie und Geochemie, TU München, Hieronymus-Verlag, 204 p.

Freiberger R, Hecht L, Cuney M, Morteani G (in press) Secondary Ca-Al silicates in plutonic rocks: Implications for their cooling history. Contributions to Mineralogy and Petrology.

Frey M, de Capitani C, Liou JG, 1991. A new petrogenetic grid for low-grade metabasites. Journal of Metamorphic Geology, 9, 497-509.

Kerrich R, 1987. Stable isotope studies of fluids in the crust. In: Short course in stable isotope geochemistry in low-temperature fluids (ed Kyser TK). Mineralogical Association of Canada, Saskatoon, 13, 258-286.

Lehmann B, 1990. Metallogeny of tin. In: Lecture Notes in Earth Sciences (eds. Bhattacharji S, Friedman GM, Neugebauer HJ, Seilacher A). Springer-Verlag, 32, 211 p.

Lespinasse M, Cathelineau M, 1990. Fluid percolations in a fault zone: a study of fluid inclusions planes in the St Sylvestre granite, North-West Massif Central, France. Tectonophysics, 184, 173-187.

Poty B, Leroy J, Jachimowicz L, 1976. Un nouvel apparail pour la mesure des temperatures sous le microscope, l'installation de microthermométrie Chaixmeca. Bulletin de la Société Francaise de la Minéralogie et Crystallographie, 99, 182-186.

Roedder E, 1984. Fluid inclusions. Reviews in mineralogy, 12, Mineralogical Society of America, 644 p.

Scaillet S, Cheilletz A, Cuney M, Farrar E, Archibald D, 1996. Cooling patterns and mineralization history of the Saint Sylvestre and Western Marche leucogranite plutons, French Massif Central. I. 40Ar/39Ar isotopic constraints. Geochimica Cosmochimica Acta, 60, 23, 4653-4671.

Sheppard SMF, 1986. Characterization and isotopic variations in natural waters. In: Stable isotopes in high temperature geological processes (eds. Valley JW, Taylor HP, O'Neil JR). Mineralogical Society of America, Reviews in Mineralogy, 16, 165-184.

Thiéry R, Vidal J, Dubessy J, 1994. Phase equilibria modelling applied to fluid inclusions liquid-vapor equilibria and calculation of the molar volume in the CO2-CH4-N2 system. Geochimica Cosmochimica Acta, 58, 1073-1082.

Turpin L, Cuney M, Friedrich M, Bouchez JL, Aubertin M, 1990. Meta-igneous origin of Hercynian peraluminous granites in NW French Massif Central: Implications for crustal history reconstitutions. Contribution to Mineralogy and Petrology, 104, 163-172.

Virlogeux D, Roux J, Guillemot D, 1999. Apport de la géophysique à la connaissance géologique du massif de Charroux-Civray et du socle poitevin. Etude du Massif de Charroux-Civray - Actes des Journées Scientifiques CNRS/Andra, Poitiers 13 et 14 octobre 1997, 33-61.

Zhang YG, Frantz JD, 1987. Determination of the homogenization temperatures and densities of supercritical fluids in the system NaCl-KCl-$CaCl_2$-H_2O using synthetic fluid inclusions. Chemical Geology, 64, 335-350.

Zheng YF, 1993. Calculation of oxygen isotope fractionation in anhydrous silicate minerals. Geochimica Cosmochimica Acta, 56, 1079-1091.

2 PENETRATION OF BRINES INTO A CRYSTALLINE BASEMENT DURING EXTENSIONAL TECTONICS: IMPLICATIONS ON FRACTURE SEALING

M.C. Boiron[a], M. Cathelineau[a], D.A. Banks[b], S. Buschaert[a,f], S. Fourcade[c], Y. Coulibaly[a], J.L. Michelot[d], A. Boyce[e], R Nitjchoua[f]

[a] *UMR G2R 7566 - CREGU, BP23, 54501 Vandoeuvre-lès-Nancy, France*
[b] *School of Earth Sciences, Univ. of Leeds, Woodhouse Lane, Leeds LS2 9JT, UK*
[c] *Géosciences Rennes UMR 6118, Univ. Rennes 1, 35042 Rennes Cédex, France*
[d] *UMR-CNRS-UPS Orsay Terre, Laboratoire d'hydrologie et de Géochimie isotopique, Université de Paris Sud, Bat 504, 91405 Orsay, France*
[e] *Scottish Universities Research and Reactor centre, East Kilbride, Glasgow G75 0QF, Scotland, UK*
[f] *Andra, French Agency for Nuclear Waste Management, 92298 Châtenay-Malabry*

Submitted to Chemical Geology

Figure captions ***2-54***
Table captions ***2-54***
Abstract ***2-55***

2.1 INTRODUCTION ***2-57***

2.2 GEOLOGICAL SETTING ***2-57***

2.3 MINERAL SEQUENCES AND STUDIED MATERIAL ***2-58***

2.4 FLUID CHARACTERISATION ***2-59***
2.4.1 Methods 2-59
2.4.2 Microthermometry and Raman results 2-60
2.4.3 Ion chemistry 2-62

2.5 STABLE ISOTOPE DATA ON QUARTZ AND CARBONATES ***2-67***
2.5.1 Analytical techniques 2-67
2.5.2 Stable isotope compositions 2-68

2.6 DISCUSSION ***2-70***
2.6.1 Salt source 2-70
2.6.2 Style of fluid migration 2-70
2.6.3 Age of the process 2-70

2.7 CONCLUSIONS ***2-72***
Acknowledgements ***2-74***
References ***2-75***

FIGURE CAPTIONS

Fig. 2.1. Map of the Charroux-Civray area with the north-western part of the Massif Central (modified from Rolin and Colchen, 1995). At the drilling locations, the basement is covered by about 150 m thick of sedimentary rocks of Jurassic age. The basement beneath Charroux-Civray is mainly composed of medium-K and high-K calcalkaline associations of which the contours have been derived from geophysical investigations. Identification of the studied drillings is given in the black rectangles. 2-58

Fig. 2.2. Photomicrographs of typical vein fillings. A: Dolomite (Dol)-Fluorite (Fl) and Calcite (Cc) mineral assemblage (sample CIV 107-1016 (253,73 -254 m). B: Adularia (Adul)- Dolomite (Dol)-Barite (Ba)-late calcite (Cc) vein filling (sample CIV 107-1018 (293,46 -293.79 m)). 2-62

Fig. 2.3. Tm ice versus Th diagram of aqueous fluid inclusions 2-63

Fig. 2.4. Na/K- Na/Li ratios of fluids determined from crush-leach analyses . Full line = sea water evaporation trend from Fontes and Matray (1993). Dotted line: temperature estimation deduced from the geothermometric cation relationships (Verma and Santoyo, 1997) 2-63

Fig. 2.5. Na versus Cl (A) and K versus Cl (B) diagrams of the composition of the fluids determined from crush-leach analyses. Full line = sea water evaporation trend from Fontes and Matray (1993). SW: sea water, G: gypsum, H: halite, E: epsomite, S: sylvite, C: carnallite, B: bischofite 2-65

Fig. 2.6. Cl/Br versus Cl diagram of the composition of the fluids determined from crush-leach analyses. Full line = sea water evaporation trend from Fontes and Matray (1993). SW: seawater, G: gypsum, H: halite, E: epsomite, S: sylvite, C: carnallite 2-66

Fig. 2.7. Na/Br versus Cl/Br diagram of the composition of the fluids determined from crush-leach analyses Full line = seawater evaporation trend from Fontes and Matray (1993). SW: seawater, H: halite, E: epsomite, S: sylvite. 2-67

Fig. 2.8. δD and $\delta^{18}O$ values of fluids (symbols) associated with fractures infillings of the Charroux-Civray site and with mineralized sites of the northwestern edge of the French Massif Central. Also represented are the compositional fields of some representative fluids (organic waters from Sheppard and Charef, 1986, Basin waters from Sheppard (1984):GC = Gulf Coast; C = California; M = Michigan) as well as a typical sea-water evaporation trends (after Knauth and Beeunas, 1986, Pierre, 1989, initial evaporation under humid conditions (curve n°1) and for arid conditions (n°2), evaporation curve (n°3) from Pierre et al. (1984)), present day waters sampled in Vienne boreholes from Michelot (1999), Zn-mineralized sites of the S.E. edge of the Aquitaine Basin (after Munoz et al., 1995 and Munoz et al., 1999), and Canadian shield brines from Frape and Fritz (1987). 2-69

Fig. 2.9. Schematic model of the hydrothermal circulations within the Charroux-Civray plutonic complex at the unconformity surface. 1-Tertiary cover, 2 - Mesozoïc limestones, 3- Impermeable shales, Toarcian formation, 4- basal silicoclastic series and dolomites, Infra Lias, 5 - Basal silicoclastic series, 6 - Weathered basement (paleosurface with supergene oxidized facies), 7 - Granitoids (hercynian basement) 2-72

TABLE CAPTIONS

Table 2.1. Investigated samples for fluid inclusion studies, with host rock type, predominant alteration type. The mineral studied for fluid inclusion is indicated in bold character. 2-59

Table 2.2. Ranges of microthermometric fluid-inclusion and stable isotopic data. 2-61

Table 2.3. Reconstructed composition (in mmole/kg solution) of fluid inclusions from crush-leach analyses. 2-66

ABSTRACT

In the north-western margin of the French Massif Central, basinal brines have percolated within the Hercynian crystalline basement and its sedimentary cover (Infra-Toarcian formations) and induced fracture or porosity sealing. These fluids were investigated in the Charroux-Civray (Vienne) crystalline basement and its sedimentary cover as well as in outcropping areas of the basement in the vicinity of northern Limousin. Dolomite, calcite (± fluorite, barite and quartz in some instances) constitute most fracture fillings, and formed from H_2O-NaCl-KCl-$CaCl_2$-($MgCl_2$) brines. Brine inclusions were found in most minerals and are characterized by Tm ice ranging from -12°C to -27.6°C, indicative of salinities in the range 16- 23 eq. wt.% NaCl, and by Th in between 75°C and 130°C for quartz and slightly lower for dolomite, barite, fluorite and calcite (90±25°C). Brines hosted by different minerals show little compositional differences and are characterized by Na/K ratios of 5 to 40, Na/ Li ratios of 20 to 530, and Cl/ Br ratios of 200 to 1000 which are rather typical of deep basinal brines. Similar fluids were found in the representative fluorite-barite-dolomite occurrences of the northern edge of the French Massif Central (Chaillac, Bernardan- Cote Moreau, Peny-Margnac) either in the infra-Toarcian sediments or in the basement. Within the sedimentary cover, $\delta^{18}O$ values are + 27 ± 2‰ for fracture calcites and dolomites and 28 ± 1‰ for quartz. The fluid $\delta^{18}O$ signature is estimated to be *c.* 6 ± 2 ‰ for a crystallisation temperature in between 80° and 120°C and the δD value is –30 ± 10‰. The fluid at the origin of the fracture filling is interpreted as a deep sedimentary brine expelled during a period of maximum subsidence. The brine produced an intense sealing of most fractures inside the basement. Among the different stages of fluid migration responsible for the sealing of macrofractures in the Hercynian crystalline basement, from Hercynian to present times, the downward percolation of brines during the Mesozoic is certainly one of the most important. In addition, the mass transfer linked to this stage is significant and accounts for the early introduction of great masses of chlorine in the granitoïd aquifer.

Keywords: deep groundwater, brines, stable isotope, unconformity, Vienne granites

2.1 Introduction

The Hercynian basement is located beneath a Mesozoic sedimentary cover (150 meters of limestones, shales, and detrital series from Hettangian up to Malm) over an area of about 125 km^2 between the Armorican massif and the "Massif Central" in France, the so-called "Poitou High", This region was recently explored by 17 continuously cored boreholes, 200 m to 1000 m deep, by Andra to investigate the setting of an underground laboratory. Exceptional and unweathered drilled material from Hercynian plutonic suites have shown that the major plutonic bodies (tonalites and granodiorites) contain rather dense sets of fractures, most of them being filled by a systematic mineral sequence: adularia-quartz-dolomite- calcite, and a minor but typical association of fluorite-barite with traces of Pb-Zn sulphides. Preliminary mineralogical and fluid inclusion studies have shown that these minerals crystallized from a brine at rather low temperatures, during a period younger than the deposition of the overlaying infra-Toarcian sedimentary series. Such features are typical of most F-Ba deposits from the northern part (Chaillac, Ziserman, 1980) or the south-eastern part (Albigeois area, Munoz et al., 1999) of the French massif central.

The aim of this work was to determine the origin and nature of brines percolating the basement and their role in the mass transfer from the basins towards the basement. Work was focused on the Poitou high basement under the sedimentary cover. In order to evaluate the extension of the process in the northern Limousin, several occurrences of the same specific paragenetic sequence filling the fractures were also sampled within the basement at various distances from the unconformity with the Mesozoic series.

2.2 Geological setting

The Charroux-Civray area is located at the north-western border of the French Massif Central (Fig. 2.1), below a 150 m thick sedimentary cover composed of Lias and Dogger marine formations. The basement is dominated by plutonites from the "Tonalitic Lineament" of the Limousin (Peiffer, 1986; Shaw et al., 1993) and contains multiple intrusions of medium-K calc-alkaline tonalites and granodiorites dated around 350-360 ± 5 Ma (U-Pb zircons; Bertrand et al., 2000) intruded later by peraluminous intrusions. (Capdevila, 1997; Cuney et al., 1999). Investigated samples from this area were taken from 17 continuously cored, 200 m to 1000 m deep, boreholes drilled by Andra (French Nuclear waste Management Company).

By means of paragenetic and fluid inclusions studies (FI frequently on quartz), the existence of at least 3 stages of fluid flow was demonstrated in a preliminary study, each stage characteristic of extremely distinct P-T conditions and geodynamic contexts (Cathelineau et al., 1999). Multiphase veins fillings (including carbonates) can be ascribed to 3 stages: i) Hercynian events (stage I) characterized by an early post-magmatic stage (retrograde crystallisation of Ca-Al silicates) followed by thermal heating and fluid circulation linked to the emplacement of peraluminous intrusions, and finally by a late retrograde alteration of plutonites, coeval with the final basement uplift stage and cooling. A small amount of sealed fractures are related to these stages and consist of quartz-hematite, or quartz-chlorite-phengite or illite veins with a small amount of carbonates. The basement was uplifted and the top of the granites

was weathered during a period of emersion (Trias), ii) Stage-II: abundant fractures filled by dolomite and calcite are found in the plutonites and in the sedimentary cover. They are recognized by the systematic presence of minor amounts of fluorite/ barite±sulphides and occur, down to 800 m underneath the basement/cover interface. As this assemblage is also observed in the lower part of the sedimentary cover either as fracture or pore infillings in all series below the Toarcian shales (Hettangian/ Sinemurian series), this indicates an age younger than Hettangian (Cathelineau et al., 1999). iii) later, stage III is characterized by late calcites (± kaolinite) crystallized at low temperatures.

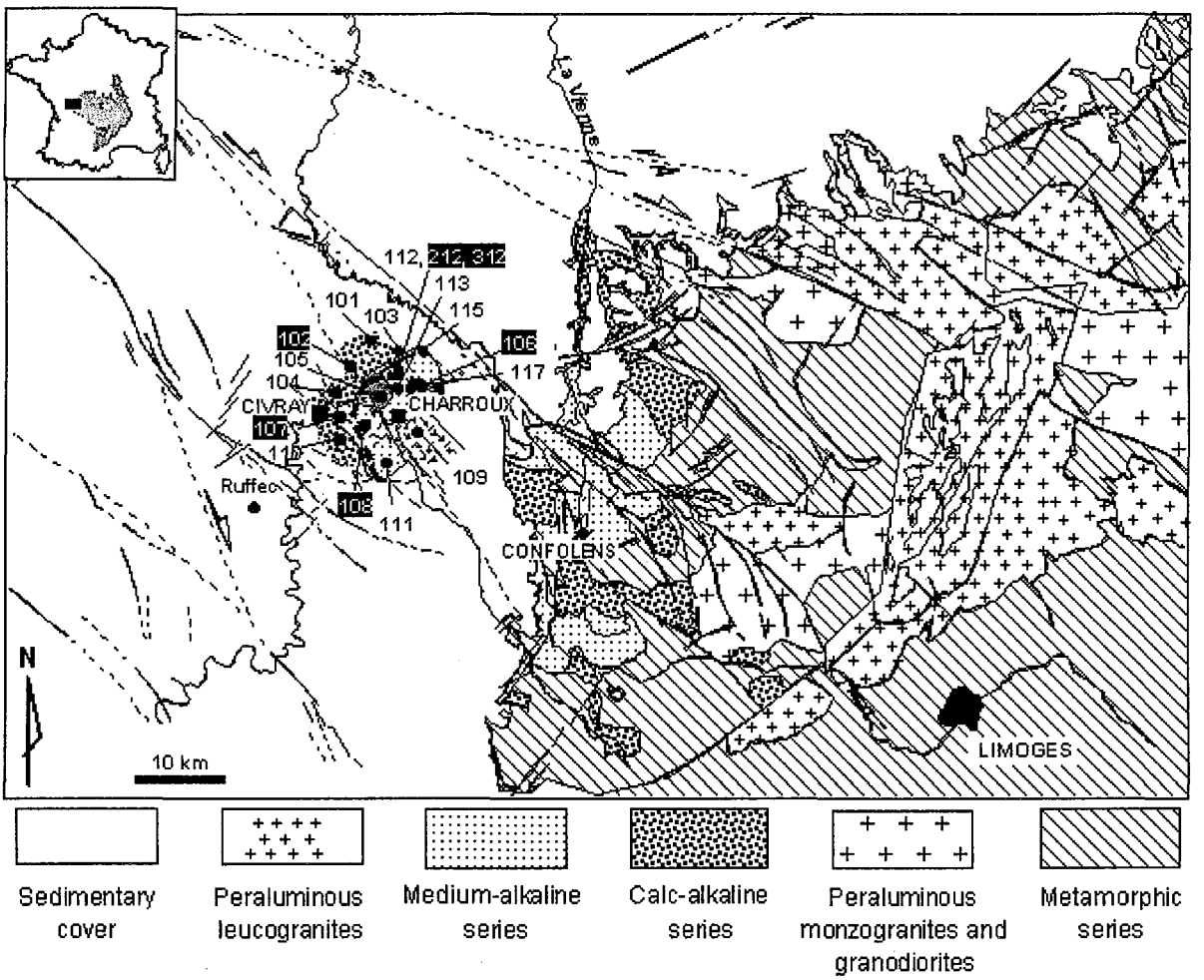

Fig. 2.1. Map of the Charroux-Civray area with the north-western part of the Massif Central (modified from Rolin and Colchen, 1995). At the drilling locations, the basement is covered by about 150 m thick of sedimentary rocks of Jurassic age. The basement beneath Charroux-Civray is mainly composed of medium-K and high-K calcalkaline associations of which the contours have been derived from geophysical investigations. Identification of the studied drillings is given in the black rectangles.

2.3 Mineral sequences and studied material

A first set of samples was selected along 10 of the 17 deep drilling cores (200 to 1000 m deep) made by Andra (Table 2.1).

In the Vienne granitoids, the mineralogical sequence is fairly constant comprising: hematite-adularia)/ quartz / dolomite (±fluorite and barite ± Cu, Zn, Fe sulphides)/calcite (Fig. 2.2 and Table 2.1). A similar mineral assemblage is also

observed in the lower part of the sedimentary cover filling the porosity of the detrital series (Hettangian to Sinemurian sandstones and conglomerates). Dolomite represents the main vein filling, calcite being much less abundant. Both have a rather low Fe content (< 0.15 per formula unit) and are close to the two carbonate end-members (pure dolomite and calcite).

The second set of samples include vein material from the outcropping northern Limousin basement: the Chaillac fluorite-barite veins, fluorite veinlets in the La Marche peraluminous granites (Bernardan-Cote Moreau area), and dolomite veins from the Margnac–Peny area in the peraluminous granite of St Sylvestre (see Fig. 2.1 for location).

At Chaillac, the main stage of fluorite deposition consists of the crystallisation of yellow to brown amber fluorite followed by grey fluorite, barite and pyrite. At Cote Moreau, fluorite occurs as yellow euhedral crystals of millimetre size, deposited on a thin hematite-bearing quartz comb. In Peny, centimetre-sized monocrystals of pink dolomite are observed in fracture infillings, with no accompanying minerals.

Drilling n°	Sample n°	Depth (m)	Host rock	Mineral succession
Vienne				
CIV 102	CIV 00667	206.5	Quartz tonalite	adularia-**dolomite**-barite-pyrite
CIV 102	CIV 671	227.02/227.18	Tonalite	**calcite**
CIV 107	CIV 1016	253.7/254	Quartz monzodiorite	**fluorite**-pyrite-chalcopyrite
CIV 107	CIV 1019	347.02/347.7	Microdiorite	**quartz**-pyrite-**dolomite**
CHA 106	CHA 1052	491.8/491.9	Monzogranite	**quartz**
CHA 106	CIV 1068	585.7/586.04	fracture dolerite -polyphased	**dolomite**-barite
CHA 108	CHA 2421	243.10/243.2	Quartz monzodiorite	**fluorite**-pyrite-barite-chalcopyrite
CHA 212	CHA 5646	607.2/607.6	Tonalite	adularia-**dolomite**-barite
CHA212	CHA8594	728.5/728.65	Tonalite	dolomite-**barite**-chalcopyrite-pyrite
CHA 212	CHA 8602	892.3/892.5	Tonalite	adularia-**dolomite**-pyrite
CHA 212	CHA 8606	800.00	Tonalite	**dolomite**-barite- pyrite
CHA 212	CHA 8598	855.5/855.8	Fine grained granite	**dolomite**-pyrite-barite-galena-calcite
CHA 312	CHA 8805	-115.25	Sedimentary cover	**quartz** in cavity
North-Western Massif Central				
Chaillac	C1		Detrital series - Hettangian	Yellow to brown **fluorite**-barite±pyrite
	C2		Detrital series - Hettangian	Yellow to brown **fluorite**-barite±pyrite
	C4		Detrital series - Hettangian	Yellow to brown **fluorite**-barite±pyrite
Cote Moreau	P284L110		Peraluminous granite	quartz - (hematite) -yellow **fluorite**
Peny	1051 E17b		Peraluminous granite	Pink **dolomite** in fracture

Table 2.1. Investigated samples for fluid inclusion studies, with host rock type, predominant alteration type. The mineral studied for fluid inclusion is indicated in bold character.

2.4 Fluid characterisation

2.4.1 Methods

Microthermometric studies of the fluid inclusions were performed on wafers using a Chaixmeca heating-freezing stage (Poty et al., 1976). The stage was calibrated with melting-point standards at T > 25°C and with natural and synthetic fluid inclusions at

T < 0°C. The rate of heating was monitored in order to obtain an accuracy of ± 0.2°C during freezing, ± 1°C when heating over the 25-400°C. Salinity, expressed as eq. wt. % NaCl, was calculated from microthermometric data using equations from Bodnar (1993). For microthermometric data, abbreviations are used as follows: Te: temperature of ice- first melting; Tm ice/hy: melting temperature of ice or undefined hydrate, Th (L-V): total homogenisation temperature (L+V to liquid or L+V to vapour).

Bulk crush-leach analysis was performed on samples of quartz devoid of mineral inclusions. Samples were prepared and cleaned using the methods of Banks et al. (2000). The amount of sample crushed was typically between 0.5 and 1 g. Analysis of anions Cl, Br, I, F and SO_4 was performed by Ion Chromatography on double distilled water leaches. Na and K were determined on the same solutions by Flame Emission Spectroscopy (FES). It was not possible to analyse Ca because all minerals are Ca-carriers or contaminated by carbonate inclusions (quartz). Therefore, calcium was estimated from Laser Induced Breakdown spectroscopy (LIBS), (see below). The major cations and anions in the fluid inclusions have been calculated in mmole/kg of solution and are discussed in the text in term of molar ratios.

2.4.2 Microthermometry and Raman results

Similar data were obtained from the analyzed minerals from Vienne, and the north-western Massif central deposits. Microthermometry and Raman microprobe investigations show the existence of a single dominant fluid type (H_2O-NaCl-KCl-$CaCl_2$ ($MgCl_2$) brine, (see below)) in primary fluid inclusions from all the minerals of the infilling sequence (Fig. 2.2). Within the zoned quartz crystals, primary fluid inclusions are distributed along the growth zones. They are generally small (≤10 □m) and irregular. Dolomite, fluorite and calcite contain two-phase aqueous inclusions of variable size (up to 20 µm), generally flat and irregular in shape. We stress the point that FIP in the host rocks never display this type of high salinity fluids. This could indicate that no FIP developed from the host granitoïds in quartz during the stage of brine circulation either because this event was not accompanied by fracturating or because the temperature was too low for quartz healing.

The first melting temperature, as low as -50°C, is diagnostic of the presence of $CaCl_2$ (and possibly $MgCl_2$; Crawford, 1981) in addition to NaCl. Two-phase fluid inclusions were found in all the minerals of the infilling sequence and show a range of melting temperature of a solid from -12°C (and some values up to -6°C for Vienne barite, and -3.8°C for Chaillac fluorite) to -27.6°C (ice ± hydrohalite melting) (Table 2.2). Most Tm ice values for dolomite and quartz are between -16 and -27°C. Only one melting was observed, this making impossible an estimation of the Na/Ca ratio on the basis of the melting of ice and hydrohalite. For this reason the chlorinity of the inclusions, showing the lowest Tm (ice), has been determined by Raman spectroscopy using the calibration curves from Lhomme et al. (1999). This could only be done on quartz because for other minerals, fluorescence makes the measurements impossible. For inclusions showing a melting of a solid around -27°C (sample CIV 1019), the measured chlorinity is around 4.2 moles/kg solution, e.g. close or slightly lower than the maximal estimate given by the consideration of the saturation with respect to halite. The Na/Ca ratio is in favour of Na (see data below), this allowing the

consideration of the simple system H_2O-NaCl. The salinity was thus calculated arbitrary on the basis of microthermometric measurements in the H_2O -NaCl system for dolomite, calcite and fluorite. In spite of a probable slight overestimation, salinities are considered to range from 16 to 23 eq. wt.% NaCl.

Location	Mineral	Sample n°	Tm ice (°C)		Th (°C)		$\delta^{18}O$ ‰ SMOW	$\delta^{13}C$ ‰ PDB	δD ‰ SMOW
Vienne	Quartz	CIV 1019	-14 ; -27.6 (-22)	n = 23	75 ; 130 (90 / 110)	n = 8			-46
	Quartz	CHA 1052	-9 ; -11.7	n=6	n.d.				
	Quartz	CHA 8805	-12.2 ; -22.6	n=5	101 ;120 (100 / 110)	n=5	27.5		
	Dolomite	CIV 00667	n.d.		n.d.		26.4	-9.7	
	Dolomite	CIV 1068	-24.9 ; -26.3 (-25.5)	n = 5	88.5 ; 95.2 (90)	n=6			-50
	Dolomite	CIV 1019 B	-21 ; -26.7 (-25.7)	n = 9	90.6 ; 113.5 (110)	n = 9	27.3	-8.8	-19
	Dolomite	CHA 5646	n.d.		n.d.		28.7	-13.4	-40
	Dolomite	CHA 8598	n.d.		n.d.		25.9	-10.7	-21
	Dolomite	CHA 8602	n.d.		n.d.		26.4	-10.0	
	Dolomite	CHA 8606	n.d.		n.d.		26.6	-9.9	-28
	Fluorite	CIV 1016	-15 ; -18 (-16)	n = 4	87 ; 102.7 (90)	n = 4			
	Fluorite	CHA 2421	-14.5 ; -22.6	n = 4	86.5 ; 95.1 (90)	n = 13			
	Calcite	CIV 671	-11.9 ; -25.1 (-19.5)	n = 8	64 ; 102 (70 ; 100)	n = 9	23.8	-10.9	-28
	Barite	CHA8594	-6 ; -16.8	n=11	84 ; 116 (110)	n=6			
North-Western Massif Central									
Chaillac	Fluorite	C1	-3.8 ; -9.8	n=6	78 ; 120 (110)	n=6			
		C2	-7.3 ; -19.4	n=12	90 ; 116 (110)	n=11			
		C4	-18.1 ; -19.4	n =7	95 ; 120 (105)	n=7			
Cote Moreau	Fluorite	P284L110	-18.4 ; -18.7	n = 6	95 ; 100 (100)	n=5			
Peny	Dolomite	1051 E17b	-19.7 ; 30.2	n = 5	109 ; 133 (110 / 130)	n=6	27.8	-7.5	

Table 2.2. Ranges of microthermometric fluid-inclusion and stable isotopic data.

Homogenisation temperatures (Th) are in between 75°C and 130°C for quartz and slightly lower for dolomite (90-115°), barite (85-115°C), fluorite (85-100°C) and calcite (65-100°C) (Fig. 2.3). Since inclusions homogenise into the liquid state, the minimum fluid pressure prevailing during this stage (estimated using the method of the fluid vapour pressure at the homogenisation temperature in the H_2O-NaCl system) can be as low as 10-20 bars. The lack of evidence for boiling, however, suggests that pressure was somewhat higher. In addition, the formation temperature estimated from the hydrothermal alteration facies (I/S R0 formed during the brines stage in the scarce older phyllosilicate-rich fractures) is in the range of the homogenisation temperature, which suggests that pressure corrections are negligible. Consequently, we estimate that the minimum fluid pressure, similar to the trapping pressure, should not exceed a few hundred of bars.

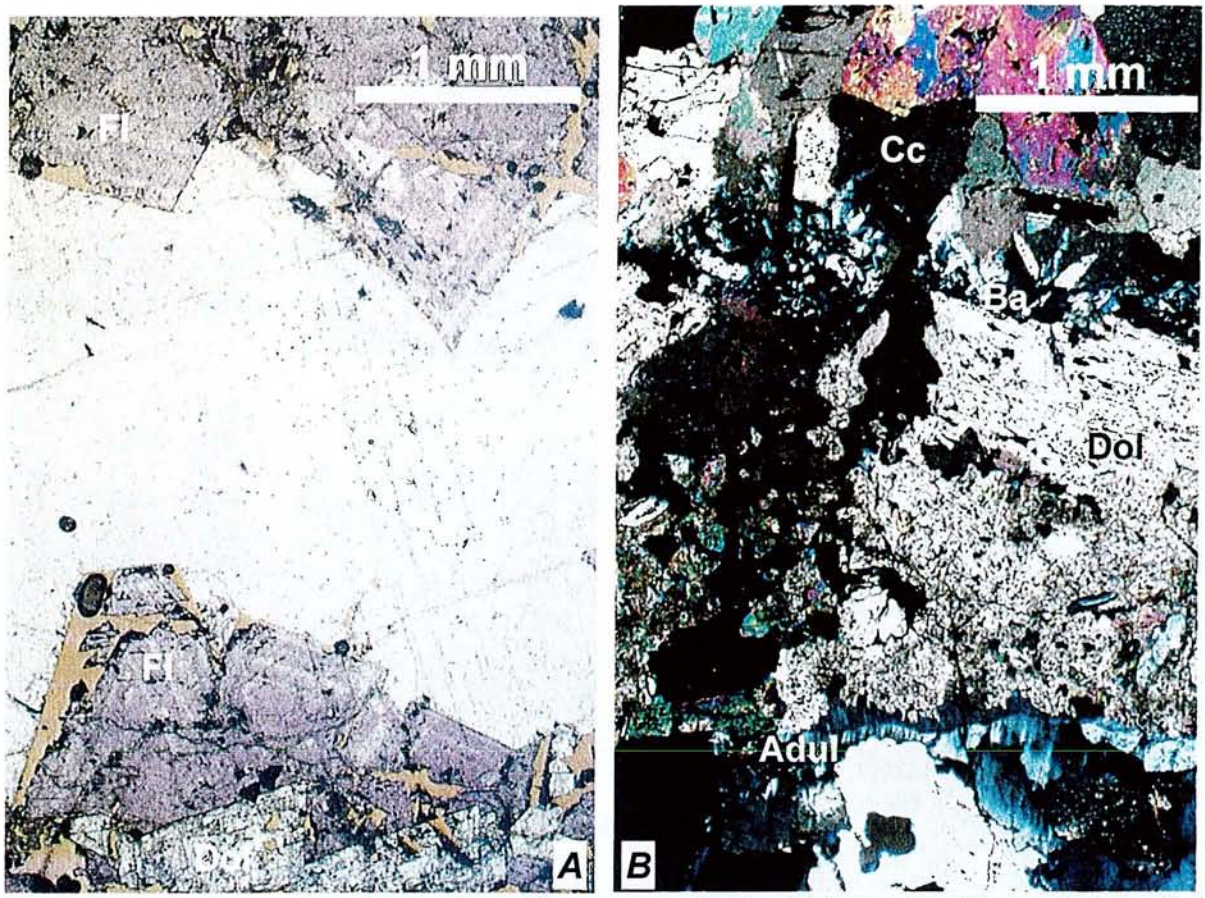

Fig. 2.2. Photomicrographs of typical vein fillings. A: Dolomite (Dol)-Fluorite (Fl) and Calcite (Cc) mineral assemblage (sample CIV 107-1016 (253,73 -254 m). B: Adularia (Adul)- Dolomite (Dol)-Barite (Ba)-late calcite (Cc) vein filling (sample CIV 107-1018 (293,46 -293.79 m)).

2.4.3 Ion chemistry

The reconstructed fluid chemistry calculated from crush leach analyses and using the average salinity deduced from microthermometry and Raman spectroscopy is reported in Table 2.3. Average salinities are evidently lower than the maximum estimates for inclusions showing the lowest Tm ice, but are probably more realistic for the bulk population of inclusions analyzed by the bulk crush-leach technique. The maximum salinity of these brines is around 23 eq. wt.% NaCl, close to the salinity resulting from sea water evaporation to halite saturation. Microthermometric data show that fluid inclusions display a significant variation in salinity (16-23 eq. wt.% NaCl), indicating probable dilution of the more saline brines, described above, by a dilute fluid. Such a dilution is shown by the Tm ice/Th trend which points out a range of Tm ice data which probably reflects mixing during the precipitation of the fracture minerals.

The dominant anion in the analyzed fluids is Cl, and there is a significant amount of SO_4 in some samples (quartz, dolomite). Major cations are Na and K. The presence of Ca, deduced from the microthermometric measurements, is confirmed by the LIBS data. The major cation ratios are the followings: Na/K ratios of 5.5 to 40, Na/Li ratios of 20 to 530, (Fig. 2.4). Na/Ca ratios are estimated to be around 3 to 5 from LIBS measurements. Mg is likely to be present as the brines precipitate dolomite as a predominant mineral.

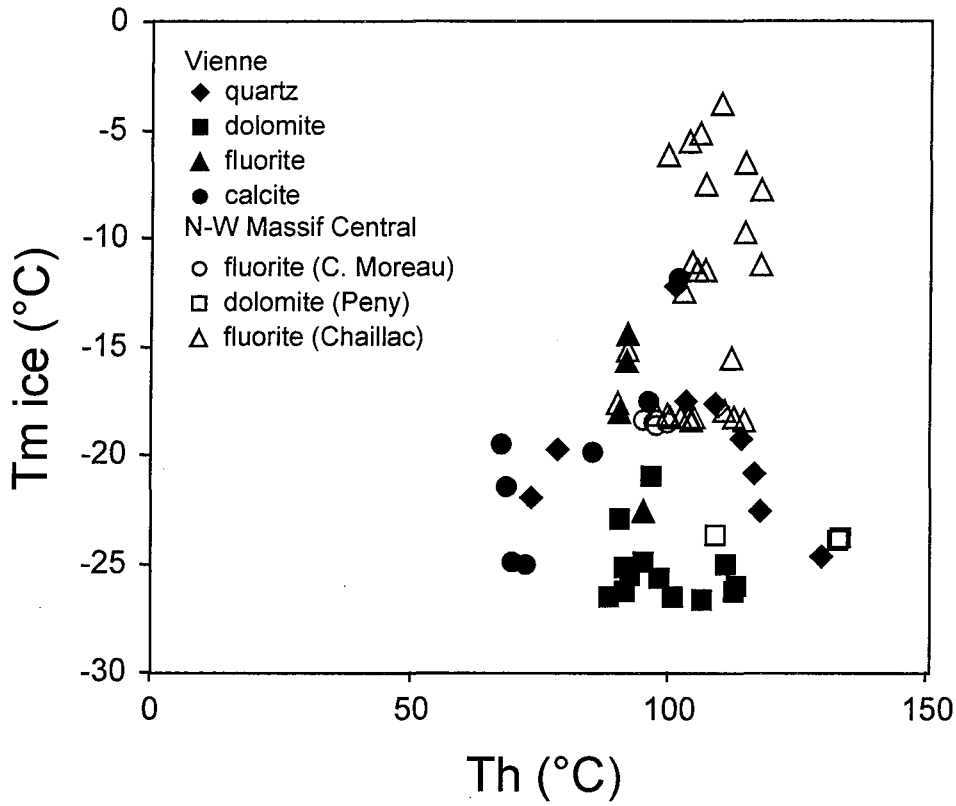

Fig. 2.3. Tm ice versus Th diagram of aqueous fluid inclusions

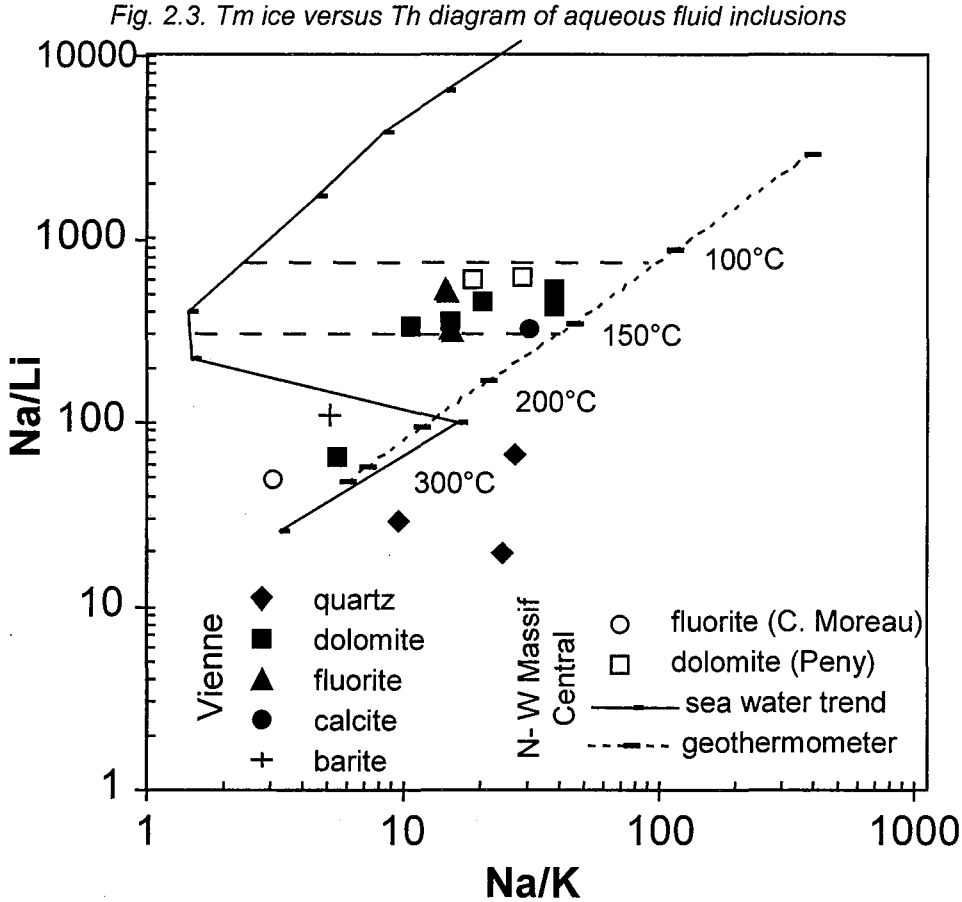

Fig. 2.4. Na/K- Na/Li ratios of fluids determined from crush-leach analyses . Full line = sea water evaporation trend from Fontes and Matray (1993). Dotted line: temperature estimation deduced from the geothermometric cation relationships (Verma and Santoyo, 1997)

Cation or anion ratios, Na/K and Na/Li indicate that the studied brines have compositions similar to those of sedimentary brines, especially those reported by Carpenter et al. (1974) and Kharaka et al. (1987) in oil fields. The Na/Li rations are surprisingly consistent with those expected at temperatures from 100 to 150°C, using the Fournier (1979) and Fouillac and Michard (1981) geothermometers revised by Verma and Santoyo (1997). The Na/K ratio plots between the geothermometric curve and the sea water trend. The evolution in the Na/K ratio from that expected after halite saturation towards that predicted for fluids equilibrated at 100-150°C with crystalline rocks could indicate a progressive chemical change due to water-rock (plutonite) interactions. Some data are quite distinct and especially enriched in Li, yielding low Na/Li ratios.

In the Na versus Cl and K versus Cl diagrams, data plot at the left-handed side of the seawater evaporation curve (Fig. 2.5A and B). The distribution is again interpreted as resulting from two factors: i) a range of Na (or K) contents which correspond to those expected for brines having passed halite saturation and may have reached epsomite saturation, ii) a slight dilution which subsequently decreased the Na, K and Cl concentration towards low salinity fluids.

The halogens Cl, Br and to a lesser degree I, can be used to distinguish sources of fluid (Bohlke and Irwin, 1992), because they display a conservative behaviour in solution and are relatively unaffected by fluid-rock interactions (Banks et al., 1991). Br contents range from 2 to 22 mmol/kg solution and I from 0.0006 to 0.0056 mmol/kg solution. Br/Cl (log Br/Cl from -2.2 to -3) and I/Cl ratios (log I/Cl from -5.8 to -6.8) are typical of deep basinal brines. Most of the Cl/Br ratios range from 200 to 1000 except for one sample which displays a higher Cl/Br ratio (1850). These ratios are similar to those of primary brines which reached saturation with respect to halite and have been also found in most deep basinal fluids. Thus, in the Cl/Br versus Cl diagram (Fig. 2.6), the composition of brines lies close to the sea water evaporation curve after halite saturation (Fontes and Matray, 1993). The Cl content is however slightly lower than expected, due to the slight dilution of the primary brine discussed above. The Cl/Br vs Na/ Br plot (Fig. 2.7), shows that most data plot around the sea water trend, and are significantly distinct from that determined by simple halite dissolution (ratio 1:1). In addition, most Na/ Br and Cl/ Br values are lower than those of sea water, as are most inclusions are found in evaporitic halite (Horita et al., 1991, Kesler et al., 1996). The I contents are rather low and typical of fluids issued from sea water evaporation and noticeably lower than the I content of brines derived from halite dissolution or of oil field brines which are enriched in I due to its concentration in organic matter.

Overall, the data suggest that the studied brines are primary brines expelled from evaporites that subsequently underwent only a moderate dilution in the regions where the minerals crystallized.

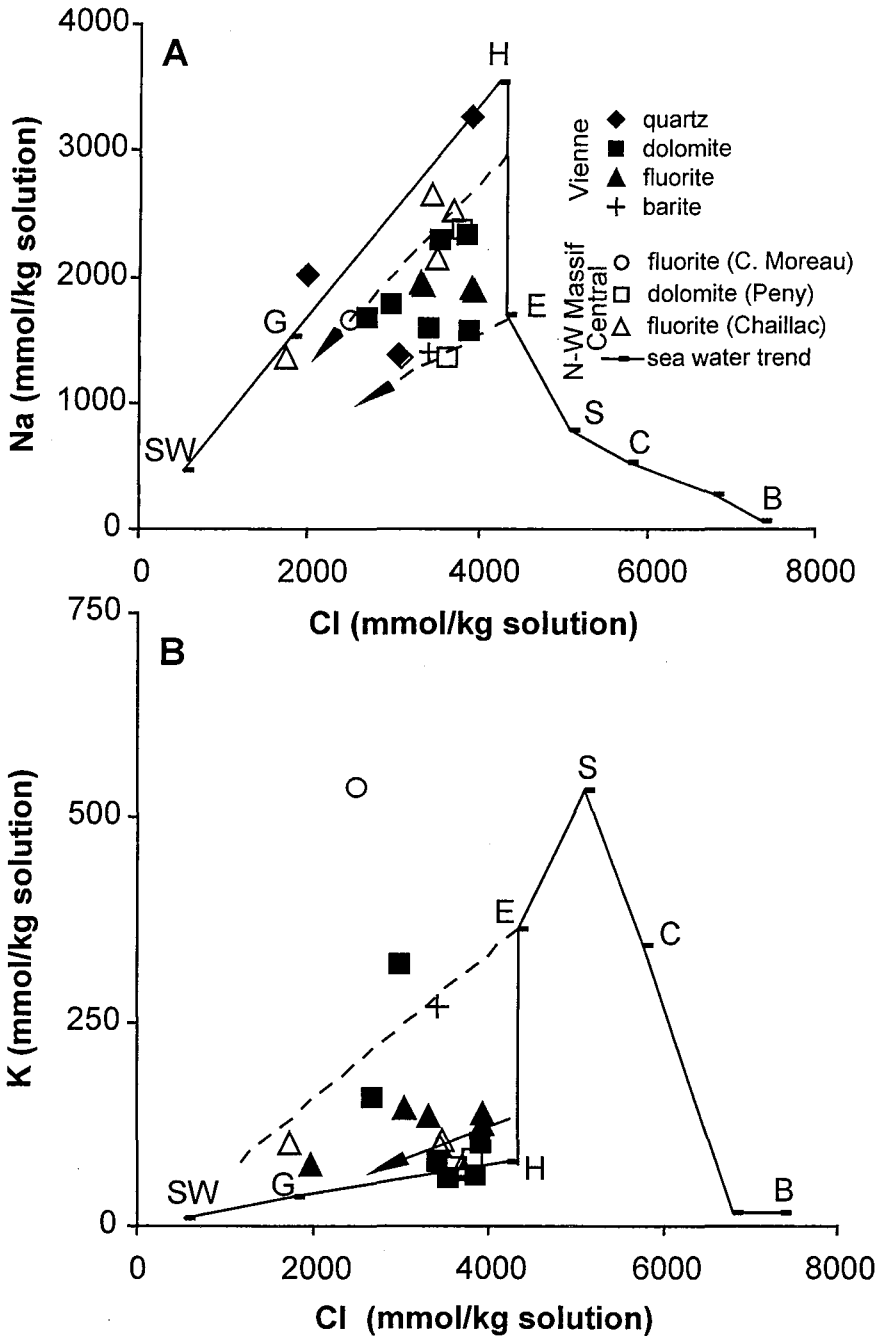

Fig. 2.5. Na versus Cl (A) and K versus Cl (B) diagrams of the composition of the fluids determined from crush-leach analyses. Full line = sea water evaporation trend from Fontes and Matray (1993). SW: sea water, G: gypsum, H: halite, E: epsomite, S: sylvite, C: carnallite, B: bischofite.

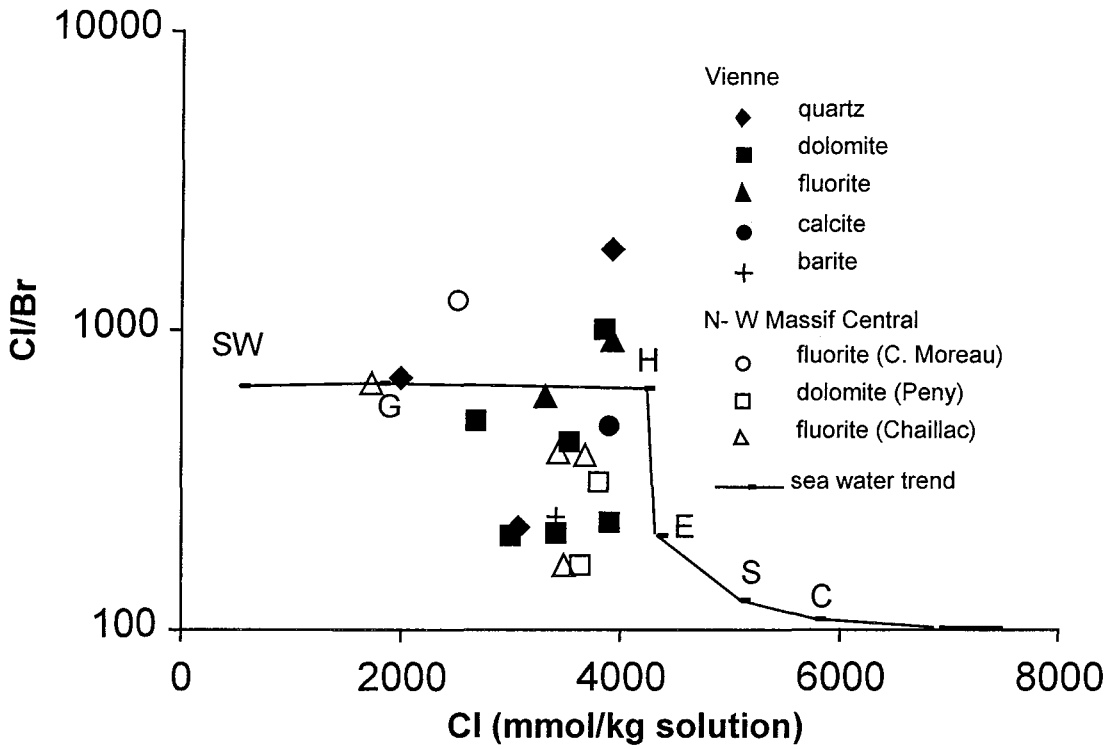

Fig. 2.6. Cl/Br versus Cl diagram of the composition of the fluids determined from crush-leach analyses. Full line = sea water evaporation trend from Fontes and Matray (1993). SW: seawater, G: gypsum, H: halite, E: epsomite, S: sylvite, C: carnallite.

Location	Sample	mineral	Na	K	Li	Cl	Br	F	SO4	I
Vienne	CIV 01019C	Quartz	1383.3	144.1	47.3	3067.9	14.1	185.3	234.1	0.0012
	CHA 1052	Quartz	2013.7	74.0	29.8	1989.2	2.9	6.5	146.4	
	CHA 8805	Quartz	3267.5	136.2	168.7	3930.9	2.1			
	CIV 00667	Dolomite	1677.8	158.0	5.0	2688.4	5.4	76.0	441.1	
	CHA 1068	Dolomite	2332.5	60.7	5.4	3856.9	3.9	26.9	23.8	0.0006
	CIV 01019A	Dolomite	1781.6	322.3	27.4	2987.9	14.7	78.6	322.2	
	CIV 01019B	Dolomite	1564.8	102.4	4.4	3896.8	17.2			0.0014
	CHA 5646	Dolomite	1583.0	78.6	3.5	3407.7	16.3	42.2	135.2	
	CHA 8602	Dolomite	2275.4	58.8	4.2	3533.6	8.4		103.6	
	CIV 1016	Fluorite	1940.8	134.2	3.6	3315.9	5.5		3.1	
	CHA 02421	Fluorite	1897.5	125.7	5.8	3926.1	4.3			
	CIV 00671	Calcite	2180.0	69.8	6.7	3911.5	8.2	10.5		0.0037
	CHA 8594	Barite	1398.8	268.9	12.8	3423.9	14.5			0.0056
North-Western Massif Central										
Chaillac	C1	Fluorite	1352.7	100.0		1738.4	2.6		19.4	
	C2	Fluorite	2140.7	105.2		3495.5	21.5		18.3	
	C3	Fluorite	2637.5	96.7		3445.7	8.9		47.1	
	C4	Fluorite	2511.6	73.5		3684.2	9.8		2.6	
Cote Moreau	P284L110	Fluorite	1655.7	536.8	33.2	2512.0	2.0		422.9	
Peny	1051 E17a	Dolomite	2368.0	82.3	3.9	3809.6	12.3	27.5	30.9	
	1051 E17b	Dolomite	1358.3	72.6	2.2	3641.6	22.1	8.2	88.6	

Table 2.3. Reconstructed composition (in mmole/kg solution) of fluid inclusions from crush-leach analyses.

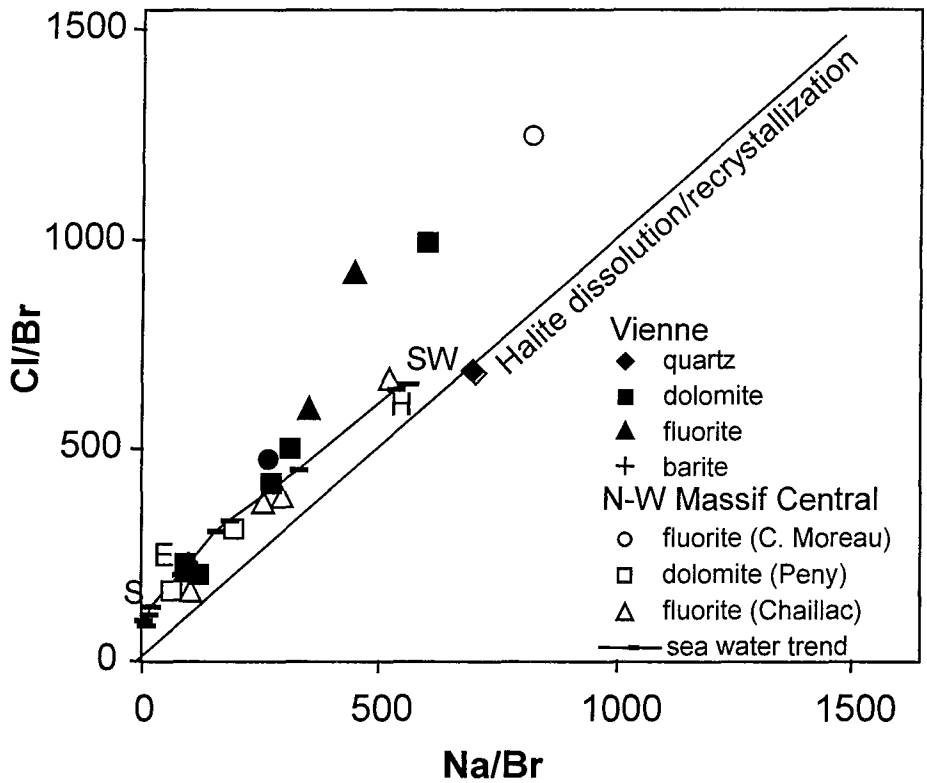

Fig. 2.7. Na/Br versus Cl/Br diagram of the composition of the fluids determined from crush-leach analyses Full line = seawater evaporation trend from Fontes and Matray (1993). SW: seawater, H: halite, E: epsomite, S: sylvite.

2.5 Stable isotope data on quartz and carbonates

2.5.1 Analytical techniques

Calcite from fractures was finely crushed. The carbonate fraction (5-10 mg) was reacted with 100% orthophosphoric acid at 25°C and we used the $\alpha(O)$ $CO_2/CaCO_3$ (extraction) = 1.01025. The oxygen isotopic composition was measured on separated quartz grains and quartz microsamples extracted from fluid inclusion wafers in which FI were studied. Extraction of oxygen was made at 650°C in Ni fluorination tubes, using BrF_5. All isotopic analysis were determined on CO_2 gas using a VG SIRA 10 mass spectrometer at Géosciences Rennes and expressed, using internal carbonate standards, NBS 19 and NBS 28 reference material, with the conventional δ notation vs. SMOW (O) and PDB (C). Data on silicates are normalized to a value of NBS 28 = 9.60‰. For carbonates, the mean precision was 0.04 ‰ on 5 replicate samples and the uncertainties related to the PDB and SMOW scales are estimated to be < 0.1‰ (C) and *c.* 0.1‰ (O). As with quartz, the uncertainty is estimated to be *c.* 0.1‰ (O) relative to SMOW, but may reach 0.3‰ for the smallest samples (<1 mg).

δD of fluid inclusions was measured directly on FI populations using standard procedures (Fallick et al., 1987) in the SURCC laboratory. The uncertainties on H and O isotope ratios are 2‰.

2.5.2 Stable isotope compositions

The $\delta^{13}C$ and $\delta^{18}O$ results obtained on calcites and dolomites are given in Table 2.2. Calcites and dolomites show a marked homogeneity in both C and O isotopic compositions: $\delta^{13}C$ values range from -9 to -12 ‰, $\delta^{18}O$ values are 27 ± 2 ‰. The $\delta^{18}O$ value of quartz in the sedimentary cover is 28 ± 1‰. Only one sample of quartz was found in the basement fractures and its $\delta^{18}O$ value is lower: 20‰. Nevertheless, because this sample is geometrically associated with a more ancient quartz in the same host fracture ($\delta^{18}O$ of the ancient quartz may be as low as + 5.1‰, Fourcade et al., 2001), we suspect that the mechanical extraction produced a composite sample, as also suggested by the high Li content of that sample (Table 2.3). Therefore, its measured $\delta^{18}O$ value is probably a minimum value.

The isotopic composition of the fluid supposed to have been in equilibrium with quartz was calculated using the quartz-H_2O fractionation equation of Zheng (1993) for a typical temperature range of 120 to 100°C (in agreement with fluid inclusion data) because quartz is known to be resistant to post-crystallisation isotope exchange in low-temperature conditions. The related fluid has a positive $\delta^{18}O$ value ($\delta^{18}O_{fluid}$ = 6.4 to 7.8‰ at 100°C, 9 to 10.3‰ at 120°C). The same kind of information is obtained using the calcite-H_2O fractionation equation of Kim and O'Neil (1997) combined with the dolomite-calcite fractionation coefficients of Sheppard and Schwarcz (1970) for the range of isotopic compositions measured in carbonates ($\delta^{18}O_{fluid}$= 4.6 to 7.5‰ at 80°C, 7.2 to 10.7‰ at 100°C). Nevertheless, the two estimates of the fluid $\delta^{18}O$ values fit only if we assume that carbonates crystallized or isotopically exchanged at temperatures which were slightly lower (-20°C) than the crystallisation temperature of quartz. This is not unreasonable if we consider the sensitivity of carbonates to post crystallisation isotopic exchange (e.g., O'Neil, 1987 and references therein). Taking into account the uncertainties of these estimates (especially the lowering of O activity in highly saline fluids) these data suggest that quartz and carbonates crystallized from a common fluid type, in agreement with paragenetic and fluid inclusions data. Two solutions exist for the estimated fluid $\delta^{18}O$ value: *c.* 6± 2 ‰ and *c.* 9 ± 1.5‰.

Measured fluid inclusion δD values range from -19 to -50 ‰ (Table 2.2) and discriminate the Poitou + (northern Limousin) mineralising fluids from those associated with similar mineralisation events in the south eastern edge of the Aquitain Basin (Fig. 2.8). Thus, in the $\delta D/\delta^{18}O$ space, our brines plot in a common sector in which compositions of metamorphic, diagenetic fluids and present-day basinal brines overlap (Fig. 2.8). On the basis of both the $\delta^{18}O$ and δD values, these fluids cannot be pristine marine waters. Such isotopic signatures may be those of fluids derived from deep and relatively high-temperature environments (metamorphic fluids, see Fig. 2.8), but this kind of source is difficult to conceive in the geodynamic context at the time and with the geometry of fluid flow (see below). Neither they correspond to fluids (of any primary origin) equilibrated at low-temperatures (100-150°C) with the basement lithologies (such as the local granitoids themselves) under low fluid/rock ratios, because such fluids would have had much lighter O isotopic ratios (e.g., in the range -3 to -8‰ if equilibrated with a granitic feldspar with $\delta^{18}O$= 8‰). They cannot be sea water, isotopically modified by evaporation, because δD values are too low for the estimated $\delta^{18}O$ range (see the evaporation trends in Fig.

2.8). Because we do not have access to direct measurement of both O and H in fluid samples, we cannot evaluate the possible existence of a correlation between $\delta^{18}O$ and δD values (equilibration vs. evaporation vs. mixing processes). Like many examples of basinal brines, the isotopic properties of our highly saline fluids, is likely to result from the combination of several processes among which evaporation and mixing effects (e.g., Knauth and Beeunas, 1986) combined with a strong interaction with ^{18}O -rich sediments at significant temperatures reaching 100-150°C (e.g., Taylor, 1987; Kyser and Kerrich, 1990 and references therein) are important. It is noteworthy that the rather homogeneous C isotopic composition of the fractures carbonates (-9 to -12 ‰) rules out the involvement of marine limestone lithologies (including the thin local overlying carbonated series of the "Poitou High") as the main source of the C in the brines. Theoretically, such values may be obtained by interaction with sediments containing both reduced and oxidized carbon (e.g., shales + carbonates). However, as discussed in another paper, the present brines scavenged carbon that was previously introduced into the basement lithologies (Fourcade et al., 2001). Actually, we must consider the brines as exotic in the sense given by Sheppard (1986).

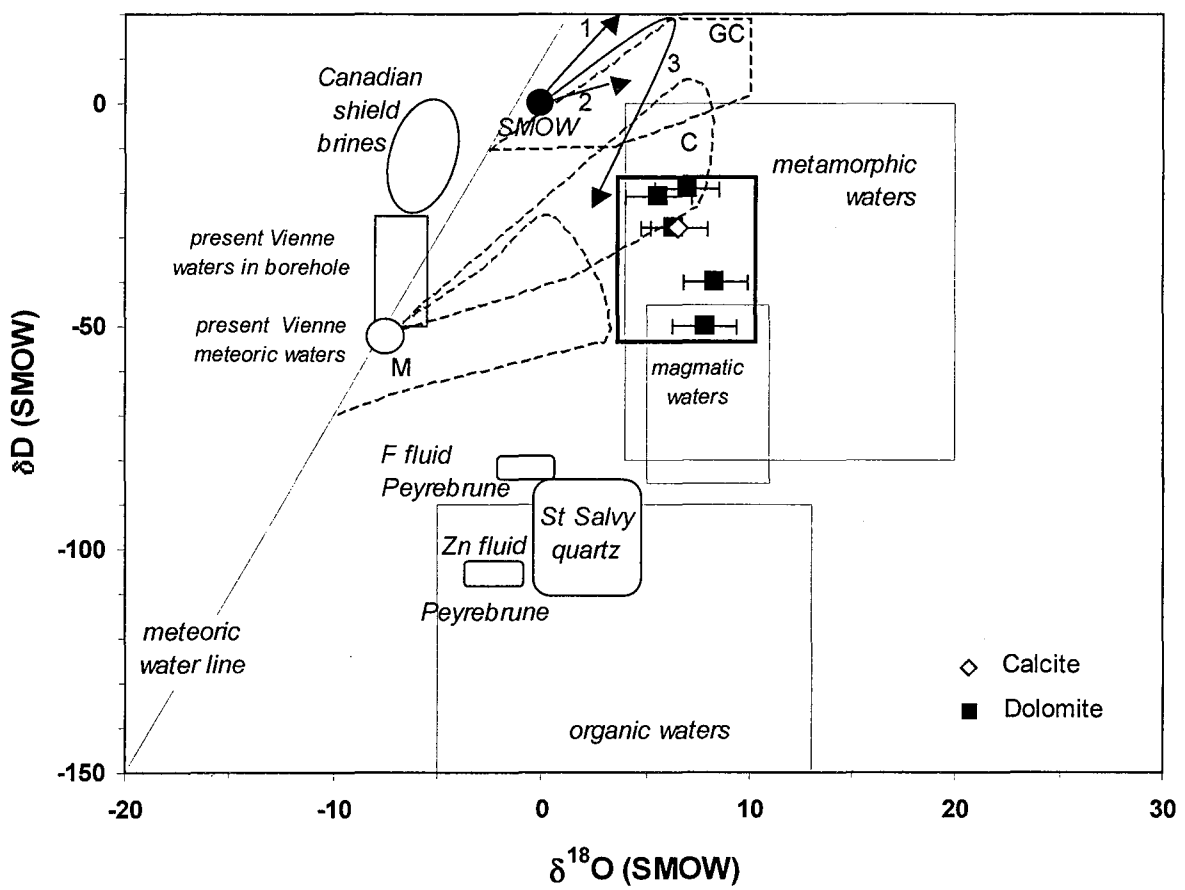

Fig. 2.8. δD and $\delta^{18}O$ values of fluids (symbols) associated with fractures infillings of the Charroux-Civray site and with mineralized sites of the northwestern edge of the French Massif Central. Also represented are the compositional fields of some representative fluids (organic waters from Sheppard and Charef, 1986, Basin waters from Sheppard (1984):GC = Gulf Coast; C = California; M = Michigan) as well as a typical sea-water evaporation trends (after Knauth and Beeunas, 1986, Pierre, 1989, initial evaporation under humid conditions (curve n°1) and for arid conditions (n°2), evaporation curve (n°3) from Pierre et al. (1984)), present day waters sampled in Vienne boreholes from Michelot (1999), Zn-mineralized sites of the S.E. edge of the Aquitaine Basin (after Munoz et al., 1995 and Munoz et al., 1999), and Canadian shield brines from Frape and Fritz (1987).

2.6 Discussion

2.6.1 Salt source

The study suggests that the solutions are primary brines, resulting from the evaporation from sea water, which evolved chemically during their migration at the unconformity between the Hercynian basement and the Infra-Liassic formations. The neighbouring Aquitaine Basin is the most obvious large-scale reservoir of evaporites which was available for such an interaction. As with the Paris Basin, the Aquitaine Basin contains two levels of salts of marine derivation: i) the first one is located at the bottom of the sedimentary pile in the Aquitaine basin and formed during an initial syn-rift phase (275 to *c.* 205 Ma, late Triassic) so-called "Salifère inférieur"; (Curnelle, 1983), ii) the second one is found in the infra-Toarcian sequence. The Hettangian series constitutes the second salt level and is found in the Charroux-Civray area: in that area, it contains horizons characterized by anhydrite nodules typical of emerged supratidal zones, and by breccias showing dissolution cavities from salt or sulfate dissolution. These levels correspond to a thick (≤ 900 m) Hettangian rhythmic evaporite sequence, which is overlain by a Sinemurian carbonate platform (Curnelle, 1983).

The primary brines involved in the studied area were probably derived from the Hettangian evaporites which cover a huge area at the base of the Aquitaine Basin series, including the northern part of the basin. The presence of evaporitic breccias in some of the drillings in the Vienne granite confirms the nearby occurrence of such levels.

2.6.2 Style of fluid migration

The temperatures indicate that the fluid flow took place at greater depths than today (present depth: 100 to 900 m) and probably, since the minimum amount of denudation is estimated in between 500 to 1000 m, for instance at more than 600 m in the infra-Toarcian paleo-aquifer. The homogeneity of the mineralogical sequence, laterally over tens of kilometers, and vertically over more than 700 m below the unconformity, indicate formation during a major fluid event that did not reoccur In this respect, the lack of mutual crosscutting relationships among the fracture infillings is very significant. From this feature, we infer that the migration of fluids was globally subhorizontal along the unconformity (Fig. 2.9). Thus, the easiest way for salty fluids, derived from the deep parts of the Aquitaine Basin, to reach the upper part of the series (the « Poitou High ») was to travel at the basement/basin boundary during the expulsion associated with maximum burial. The lack of mineralized fractures above the Toarcian could indicate that the fluid migration did not occur above the series of impermeable shales.

2.6.3 Age of the process

The age of brine circulation is not precisely known. The burial of sediments and the basement fractures is linked to the role of distensive movements affecting the

basement and its sedimentary cover after Toarcian. The "post-rift" period, which lasted until Upper Jurassic, is however dominated by thermal subsidence (Brunet, 1983). The maximum compaction in that part of the basin may have occurred during or slightly after the Barremian (Brunet, 1983). Over a long period, the evolution of the Aquitaine Basin can be explained in terms of crustal stretching and lithospheric thinning. Thus, the optimum epochs for fluid circulation were likely to be the extension periods, when the geothermal gradient was elevated. In the absence of absolute dating of the fractures, we speculate that this fluid flow could have occurred during either:

(a) the Lias-Dogger: indirect dating of the process was given by K-Ar dates obtained on the finest fractions of clays sampled within fractures of the Vienne granites, fractures that have experienced the brine episode (*c.* 160-170 Ma, Cathelineau et al., 2001); the most significant extensional episode occurred at the Lias-Dogger transition, around 180 Ma ago (Bonhomme, 1982, Curnelle and Dubois, 1986). Coeval with this extension, a significant hydrothermal event is recorded in several sites from the southern Massif Central (Leveque et al., 1988; Lancelot and Vella, 1989; Respault et al., 1991). At this period, the thickness of the sediments around the " Poitou High " may have not have been more than two or three hundreds of meters and the temperature at the level of the unconformity could not have exceeded a few tens of degrees (30-40°C at maximum). Nevertheless, long-distance migration of fluids, in complete thermal disequilibrium (*c.* 100°C), circulating at the basin-basement boundary, i.e., in a cold aquifer, without significant cooling is difficult to envisage;

(b) the Oxfordian-Kimmeridgian (*c.* 145 Ma), or (c) the Barremian-Aptian intervals (*c.* 110 Ma) which also coincide with new rifting episodes (Brunet, 1983), especially the Gascogne Gulf rifting. A K-Ar date of 112 Ma was obtained on one sample of adularia extracted from a fracture infilling in the Vienne granite (Cheilletz et al., 1997). Although the thickness of the sedimentary sequence at that time is debated in the Poitou High, more than 6 km of sediments were deposited in the Aquitaine Basin at that time. This situation is also very favourable to a release of hot fluids (around 180°C for a thermal gradient of 30°C/ km).

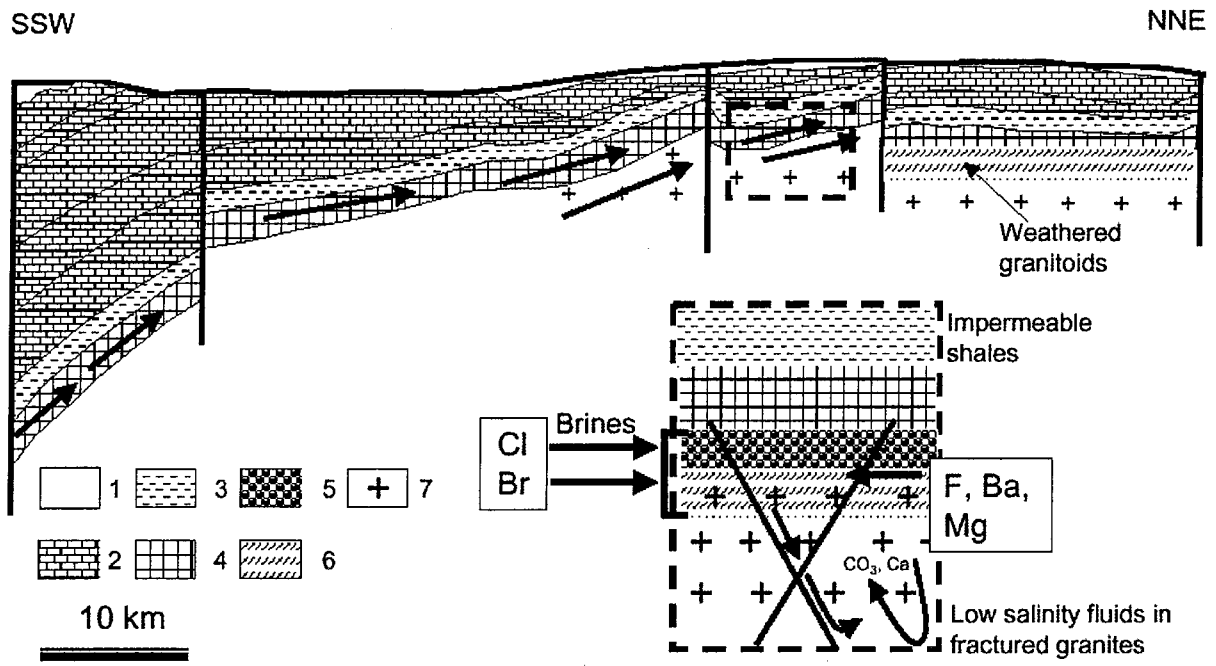

Fig. 2.9. Schematic model of the hydrothermal circulations within the Charroux-Civray plutonic complex at the unconformity surface. 1-Tertiary cover, 2 - Mesozoïc limestones, 3- Impermeable shales, Toarcian formation, 4- basal silicoclastic series and dolomites, Infra Lias, 5 - Basal silicoclastic series, 6 - Weathered basement (paleosurface with supergene oxidized facies), 7 - Granitoids (hercynian basement).

2.7 Conclusions

Distensive movements, probably Mesozoic in age, related to the opening of the Atlantic ocean or of the Gascogne gulf produced significant fluid movements at the basement/cover interface in the north-western margin of the French Massif Central.

90% of the present day sealed fractures are fractures that were opened (or re-opened if formed earlier during Hercynian stages) and re-sealed at that time. The settling of a palaeo-aquifer at the bottom of the sedimentary sequence and at the top of the granites, previously weathered during the emersion period (post-Trias, ante-Hettangian), introduced a significant connexion between the top of the aquifer and the fractured granite at depth and favoured the systematic sealing of fractures down to at least 800 m depth. The extreme efficiency of the sealing process can be attributed to: i) a major interaction between brines and the host granite, with a redistribution of the stock of ancient carbonates disseminated in granites (Fourcade et al., 2001) and local extraction of Ba and F from weathered feldspars and biotite (± amphibole) respectively, and to ii) the cooling of the hot fluids expelled from the deepest part of the Aquitain Basin to its rather cool edge (the top part of the Poitou High).

The chemical consequence of brine migration was the introduction of F, Ba, Cl, into the basement. Since no brines were significantly trapped as fluid inclusions in the host rocks (no healing of microfissured quartz, very limited mineral crystallisation in fractures), this indicates: i) either that the conditions allowing an efficient trapping of fluids in rock-forming minerals were not matched, or possibly; ii) that the intrinsic

permeability of basement rocks in the volumes located between drains was rather small.

Actually, the fact that carbonates in the host granites were somewhat remobilized argues that the small-scale permeability was not negligible at the time scale of the sealing event, and also indicates that a part of the material filling fractures in the granite was of local provenance. Thus, the image suggested by the palaeofluid circulations in the Charroux-Civray site is that of a system in which the fluid movements were controlled by a double-permeability medium, most of the fluid flow being accommodated by macroscopic (cm wide, dm to meter long) fractures and not by microfractures. The brines probably penetrated deeply downwards in the basement as shown by samples at more than 700m depth (maximal depth reached by drillings) through dense sets of connected macrofractures. The sealing is likely to be linked to the mixing between the brines and a dilute fluid probably of meteoric origin, infiltrated from emerged zones. The mixing process is likely the key factor that promoted precipitation of the dolomite/ fluorite (± sulphide) association as modelled by Azaroual and Fouillac (1999). According to these authors, dilution of brines with only 10% of cold meteoric water is able to explain a significant amount of mineral precipitation and reproduces the mineral crystallisation sequence which is observed in the studied case.

The mass transfer linked to the brine introduction had probably a significant impact on the geochemical features of the interstitial fluids in granites since Mesozoïc times. The discovery of deep saline (up to 10g/kg solution) groundwaters in the Vienne granitic rocks (Casanova et al., 2001) can be explained by the early penetration of the brines (up to 150 g/ kg solution), probably followed at a lesser extent by marine water percolation. The history of palaeo-fluid migration in the Hercynian basement is therefore of great interest for the understanding of the present water chemistry in deep aquifers.

ACKNOWLEDGEMENTS

This work has been initiated within the framework of contracts commissioned by Andra (Agence Nationale pour la gestion des Déchets Radioactifs = French Nuclear Waste Management Company) and within the framework of the group "Cristallisations dans les fractures" leaded by J.F. Aranyossy. This study was then supported by the GdR FORPRO - Action 98-III (paper FORPRO n° 2001/11 A), a National Research Program between CNRS and Andra. Andra is acknowledged for the facilities and permission of sampling the drill cores. S. Buschaert benefits of a grant from Andra for completion of his PhD.

S.C.D. - U.H.P. NANCY 1
BIBLIOTHÈQUE DES SCIENCES
Rue du Jardin Botanique - BP 11
54601 VILLERS-LES-NANCY Cédex

REFERENCES

Azaroual, M., Fouillac, C., 1999. Thermodynamic modelling of modern basinal brines from the Paris Basin: Implication for MVT ore genesis. In Mineral Deposits, Process to Processing, Stanley et al., Eds, Balkema, vol. 2, 809-812.

Banks, D.A., Davies, G.R., Yardley, B.W.D., McCaig, A.M., Grant, N.T., 1991. The chemistry of brines from an Alpine thrust system in the Central Pyrenees: An application of fluid inclusion analysis to the study of fluid behaviour in orogenesis. Geochim. Cosmochim. Acta 55, 1021-1030.

Banks, D.A. Giuliani, G., Yardley, B.W.D., Cheilletz, A. 2000. Emerald mineralisation in Colombia: Fluid chemistry and the role of brine mixing. Mineral. Deposita 35, 699-713.

Bertrand, J.M., Leterrier, J., Delaperrière, E., Brouand, M., Cuney, M., Stussi, J.M., Virlogeux, D., 2000. Géochronologie U-Pb sur zircon de granitoides du Confolentais, du massif de Charroux-Civray (seuil du Poitou) et de Vendée. Bull. Soc. Geol. Fr. in press.

Bodnar, R. J., 1993. Revised equation and table for determining the freezing point depression of H_2O-NaCl solutions. Geochim. Cosmochim. Acta 57, 683-684.

Bohlke, J.K., Irwin, J.J., 1992. Laser microprobe analyses of noble gas isotopes and halogens in fluid inclusions: Analyses of microstandards and synthetic inclusions in quartz. Geochim. Cosmochim. Acta 56, 187-201.

Bonhomme, M.G., 1982. Age triasique et jurassique des argiles associées aux minéralisations filoniennes et des phénomènes diagénétiques tardifs en Europe de l'Ouest - Contexte géodynamique et implications génétiques. C.R. Acad. Sci. 294, 521-524.

Brunet M.F., 1983. La subsidence du bassin d'Aquitaine au Mésozoïque et au Cénozoïque. C.R. Acad. Sci. 297, 599-602.

Capdevila R., 1997. Les suites plutoniques métaalumineuses recoupées par les forages Andra de la Vienne: caractérisation, mode de mise en place et discussion du contexte géodynamique. Journées Scientifiques Andra, Poitiers, p.7.

Carpenter, A.B., Trout, M.L., Pickett, E.E., 1974. Preliminary report on the origin and chemical evolution of lead- and zinc-rich oil field brines in central Mississippi. Econ. Geol. 69, 1191-1206.

Casanova, J., Negrel, P., Kloppmann, W., Aranyossy, J.F., 2001. Origin of deep saline groundwaters in the Vienne granitic rocks (France): constraints inferred from boron and strontium isotopes. Geofluids 1, 91-102.

Cathelineau, M., Cuney, M., Boiron, M.C., Coulibaly, Y., Ayt Ougougdal, M., 1999. Paléopercolations et paléointeractions fluides/roches dans les plutonites de Charroux-Civray - Etude du Massif de Charroux-Civray. Actes des Journées Scientifiques CNRS/Andra, Poitiers, EDP Sciences, 159-179.

Cathelineau, M., Fourcade, S., Clauer, N., Buschaert, S., Rousset, D., Boiron, M.C., Martineau, F., Meunier, A., Javoy, M., Nitjchoua, R., 2001. Multistage paleofluid percolations in granites: A stable isotope and K-Ar study of fracture illite from Vienne plutonites (N.W. of the french Massif Central). Clay Min., submitted.

Cheilletz, A., Cuney, M., Coulibaly, Y., Brouand, M., Cathelineau, M., Stussi, J.M., 1997. L'adularisation à l'interface socle/couverture dans la région de Charroux - Civray. Journées. Scientifiques. Andra, Poitiers, p 16.

Crawford M.L., 1981. Phase equilibria in aqueous fluid inclusions. In MAC short course on fluid inclusions, Mineral. Assoc. Can., Hollister and Crawford Eds, 75-100.

Cuney, M., Brouand, M., Stussi, J.M., Gagny, C. 1999. Le massif de Charroux-Civray (Vienne): un exemple caractéristique des premières manifestations plutoniques de la chaîne hercynienne - Etude du Massif de Charroux-Civray. Actes des Journées Scientifiques CNRS/Andra, EDP Sciences, Poitiers, 63-104.

Curnelle, R., 1983. Evolution structuro-sédimentaire du Trias et de l'infra-lias d'Aquitaine. Bull. Cent. Rech. Explor. Prod. Elf Aquitaine 7-1, 69-99.

Curnelle, R., Dubois, P., 1986. Evolution mésozoïque des grands bassins sédimentaires français, bassin de Paris, d'Aquitaine et du Sud-Est. Bull. Soc. Géol. Fr. 8, 529-546.

Fallick, A.E., Jocelyn, J., Hamilton, P.J., 1987. Oxygen and hydrogen stable isotope systematics in Brazilian agates. In: Rodriguez Clemente, E. (Ed.), Geochemistry of the Earth Surface and Processes of Mineral Formation, 99-117.

Fontes, J.C., Matray, J.M., 1993 . Geochemistry and origin of formation brines from Paris Basin, France. 1. Brines associated with triassic salts. Chem. Geol. 109, 149-175.

Fouillac, C., Michard, G., 1981. Sodium/lithium ratio in water applied to geothermometry of geothermal reservoirs. Geothermics 10, 55-70.

Fourcade, S., Michelot, J.L., Buschaert, S., Cathelineau, M., Freiberger, R., Coulibaly, Y., Nitjchoua, R., 2001. Early introduction of carbon in plutonic rocks and its successive remobilizations during subsurface fluid-rock interactions : the case study of the Vienne granitoids (France). In prep.

Fournier, R.O., 1979. A revised equation for Na/K geothermometer. Geotherm. Res. Counc. Trans., 3, 221-224.

Frape, S.K., Fritz, P., 1987, Geochemical trends from groundwaters from the Canadian Shield. In: Saline waters and gases in crystalline rocks. Fritz, P and Frape, S.K. Eds. Geol. Assoc. Canada Spec. Paper, 33, 19-38.

Horita, J., Friedman, T.J., Lazar, B., Holland, H.R., 1991. The composition of Permian seawater. Geochim. Cosmochim. Acta 55, 417-432.

Kesler, S.E., Martini, A.M., Appold, M.S., Walter, L.M., Huston, T.J., Furman, F.C., 1996. Na-Cl-Br systematics of fluid inclusions from Mississippi Valley-type deposits, Appalachian basin: Constraints on solute origin and migration paths. Geochim. Cosmochim. Acta 60, 225-233.

Kharaka, Y.K., Maest, A.E., Carothers, W.W, Law, L.M., Lamothe, P.J., Fries, T.L., 1987. Geochemistry of metal-rich brines from central Mississippi Salt dome Basin, USA. Applied Geoch., 2, 543-561.

Kim, S.T., O' Neil, J.R., 1997. Equilibrium and non-equilibrium oxygen isotope effects in synthetic carbonates. Geochim. Cosmochim. Acta 61, 3461-3475.

Knauth, L.P., Beeunas, M.A., 1986. Isotope geochemistry of fluid inclusions in Permian halite with implications for the isotopic history of ocean water and the origin of saline formation waters. Geochim. Cosmochim. Acta 50, 419-433.

Kyser, T.K., Kerrich, R., 1990. Geochemistry of fluids in tectonically active crustal regions. In " Short Course on Fluids in Tectonically Active Regimes of the Continental Crust ", Min. Assoc. Canada, Vancouver, Nesbitt, B.E., ed,.18, 133-230.

Lancelot, J., Vella, V., 1989. Datation U-Pb liasique de la pechblende de Rabajac - Mise en évidence d'une préconcentration uranifère permienne dans le bassin de Lodève (Hérault). Bull. Soc. Géol. Fr. 8, 309-315.

Leveque, M.H., Lancelot, J.R., George, E., 1988. The Bertholène uranium deposit-mineralogical characteristics and U-Pb dating of primary U mineralisation and its subsequent remobilization: consequences for the evolution of the U-deposits of the Massif Central, France. Chem. Geol. 69, 147-163.

Lhomme, T., Dubessy, J., Rull, F., 1999. Determination of chlorinity in aqueous fluids using Raman spectroscopy at room temperature. GeoRaman'99, Valladolid, Spain, 93-94.

Michelot, J.L., 1999, Les eaux du système granitique de la Vienne: reconnaissance hydrogéochimique et isotopique, In: Etude du Massif de Charroux-Civray, Actes des journées scientifiques Andra, Poitiers, EDP Sciences. 181-199.

Munoz, M., Boyce, A.J., Courjault-Rade, P., Fallick, A.E., Tollon, F., 1995. Multi-stage fluid incursion in the Palaeozoic basement-hosted Saint-Salvy ore deposit (NW Montagne Noire, southern France), International Journal of Rock Mechanics and Mining Science & Geomechanics Abstracts, 32, 5, 202A .

Munoz M.,. Boyce A. J, Courjault-Rade P., Fallick A. E., Tollon F., 1999. Continental basinal origin of ore fluids from southwestern Massif Central fluorite veins (Albigeois, France): evidence from fluid inclusion and stable isotope analyses, Appl. Geochem. 14, 447-458

O' Neil, J.R., 1987. Preservation of H, C, O isotopic ratios in the low temperature environment. In " Short Course in Stable Isotope Geochemistry of Low Temperature Fluids ", Min. Assoc. Canada, Saskatoon , Kyser, T.K., ed., 13, 85-128.

Peiffer, M.-T., 1986. La signification de la ligne tonalitique du Limousin. Son implication dans la structuration varisque du Massif Central français. C.R. Acad. Sci. Paris 303-II, 305-310.

Pierre, C., Ortlieb L., Person A., 1984. Supratidal evaporitic dolomite at Ojo de Liebre lagoon: mineralogical and isotopic arguments for primary crystallization. J. Sedimen. Petrol. 54, 1049-1061.

Pierre, C., 1989. Sedimentation and diagenesis in restricted marine basins. In " Handbook of Environmental Isotope Geochemistry, 3. The Marine Environment ", Fritz, P. and Fontes, J.C., eds, Elsevier, Amsterdam, 257-315.

Poty, B., Leroy, J., Jachimovicz L., 1976. Un nouvel appareil pour la mesure des températures sous le microscope: l'installation de la microthermométrie Chaixmeca. Bull. Soc. Fr. Minéral. Cristallogr., 99, 182-186.

Respault, J. P., Cathelineau M., Lancelot J.R., 1991. Multistage evolution of the Pierres Plantées uranium ore deposit (Margeride, France) : evidence from mineralogy and U-Pb systematics. Eur.J. Mineral. 3, 85-103.

Rolin, P., Colchen M., 1995. Le socle cristallin du Confolentais le long de la vallée de la Vienne. Andra Report # OUTPT 95001, 91p.

Shaw, A., Downes H., Thirlwall M.F., 1993. The quartz diorites of Limousin: elemental and isotopic evidence for Devono-Carboniferous subduction in the Hercynian belt of the French Massif Central. Chem. Geol. 107, 1-18.

Sheppard, S.M.F., 1984. Stable isotopes studies of formation waters and associated Pb-Zn hydrothermal ore deposits. In: Thermal phenomena in sedimentary basins. Ed. Technip 301-317.

Sheppard, S.M.F., 1986. Characterization and isotopic variations in natural waters. In " Stable isotopes in high temperature geological processes ", Reviews in Mineralogy Min. Soc. Am., Valley, J.W., Taylor, H.P., Jr., O'Neil, J., eds, 16, 165-183.

Sheppard, S.M.F., Schwarcz, H.P., 1970. Fractionation of C and O isotopes and magnesium between coexisting metamorphic calcite and dolomite. Contrib. Mineral. Petrol. 26, 161-198.

Sheppard, S.M.F., Charef, A., 1986. Eau organique: caractérisation isotopique et évidence de son rôle dans le gisement Pb-Zn de Fedj-el-Adoum, Tunisie. C.R. Acad. Sci. 302-II, 1189-1192.

Taylor, B.E., 1987. Stable isotope geochemistry of ore-forming fluids. In " Short Course in Stable Isotope Geochemistry of Low Temperature Fluids ", Min. Assoc. Canada, Saskatoon, Kyser, T.K., ed., 13, 337-345.

Verma, S., Santoyo, E., 1997. New improved equations for Na/K, Na/Li and SiO_2 geothermometers by outlier detection and rejection. J. Volcanol. Geotherm. Res. 79, 9-23.

Zheng, Y.F., 1993. Calculation of oxygen isotope fractionation in anhydrous silicate minerals. Geochim. Cosmochim. Acta 56, 1079-1091.

Ziserman A., 1980. Le gisement de Chaillac (Indre): la barytine des Redoutières, la fluorine du Rossignol. Association d'un gite stratiforme de couverture et d'un gite filonien du socle . 26° CGI, Gisements français, Fascicule E3.

3 MULTISTAGE PALEOFLUID PERCOLATIONS IN GRANITES: A STABLE ISOTOPE AND K-AR STUDY OF FRACTURE ILLITE FROM THE VIENNE PLUTONITES (N.W. OF THE FRENCH MASSIF CENTRAL)

M. Cathelineau[a], S. Fourcade[b], N. Clauer[c], S. Buschaert[a,f], D. Rousset[c], M.C. Boiron[a], F. Martineau[b], A. Meunier[d], V. Lavastre[e,f], M. Javoy[e]

[a] UMR G2R 7566 - CREGU, BP23, 54501 Vandoeuvre-lès-Nancy, France
[b] Géosciences Rennes (UMR 6118), Univ. Rennes 1, 35042 Rennes Cedex, France
[c] CGS - Université de Strasbourg, France
[d] HydrAsa - Université de Poitiers, France ; [e] IPGP, Univ. Paris VII, France
[f] Andra, French Agency for Nuclear Waste Management, 92298 Châtenay-Malabry

Submitted to Clay minerals

Figure captions ***3-82***
Table captions ***3-82***
Abstract ***3-83***

3.1 INTRODUCTION ***3-85***

3.2 SAMPLE DESCRIPTION ***3-87***

3.3 ANALYTICAL METHODS AND RESULTS ***3-90***
3.3.1 Mineral separation and characterization 3-90
3.3.2 Crystal-chemistry of illite and chlorite 3-92
3.3.3 K-Ar measurements 3-95
3.3.4 Stable isotopes measurements 3-96
3.3.5 Results 3-96

3.4 DISCUSSION ***3-100***
3.4.1 Isotopic signatures of the fluids 3-100
3.4.2 Age and geodynamic context of brines circulation 3-101

3.5 CONCLUSIONS ***3-103***
Acknowledgements ***3-104***
References ***3-105***

FIGURE CAPTIONS

Fig. 3.1. Map of the Charroux-Civray area with the northwestern part of the Massif Central and locations of the drilling sites (modified from Rolin and Colchen, 1995). At the drilling locations, the basement is covered by about 150 m thick sedimentary rocks of Jurassic age (white area). The basement beneath Charroux-Civray is mainly built-up by medium-K and high-K calcalkaline intrusions and its local contours have been derived from geophysical investigations. 3-86

Fig. 3.2. Photomicrographs of typical alteration assemblages in the clay rich fractures and their host rocks. Clay rich fracture (breccia in fault) impregnated with iron hydroxides. A: macroscopic features, B: breccia with clasts of deformed granodiorite cimented by illite and iron hydroxides; C: illite , D : illite and chlorite (+ pyrite). 3-89

Fig. 3.3. Examples of deconvoluted XRD patterns of the K-micas populations using Lansons' method (Lanson, 1990). 3-91

Fig. 3.4. Diagrams for K-micas identification. A: Si^{IV} - interlayer charge, and chlorite B: Fe/Mg vs Si^{IV} from the clay-rich fractures. 3-93

Fig. 3.5. MR3-2R3-3R2 diagram from Velde (1977) applied to clay particle analyses from the clay rich fractures. 3-95

Fig. 3.6. Oxygen isotopic composition of clay fractions in the fractures from the Vienne plutonites as a function of their K-Ar age. Except for fractions of the 8606f sample, the lines are the best fits corresponding to the different size fractions of the samples 5183f, 8799f and 2422f. 3-98

Fig. 3.7. Depth distribution of O isotopic data (A) and K/Ar ages (B) on clay fraction from the clay rich fractures. 3-99

TABLE CAPTIONS

Table 3.1. Main features of the studied samples (drilling, type of enclosing rock, petrography and XRD mineralogy). 3-88

Table 3.2. Crystal-chemistry of chlorites with indication of mean compositions and standard deviation (s.d.). 3-92

Table 3.3. Crystal-chemistry of K-micas with indication of mean compositions and standard deviation (s.d.). 3-94

Table 3.4. Isotopic data ($\delta^{18}O$ and δD vs. SMOW and K-Ar ages) obtained on the clay-rich material filling the fractures within the Vienne granitoids. 3-97

ABSTRACT

Age determination of fluid percolations in old fractures from basement rocks is of particular interest for the reconstruction of palaeo-hydraulic regimes at depth. However, in most cases no material is suitable to be easily dated. In the specific case of the north-western margin of the French Massif Central, basinal brines have percolated within the Hercynian crystalline basement and its sedimentary cover (Infra-Toarcian formations) yielding to subsequent fracture or porosity sealing. The fluid at the origin of the fracture fillings was interpreted as either a deep sedimentary brine expelled during a period of maximal subsidence or a fluid travelling upward along unconformities, throughout the evaporite sequences of infra-Toarcian age (Rhaetian-Hettangian, or Keuper) at an unknown period of time. These fluids produced an intense sealing of most fractures from the basement as carbonates, and a discrete re-crystallization of the early Hercynian phyllosilicates (phengite-chlorite) into (illite/smectite) minerals in the earlier phyllosilicate (chlorite-illite) rich fractures.

Using a specific method for the extraction without contamination of the finest newly formed fractions, clay fractions are identified by XRD, MEB, MET, and then analyzed for stable isotope composition (D/H, $\delta^{18}O$) and dated by the K-Ar method. DRX patterns show that the clay fraction is by far dominated by illite layers and ordered mixed-layer minerals having a rather high amount of illite (R3 I/S). These 10 Å layers are accompanied by chlorite, and minor amounts of pyrite, kaolinite, and other I/S minerals. The late assemblage attributable to the brine stage is observed in some samples, and is identified as a mixture of I/S minerals and 10/14 Å mixed-layer minerals, but not separable from the other clay minerals.

D/H values of the clay fractions is fairly constant around -50‰ ± 10‰, but $\delta^{18}O$ values of the same clay fractions display a wide range from 8 to 18‰ (SMOW). The study of the granulometric fractions between 2 and 0.2 μm reveals a correlation between K-Ar ages and $\delta^{18}O$ values, although no significant variation is registered in the relative amounts of chlorite and illite. The finest fraction (<0.2 μm) dated at 188± 5 Ma presents a $\delta^{18}O$ value of 15.73‰. This value is similar to that of the clay fraction issued from fractures affected by the palaeo-surface. Deep fractures (at depth of 570 and 923 m) are, on the contrary, characterized by $\delta^{18}O$ values around 10.3 ± 0.4 ‰ SMOW and rather old ages, in between 253 Ma and 272 Ma. Newly formed clay fractions are interpreted as formed at an age younger than 188 Ma from a fluid having a $\delta^{18}O$ of around 5 ± 2 ‰ compatible with the data obtained on other contemporaneous minerals (quartz, carbonates). This age is intermediate between the main distensive stages known at 180 Ma and 110 Ma, corresponding to the main rifting episodes linked to the rifting of the Atlantic ocean and Gascogne gulf.

Keywords : illite, fracture, multiphase hydrothermal alteration, stable isotopes, K-Ar dating, fluid-rock interaction.

3.1 Introduction

In fractured basement rocks, the precise determination of the relative and even the absolute chronology of fluid flow events is of critical interest to understand and predict the hydraulic regimes at depth. However, dating fluid circulations in fractures of basement rocks is a difficult task because the fluid events did not necessarily induce the growth of newly-formed minerals. Moreover, most fractures of crystalline basement rocks are often filled with minerals which are not suitable for isotopic dating (quartz, sulphates, carbonates). The knowledge of this chronological information is important for any research project dealing with the safety of deep aquifers near underground laboratories or testing potential areas for nuclear waste disposal. The nature of fluids circulating within a basement and within its sedimentary cover, their geometry and the causes of fluid migrations are also important to be constrainted (Blyth et al., 2000; Fourcade et al., 2001).

An alternative for direct isotopic datation of fluid circulations in fractures is to examine in great detail the phyllosilicates contained in host rocks at the vicinity of fractures or in the composite fracture fillings made of vein material and host rocks. It might be expected that, in some instances, phyllosilicates of detrital origin (or inherited from early alteration stages), when submitted to a new fluid flow event, may react with the fluids to form small amounts of newly-formed or recrystallized minerals. The main difficulty encountered concerns the separation of the minute amounts of newly-formed or recrystallized particles from inherited (or partly reequilibrated) phyllosilicates. A best-suited methodology is therefore needed to extract and carefully characterize the finest newly formed clay mineral fractions before any dating attempt. XRD together with MEB, MET and stable (H, O) isotopic studies, are used to identify the clay minerals fractions and to assess the related conditions of fluid circulation, while K-Ar systematics may enlight the epoch(s) of fluid flow(s).

An attempt to date fluid flow by this method was performed on the Hercynian fractures located in the Vienne basement plutonites, in the north-western edge of the French Massif Central (the Charroux-Civray granitoids, Fig. 3.1). This area was investigated by the Andra (French national agency for nuclear waste management) for a possible setting of an experimental underground laboratory devoted to long term nuclear waste disposal. The Vienne plutonites display irregularly distributed but well-developped sets of fractures. Using paragenetic and fluid-inclusion studies (Fluid Inclusions frequently on quartz), at least three main stages of fluid flows were identified in the Charroux-Civray granitoids, each stage being characterized by extremely distinct P-T conditions and geodynamic contexts (Cuney et al., 1999, Coulibaly, 1998, Cathelineau et al., 1999, Boiron et al., 2001, Fourcade et al., 2001).

The early stage (noted I) of hydrothermal (s.l.) origin and Hercynian age, is characterized by veins filled by rather "high temperature" mineral assemblages involving phyllosilicates: (epidote)-quartz-chlorite-phengite (hematite) ± carbonates (dolomite I, calcite I) ± adularia, quartz-muscovite, quartz-sulphides-illite. This stage and its typical parageneses are widespread and well known in the northern Massif Central (Boiron et al., 1989; Essarraj et al., 2001). It involved late metamorphic fluids (or externally-derived fluids close to chemical and thermal equilibrium with basement lithologies at c. 350 - 450°C) followed by convective geothermal fluids near shallowly located peraluminous granitic intrusions (4-5 km).

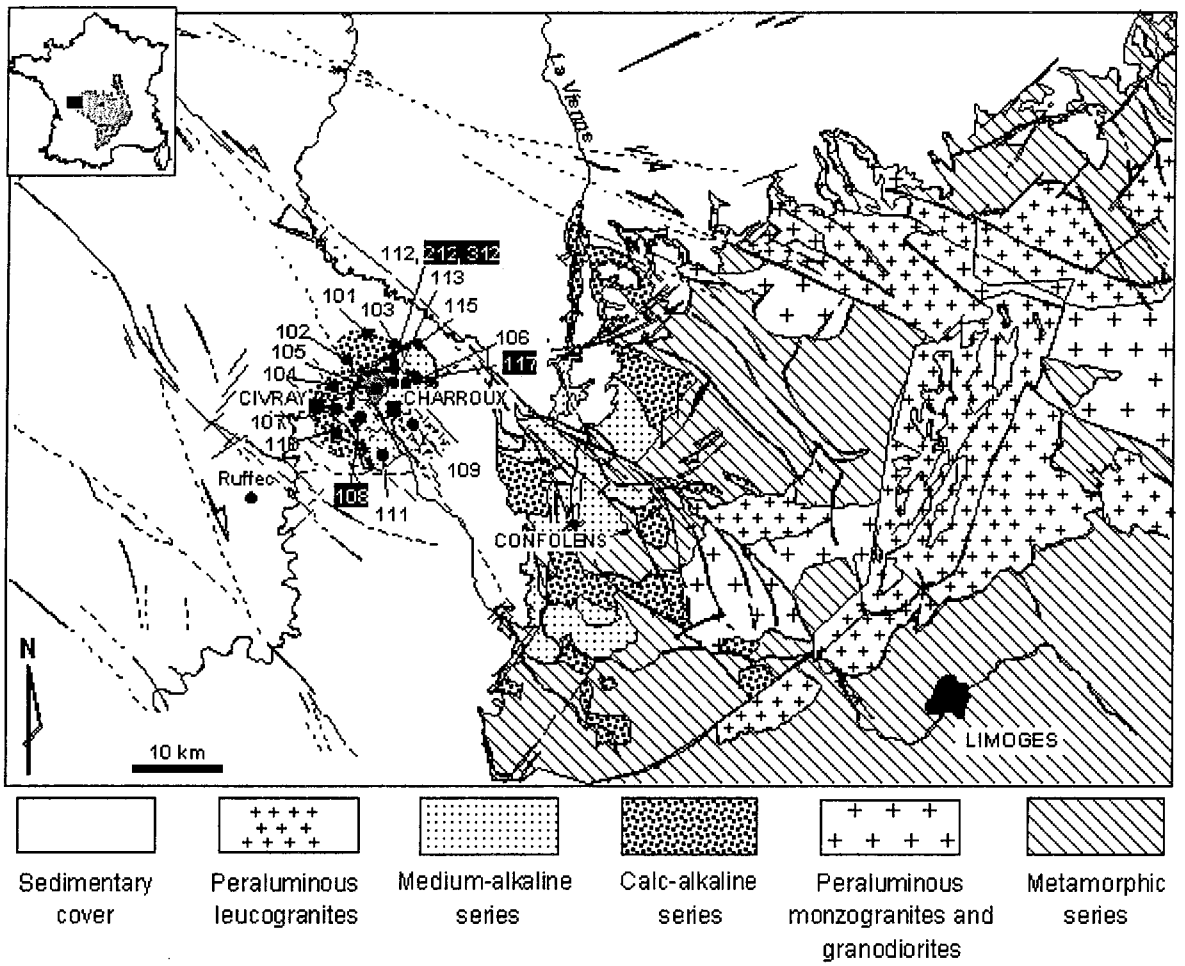

Fig. 3.1. Map of the Charroux-Civray area with the northwestern part of the Massif Central and locations of the drilling sites (modified from Rolin and Colchen, 1995). At the drilling locations, the basement is covered by about 150 m thick sedimentary rocks of Jurassic age (white area). The basement beneath Charroux-Civray is mainly built-up by medium-K and high-K calcalkaline intrusions and its local contours have been derived from geophysical investigations.

The second stage (noted II) of fluid flow produced a carbonate dominated (+ fluorite and barytine) assemblage without clay minerals. This event occurred during the Mesozoic, after the Hettangian, since the sediments overlying the granitoids display in their cavities, the same mineral assemblages as those filling the poral system of the plutons. Such veins are largely predominant in the studied drill cores of the basement down to 800 m beneath the basement - cover interface. They are also observed in the lower part of the sedimentary cover (Hettangian/ Sinemurian series). This stage II was interpreted as following the migration of brines along the basement/cover boundary (Boiron et al., 2001) during extensional tectonics, brines which were expelled from the deepest parts of the Aquitanian sedimentary basin (Fig. 3.1). Mesozoic brines event produced a very efficient sealing of the ancient (and possibly newly-formed) fractures in the granitic basement, while the porosity of the overlaying sedimentary cover (infra-Toarcian) was partially reduced. However, the process is not yet precisely dated.

These two kinds of fractures are frequently crosscut by later veins (stage III) filled with kaolinite and calcite.

All these fractures are almost partially to totally sealed and, probably, they never experienced re-opening after sealing. They do not contribute really to the present-day hydrological system. Nevertheless, a few clay-rich fractures are characterized by recurrent fluid circulations from Hercynian to the present time. Some of them were water productive during the drilling process and collected during the hydrological survey (Casanava et al., 2001). These are originally Hercynian faults formed under high temperature conditions and affected by ductile, then brittle deformations. The nature of their fillings (phengite-chlorite), in the lack of quartz or predominant carbonate, is in relation with a rather high hydraulic conductivity. They experienced, therefore, different events of fluid flow, including the Mesozoic one, and were affected geochemically and mineralogically by the related fluid-rock interactions.

The events of fluid circulations are not well known, but according to their temperatures, fluid densities, compositions and origins, a model has been achieved (Fourcade et al., 2001; Boiron et al., 2001). The aim of the present work is to constrain in time this model by dating the post-Hercynian circulation stages which affected the Hercynian fractures. The analytic procedure comprised extraction, oxygen and hydrogen isotopic characterization and K-Ar dating of the clay fractions in different types of Hercynian plutonic basement fractures.

3.2 Sample description

An outstanding suite of unweathered rocks has been revealed by a recent detailed study of a 125-km^2 area of Hercynian granitic plutons located between the Armorican Massif and the Massif Central in western France, underneath a 150-m thick sedimentary cover consisting of Mesozoic limestones and clay rocks. Clay-rich fractures were selected from four deep drillings of the Charroux-Civray area (Fig. 3.1; drill holes CIV108, CHA117, CHA212 and CHA312). Some specific features of the host-rocks are presented in Table 3.1 on the basis of petrographic observations and XRD analysis. Two main types of samples were identified: i) samples located close to the basement/cover unconformity (in fact a few tens of meters below). This brownish zone due to a significant impregnation by hematite and goethite clearly displays oxidation features linked to an emersion stage that occurred between the Hercynian cycle and the transgression of the Mesozoic sea. ii) samples from slightly (around 240 ± 10 m) to significantly deeper (570 m, 923 m) levels are devoid of oxidation.

A <u>first pervasive alteration stage,</u> post-dating early retrograde metamorphic assemblages (Ca-silicates) is widespread in all samples. It corresponds to the largest alteration halos, frequently along major fractures in highly fractured plutonites, and it is characterized by this association: chlorite, phengite, dolomite, calcite, pyrite (or hematite). Alteration minerals are mostly found in close association with primary minerals: hornblende is frequently altered to chlorite, calcite and hematite, biotite is partially or totally replaced by chlorite (± K-feldspar as adularia) which is frequently associated with anatase and hematite. Ca-plagioclase is replaced by calcite and phengite, and carbonate may be locally oriented parallel to the biotite cleavage. K-feldspars are better preserved but display also some phengite patches. Titanite is replaced by anatase and carbonate. The whole mineral association can also be

found in thin microfractures. The studied samples correspond to fractures with long-lived activity starting under ductile deformation (C-S structures), and continuing in brittle context, the fault producing breccia with elements of the ductile deformed plutonites (Fig. 3.2).

An illite or an ordered I/S, with a high content of illite layers, may be found locally together with chlorite and dolomite. This mineral association, which is locally well developed, replaces or invades earlier alteration minerals crystallized at lower temperatures, as indicated by the association of a low-temperature epithermal type of quartz (quartz combs) and of fluid-inclusion data (Freiberger et al., 2001; Fourcade et al., 2001). Such minerals are locally described in macroscopic veins in association with chlorite-euhedral quartz-dolomite (Fig. 3.2). The supergene alteration which affected the first tens of meters near the top of the granite after emersion (reddening, hematization, adularisation) is well marked in the two samples at the top of the CHA312 drilling.

The second stage (noted II) of alteration is mostly marked by the crystallization of newly formed minerals in microfractures corresponding to a re-opening of macrofractures filled by the stage I paragenetic association. It produced a specific mineral assemblage observed over more than 700 meters depth with almost no variation in the paragenetic sequence: hematite-adularia/ quartz /dolomite (II)/ fluorite/ barite ± sulphides / calcite (II). It also produced patches or small fillings of cavities displaying the whole or a part of that specific mineral association (Fig. 3.2).

Sample	Depth (m)	Borehole	Rock type	Sample type	Petrography	fraction (µm)	XRD description
8795	159.8	CHA312	Tonalite	Reddened & oxidized clay fracture	FeOx/ill/Dol/Ba/	<2	60 % ill., 40 % IS R0 (ill.> 90%)
8799	169.0	CHA312	Tonalite	Fracture with green clay & carbonates	Chl/Ph/IS/Ad/Dol/Ba/Ga/Cc	<2	30 % ill., 40 % chl., 30 % IS R0 (ill.> 90%)
						0-0.2	30 % ill., 30% chl., 40 % IS
						0.2-0.4	25 % ill., 40% chl., 35 % IS
						0.4-1.0	25 % ill., 45% chl., 30 % IS
						1.0-2.0	30 % ill., 40% chl., 30 % IS
5183	233.3	CHA117	Monzo granite	Oxidized clay fracture	FeOx/Ph/ill/Ga/Dol	<2	85%(ill.+IS>90% ill),15%chl.
						0-0.2	85% ill., 15% chl.
						0.2-0.4	75% ill., 25% chl.
						0.4-1.0	65% ill., 35% chl.
						1.0-2.0	65% ill., 35% chl.
2420	242.6	CHA108	Monzo diorite	Fracture with green clay, quartz & fluorite	Chl/ill/Ad/Fl/Ba/Dol	<2	30 % ill., 60 % chl., 10% IS (R0:Sm<40%)
2422	260.3	CHA108	Granite with biotite	Zoned clay fracture	Chl/ill/Ba/Py/Cc	<2	85% (ill. + εIS), 15% chl.
-	-	-				0-0.4	80 % ill., 10 % chl., 10% IS
-	-	-	-			0.4-1.0	75 % ill., 15 % chl., 10% IS
-	-	-	-			1.0-2.0	70 % ill., 20 % chl., 10% IS
5799	494.5	CHA212	Tonalite	Clay fracture	Chl/ill/Qz	<2	40 % (ill.+IS: >90% ill), 25% chl., 35% chl/sm
8606	800.0	CHA212	Tonalite	Clay fracture & galena & carbonates	ill/Chl/Ga/Dol/Ba/Py	<2	70% (ill.+IS:>90% ill), 30% chl.
-	-	-	-			0-0.2	80% ill., 20% chl.
-	-	-	-			0.2-0.4	70% ill., 30% chl.
-	-	-	-			0.4-1.0	65% ill., 35% chl.
-	-	-	-			1.0-2.0	40% ill., 40% chl.

Table 3.1. Main features of the studied samples (drilling, type of enclosing rock, petrography and XRD mineralogy).
chl: chlorite, ill: illite, sm: smectite, IS: mixed-layered mineral constituted of sm and ill, corr: corrensite.

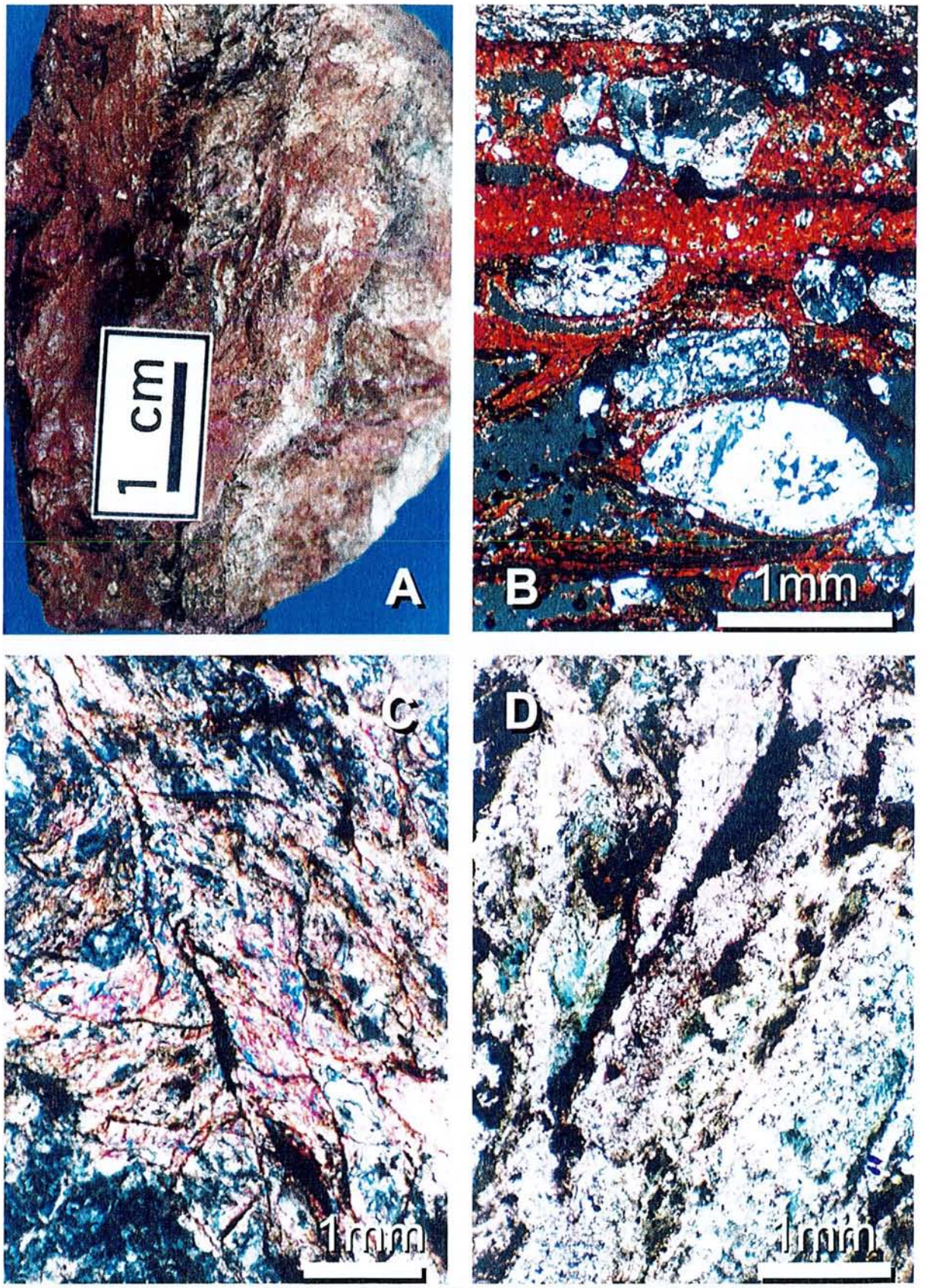

Fig. 3.2. Photomicrographs of typical alteration assemblages in the clay rich fractures and their host rocks. Clay rich fracture (breccia in fault) impregnated with iron hydroxides. A: macroscopic features, B: breccia with clasts of deformed granodiorite cimented by illite and iron hydroxides; C: illite , D : illite and chlorite (+ pyrite).

3.3 Analytical methods and results

3.3.1 Mineral separation and characterization

The clay fractions were extracted by gentle methods based on short repetitive ultrasonic treatments to preserve the mineral textures and the initial nature of the finest fractions, limit the amount of fine-grained material. Several granulometric fractions were obtained by settling in distilled water and further ultra-centrifuge separation. The XRD characterization was carried out at the Centre de Géochimie de la Surface (Strasbourg, France) and at Etudes Recherches Matériaux (Poitiers, France).

The XRD patterns have been recorded at CGS on a Philips PW 1050 diffractometer using a diffracted-beam Cu Kα radiation of 40 kV and 20 mA. The diffracted beam was filtered by a nickel filter and a monochromator together with a second nickel filter. The diffractograms were recorded from 2° to 35° 2q, with a step of 0.02° 2q and an accumulating time of 2 seconds by step.

At ERM, the XRD patterns were recorded using a Philips PW 1730 diffractometer (Ni-filtered Cu Kα radiation generated at 40 kV and 40 mA), equipped with a Kevex PSI detector and a stepping motor drive on the goniometer (SOCABIM DACO system). Oriented preparations of Ca-saturated <2 µm fraction were first analyzed in air-dried state and then after ethylene-glycol saturation. Additional analyses were carried out on K-ethylene glycol and Li-300°C-ethylene glycol saturated samples. The analytical conditions were 2-35°2θ as usual data collection range, 0.025°2θ as scanning step size and 6 s as counting time.

The respective amounts of illite and smectite layers were determined by comparison with XRD calculated patterns using the computer program Newmod (Reynolds and Hower, 1970) and modeled using the DECOMPXR program by Lanson (1990).

The XRD patterns (Fig. 3.3) demonstrate that the clay fraction is dominated by illite and ordered mixed-layer minerals with a high amount of illite (R3 I/S). The late paragenetic assemblage linked to the brine stage is observed in some samples and is identified as a mixture of I/S and mixed-layer illite/chlorite. These 10 Å layers are accompanied by chlorite and minor amounts of pyrite, kaolinite and other I/S minerals.

Deconvolution of the illite (001) peak by Lanson's (1990) method shows that I/S consists in more than 85% illite layers (broad bands in the 10.5 to 10.1 Å range in the air dried state which shifts to lower d–spacing values after ethylene glycol solvation) and that I/S is ordered in most samples. In a few cases, illite/vermiculite/smectite mixed layers were suspected. Exceptions concern the two samples from the shallowest levels (CHA 8795 and 8799) where I/S are found. On the basis of their swelling properties (the large band at 15 Å in the air-dried state shifts to 17 Å after ethylene glycol solvation), it can be concluded that they are I/S of R0 type, e.g. with random ordered interstratification of more than 70% smectite layers (Reynolds, 1980). The expandable layer charge in ordered and randomly ordered mixed layer minerals is not homogeneous since some of them collapse irreversibly to 10 Å, increasing the "illite" amount in K-saturated preparations in the ethylene glycol solvated state. This indicates the presence of vermiculite-type layers (Drits et al.,

1997) in the stacking. The I/S expandability is reduced but not totally neutralized after the Hoffman-Klemen treatment. Thus, a part of the expandable layer charge originates in the tetrahedral sheets.

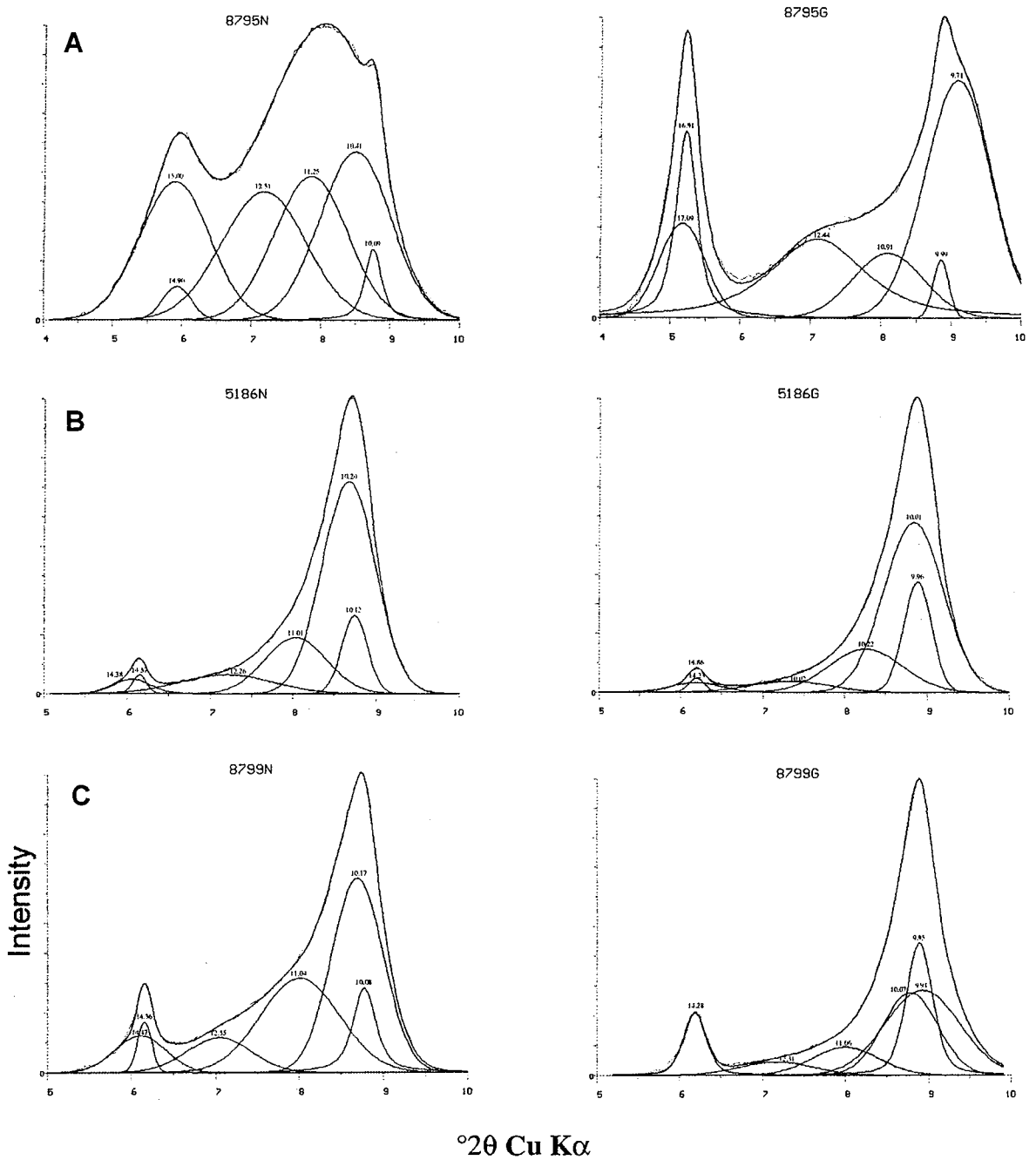

Fig. 3.3. Examples of deconvoluted XRD patterns of the K-micas populations using Lansons' method (Lanson, 1990).
A: sample CHA 8795, B: sample CHA 5186, C: sample CHA8799. Left hand side: air dried, right hand side: glycolated.

3.3.2 Crystal-chemistry of illite and chlorite

Microprobe analyses have been carried out at the University Henri Poincaré (Nancy, France) on a CAMECA SX microprobe. K-smectite and run products, previously dispersed in a small volume of distilled water were mounted on a pure carbon slide. The analytical conditions were: 10 kV, 4 to 6 nA, 10-µm diameter for the investigation area, ZAF COR 2 as correction program and 3% for the maximum analytical error.

Analyses of the two main phases found in clay rich fractures, illite and chlorite are given in Table 3.2 and in Table 3.3. Binary diagrams Si – Interlayer charge for illites show that they display rather typical crystal chemistry with an interlayer charge between 0.75 and 0.9 dominated by K, and a slight octahedral substitution (phengite substitution) which shifts weakly the chemical features of the analyzed illites from Pyrophyllite-muscovite ideal mixing line (Fig. 3.4). One exception is the sample from surficial level (8799 at –169m) where I/S enriched in smectite (R0) are present, confirming the XRD results.

Chlorites are trioctahedral with crystal-chemistry close to the brunsvigite field, and the chamosite - brunsvigite boundary (Fe/Mg around 0.75). The sample 8799 is characterized by mixed layered phases, probably I/S characterized by an interlayer charge, and increased Si content due to the presence of di-octahedral layers (probably illite, Fig. 3.4 and Fig. 3.5).

Mineral/ Sample depths	sample/analyses	Si	Al^{IV}	Al^{VI}	Fe^{2+}	Mg	Mn	Ca	Na	K
Chlorite	8799-1	2.94	1.06	1.46	1.85	2.39	0.07	0.01	0.02	0.03
169 m	8799-2	3.18	0.82	1.69	1.37	2.38	0.05	0.02	0.01	0.09
Chlorite	2422-1	2.88	1.12	1.31	1.99	2.49	0.05	0.02	0.02	0.02
260 m	2422-2	2.73	1.27	1.35	2.06	2.47	0.04	0.01	0.00	0.00
Chlorite	5799-1	2.81	1.19	1.59	2.36	1.79	0.04	0.02	0.00	0.01
495 m	5799-2	2.80	1.20	1.61	2.33	1.84	0.00	0.01	0.00	0.01
	5799-3	2.85	1.15	1.66	2.25	1.72	0.06	0.04	0.03	0.00
	5799-4	2.76	1.24	1.71	3.09	0.92	0.01	0.02	0.00	0.01
	5799-5	2.73	1.27	1.76	3.02	0.94	0.02	0.02	0.00	0.01
	5799-6	2.78	1.22	1.77	2.95	0.96	0.01	0.01	0.00	0.00
	5799-7	2.73	1.27	1.63	3.21	0.91	0.04	0.00	0.00	0.01
	5799-8	2.88	1.12	1.73	2.26	1.65	0.00	0.02	0.00	0.02
	5799-9	2.79	1.21	1.70	3.09	0.91	0.04	0.01	0.01	0.01
	5799-10	2.79	1.21	1.72	3.10	0.90	0.00	0.00	0.00	0.01
	mean	*2.79*	*1.21*	*1.69*	*2.77*	*1.25*	*0.02*	*0.01*	*0.00*	*0.01*
	s.d.	*0.05*	*0.05*	*0.06*	*0.39*	*0.41*	*0.02*	*0.01*	*0.01*	*0.01*
Mixed layered	8799-1	3.37	0.63	1.39	1.74	2.38	0.00	0.02	0.01	0.18
Illite/chlorite	8799-2	3.64	0.36	1.70	1.54	1.89	0.03	0.03	0.01	0.27
169 m	8799-3	3.41	0.59	1.59	1.52	2.24	0.02	0.03	0.03	0.18
	8799-4	3.48	0.52	1.51	1.69	2.13	0.00	0.05	0.02	0.24
	8799-5	3.42	0.58	1.44	1.66	2.32	0.01	0.06	0.02	0.15
	8799-6	3.40	0.60	1.68	1.40	2.21	0.01	0.02	0.02	0.26
	8799-7	3.46	0.54	1.69	1.49	2.09	0.01	0.03	0.01	0.21
	8799-8	3.62	0.38	1.66	1.45	2.06	0.01	0.02	0.00	0.29
	mean	*3.47*	*0.53*	*1.58*	*1.56*	*2.17*	*0.01*	*0.03*	*0.02*	*0.22*
	s.d.	*0.10*	*0.10*	*0.12*	*0.11*	*0.15*	*0.01*	*0.01*	*0.01*	*0.05*
Mix. layered ill/chl 233 m	5183-1	3.42	0.58	1.90	1.27	2.06	0.00	0.01	0.02	0.19

Table 3.2. Crystal-chemistry of chlorites with indication of mean compositions and standard deviation (s.d.).

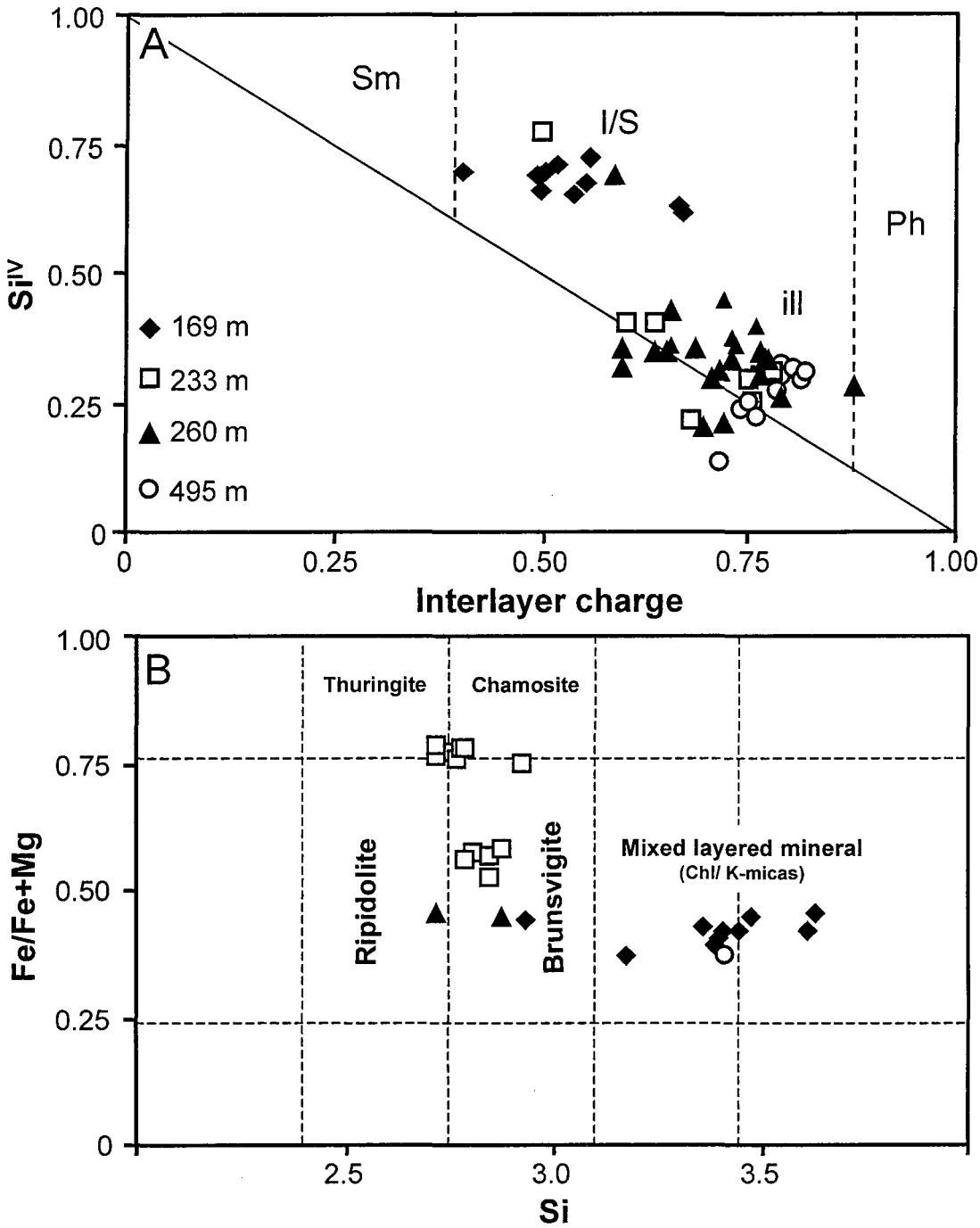

Fig. 3.4. Diagrams for K-micas identification. A: Si^{IV} - interlayer charge, and chlorite B: Fe/Mg vs Si^{IV} from the clay-rich fractures.

Mineral Sample depths	Sample-analyses	Si	Al^{IV}	Al^{VI}	Fe^{3+}	Mg	Mn	Ca	Na	K
Illite	5183-1	3.39	0.61	1.51	0.25	0.33	0.00	0.02	0.01	0.60
233 m	5183-2	3.20	0.80	1.67	0.20	0.24	0.00	0.02	0.02	0.63
	5183-3	3.39	0.61	1.77	0.10	0.20	0.00	0.03	0.01	0.55
	mean	*3.33*	*0.67*	*1.65*	*0.19*	*0.26*	*0.00*	*0.02*	*0.01*	*0.60*
	s.d.	*0.09*	*0.09*	*0.11*	*0.06*	*0.06*	*0.00*	*0.00*	*0.01*	*0.04*
Illite	2422-1	3.27	0.73	1.77	0.10	0.10	0.01	0.02	0.00	0.84
260 m	2422-2	3.38	0.62	1.68	0.12	0.22	0.01	0.00	0.00	0.76
	2422-3	3.29	0.71	1.72	0.12	0.20	0.00	0.01	0.00	0.75
	2422-4	3.32	0.68	1.75	0.13	0.15	0.00	0.00	0.02	0.72
	2422-5	3.43	0.57	1.73	0.10	0.16	0.00	0.01	0.01	0.70
	2422-6	3.33	0.67	1.73	0.14	0.14	0.00	0.02	0.01	0.74
	2422-7	3.34	0.66	1.76	0.11	0.15	0.00	0.02	0.01	0.64
	2422-8	3.31	0.69	1.59	0.24	0.29	0.00	0.00	0.01	0.60
	2422-9	3.19	0.81	1.59	0.28	0.23	0.00	0.00	0.01	0.72
	2422-10	3.25	0.75	1.73	0.15	0.15	0.00	0.00	0.00	0.79
	2422-11	3.36	0.64	1.72	0.16	0.14	0.00	0.01	0.01	0.70
	2422-12	3.28	0.72	1.83	0.09	0.11	0.00	0.01	0.01	0.69
	2422-13	3.32	0.68	1.83	0.06	0.11	0.01	0.01	0.02	0.70
	2422-14	3.33	0.67	1.75	0.14	0.16	0.01	0.01	0.01	0.62
	2422-15	3.33	0.67	1.66	0.24	0.14	0.00	0.00	0.01	0.65
	2422-16	3.35	0.65	1.72	0.13	0.18	0.01	0.01	0.01	0.73
	2422-17	3.41	0.59	1.72	0.13	0.18	0.01	0.00	0.01	0.66
	2422-18	3.30	0.70	1.78	0.12	0.12	0.02	0.02	0.01	0.68
	2422-19	3.19	0.81	1.87	0.08	0.10	0.01	0.02	0.01	0.65
	2422-20	3.34	0.66	1.79	0.15	0.11	0.01	0.00	0.01	0.60
	2422-21	3.35	0.65	1.75	0.14	0.15	0.01	0.00	0.00	0.66
	2422-22	3.32	0.68	1.71	0.13	0.18	0.01	0.01	0.01	0.75
	mean	*3.32*	*0.68*	*1.74*	*0.14*	*0.16*	*0.01*	*0.01*	*0.01*	*0.70*
	s.d.	*0.06*	*0.06*	*0.07*	*0.05*	*0.05*	*0.01*	*0.01*	*0.00*	*0.06*
Illite	5799-1	3.31	0.69	1.81	0.09	0.11	0.00	0.06	0.02	0.67
495 m	5799-2	3.29	0.71	1.83	0.07	0.11	0.00	0.04	0.02	0.70
	5799-3	3.26	0.74	1.80	0.10	0.13	0.00	0.03	0.03	0.71
	5799-4	3.31	0.69	1.82	0.07	0.10	0.01	0.04	0.01	0.73
	5799-5	3.29	0.71	1.80	0.08	0.12	0.03	0.03	0.01	0.70
	5799-6	3.28	0.72	1.79	0.09	0.11	0.04	0.03	0.01	0.69
	5799-7	3.29	0.71	1.81	0.09	0.12	0.00	0.03	0.01	0.72
	5799-8	3.26	0.74	1.84	0.07	0.09	0.02	0.03	0.02	0.72
	5799-9	3.24	0.76	1.84	0.06	0.15	0.00	0.03	0.01	0.69
	5799-10	3.22	0.78	1.86	0.08	0.11	0.00	0.03	0.01	0.69
	5799-11	3.24	0.76	1.85	0.06	0.11	0.02	0.04	0.01	0.68
	5799-12	3.21	0.79	1.83	0.09	0.12	0.01	0.03	0.01	0.69
	5799-13	3.12	0.88	1.91	0.08	0.08	0.00	0.04	0.01	0.63
	5799-14	3.28	0.72	1.81	0.08	0.10	0.00	0.05	0.02	0.72
	5799-15	3.30	0.70	1.79	0.09	0.11	0.00	0.05	0.03	0.71
	mean	*3.26*	*0.74*	*1.83*	*0.08*	*0.11*	*0.01*	*0.04*	*0.01*	*0.70*
	s.d.	*0.05*	*0.05*	*0.03*	*0.01*	*0.02*	*0.01*	*0.01*	*0.01*	*0.02*
Mixed layered	8799-1	3.70	0.30	1.53	0.18	0.31	0.00	0.04	0.05	0.40
Illite/smectite	8799-2	3.68	0.32	1.54	0.20	0.32	0.01	0.02	0.01	0.36
169 m	8799-3	3.65	0.35	1.47	0.27	0.32	0.00	0.03	0.03	0.42
	8799-4	3.71	0.29	1.53	0.18	0.30	0.00	0.05	0.02	0.44
	8799-5	3.68	0.32	1.50	0.20	0.33	0.00	0.05	0.01	0.41
	8799-6	3.66	0.34	1.48	0.24	0.31	0.00	0.04	0.01	0.46
	8799-7	3.63	0.37	1.51	0.21	0.33	0.00	0.06	0.02	0.42
	8799-8	3.67	0.33	1.49	0.22	0.33	0.01	0.05	0.01	0.41
	8799-9	3.67	0.33	1.54	0.14	0.37	0.02	0.04	0.01	0.43
	8799-10	3.71	0.29	1.51	0.16	0.36	0.00	0.03	0.01	0.49
	8799-11	3.60	0.40	1.43	0.22	0.38	0.01	0.04	0.00	0.59
	8799-12	3.62	0.38	1.46	0.21	0.35	0.00	0.04	0.00	0.60
	mean	*3.67*	*0.33*	*1.50*	*0.20*	*0.33*	*0.00*	*0.04*	*0.02*	*0.45*
	standard deviation	*0.03*	*0.03*	*0.03*	*0.03*	*0.03*	*0.01*	*0.01*	*0.01*	*0.07*
Mixed layered	5183-1 (233 m)	3.76	0.24	1.45	0.24	0.31	0.01	0.01	0.01	0.47
Illite/smectite	2422-1 (260 m)	3.68	0.32	1.77	0.08	0.08	0.01	0.00	0.01	0.59

Table 3.3. Crystal-chemistry of K-micas with indication of mean compositions and standard deviation (s.d.).

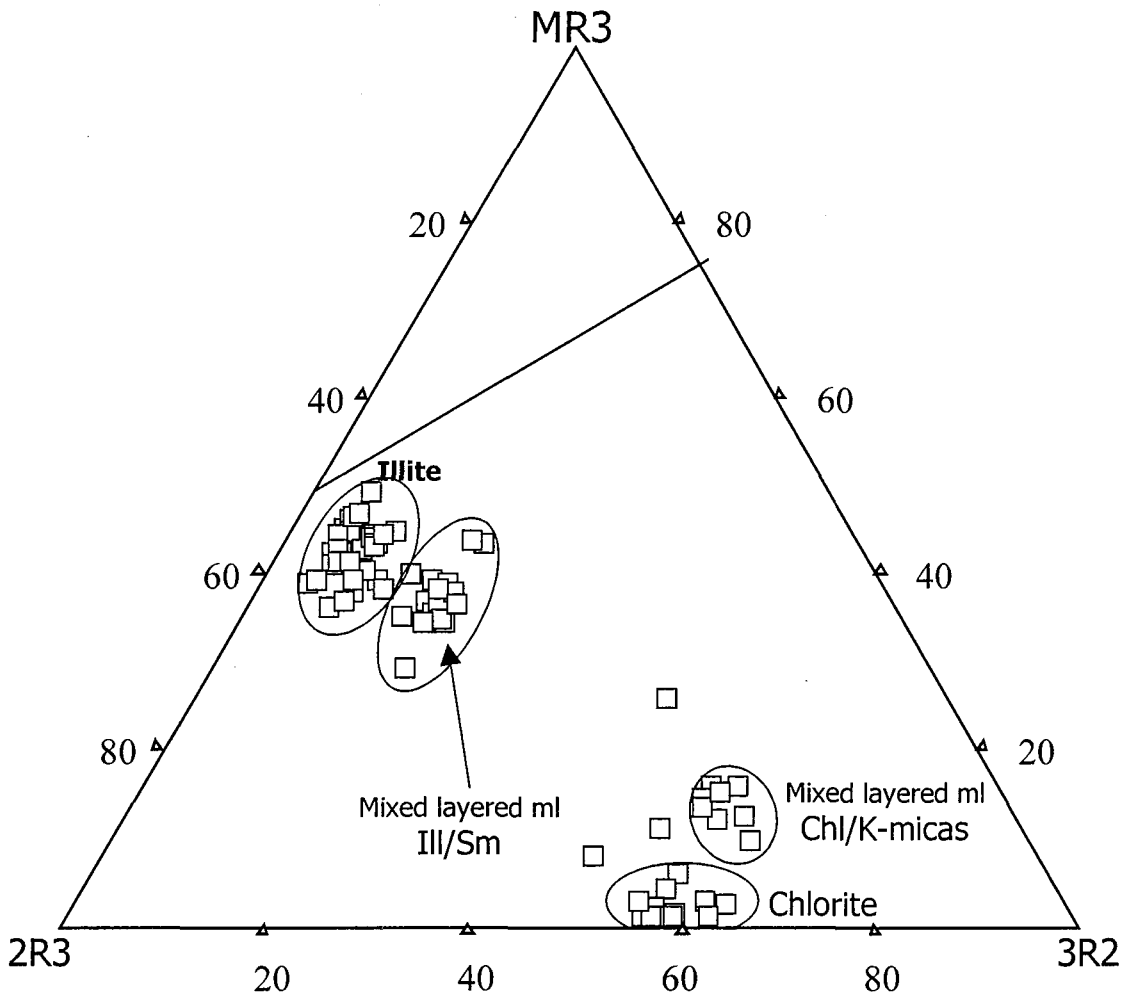

Fig. 3.5. MR3-2R3-3R2 diagram from Velde (1977) applied to clay particle analyses from the clay rich fractures.

3.3.3 K-Ar measurements

The extracted clay fractions were finely hand-crushed in a mortar. The separated fractions were dated by the K-Ar method following a procedure similar to that of Bonhomme (1982). The samples were stored under vaccum for at least 12 h and heated at 100°C before Ar analysis to remove the Ar of atmospheric origin. Potassium analyses were carried out by flame spectrophotometry with an accuracy better than $\pm$ 1.5%. Argon isotopic results were controlled by measuring the international GLO-glauconite standard which averaged 24.86 $\pm$ 0.15 (2σ).10^{-6} cm^3 radiogenic ^{40}Ar/STP for 4 independent determinations, and the atmospheric $^{40}Ar/^{36}Ar$ ratio which averaged 301.7 $\pm$ 2.1 (2σ) for 5 independent controls during the course of the study. As these values were close to the references and as the residual atmospheric Ar of the mass spectrometer and the extraction line never exceeded 10^{-8} cm^3 of radiogenic ^{40}Ar, no corrections were applied to the raw data. The decay constants used for age calculation are those recommended by Steiger and Jäger (1977).

3.3.4 Stable isotopes measurements

Oxygen and hydrogen isotopic compositions were measured on separated clay fractions. After drying at 80°C in an oven, the clay powder was mechanically homogenized in a boron carbide mortar.

For O isotope analysis, 5 to 12 mg samples were dehydrated under high vacuum at room temperature for 1-2 hours, then at increasing temperatures up to 160-170°C to remove physico-chemically adsorbed water. Samples were transferred into the Ni vessels of the fluorination line under a dry nitrogen conditioning. After 4 hours of outgassing under high vacuum at room temperature, the samples were reacted overnight with BrF_5 at 650°C. Oxygen isotopic ratios were measured on CO_2 gas using a VG SIRA 10 mass spectrometer at the Geosciences Department of Rennes. The procedure (from weighting to mass spectrometer) was duplicated for most of the samples and the error quoted in the Table 3.4 corresponds to the deviation observed between two extractions done in different Ni tubes. The isotopic composition is expressed with the conventional δ notation with respect to the SMOW reference. The NBS 28 quartz reference, and additional internal standards (basaltic glass Circé 93 and Madagascar granite A 1113) were used to calibrate the fluorination line with respect to carbonate reference samples (NBS19 and two internal standards). The results given in the table are thus normalized to the NBS 28 reference (+9.6‰ vs. SMOW). The total uncertainties are estimated to be in the 0.1-0.2‰ range.

For hydrogen isotope analysis, 20 ± 5 mg samples were outgassed during 2 hours at 180°C using silica glass tubes that were previously outgassed at 1400°C during 1 h. Water was released from the sample by heating the silica glass tube at 1400°C for 20 mn in the presence of hot, pure CuO and the condensable gazes (H_2O and minor amounts of CO_2) were trapped in liquid nitrogen. After cryogenic removal of CO_2, H_2O was reduced by U metal at 800°C using a toepler pump for gaz circulation and pumping. D/H ratios were measured on a Finnegan Mat Delta E mass spectrometer on H_2 gaz of the Institut de Physique du Globe of Paris. The isotopic composition is expressed with the conventional δ notation with respect to the SMOW reference. Some samples have been duplicated and the error (Table 3.4) corresponds to the deviation observed between two different extractions. Internal water standards calibrated with respect to the V-SMOW, SLAP, GISP international references were used for calibration. The total uncertainties are estimated to be in the 1-2‰ range. Fourcade and Martineau (2000) have already checked that the D/H isotopic ratio was not significantly affected by the separation procedure (more specifically by the HCl treatement).

3.3.5 Results

The $\delta^{18}O$ values were determined on the clay fractions dated by the K-Ar method. Bulk samples are composite and made of chlorite and illite as the main components (Table 3.1) with relative proportions of chlorite ranging between 0% (CHA312/8795) and 50% (CHA108/2420). Because the mineral size was too small, the separation of pure end-members could not be realized. Therefore, we measure the isotopic compositions of a clay mixture. The range of measured $\delta^{18}O$ values is rather large: between +8‰ and +18.2‰ (Fig. 3.6) and the samples pertain to two groups. The first

group displays low $\delta^{18}O$ values (+8 to +11.2 ‰) and corresponds to samples yielding relatively ancient K-Ar dates (247 to 272 Ma). The second group presents the highest $\delta^{18}O$ values (*c.* 18‰) and displays younger ages (194-198 Ma).

The samples of the first group are issued from deep-seated fractures (Table 3.4) while the other samples are shallow-seated fractures. This upper part of the granite, near the paleo-surface has experienced weathering during the pre-Hettangian emersion period (Fig. 3.7). For the different size fractions of sample 5183, the $\delta^{18}O$ values and the K-Ar dates display a negative correlation (Fig. 3.6), connecting the two aforementioned groups. The finest fraction (< 0.2 μm) showing the highest $\delta^{18}O$ value (+15.73 ± 0.25‰) is also the youngest (188 ± 5 Ma). The K-Ar date and the $\delta^{18}O$ value vary among the size fractions of sample 5183 without large corresponding variations of the chlorite/illite abundance ratio.

The δD values obtained on the different clay fractions range from -45 to -61‰. They are apparently independent of the clay size and are correlated neither to the K-Ar dates nor to the $\delta^{18}O$ values.

Sample	fraction (μm)	Depth (m)	Borehole	Age K/Ar (Ma)	± Ma	$\delta^{18}O$ (SMOW)	± ^{18}O	δD (SMOW)	± δD
8795	<2	159.80	CHA 312	198	5	18.22	0.05	-66.82	
8799	<2	169.00	CHA 312	198	5	17.30	0.30	-45.72	0.07
-	0-0.2	-	-	199	5	18.14	0.11		
-	0.2-0.4	-	-	211	5	16.84	0.11		
-	0.4-1.0	-	-	212	5	15.87	0.16		
-	1.0-2.0	-	-	218	5	14.31	0.12		
5183	<2	233.35	CHA 117	207	5	13.69	-	-53.39	1.44
-	0-0.2	-	-	188	4	15.73	0.25	-49.44	1.77
-	0.2-0.4	-	-	222	5	13.36	0.15	-49.01	2.33
-	0.4-1.0	-	-	238	5	11.96	0.01	-51.79	
-	1.0-2.0	-	-	250	6	10.75	-		
2420	<2	242.60	CHA 108	247	6	7.98	0.02	-60.76	4.96
2422	<2	260.35	CHA 108	259	6	11.13	0.01	-59.60	0.73
-	0-0.4	-	-	250	5	11.46	0.05		
-	0.4-1.0	-	-	262	6	10.18	0.11		
-	1.0-2.0	-	-	263	6	10.02	0.11		
5799	<2	494.50	CHA 212	272	6	10.74	0.20	-50.13	
8606	<2	800.00	CHA 212	253	6	10.20	0.24	-45.90	1.15
-	0-0.2	-	-	253	5	10.17	0.13		
-	0.2-0.4	-	-	263	6	9.37	0.07		
-	0.4-1.0	-	-	291	6	7.95	0.03		
-	1.0-2.0	-	-	275	6	7.93	0.19		

Table 3.4. Isotopic data ($\delta^{18}O$ and δD vs. SMOW and K-Ar ages) obtained on the clay-rich material filling the fractures within the Vienne granitoids.

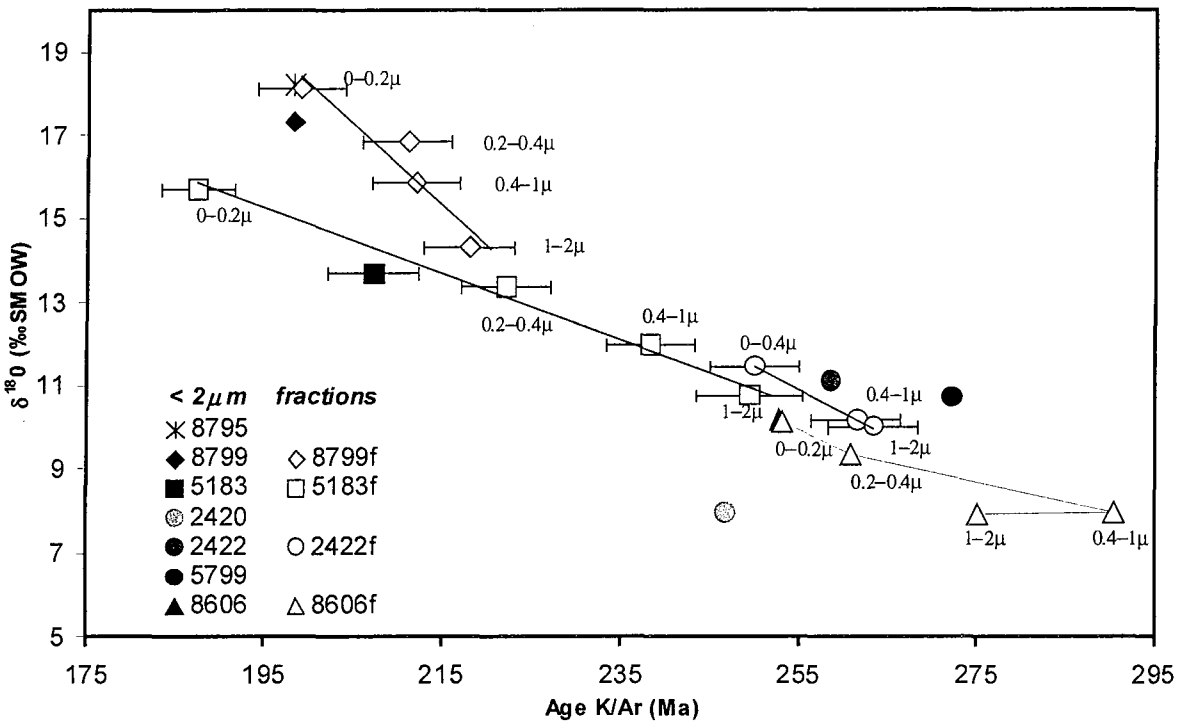

Fig. 3.6. Oxygen isotopic composition of clay fractions in the fractures from the Vienne plutonites as a function of their K-Ar age. Except for fractions of the 8606f sample, the lines are the best fits corresponding to the different size fractions of the samples 5183f, 8799f and 2422f.

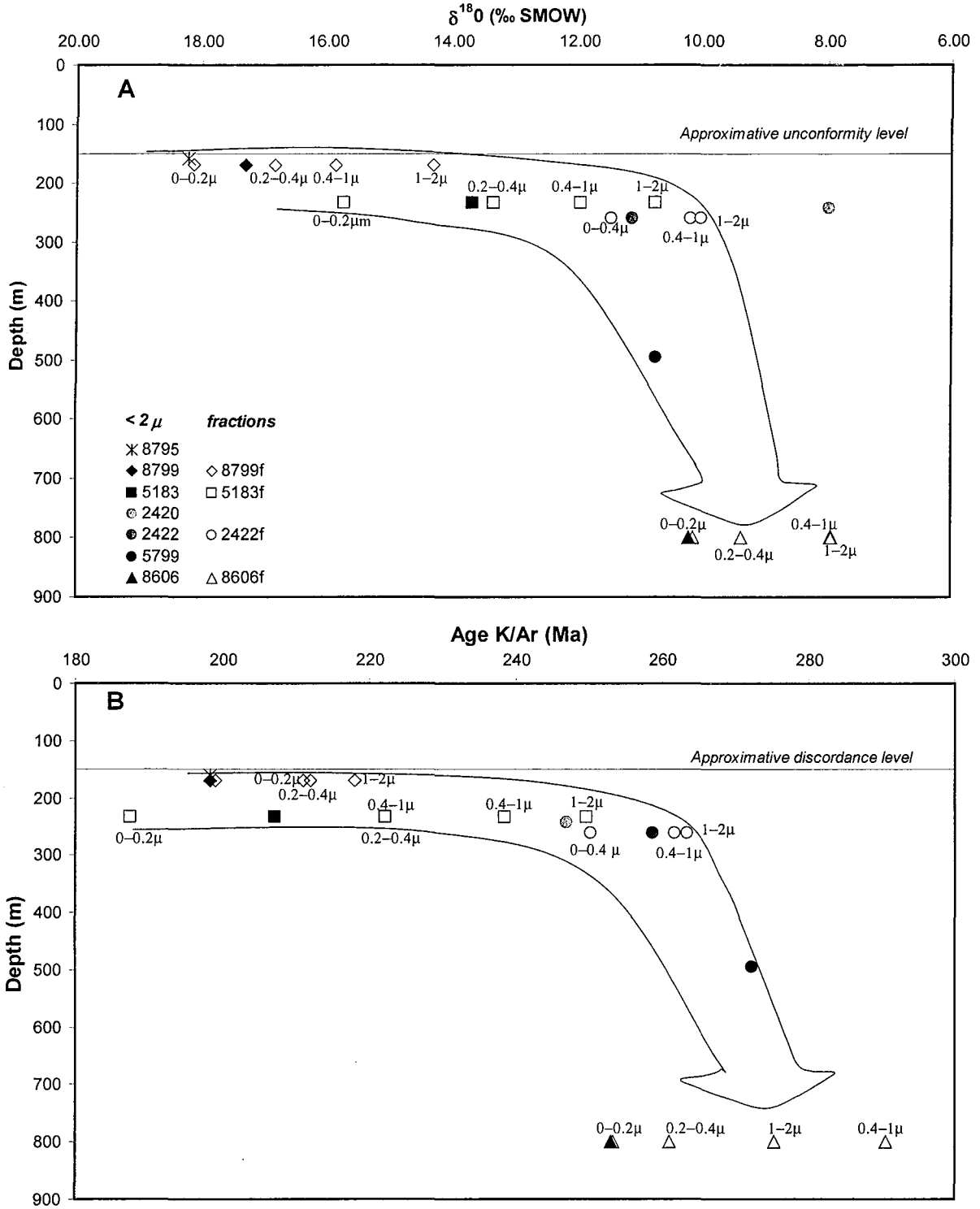

Fig. 3.7. Depth distribution of O isotopic data (A) and K/Ar ages (B) on clay fraction from the clay rich fractures.

3.4 Discussion

The present data lead to two main questions: Are each group aforementioned assignable respectively to one of the two major stages of identified fluid flow in the Vienne granitoids and how could these stages be registered in the minerals ?

3.4.1 Isotopic signatures of the fluids

The isotopic composition of the minerals may be helpful to evaluate the nature of the fluid provided that the crystallization or equilibration of that mineral is attributable to a single event and that the temperature of the mineral/fluid interaction could be estimated. The first (Hercynian) event is still recorded in the most deep-seated fractures (8766 at 800m depth and 5799 at 500 m depth) with K-Ar values up to 291 ± 6 Ma (Table 3.4). If we use the most deep-seated samples, the oxygen isotopic compositions of the major mineral components, namely chlorite and illite, may be estimated assuming that each mineral keeps a constant isotopic composition among these samples. Sample 2420 contains the largest content of chlorite (55% by volume) and has also a significant lower $\delta^{18}O$ value (7.98‰), suggesting that chlorite has a lower isotopic composition than illite in the mixture. Using the mass abundance ratios (molar weights for chlorite and illite taken as 0.625 and 0.390 Kg. mole^{-1}, respectively) and the isotopic compositions of samples 2420, 2422, 5799, 8606, we estimate the $\delta^{18}O$ value of chlorite to be *c.* 5.5 ± 0.5‰ and that of illite *c.* +13 ±1‰. Reasonable estimates of the crystallization temperatures are 350° to 400°C for chlorite and 150°- 250°C for illite (Freiberger et al., 2001, Cathelineau, 1988). Available fractionation equations for the systems chlorite-water (e.g., Wenner and Taylor, 1971; Zheng, 1993) or illite-water (Zheng, 1993) yields estimates of the ancient fluid $\delta^{18}O$ value at *c.* +6 to +7‰ for chlorite and *c.* +5 to +10‰ for illite. Although such estimates are too approximate to conclude that the fluids were the same, this calculation indicates that the fluids responsible for the early alteration in the Hercynian faults were generated in hot rock-dominated systems (e.g., metamorphic fluids).

Now, once crystallized chlorite is a mineral known to be rather resistent to oxygen isotopic re-equilibration in low-temperature conditions, as documented by studies of altered oceanic crust. We will thus consider that chlorite remained isotopically inert in its oxygen isotopic composition during the brine circulations. Concerning the second stage of fluid circulation, and using the 0 - 0.2 µm size fraction of sample 5783 which gives the highest isotopic composition (+15.73 ± 0.25‰) as well as the youngest K-Ar age (188 ± 4 Ma), the □$\delta^{18}O$ value of the re-equilibrated illite fraction may be calculated to be *c.* + 20‰.

If illite of that fraction is only partly re-equilibrated, the illite fraction reset during the young event could have had a higher oxygen isotope composition. According to the fractionation equations of Zheng (1993), an illite at +20‰ could have been in isotopic equilibrium with a fluid yielding a $\delta^{18}O$ value of *c.* +8‰ for a temperature of *c.* 100°C (typical temperature derived from the fluid inclusion studies of quartz and carbonate infillings related to brine circulations). If chlorite re-equilibrated during the brines episodes, a fluid $\delta^{18}O$ value of *c.* +5‰ (Zheng, 1993) is obtained from the 0 - 0.2 µm

size chlorite+illite mixture. This range of fluid isotopic compositions is the same obtained using the oxygen isotopic compositions of quartz and carbonate infillings deposited by the brines inside the granitic basement and the overlying Hettangian sediments (Boiron et al., 2001).

The δD values do not correlate either with $\delta^{18}O$ values nor with the chlorite/illite ratio of the clay fraction (Table 3.4). Unfortunately, the variations of mineral-fluid isotopic fractionations with temperature and chemical compositions are not well established for illite and especially chlorites (Savin and Lee, 1988). Therefore, considering also possible isotopic fractionations during the illite - I/S transition (Yeh, 1980) and the poor knowledge of the degree of re-equilibration of each mineral species during the two (or more) stages of fluid flow, attempts to estimate the D/H signatures of the fluids are very speculative. We may just state that since hydrogen isotopes are known to re-equilibrate faster than oxygen isotopes and rather easily in the presence of fluids even at relatively moderate temperatures (e.g., O'Neil, 1987; Savin and Lee, 1988 and references therein). So, the samples displaying reset of K-Ar dates and $^{18}O/^{16}O$ ratios likely experienced hydrogen isotope exchanges with the brines. In that case, the D/H fractionation between illite and water is about -27‰ at 100°C (Yeh, 1980). It represents a reasonable value considering the estimation for minerals of similar compositions and structures. For chlorite-water, the fractionation factors reported in the literature display large discrepancies at low temperatures. The calibration of Sakai and Tsutsumi (1978) gives δD Chlorite-H_2O = +32‰ and that of Marumo et al. (1980) suggests values around -10‰. For a chlorite-illite mixture with volume proportions of 0.2/0.8 (representative of the most analyzed samples, see Table 3.4) and taking into account the molecular weights as well as the hydrogen concentration ratio (chlorite/illite ≈ 2.7), we obtain a global fractionation factor with water in between *c.* 0 and -20‰. Accordingly, the range of measured δD values in our " re-equilibrated " clay fraction (-46 to -67‰, Table 3.4) is in agreement with that directly measured on the highly saline fluid inclusions contained in minerals (quartz, carbonates) crystallized during the brines circulation: -20 to -50‰ (Boiron et al., 2001). As hydrogen isotopic exchange is probable, we cannot exclude that the D/H ratios in the totality of the analyzed clay fractions were reset during the *c.* 100°C-brines event or even subsequently for some of them, during the circulation of surface-derived water knowing that some of these fractures still act as drains today.

3.4.2 Age and geodynamic context of brines circulation

The maximum of compaction in that part of the basin may have occurred during or slightly after the Barremian (Brunet, 1983). Over a long period, the evolution of the Aquitain Basin can be explained in terms of crustal stretching and lithospheric thinning (Brunet, 1983). Burial of sediments and tectonic activity are the mechanisms which could promote fluid expulsions from basin. The basement fracturation is apparently linked to distensive movements affecting both the basement and its sedimentary cover after Sinemurian. Thus, the optimum periods for fluid circulation were likely the extension periods, especially because they could correspond to increases in the geothermal gradient. On the present data, we speculate that these brine flows could have occurred either:

(a) during the Lias-Dogger: the lowest K-Ar dates obtained on the finest clay fractions are apparently consistent with this scenario (188 to 198 Ma, Table 3.4) since they are contemporaneous or slightly younger than the age of the stratigraphic unit which hosts them: 200 to 197 Ma for the Hettangian, according to Okulitch (1999). Moreover, a very significant extensional episode occurred in the Aquitanian Basin at the Lias-Dogger Transition, at about 180 Ma (Bonhomme, 1982, Curnelle and Dubois, 1986). Coeval with this extension, a significant hydrothermal event is recorded in several sites from southern Massif Central (Leveque et al., 1988; Lancelot and Vella, 1989; Respault et al., 1991). However, the thickness of deposited sediments around the "Poitou High" may have been lower than two or three hundreds of meters at this period (on the basis of the present-day thickness of the series) and the temperature at the I unconformity could not have exceeded a few tens of degrees (30-40°C at maximum). As a high porosity existed in the upper part of the granitic basement (strongly altered during the emersion period) as well as in the overlying Triassic to Hettangian sediments, the unconformity was certainly a cold aquifer. In that context, it is very difficult to predict i) how a pervasive invasion of hot brines has penetrated to 800 m deep in the granite fractures, ii) how such hot fluids could have been generated, even from more internal parts of the Aquitanian Basin (beginning of the basin filling).

(b) during the Oxfordian-Kimmeridgian (*c.* 156-151 Ma; Okulitch, 1999), or (c) the Barremian-Aptian intervals (*c.* 127 - 112 Ma; Okulitch, 1999) which also coincide with new rifting episodes (Brunet, 1983), especially the opening of the Gascogne gulf. One K-Ar date at 112 Ma was obtained on a sample of adularia extracted from a fracture infilling in the Vienne granite (Cheilletz et al., 1997). Although the thickness of the sedimentary sequence at that time is debated in the Poitou High ("Detroit Poitevin"), more than 6 km of sediments were deposited in the centre of the Aquitanian Basin. This situation is favorable to a release of rather hot fluids (around 180°C for a thermal gradient of 30°C/ km). Moreover, some chemical characteristics of the Vienne brines (K/Na ratios) suggest that they were recharged in hotter zones (*c.* 170°C; Boiron et al., 2001) than those estimated in the Vienne unconformity. Thus, it shall be admitted that neither the lowest K-Ar dates nor the heaviest oxygen isotopic compositions measured in the finest clay fractions are reliable records of the brine event: these fractions may be themselves mixtures of material pertaining to the Hercynian event and material re-equilibrated during the brine event. The extrapolation of the dates vs. the $\delta^{18}O$ correlation trend towards younger K-Ar ages (110 -120 Ma) indicates that the "neoformed" clay fraction could have a $\delta^{18}O$ value in the range of 21 to 22‰.

3.5 Conclusions

The study yields the following conclusions:

1- Clay-enriched fractures of plutonites from the western part of the French Massif Central, were subjected to multistage fluid circulations in spite of low hydraulic conductivity. These fractures were thus conductive and ensured the connection between highly percolated fracture blocks (areas of dense sets of fractures sealed by the Mesozoic fluids), and the fluid supply areas which are probably palaeo-aquifers circulating in the upper part of the granite and in the infra-Toarcian formations.

2- The good preservation of the late Hercynian assemblage (chlorite/ K-micas) suggests either: i) the lack of major thermodynamic disequilibrium between the percolating fluids and the Hercynian mineral assemblages, or ii) the lack of significant fluid fluxes (low hydraulic conductivity),

3- Clay-rich fractures were formed during late Hercynian stages, by undergoing the successive significant phases of fluid migration, mainly the Mesozoic brine stage. They are still conductive, as some produced present-day waters. However, only the Mesozoic stage, already known at the periphery of the French Massif Central, was recorded by the illite fraction. This indicated that the clays are probably stable and insensitive to further recent fluid circulations of colder waters also identified in the Vienne granite.

ACKNOWLEDGEMENTS

This study was financially supported by CNRS and Andra (French Nuclear Waste Management Company) through the GdR FORPRO - Action 98-III. It corresponds to the GdR FORPRO contribution number 2001/10 A. Andra is acknowledged for the facilities and permission of sampling the drill cores. Stéphane Buschaert & Véronique Lavastre benefitted of a grant by Andra for completion of their PhD.

REFERENCES

Blyth, A., Frape, S., Blomqvist, R., Nissinen, P., 2000. Assessing the past thermal and chemical history of fluids in crystalline rocks by combining fluid inclusion and isotopic investigations on fracture calcite. Applied Geochem. 15, (10), 1417-1437.

Boiron M.C., Cathelineau M., Banks D.A., Buschaert S., Fourcade S., Coulibaly Y., Michelot J.L., Boyce A., Nitjchoua R., 2001. Penetration of brines into a crystalline basement during extensional tectonics: role on fracture sealing, and mass transfer. submitted

Boiron, M.C., Cathelineau, M., Trescases, J.J., 1989. Conditions of gold-bearing arsenopyrite crystallization in the Villeranges basin, Marche-Combrailles shear zone, France. A mineralogical and fluid inclusion study. Econ. Geol., 84, 1340-1362.

Bonhomme M.G., 1982, Age triasique et jurassique des argiles associées aux minéralisations filoniennes et des phénomènes diagénétiques tardifs en Europe de l'Ouest - Contexte géodynamique et implications génétiques. C.R. Acad. Sci. 294, 521-524.

Brunet M.F., 1983. La subsidence du bassin d'Aquitaine au Mésozoïque et au Cénozoïque. C.R. Acad. Sci. Paris, 297, 599-602.

Casanova, J., Negrel, P., Kloppmann, W., Aranyossy, J.F., 2001, Origin of deep saline groundwaters in the Vienne granitic rocks (France): constraints inferred from boron and strontium isotopes. Geofluids, 1, 91-102.

Cathelineau, M., 1988. Cation site occupancy in chlorites and illites as a function of temperature. Clay Minerals, 23, 471-485.

Cathelineau M., Cuney M., Boiron M.C., Coulibaly Y., Ayt Ougougdal M., 1999. Paléopercolations et paléo-interactions fluides - roches dans les plutonites de Charroux-Civray. Actes des Journées Scientifiques CNRS- Andra, Etude du massif de Charroux - Civray, EDP Sciences 159-179.

Cheilletz A., Cuney, M., Coulibaly, Y., Brouand M., Cathelineau, M., Stussi J.M., 1997. L'adularisation à l'interface socle-couverture dans la région de Charroux-Civray .. Actes des Journées Scientifiques CNRS/Andra, Poitiers 13 et 14 octobre 1997, abstract VG12, p16.

Coulibaly Y., 1998. Recherche des traces de circulation récentes en milieu cristallin : Une approche analytique sur les cristallisations dans les fractures et les paléofluides, Thèse INPL, Nancy, 453p.

Cuney, M., Brouand, M., Stussi, J.M., Gagny, C., 1999. Le massif de Charroux-Civray (Vienne): un exemple caractéristique des premières manifestations plutoniques de la chaîne hercynienne - Etude du Massif de Charroux-Civray.- Actes des Journées Scientifiques CNRS/Andra, Poitiers 13 et 14 octobre 1997, 63-104.

Curnelle R., Dubois P., 1986. Evolution mésozoïque des grands bassins sédimentaires français, bassin de Paris, d'Aquitaine et du Sud-Est. Bull. Soc. Géol. Fr., 8, 529-546.

Drits V.A., Lindgreen H., Sakharov B.A., Salyn A.S., 1997, Sequence structure transformation of illite-smectite-vermiculite during diagenesis of Upper Jurassic shales, North sea. Clay Minerals, 33, 351-371.

Essarraj S., Boiron M.C., Cathelineau M., Fourcade S., 2001. Multistage deformation of Au-quartz veins : Evidence for late gold introduction from microstructural, Isotopic and fluid inclusion studies. Tectonophysiscs, in press.

Fourcade, S., Michelot J.L., Buschaert S., Cathelineau M., Freiberger R., Coulibaly Y., Aranyossy J. F., 2001. Multi-stage fluid circulation with early introduction and recurring remobilizations of carbon during subsurface fluid-rock interactions: the case study of

the vienne granitoids (france), submitted.Fourcade, S., Martineau, F., 2000. Composition isotopique de l'oxygène et de l'hydrogène dans les fractions argileuses des sites de Mont-Terri et de Tournemire. Rapport Final Action 99-I (eaux intersticielles), Forpro-Andra, 11p.

Freiberger, R., Hecht, L., Cuney, M., Morteani, G., 2001. Secondary Ca-Al-silicates from Mid-European Hercynian granitoids: Implications for the cooling history of granitic plutons. Contributions to Mineralogy and Petrology, in press.

Lancelot J., Vella V., 1989. Datation U-Pb liasique de la pechblende de Rabajac - Mise en évidence d'une préconcentration uranifère permienne dans le bassin de Lodève (Hérault). Bull. Soc. Géol. Fr., 8, 309-315.

Lanson B., 1990. Mise en évidence des mécanismes de transformation des interstratifiés illite/smectite au cours de la diagénèse.Thèse de l'Université Paris 6-Jussieu, 366 p

Leveque M.H., Lancelot J.R., George E., 1988. The Bertholène uranium deposit-mineralogical characteristics and U-Pb dating of primary U mineralization and its subsequent remobilization: consequences for the evolution of the U-deposits of the Massif Central, France. Chem. Geol., 69, 147-163.

Marumo, K., Nagasawa, K., Kuroda, Y., 1980. Mineralogy and hydrogen isotope geochemistry of clay minerals in the ohnuma geothermal area, northeast Japan. Earth Planet. Sci. Letters, 47, 255-262.

O'Neil, J.R., 1987. Preservation of H, C, and O isotopic ratios in the low temperature environment. In " Stable isotope geochemistry of low temperature fluids ", Vol. 13 (Kyser, T.K., ed.), Saskatoon, Min. Assoc. of Canada, 85-128.

Okulitch, A.V., 1999. Geological time scale, 1999. Geol. Surv. of Canada, Open file 3040 (National Earth Sci. Ser., Geol. Atlas).

Respault .J. P., Cathelineau M., Lancelot J.R., 1991, Multistage evolution of the Pierres plantées uranium ore deposit (Margeride, France) : evidence >from mineralogy and U-Pb systematics. Eur.J. Mineral., 3, 85-103.

Reynolds R.C., Hower J., 1970. The nature of interlayering in mixed-layer illite-montmorillonite. Clays and Clay Minerals, 18, 25-36.

Rolin P., Colchen M., 1995. Le socle cristallin du confolentais le long de la vallée de la Vienne. Andra Report # OUTPT 95001, 91p.

Sakai, H. and Tsutsumi, M., 1978. D/H fractionation factors between serpentine and water at 100°C to 500°C and 2000 bar water pressure. Earth Planet. Sci. Letters, 40, 231-242.

Savin, S.M., Lee, M., 1988. Isotopic studies of hydrous phyllosilicates. In " Hydrous Phyllosilicates (exclusive of micas) " (Bailey, S.W., ed.), Rev. of Mineralogy, Vol. 19, Min. Soc. America, 189-233.

Steiger RH, Jäger, E., 1977. Subcomission on Geochronology: Convetion on the use of decay constants in geo-and cosmogeochronology. Earth PlanetSci. Lett., 36:359-362.

Velde B., 1977. Clays and clay minerals in natural and synthetic systems. in: Developments in Sedimentology, 21.

Wenner, D.B., Taylor, H.P., Jr., 1971. Temperatures of serpentinzation of ultramafic rocks based on $^{18}O/^{16}O$ fractionation between coexisting serpentine and magnetite. Contrib. Mineral. Petrol., 32, 165-185.

Yeh, H.W., 1980. D/H ratios and late-stage dehydration od shales during burial. Geochim. Cosmochim. Acta, 44, 341-352.

Zhang, Y. G., Frantz, J. D., 1987. Determination of the homogenization temperatures and densities of supercritical fluids in the system NaCl-KCl-$CaCl_2$-H_2O using synthetic fluid inclusions. Chem. Geol. 64, 335-350.

Zheng, Y.F., 1993. Calculation of oxygen isotope fractionation in hydroxyl-bearing silicates. Earth Planet. Sci. Letters, 120, 247-263.

4 MULTISTAGE FLUID CIRCULATION WITH EARLY INTRODUCTION AND RECURRING REMOBILIZATIONS OF CARBON DURING SUBSURFACE FLUID-ROCK INTERACTIONS: THE CASE STUDY OF THE VIENNE GRANITOIDS (FRANCE)

S. Fourcade[a], J.L. Michelot[b], S. Buschaert[c,f], M. Cathelineau[c], R. Freiberger[d,c], Y. Coulibaly[e,c], J. F. Aranyossy[f]

[a] *Géosciences Rennes (UMR 6118), Univ. Rennes 1, 35042 Rennes Cedex, France*
[b] *Laboratoire d'Hydrologie et de Géochimie Isotopique "OrsayTerre", Univ. Paris-Sud, 91405 Orsay, France*
[c] *CREGU-UMR G2R 7566, BP23, 54501 Vandoeuvre-lès-Nancy Cedex, France*
[d] *Institut für Mineralogie, Petrologie und Geochemie Albert-Ludwigs-Universität Freiburg, Albertstr. 23b, 79104 Freiburg, Germany*
[e] *UFR STRM, Université de Cocody, 22 BP 582 Abidjan 22, Côte d'Ivoire*
[f] *Andra, French Agency for Nuclear Waste Management, 92298 Châtenay-Malabry*

Submitted to Chemical Geology

Figure captions ***4-112***
Table captions ***4-112***
Abstract ***4-113***

4.1 INTRODUCTION ***4-115***

4.2 GEOLOGY AND DESCRIPTION OF THE STUDIED MATERIAL ***4-116***
4.2.1 The Vienne granitoids 4-116
4.2.2 The fluid circulations 4-117
- Stage-I: Hercynian events 4-119
- Stage-II: Brines events 4-120
- Stage-III: Late calcite 4-121

4.3 C AND O ISOTOPES ON BULK ALTERED ROCKS AND VEINS ***4-121***
4.3.1 Analytical techniques 4-121
4.3.2 Isotopic data 4-123
- Hercynian stage (I) 4-123
- Brine stage (II) 4-123
- Late stage (III) 4-125

4.4 DISCUSSION ***4-130***
4.4.1 Possible origin of the fluids and elements 4-130
- The Hercynian fluids 4-130
- Stage II Mesozoic fluids 4-131
- Late (Stage III) fluids: 4-132
4.4.2 Redistribution of the early stock of carbon. 4-132

4.5 CONCLUDING REMARKS ***4-134***
Acknowledgments ***4-136***
References ***4-137***

FIGURE CAPTIONS

Fig. 4.1. Map of the Charroux-Civray area with the north-western part of the Massif Central. At the drilling locations, the basement is covered by about 150 m - thick sedimentary rocks of Jurassic age (white area). The basement beneath Charroux-Civray is mainly built-up by medium-K and high-K calc-alkaline intrusions and its local contours have been derived from the geophysical investigations. *4-117*

Fig. 4.2. A: Photomicrographs of typical early Hercynian infillings (I_A). Deformed and microfractured quartz is intersected by several later generations of dolomite (CHA106 - 491.80 m). B: Macroscopic late Hercynian paragenesis (I_B) showing zoned euhedral quartz followed by the crystallization of dolomite (CHA212 – 583.27 m). C: Complex assemblage of Hercynian and Mesozoic quartz/dolomite paragenesis. D: Disseminated carbonates replacing calcic mineral precursors, in that case, a plagioclase crystal. *4-118*

Fig. 4.3. Schematic representation of the main types (I, II, III) of carbonates and quartz infillings found in the Vienne plutonites and their textural relationships. *4-120*

Fig. 4.4. Borehole – depth (m) diagram showing the location and the type (I, II or III) of fracture filling samples. Boreholes are projected along a SW-NE cross-section (see inset). *4-122*

Fig. 4.5. $\delta^{13}C$ - $\delta^{18}O$ binary plot for calcites and dolomites filling the Hercynian and Mesozoic fractures (A) and for carbonates disseminated in the matrix of whole rock plutonites (B). *4-124*

Fig. 4.6. $\delta^{13}C$ - $\delta^{18}O$ binary plot for the latest stage (III) calcites and from the sedimentary cover, with the field of the host rock (Mesozoic limestones) compositions. Envelopes for carbonates filling the Hercynian and Mesozoic fractures and those disseminated in plutonites (see Fig. 4.5) are given for reference. *4-125*

Fig. 4.7. $\delta^{13}C$ -depth section for all studied fracture carbonates and the Mesozoic limestones and their geodic calcitic infillings. Sample depths from CHA212 oblique borehole are recalculated relative to the surface. *4-126*

Fig. 4.8. Temperature vs. $\delta^{18}O$ binary plot for quartz filling the Hercynian and Mesozoic fractures in the Vienne plutonites. *4-126*

TABLE CAPTIONS

Table 4.1. Stable isotope ($\delta^{13}C$ (PDB) and $\delta^{18}O$ (SMOW)) data of investigated carbonate fracture infillings of the stages I and II, with indication of host rock type. In the fracture paragenesis, the analyzed carbonate is in heavy symbol and the number corresponds to the attributed stage. The O isotopic composition of corresponding fluid is calculated for a range of 2 assumed temperatures (see text for explanations). For samples from the CHA212 sloping drillings, depths are recalculated below the surface. *4-128*

Table 4.2. Stable isotope ($\delta^{13}C$ (PDB) and $\delta^{18}O$ (SMOW)) data of investigated late calcite (III) fracture infillings in granitoids and the geodic calcite III in sedimentary cover. *4-128*

Table 4.3. Stable isotope ($\delta^{18}O$ (SMOW)) data of investigated quartz infillings in granitoids and in sedimentary cover. *4-129*

Table 4.4. Stable isotope ($\delta^{13}C$ (PDB) and $\delta^{18}O$ (SMOW)) data of investigated disseminated carbonates in granitoids and of bulk limestones of sedimentary cover. *4-130*

ABSTRACT

The history of C transfers in a crystalline basement is discussed in the case study of a granitoid body (Vienne, Western part of French massif central) overlaid by a carbonate sedimentary sequence, a situation which is representative of most of the Variscan basement in Western Europe. The basement underwent three major stages of fluid circulation as shown by the study of carbonate and quartz fracture infillings: 1) Hercynian fluids circulated in fractures developed during uplifting of the basement in conditions of high heat flow related to the intrusion of late peraluminous granites; 2) diagenetic brines were expelled laterally along the basement/cover unconformity and were able to deeply percolate in the basement during distensive episodes linked to the basin evolution; 3) late infiltration of diagenetic/marine waters occurred in the upper part of the granitoid body.

An overwhelming majority of analyzed vein carbonates from the three stages displayed a rather restricted range of C isotopic compositions ($\delta^{13}C$ between -14 and -9‰/PDB) whatever the stage in which they were deposited and despite large variations of O isotopic ratios ($\delta^{18}O$ in the range + 3 to +30‰/SMOW). Carbon in pervasively altered rocks display the same features and is distributed among the two broad groups defined using O isotopic ratios in veins and fluid inclusions data, namely the Hercynian and the Mesozoic carbonates. Isotopic data argue that carbon was introduced as carbonates in the early stages of the retrograde Hercynian metamorphism and was systematically reworked by subsequent fluids without any significant carbon introduction from external sources. The only exception corresponds to the stage III calcite veins which are located in the upper sections of the cores, at depths lower than 350 m beneath the basement/cover boundary. These carbonates display the isotopically heaviest carbon ($\delta^{13}C$ up to -5‰/PDB) and are thus the only witnesses of element transfer from the sediments towards the basement. The trapping of oxidized carbon by Ca-rich plutonic rocks during their cooling history confers on these rocks an efficient self-sealing capacity during later fracturing and fluid flow. In the event of poly-cyclic carbonate redistribution, the use of carbon isotopic composition to unravel the fluid origins must be exercised with caution, as early C could be easily redistributed with the later fluid inputs.

Keywords: fracture sealing, carbonate, quartz, pervasive calcite, stable isotopes, carbon remobilization, fluid-rock interaction.

S.C.D. - U.H.P. NANCY 1
BIBLIOTHÈQUE DES SCIENCES
Rue du Jardin Botanique - BP 11
54601 VILLERS-LES-NANCY Cédex

4.1 Introduction

Preliminary investigations of the geochemistry of fracture infillings (calcites, dolomites and occasionally quartz) in the Vienne granitoïds were undertaken a few years ago (Coulibaly, 1998; Cathelineau et al., 1999, Sacchi and Michelot, 1996) to determine the past chemical, isotopic and thermal conditions of the fluid circulations in plutonic rocks of the Vienne covered basement. The first aim of these studies was to reconstruct the history of the successive fluid events in that area. However, these studies also lead to an important question about the carbon source of carbonate infillings in crystalline basement rocks. These rocks, indeed, among them granitoids, often contain small amounts of carbonate minerals, either as fractures infillings, or as disseminated crystals within the silicate matrix, or as crystals replacing calcic mineral precursors (e.g., plagioclase). Morphological, compositional and thermoluminescence properties are then used to characterize these different varieties of carbonates, which may be dolomitic, ankeritic or calcitic. (e.g., Komor, 1995; Wallin and Peterman, 1999; White et al., 1999). The source of the related C may be very different from case to case. The protoliths of metasediments may initially contain some carbon (either oxidised or reduced) which could be remobilized during metamorphism or hydrothermal alteration. For crystalline rocks which have been submitted to surface or subsurface conditions, a pedogenic source of C may also exist. Recrystallized glassy igneous rocks may contain C of magmatic derivation since the content of C in volcanic glasses is not negligible (Pineau and Javoy, 1994; Jendrzejewski et al., 1996; Macpherson et al., 1999).

In fresh (i.e., non weathered) granitoid rocks, the amount of carbonates may be noticeable, currently in the permil-percent range (up to a few %) although weathering drastically decreases that content (White et al., 1999 and references therein). Considering the size of granitic batholiths, this corresponds to a huge mass of carbon. In acidic plutonic rocks, the existence of an inner (magmatic) stock of carbonates has never been established and is unlikely because i) the high SiO_2 (+ H_2O) activities in granitic systems make the crystallization of carbonates in magmatic conditions improbable, ii) the total crystallization of magma would lead to the loss of the volatile phase (in which CO_2 is certainly the dominant C species). Thus, in the lack of magmatic carbonates, the source of carbon in granitoids must be external and this implies that fluid circulation is responsible for C transfer; the fluids may be surface-derived, migrating from neighbouring C-bearing rocks, outgassed from various crustal or mantle deep-seated levels. Carbonates present in granitoid rocks are therefore a clue to decipher the history of fluid migration from the initial sub-solidus cooling stage to the surficial stage. Many studies on fluid migrations are available in sedimentary systems (e.g., Muchez et al., 2000; Winter et al., 1995 and references therein) as well as in metamorphic basement lithologies (e.g., Blyth et al., 2000; Trave et al., 2000; Wallin and Peterman, 1999; Komor, 1995) but are relatively rare in granitoids (Blyth et al., 2000; Valley et al., 1988, Clauer et al., 1989).

The scope of this paper is to discuss the fluid circulation history and the C transfers in a granitoid basement in Vienne area overlaid by a carbonate sedimentary sequence, a situation representative of most of the Variscan basement in western Europe. Previous petrographic and stable isotopic works on carbonate veins (Coulibaly, 1998; Cathelineau et al., 1999, Sacchi and Michelot, 1996) lead to a striking feature: an overwhelming majority of analyzed vein carbonates displayed a rather restricted range of C isotopic compositions ($\delta^{13}C$ between -14 and -9‰/PDB)

whatever the stage of deposition and despite large variations of O isotopic ratios. $\delta^{18}O$ for carbonates and also for quartz are in the range + 3 to +30‰/SMOW. However, the reason why successive fluid inputs with very different histories could produce carbonates with a rather constant and relatively light carbon isotopic composition remains unclear. The C source problem was still more intriguing taking into account the high amount of carbonates (commonly in the percent range) observed in large rock volumes in that area.

Besides the academic scope, this approach must be performed to increase our knowledge of the (self)-sealing capacity of this type of granitoid, an important property for a potential use as a repository site for nuclear or chemical wastes. To re-investigate the question of C source and assess the fluid events, we carefully studied the paragenetic sequences including the carbonates (calcites and dolomites) and the associated quartz in the fractures. We paid special attention to a comparison of carbonate geochemistry in veins and in bulk rocks containing dispersed fine-grained carbonates. The present work combines petrographic, mineralogical, chemical, fluid inclusions and stable isotopes approaches on the different carbonate and quartz generations.

4.2 Geology and description of the studied material

4.2.1 The Vienne granitoids

The Charroux-Civray plutonic complex is located at the northwestern border of the NW edge of the French Massif Central (Fig. 4.1), below a 150 m - thick sedimentary cover. It is part of the "Tonalitic Line" of the Limousin (Peiffer, 1986; Shaw et al., 1993) and contains multiple intrusions of mafic to acidic plutonic rocks dated around 350-360 ± 5 Ma (U-Pb zircons; Bertrand et al., 1996) at an early stage of the mid-European Hercynian orogeny. Three magmatic suites have been identified: medium K calc-alkaline, high-K calc-alkaline and shoshonitic (Capdevila, 1997, 1998; Cuney et al., 1999) and the main lithologies consist of medium-K calc-alkaline gabbros, diorites, tonalites, granodiorites and high-K calc-alkaline monzogabbros, monzodiorites, monzonites, and monzogranites. The different intrusions exhibit magmatic contacts and magmatic mingling. Basic enclaves and basic to acid dikes are widespread over the whole studied complex. The main rock-forming minerals consist of zoned plagioclase (An_{45} - An_{25}), green Mg-hornblende, biotite, quartz, rare relics of clinopyroxene and alkali feldspar in varying abundance according to each rock type. Sphene, magnetite, apatite, zircon, pyrite, chalcopyrite and allanite are the main accessories. Drillings have revealed the local existence of a body of two-micas granite cross-cutting the afore mentioned granitoids at depth. According to gravimetric studies, this granitic type, enriched in rare metals (W, Ta, U; Cuney et al., 1999) has a probable larger extension at greater depths (Virlogeux et al., 1997).

Investigated samples were taken from 17 continuously cored, 200 m to 1000 m - deep boreholes performed by Andra (French Nuclear waste Management Company). The drillings were carried out to explore a potential site for the construction of an underground laboratory devoted to the study of radioactive waste disposal in crystalline rocks.

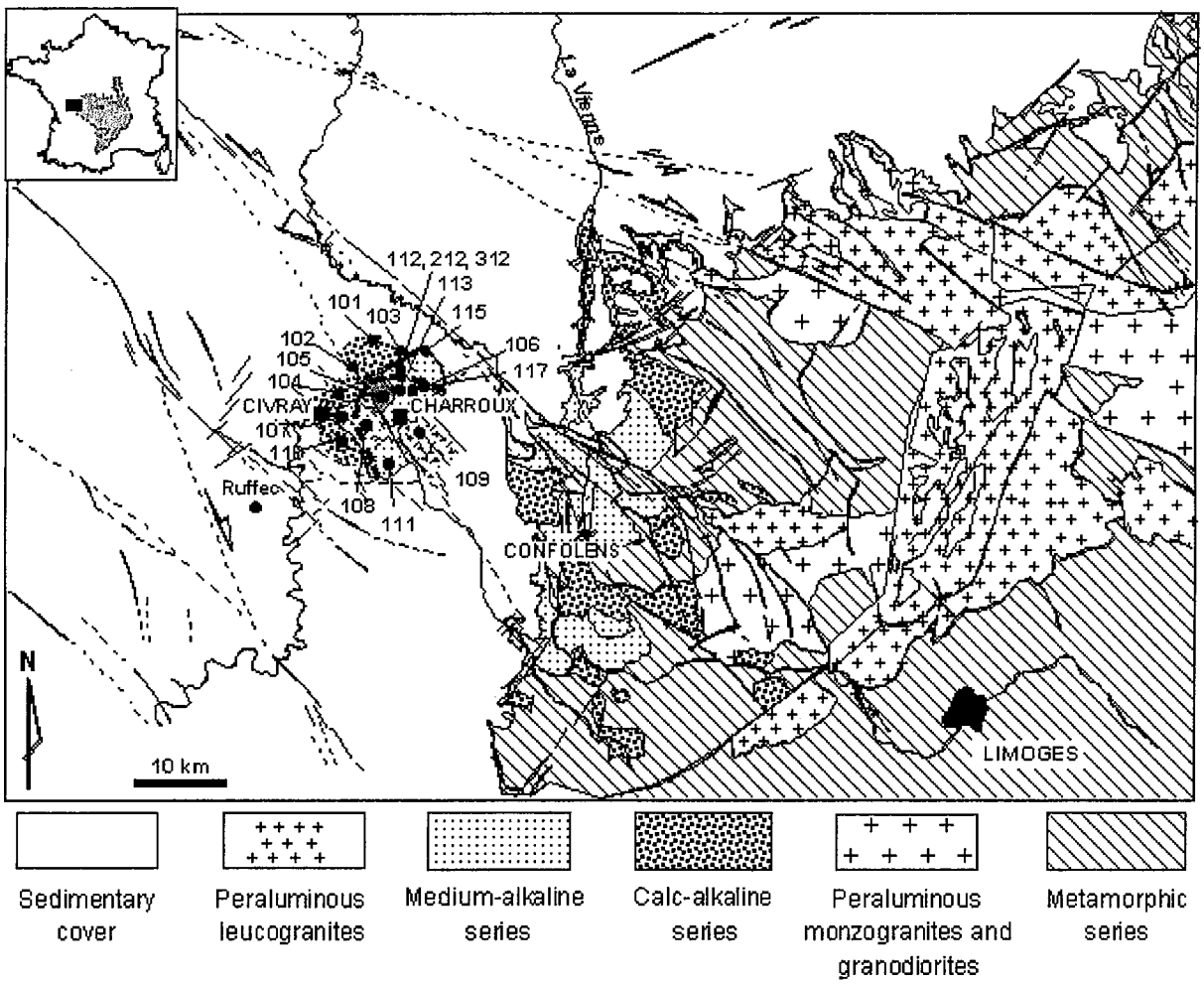

Fig. 4.1. Map of the Charroux-Civray area with the north-western part of the Massif Central. At the drilling locations, the basement is covered by about 150 m - thick sedimentary rocks of Jurassic age (white area). The basement beneath Charroux-Civray is mainly built-up by medium-K and high-K calc-alkaline intrusions and its local contours have been derived from the geophysical investigations.

4.2.2 The fluid circulations

By means of paragenetic and fluid inclusions studies (FI more frequently in quartz than in carbonates), the existence of at least 3 stages of fluid flow was demonstrated in the Charroux-Civray granitoids, each stage being characteristic of extremely distinct P-T conditions and geodynamic contexts (Cathelineau et al., 1999). Multiphase veins fillings (including carbonates and quartz) can be attributed to 3 stages of fluid circulation events (Fig. 4.2 and Fig. 4.3), summarized in the following paragraph from previous studies (Cathelineau et al., 1999; Freiberger et al., submitted).

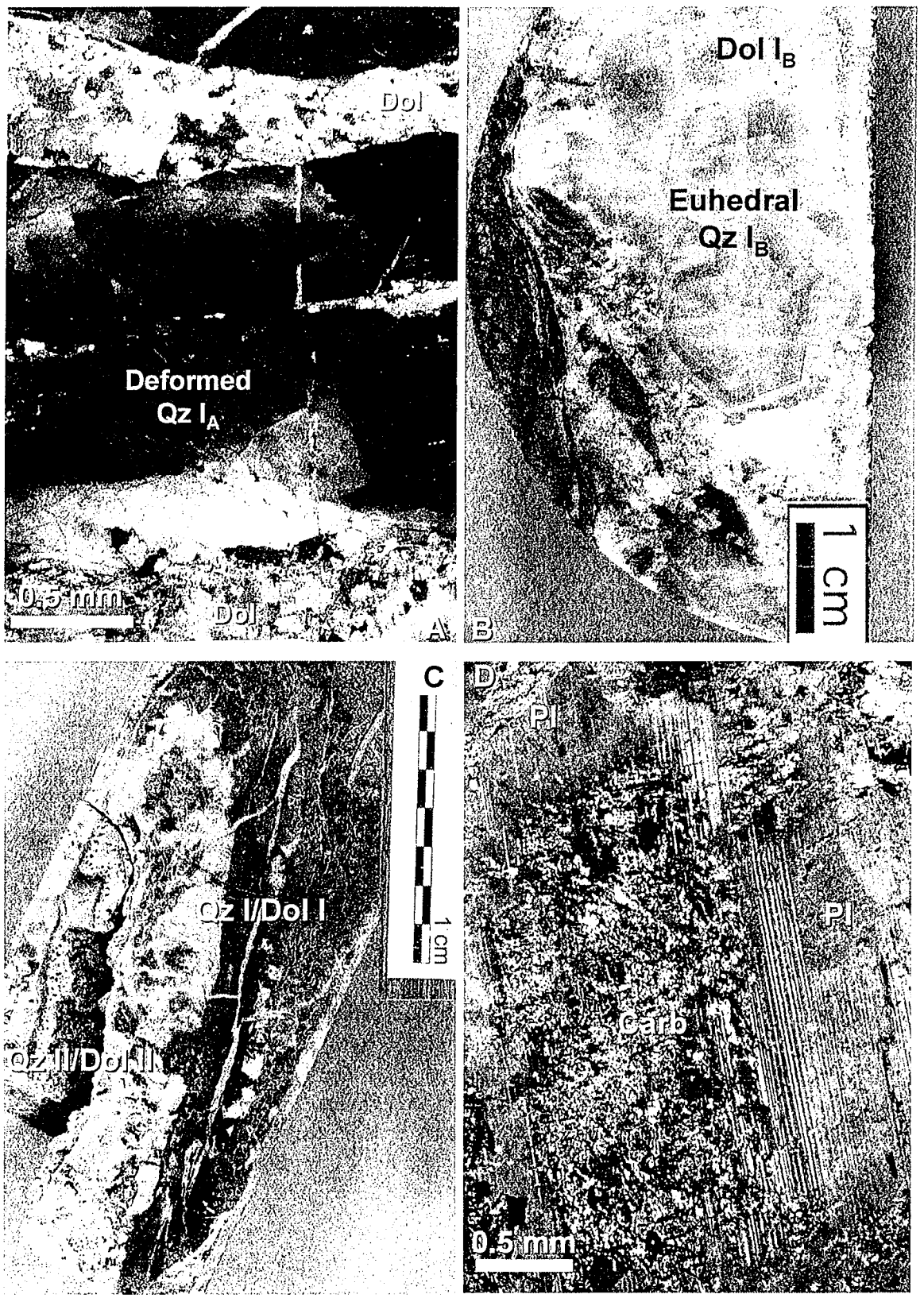

Fig. 4.2. A: Photomicrographs of typical early Hercynian infillings (I_A). Deformed and microfractured quartz is intersected by several later generations of dolomite (CHA106 - 491.80 m). B: Macroscopic late Hercynian paragenesis (I_B) showing zoned euhedral quartz followed by the crystallization of dolomite (CHA212 – 583.27 m). C: Complex assemblage of Hercynian and Mesozoic quartz/dolomite paragenesis. D: Disseminated carbonates replacing calcic mineral precursors, in that case, a plagioclase crystal.
Dol: Dolomite, Qz: Quartz, Carb: Carbonates, Pl: Plagioclase.

- Stage-I: Hercynian events

Early events (Stage-I_A): The early post-magmatic stage of Hercynian age is characterized by a first retrograde crystallization of Ca-Al silicates like hydrogarnet, prehnite, pumpellyite, pistacite and laumontite during successive cooling of the granitoids (Freiberger et al., submitted). The development of the common paragenesis prehnite + pumpellyite indicates a rather narrow temperature range of 200° to 280°C and pressures of 2 to 3 kbar (Frey et al., 1991). Earliest carbonates occur mostly as grains located at crystals boundaries or as alteration product of Ca-plagioclase, sometimes as thin microfractures (= 100 µm) fillings (Freiberger et al., submitted). Early carbonates also occur in fracture, which are then affected by a slight ductile deformation as the early vein quartz. These late deformational stages of the Hercynian orogeny are more or less coeval with the intrusion of peraluminous granitoid bodies at depth and a subsequent temperature increase up to 450°C (Cathelineau et al., 1999). Trapping temperatures of FI in carbonates of the early stage are unknown because no reliable fluid inclusion could be studied due to the deformation. Since the earliest carbonates are synchronous or slightly anterior to the deformation and to the thermal stage related to the peraluminous intrusion, they can be considered as formed in between the lowest minimal temperature (prehnite-pumpellyite stage) reached prior to the leucogranite intrusion, and the temperatures reached at the intrusion stage, i.e., in between 250 to 450°C.

On the other hand, fluids associated with pervasive alteration at that stage have been trapped in fluid inclusions planes in rocks and in deformed quartz veins. According to its deformation state, quartz can be divided into two main types. The first quartz type is affected by an intense ductile deformation and contains FI with H_2O-NaCl fluids of variable CO_2 contents (from 5 to 80 mol% in calculated bulk composition). The second type is a less deformed mosaic quartz, which has trapped only H_2O-NaCl fluids. For the two types of quartz, homogenization temperatures (T_h) are higher than 250°C and may reach more than 400°C. The related trapping conditions are estimated at around 1-2 kbar pressure and *c.* 350° to 400°C (around or slightly above the maximal T_h) up to 450°C (Freiberger et al., 2001 and submitted). During this thermal intrusive event, pervasive alteration of primary minerals occurred in relatively large rock volumes and is characterized by the following association: chlorite, phengite, quartz, dolomite, calcite, pyrite (or hematite).

Late events (Stage-I_B): undeformed macroscopic veins are filled by a chlorite + euhedral or mosaic quartz + Fe-rich dolomite (close to ankerite) assemblage formed during the second late retrograde alteration stage of plutonites (after the leucogranite intrusion), and coeval with the final basement uplifting stage and cooling. Three generations of quartz have been identified in the veins on the basis of petrographic characters and microthermometric studies without firm constraints upon their relative chronology except T_h: *i)* a mosaic/ microcrystalline vein type quartz, *ii)* an euhedral type quartz of centimeter size, and *iii)* a prismatic comb structure quartz.

The analyses of primary fluid inclusions from macroscopic dolomite-quartz veins display melting temperatures of ice (T_m) ranging from -3.2° to -0.3°C. In dolomite, T_h are in the range of 150° to 170°C, while in quartz, they range from 130° to 200°C as a function of the generation type. All these late infillings were deposited from

aqueous-type fluids of rather moderate salinities (0.5 to 5.3 wt.% eq. NaCl) at temperatures ranging from 150 to 250°C.

Both early and late analyzed dolomites are ferriferous with rather large ranges of Fe contents within a same crystal: in the formula $Ca(Mg_{1-x}, Fe_x)(CO_3)_2$, x varies between 0.1 up to 0.5 (i.e. evolves towards the ankerite end-member), while calcite displays a Fe content ranging from 0.01 up to 0.1 Fe per CO_3 unit. Such compositional variations can be observed within the same crystal.

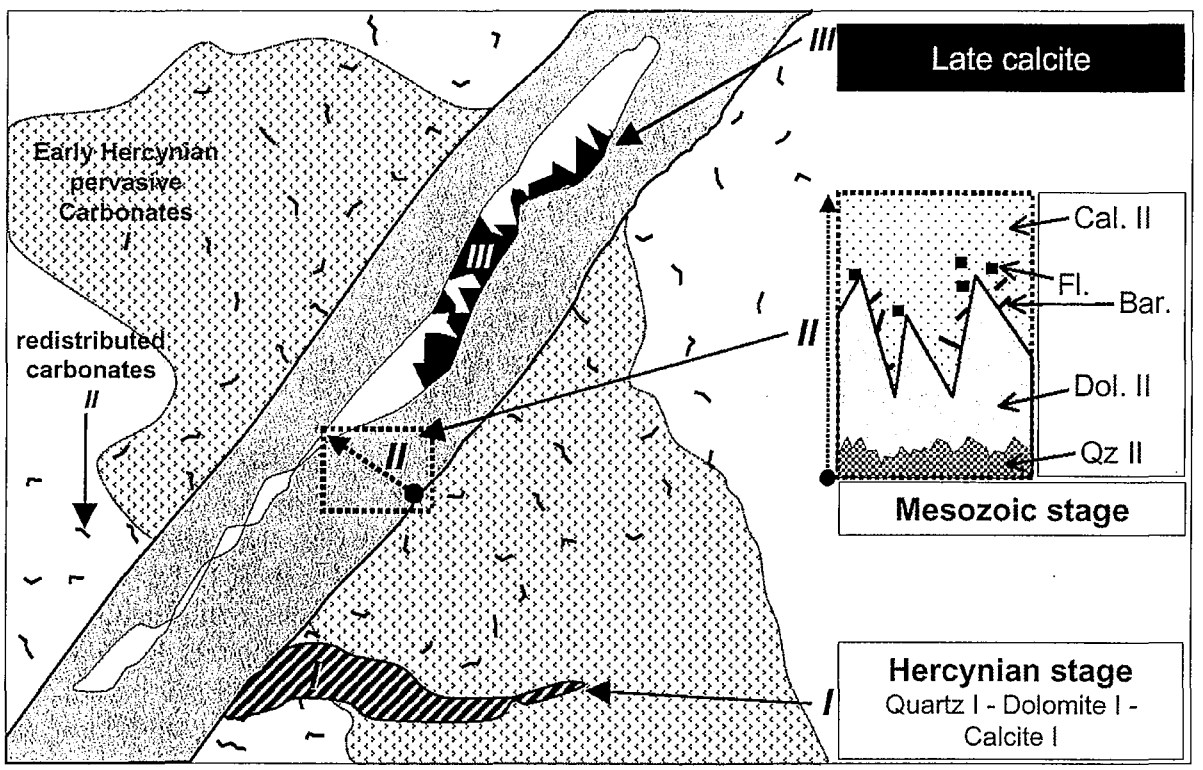

Fig. 4.3. Schematic representation of the main types (I, II, III) of carbonates and quartz infillings found in the Vienne plutonites and their textural relationships.
Cal.: Calcite, Fl.: Fluorite, Bar.: Barite, Dol.: Dolomite, Qz.: Quartz.

- Stage-II: Brines events

About 70 % of the macroscopic veins which are found in the plutonites are considered as linked to the second main stage of fracture re-opening and filling (Mesozoic stage). This stage II produced veins with a specific and constant paragenetic sequence: hematite-adularia/ quartz (II) / dolomite (II)/ fluorite/ barite± sulphides / calcite (II) (Fig. 4.2). These veins are largely predominant over the studied drill cores in the basement, down to 800 m underneath the basement/ cover interface and are also identified as quartz veins in the lower part of the sedimentary cover (Hettangian/ Sinemurian/ InfraToarcian series). This indicates an age at least younger than Hettangian.

Dolomite II represents the main vein infillings in stage II veins, calcite II and quartz II being much less abundant. Dolomite II and calcite II have a rather low Fe content (< 0.15 per formula unit) and are close to the two carbonate end-members (pure dolomite and calcite).

Brine inclusions were found in quartz, barite, dolomite and calcite from this stage-II assemblage and are characterized by a T_m ice of -23° ± 5°C, indicative of salinities around 25 wt.% equiv. NaCl, and by T_h of 90°± 20°C for quartz and slightly lower (80±20°C) for dolomite, barite and calcite. Trapped brines are interpreted as expelled basinal brines migrated across the bottom of the sedimentary cover (InfraToarcian) through structural and sedimentary discontinuities and they sealed the fractures in the underlying basement (Cathelineau et al., 1999; Boiron et al, submitted).

- Stage-III: Late calcite

A third stage is identified as late vein infillings containing calcite, or sometimes kaolinite-calcite. They are found at the upper part of the granite and in the Mesozoic sedimentary cover, but also in deeper parts (-500 to -600m in drill hole CHA 212 for instance) where they frequently occur in fractured blocks, as geodic infillings of previous stage-II veins. No morphological evolution with depth has been detected. The latest calcites record a change in the fluid salinities and temperature ($T_h \leq$ 50-55°C), suggesting a probable involvement of marine or diagenetic waters related to the cover deposition (especially the Dogger) (Cathelineau et al., 1999).

Calcite is almost pure and has very low trace elements contents. Estimated temperatures of calcite crystallization are at the maximum around 50/60°C for two-phase inclusions ($T_h \leq 50°$) or may be lower in the more common one-phased inclusions. The salinities can be measured exactly only on scarce two-phase inclusions. They are also low (about 1-2 wt.% eq. NaCl), except in some deep-seated samples (CHA 103/2424, 615.05 m; CHA 212/8600, 743.48m) for which salinities are around 4 wt.% eq. NaCl.

4.3 C and O isotopes on bulk altered rocks and veins

4.3.1 Analytical techniques

In veins, calcite, dolomite and quartz were handpicked and crushed before reaction. Isotopic analyses of carbonates were performed (both in the Rennes and in the Paris-Sud universities) on CO_2 gaz with 2 VG SIRA 10 triple collector instruments. Quartz analyses were made only in the Rennes laboratory. The " matrix " carbonates were analyzed in a global way (bulk rocks) by working on carefully selected whole rock samples devoid of any proximal carbonate vein pollutions. These powdered samples were thus reacted with anhydrous orthophosphoric acid at 25°C (McCrea, 1950). Because such bulk samples contain both disseminated calcite (dominant) and dolomite, we have used the isotope fractionation factor of calcite for acid digestion (α= 1.01025; Friedman and O'Neil, 1977). Isotope compositions are quoted using the δ notation with respect to SMOW (O) and PDB (C). Using internal carbonate standards, the reference material NBS 19 as well as replicate analyses of samples, the reproducibility of C and O analyses was better than ± 0.1‰ or than ± 0.2‰.

However, in whole rock carbonates, the true uncertainties are certainly higher for O (in the 0.2 - 0.3‰ range) because disseminated calcite and dolomite were reacted together (α = 1.01025, see above). For the quartz analyses, the reference material was NBS 28. Most quartz analyses were duplicated. The reproducibility related to these duplicates for O was ranging from 0.005 to 0.39 ‰ with an average value of 0.10 ‰. The location and the number of all the fracture filling samples are illustrated in Fig. 4.4.

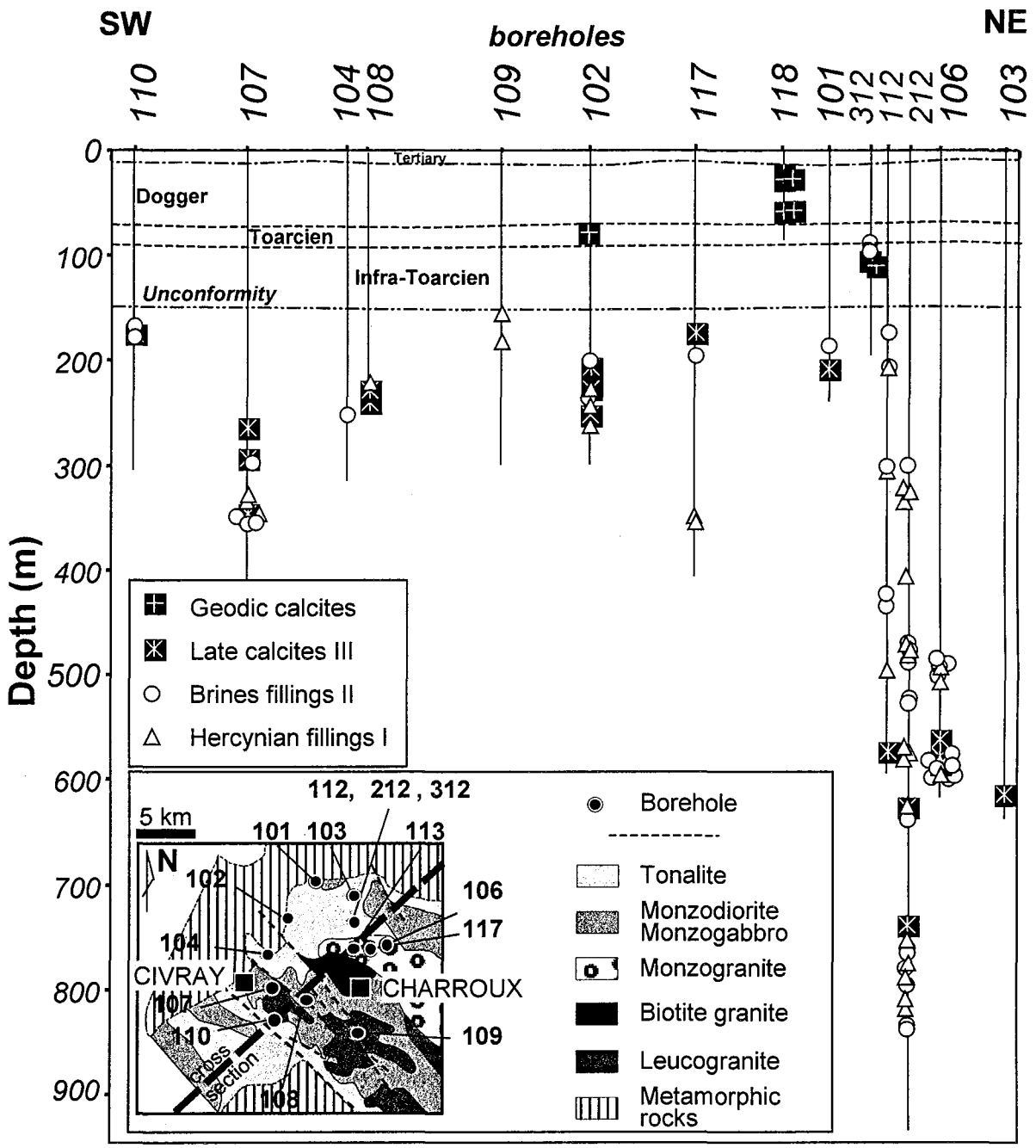

Fig. 4.4. Borehole – depth (m) diagram showing the location and the type (I, II or III) of fracture filling samples. Boreholes are projected along a SW-NE cross-section (see inset).

4.3.2 Isotopic data

Isotopic data (Table 4.1 to Table 4.4) are illustrated for carbonates as $\delta^{18}O$ vs. $\delta^{13}C$ diagrams (Fig. 4.5 and Fig. 4.6) as well as $\delta^{13}C$ vs. depth diagrams (Fig. 4.7) and for quartz as T(°C) of estimated crystallization vs. $\delta^{18}O$ diagram (Fig. 4.8). In these figures, the different groups of samples are identified on the basis of their morphological properties, their paragenetic associations, their mutual relationships, as well as, for some of them, by the fluid inclusions characteristics. In summary (see below for detail), carbonates and quartz contained in the Vienne granitoids display a huge range of O isotopic compositions (Fig. 4.5, Fig. 4.6 and Fig. 4.8). $\delta^{18}O$ values vary between +3 and +30‰/SMOW. The $\delta^{13}C$ values of vein carbonates are less variable, from -14 to -5‰.

- Hercynian stage (I)

The different hercynian carbonates show some tendencies in their isotopic features. In stage I (Hercynian) veins carbonates have globally the lowest O isotopic compositions and (with one exception) the $\delta^{13}C$ values range from -14 to -8‰ (Fig. 4.5.A). Among them, the early carbonates (stage I_A) display higher O isotopic compositions ($\delta^{18}O$ =+13 to +18.2‰) than the late Hercynian fractures (stage I_B, $\delta^{18}O$ = +3 to +13 ‰). Hercynian veins quartz display an isotopic behaviour relatively similar to that of hercynian carbonates (Fig. 4.7): $\delta^{18}O$ values of stage I_A deformed quartz are grouped close to +10‰ ±2, which differs markedly from stage I_B quartz for which a broad evolution of $\delta^{18}O$ values from +5 to +17‰, is associated to decreasing quartz FI T_h (Fig. 4.8).

Disseminated carbonates within fresh plutonites (Fig. 4.5.B) display O isotopic compositions (+12 to +16‰) very comparable to those of early Hercynian (I_A) veins.

- Brine stage (II)

The group of carbonate veins related to the Mesozoic brines event (stage II) shows a range of $\delta^{13}C$ values (-13.2 to -8.9‰) similar to that of Hercynian veins and rocks disseminated carbonates (Fig. 4.5A), but their O isotopic compositions are distinctly higher: $\delta^{18}O$ =+ 22.8 to +30‰. Similarly, brines quartz (Fig. 4.8), is ^{18}O-enriched ($\delta^{18}O$ =+20 to +29‰) and in the range observed for brines carbonates

The carbonate fraction in whole rocks affected by pervasive carbonitization displays isotopic characteristics similar to those of the Mesozoic brines event. A few of these bulk carbonates have $\delta^{18}O$ values intermediate between those of the Hercynian and Mesozoic groups.

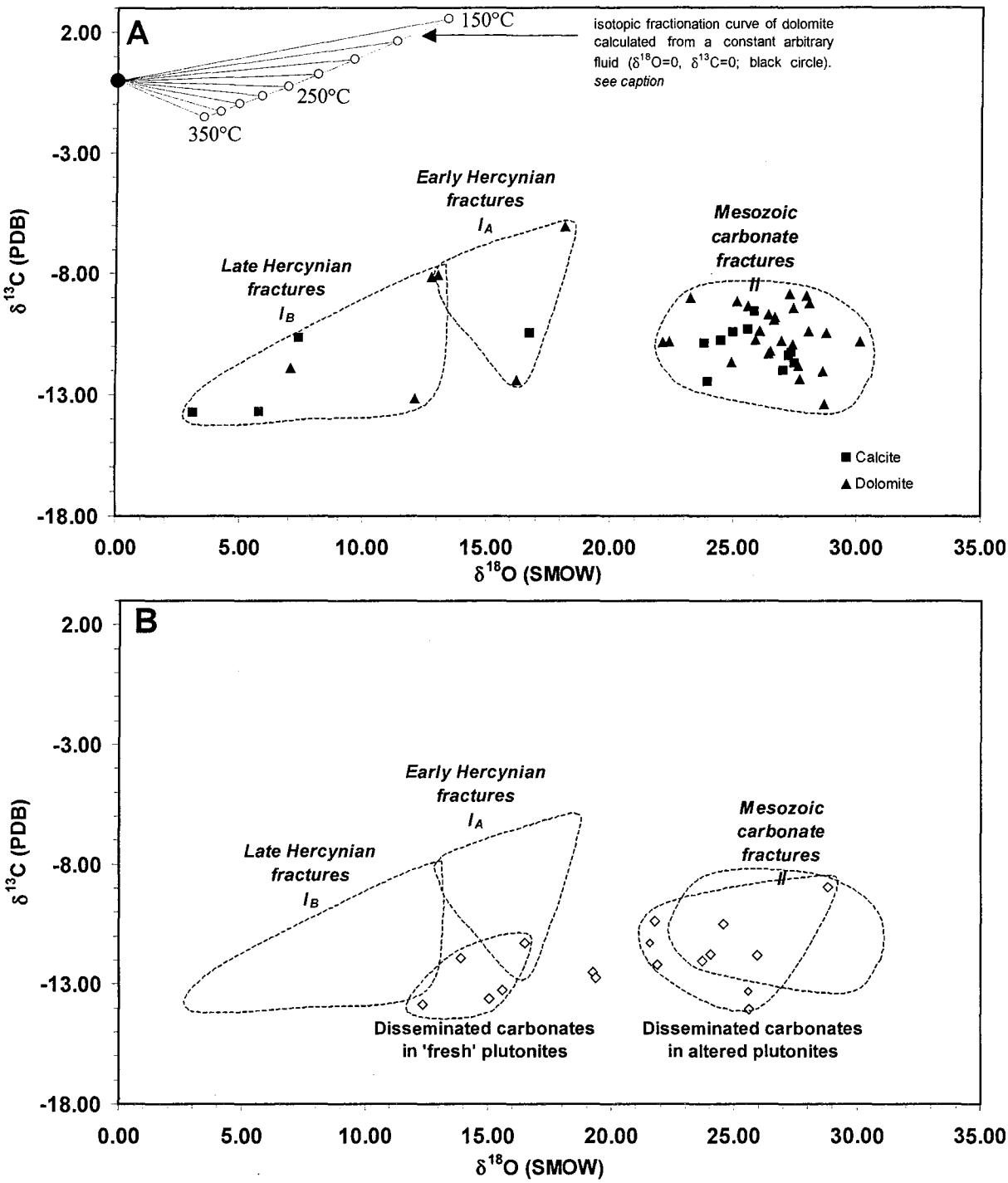

Fig. 4.5. $\delta^{13}C$ - $\delta^{18}O$ binary plot for calcites and dolomites filling the Hercynian and Mesozoic fractures (A) and for carbonates disseminated in the matrix of whole rock plutonites (B).
In figure (A) is represented the isotopic fractionation curve of dolomite calculated for a constant arbitrary fluid ($\delta^{18}O$=0; $\delta^{13}C$=0) for different temperatures assuming that the $\delta^{13}C$ value of H_2CO_3 (apparent) is very close to the $\delta^{13}C$ values of CO_2 (gas) (Ohmoto, 1972, p. 566). The C isotopic fractionation factors between dolomite and carbon in solution were obtained from the dolomite-calcite fractionation curve of Sheppard and Schwarcz (1970) and the calcite–CO_2 fractionation equation of Ohmoto and Rye (1979). The O isotopic fractionation factors between dolomite and water were derived from the dolomite-calcite fractionation curve of Sheppard and Schwarcz (1970) and the calcite–H_2O fractionation equation of O'Neil (1969). See the discussion for details.

- Late stage (III)

The last stage vein calcites display a rather restricted range of O isotopic compositions: $\delta^{18}O$ = +20.2 to 25.6‰. The majority of samples have C isotopic compositions similar to those of stages I and II with a tendency for some of them to show heavier $\delta^{13}C$ values (Fig. 4.6). It is worth noting that those ^{13}C-enriched calcites are found only in the upper part of the granitoid body (Fig. 4.7). As a whole, stage III calcites show a trend of enrichment in $\delta^{13}C$ at more or less constant $\delta^{18}O$ values towards the group of geodic calcites that fill the cavities of the overlying Mesozoic limestones ($\delta^{18}O$ = +22.6 to 25.6‰, $\delta^{13}C$ = -1.54 to +1.36‰).

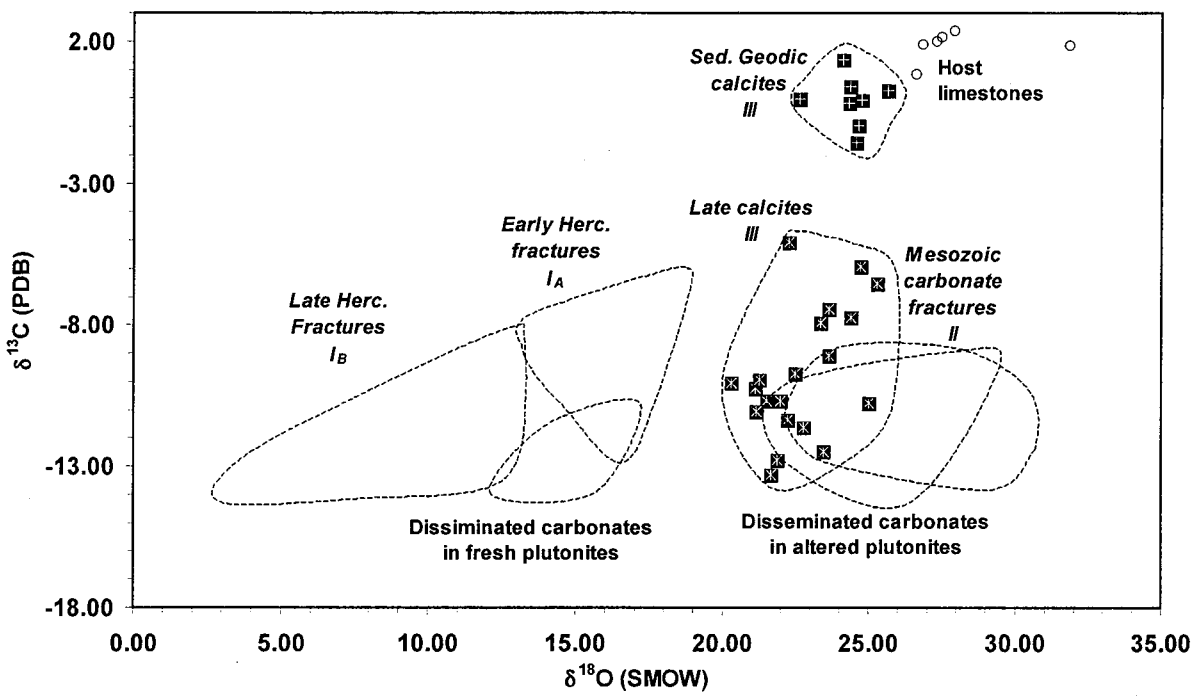

Fig. 4.6. $\delta^{13}C$ - $\delta^{18}O$ binary plot for the latest stage (III) calcites and from the sedimentary cover, with the field of the host rock (Mesozoic limestones) compositions. Envelopes for carbonates filling the Hercynian and Mesozoic fractures and those disseminated in plutonites (see Fig. 4.5) are given for reference.

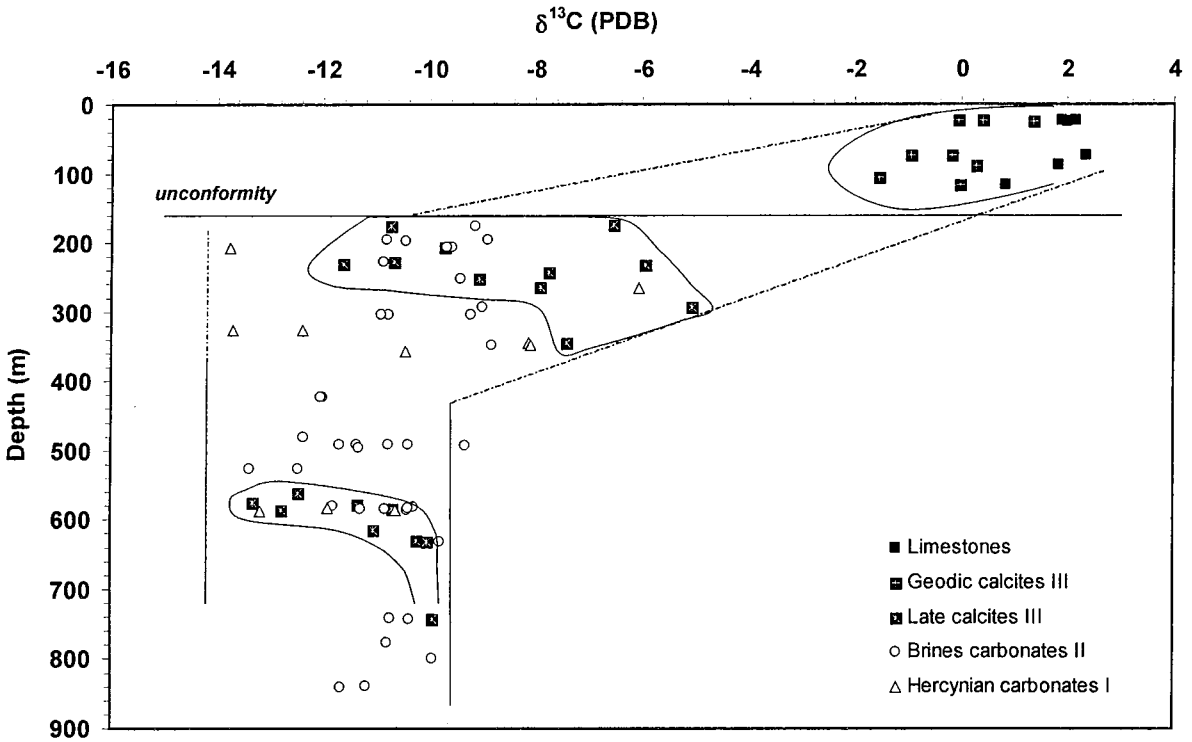

Fig. 4.7. $\delta^{13}C$ -depth section for all studied fracture carbonates and the Mesozoic limestones and their geodic calcitic infillings. Sample depths from CHA212 oblique borehole are recalculated relative to the surface.

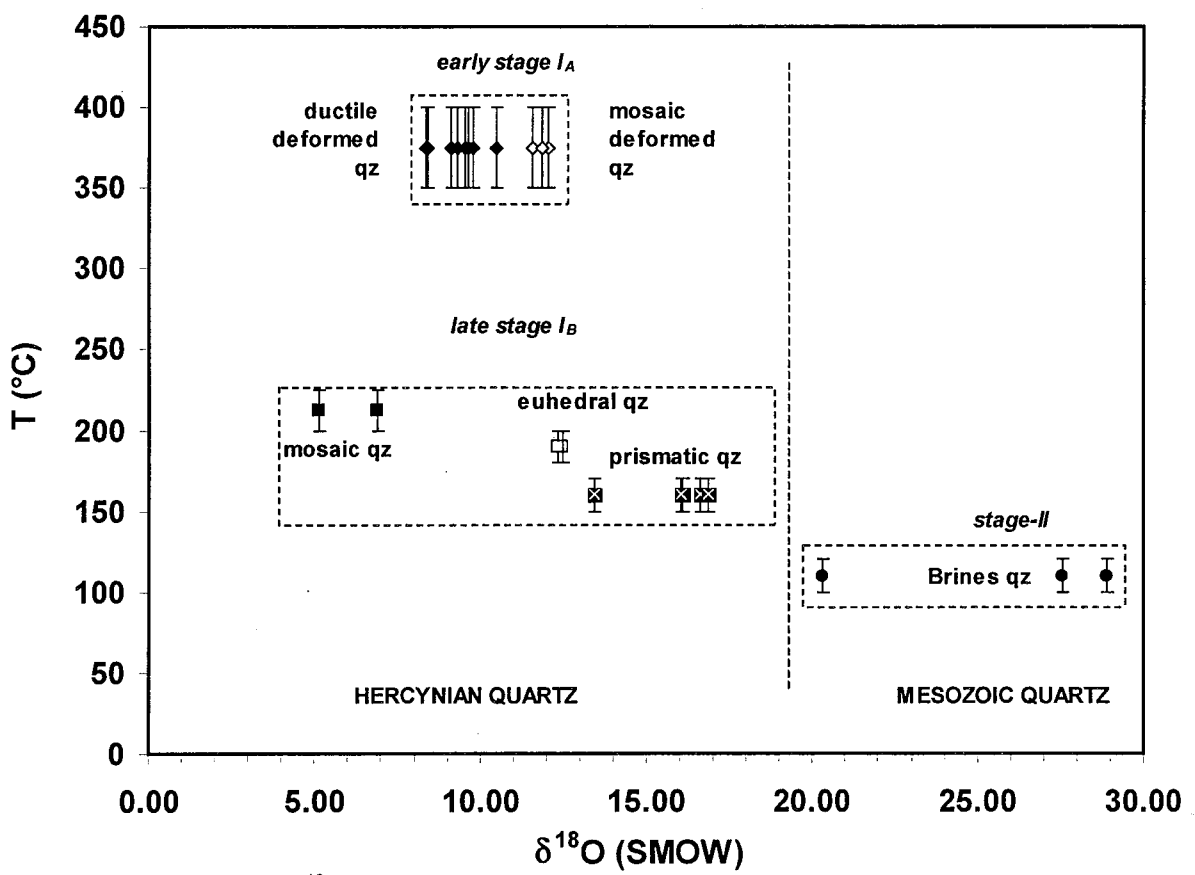

Fig. 4.8. Temperature vs. $\delta^{18}O$ binary plot for quartz filling the Hercynian and Mesozoic fractures in the Vienne plutonites.

Sample ref.	Depth (m)	Borehole	Rock type	Fracture paragenesis	$\delta^{13}C$	$\delta^{18}O$	$\delta^{18}O_{fluid}$	
Early Hercynian dolomites I_A							*T= 250°C*	*T= 400°C*
670	265.20	CIV102	to	Ill/FeOx/Qz1/Py/**Dol1**//Qz2/Dol2	-6.06	18.19	10.79	15.51
5410	326.00	CHA212	to	Qz/Cc1/**Dol1**	-12.39	16.26	8.85	13.57
1019	347.35	CIV107	mzd	Qz1/**Dol1**//Qz2/Py/Dol2/Ba2//Cc3	-8.08	13.05	5.65	10.37
Early Hercynian calcites I_A							*T= 250°C*	*T= 400°C*
5182	356.80	CHA117	to	Py/Chl/Ad/**Cc1**	-10.45	16.79	10.01	14.04
Late Hercynian dolomites I_B							*T= 170°C*	*T= 200°C*
1017	345.50	CIV107	mzd	Py/**DolAnk1**//Qz2/Dol2//Cc3	-8.13	12.80	0.70	2.74
6871	583.30	CHA212	to	Qz/**Dol1**	-11.90	7.10	-5.00	-2.96
8610	588.00	-	d	Qz1/Chl/**DolAnk1**//Qz2/Ga	-13.17	12.13	0.03	2.07
Late Hercynian calcites I_B							*T= 170°C*	*T= 200°C*
5174	206.90	CHA112	mzd	Chl/ill/Ad/FeOx/**Cc1**//Cc2	-13.76	3.17	-7.61	-5.87
5410	326.00	CHA212	to	Qz/**Cc1**-Dol1	-13.70	5.83	-4.95	-3.21
1067	585.00	CHA106	mzgd	Dol1/**Cc1**//Cc3	-10.64	7.44	-3.34	-1.60
Brine dolomites II							*T= 80°C*	*T= 100°C*
2770	174.90	CHA110	d	Ad/Dol1//Ad/**Dol2**//Cc3	-9.14	25.17	3.52	6.25
5176	174.92	CHA112	to	**Dol2**/Bar	-8.41	30.32	8.67	11.40
385	195.30	CHA101	to	Ad/**Dol2**/**Cpy**/Bar	-10.82	30.13	8.47	11.21
2729	196.00	CHA110	to	**Dol2**	-8.90	28.00	6.35	9.08
5179	197.10	CHA117	mzg	Ad/Py/**Dol2**/Bar	-10.45	28.79	7.13	9.86
298	251.95	CIV104	d	Chl/ill/Hem/Qz//Ba2/**Dol2**/Py//Cc3	-9.41	27.46	5.80	8.53
1018	293.60	CIV107	mzd	Ad/**Dol2**/Cpy/Py/Bar/Cc3	-9.00	23.28	1.63	4.36
5175	303.15	CHA112	to	**Dol2**/Cc2	-10.91	27.42	5.76	8.49
5408	303.18	CHA212	to	**Dol2**	-9.22	28.09	6.43	9.16
1017	345.50	CIV107	mzd	Py/Dol1//Qz2/**Dol2**//Cc3	-7.38	23.59	1.94	4.67
1019	347.35	-	mzd	Qz1/Ank1//Qz2/Py/**Dol2**/Ba2//Cc3	-8.82	27.29	5.64	8.37
5173	422.40	CHA112	to	Chl/ill/Ad//**Dol2**/Cc2	-12.05	28.62	6.97	9.70
5654	480.50	CHA212	lto	Qz/Py/ill/Chl/**Dol2**/Bar	-12.37	27.71	6.06	8.79
1051	491.72	CHA106	mzg	Cpy/Qz/Dol1//Ba2/**Dol2**/Cc2	-10.77	26.97	5.32	8.05
1052	491.85	-	mzg	Dol1//Ba2/**Dol2**/Cc2	-10.40	26.10	4.45	7.18
5644	492.00	CHA212	lto	Qz/Py/Cpy/**Dol2**/Bar	-9.33	25.60	3.95	6.68
1053	495.34	CHA106	mzg	Ad/Py/Qz/Dol1//Py/**Dol2**/Ba2	-11.32	26.44	4.79	7.52
1056	579.58	-	mzgd	Ad/Cpy/**Dol**	-11.81	27.66	6.01	8.74
1065	581.47	-	mzgd	**Dol2**/Bar	-10.45	27.85	6.20	8.93
1063	582.66	-	mzgd	**Dol2**/Bar	-10.40	28.04	6.39	9.12
1057	583.97	-	mzgd	**Dol2**/Cc2	-10.83	22.16	0.51	3.24
8593	630.80	CHA212	to/d	Chl/ill/Qz//**Dol2**/Bar//Cc3	-9.80	26.69	5.04	7.77
8598	741.00	-	lto	Qz//Bar/**Dol2**/Hal/Py-Cpy/Ga//Cc3	-10.74	25.91	4.26	6.99
8600	743.40	-	lto	ill/Dol1//**Dol2**/Py/Bar//Cc3	-10.37	26.06	4.41	7.14
8603	777.10	-	lto	Qz/**Dol2**/Bar/Py	-10.79	22.42	0.76	3.49
8606	800.00	-	to	ill/Chl//Gal/Py/**Dol2**/Bar	-9.93	26.66	5.01	7.74
8605	838.70	-	mzg	ill/Qz/**Dol2**/NaCl/Py	-11.18	26.52	4.87	7.60
8604	839.75	-	mzg	Qz/Ad/ill//Gal/**Dol**	-11.67	24.93	3.28	6.01
Brine calcites II							*T= 80°C*	*T= 100°C*
667	206.55	CIV102	to	Dol2/Ba2/**Cc2**//Cc3	-9.57	25.86	6.94	9.27
5174	206.90	CHA112	mzgd	Chl/ill/Ad/FeOx/Cc1//**Cc2**	-8.90	25.88	6.96	9.29
671	227.10	CIV102	to	Dol/**Cc2**//Cc3	-10.88	23.85	4.93	7.26
5175	303.15	CHA112	to	Dol2/**Cc2**	-10.78	24.51	5.59	7.92
5173	422.40	-	to	Chl/ill/Ad//Dol2/**Cc2**	-12.00	27.04	8.12	10.45
1051	491.72	CHA106	mzg	Cpy/Qz/Dol1//Ba2/Dol2/**Cc2**	-11.37	27.26	8.34	10.67
1052	491.85	-	mzg	Dol1//Ba2/Dol2/**Cc2**	-11.68	27.50	8.58	10.91
5646	526.00	CHA212	to	Qz1/ill/Chl//Qz2/Py/Dol2/**Cc2**	-12.47	24.00	5.08	7.41
1061	581.80	CHA106	mzgd	**Cc2**	-10.29	25.61	6.69	9.02
1057	583.95	-	mzgd	Dol2/**Cc2**	-11.28	27.36	8.44	10.77
1068	585.90	-	do	Dol1//Dol2/Py/Bar/**Cc2**	-10.41	25.02	6.10	8.43

Table 4.1. Stable isotope ($\delta^{13}C$ (PDB) and $\delta^{18}O$ (SMOW)) data of investigated carbonate fracture infillings of the stages I and II, with indication of host rock type. In the fracture paragenesis, the analyzed carbonate is in heavy symbol and the number corresponds to the attributed stage. The O isotopic composition of corresponding fluid is calculated for a range of 2 assumed temperatures (see text for explanations). For samples from the CHA212 sloping drillings, depths are recalculated below the surface.
Rock abbreviations: ap: aplite, br: breccia, d: diorite, do: dolerite, gb: gabbro-diorite, gn: gneiss, hem: hematite, lto: leucotonalite, mg: monzogranite, mzd: monzodiorite, mzgd: monzograbbro-diorite, to: tonalite; Mineral abbreviations: Ank: ankerite, Ad: adularia, Bar: barite, Cc: calcite, Chl: chlorite, Dol: dolomite, ill: illite, Gal: galena, Py: pyrite, Qz: quartz. For paragenesis, number 1, 2, 3 correspond to stage I, II, and III respectively.

Sample ref.	Depth (m)	Borehole	Rock type	Fracture paragenesis	$\delta^{13}C$	$\delta^{18}O$	$\delta^{18}O_{fluid}$	
Late calcites III in granitoids							*T= 50°C*	*T= 60°C*
5178	174.65	CHA117	mzg	**Cc3**	-6.54	25.30	2.05	3.62
2770	174.90	CHA110	d	Ad/Dol1//Ad/Dol2//**Cc3**	-10.74	24.99	1.74	3.31
667	206.55	CIV102	to	Dol2/Ba2/Cc2//**Cc3**	-9.72	22.48	-0.78	0.80
671	227.10	-	to	Dol/Cc2//**Cc3**	-10.68	21.52	-1.74	-0.16
387	230.30	CHA101	gn	Bar/Dol//**Cc3**	-11.62	22.78	-0.48	1.10
2419	231.60	CHA108	mzd	Chl/Ad/Py/Fl/Bar/Cpy//**Cc3**	-5.94	24.72	1.47	3.04
2421	243.15	-	mzd	Ad/Dol/Fl/Py/Bar/Cpy//**Cc3**	-7.74	24.37	1.12	2.69
298	251.95	CIV102	d	Chl/ill/Hem/Qz//Ba2/Dol2/Py//**Cc3**	-9.07	23.64	0.39	1.96
1016	263.90	CIV107	mzd	Ad/Dol/Py/Cpy/Fl//**Cc3**	-7.91	23.33	0.08	1.65
1018	293.60	-	mzd	Ad/Dol2/Cpy/Py/Bar//**Cc3**	-5.07	22.28	-0.98	0.60
1017	345.50	-	mzd	Py/Dol1//Qz2/Dol2//**Cc3/Py**	-7.42	23.62	0.36	1.94
1064	560.97	CHA106	mzg	**Cc3**/Py	-12.46	23.46	0.20	1.78
5171	574.50	CHA112	to	Chl/ill/Ad/Bar/Py//**Cc3**	-13.31	21.66	-1.60	-0.02
1066	577.50	CHA106	do	**Cc3**	-11.34	22.22	-1.04	0.54
1058	584.10	-	do	Dol//**Cc3**	-10.69	21.98	-1.27	0.30
1067	585.00	-	do	Dol1/**Cc1**//**Cc3**	-12.78	21.87	-1.39	0.19
2424	615.05	CHA103	to/d	Ad/Dol//**Cc3**/Py	-11.05	21.16	-2.09	-0.52
8593	630.70	CHA212	to/d	Chl/ill/Qz//Dol/Bar//**Cc3**	-10.23	21.12	-2.14	-0.56
8594	630.99	-	to	Chl/Iill/Qz//Ad//**Cc3**	-10.03	20.27	-2.99	-1.41
8600	743.48	-	ap	ill/Dol1//Dol2/Py/Bar//**Cc3**	-9.93	21.26	-2.00	-0.42
Geodic calcites III in limestones							*T= 25°C*	*T= 50°C*
7251	22.60	CHA118	Bathonian	Geodic **Cc3**	0.41	24.37	-3.55	1.11
7253	23.10	-		-	-0.06	24.74	-3.18	1.48
7248	24.80	-		-	1.36	24.10	-3.82	0.84
7243	72.75	-		-	-0.96	24.64	-3.27	1.39
7245	73.45	-		-	-0.17	24.33	-3.58	1.08
397	88.25	CIV102	Toarcian	-	0.28	25.66	-2.25	2.41
7268	105.50	CHA312	Infra-	-	-1.54	24.56	-3.36	1.30
7271	116.00	-	Toarcian	-	-0.02	22.63	-5.28	-0.62

Table 4.2. Stable isotope ($\delta^{13}C$ (PDB) and $\delta^{18}O$ (SMOW)) data of investigated late calcite (III) fracture infillings in granitoids and the geodic calcite III in sedimentary cover.
(see Table 4.1 caption for more details and abbreviation descriptions).

Sample ref.	Depth (m)	Borehole	Rock type	Fracture paragenesis	$\delta^{18}O$	±	$\delta^{18}O_{fluid}$	
Early Hercynian ductile deformed qz I_A							*T=350°C*	*T=400°C*
2420	243.00	CHA108	mzd	**Qz1**	8.36	0.03	2.28	3.40
6860	407.59	CHA212	pegm	**Qz1**	9.30	0.12	3.22	4.34
1052	491.80	CHA106	mzg	Py/Cpy/**Qz1**/Dol1//Ba2/Dol2/Cc2	9.11	0.00	3.03	4.15
5093	506.50	CHA112	br	**Qz1**	9.76	0.07	3.68	4.80
8598	741.05	CHA212	lto	**Qz1**//Ba/Dol2//Py/Ga//Cc3	9.63	0.12	3.55	4.67
8603	777.10	-	lto	**Qz1**//Dol2/Ba/Py	10.51	0.27	4.44	5.55
6880	838.31	-	To	**Qz1**	9.52	0.08	3.45	4.56
8709	850.52	-	lto	**Qz1**	8.40	0.10	2.32	3.44
Early Hercynian mosaïc deformed qz I_A							*T=350°C*	*T=400°C*
1506	141.00	CHA109	lto	**Qz1**	12.05	0.12	5.97	7.09
1610	177.50	CHA109	lto	**Qz1**	11.56	0.07	5.48	6.60
5643	473.70	CHA212	lto	**Qz1**/Chl/Dol1//Dol2/Py/Ba	11.89	0.08	5.81	6.93
Late Hercynian mosaïc qz I_B							*T=200°C*	*T=225°C*
668	250.50	CIV102	ap	**Qz1**/ill//Dol2/Ba/Cpy/Py	5.15	0.03	-7.13	-5.65
1019	347.00	CIV107	mzd	**Qz1**/ill/Dol1//Qz2/Py/Dol2/Ba//Ca3	6.89		-5.39	-3.91
Late Hercynian euhedral qz I_B							*T=180°C*	*T=200°C*
6871	583.27	CHA212	to	**Qz1**/Dol1	12.49	0.11	-1.19	0.20
8610	587.85	-	d	**Qz1**/Chl/Dol1//Qz2/Ga	12.36	0.12	-1.31	0.08
Late Hercynian prismatic qz I_B							*T=150°C*	*T=170°C*
5634	356.80	CHA212	gd	**Qz1**/Py/Cpy/Dol1//Dol2	16.08		-0.10	1.63
5638	485.30	-	d	**Qz1**/Dol1//Dol2/Ba	16.60	0.02	0.42	2.15
5648	492.25	-	to	Py/Chl/ill/**Qz1**//Ba/Dol2/Cc2	13.41		-2.77	-1.04
8593	630.70	-	to/d	Chl/ill/**Qz1**//Dol2/Ba//Cc3	16.06	0.08	-0.12	1.61
8606	800.00	-	to	ill/Chl/**Qz1**//Gal/Py/Dol2/Ba	16.84	0.06	0.66	2.39
Brines qz II							*T=100°C*	*T=120°C*
8803	114.80	CHA312	dol	**Qz2**	28.91	0.16	6.98	9.56
8805	115.25	CHA312	dol	**Qz2**	27.56	0.39	5.64	8.22
1019	347.00	CIV107	mzd	Qz1/Dol1//**Qz2**/Py/Dol2/Ba2//Cc3	20.30		-1.63	0.96

Table 4.3. Stable isotope ($\delta^{18}O$ (SMOW)) data of investigated quartz infillings in granitoids and in sedimentary cover.
(see Table 4.1 caption for more details and abbreviation descriptions).

Sample ref.	Depth (m)	Borehole	Rock type	Carbonate %	$\delta^{13}C$	$\delta^{18}O$
Disseminated carbonates in granitoids						
8582	567.59	CHA212	Gabbro-diorite	1.45	-13.85	12.34
8651	638.41	-	Leucotonalite	0.84	-11.92	13.91
5421	434.70	-	Tonalite	0.70	-13.63	15.05
8678	762.16	-	Leucotonalite	0.21	-13.25	15.58
8657	599.52	-	Gabbro-diorite	-	-11.29	16.50
5396	237.05	-	Tonalite	0.33	-12.51	19.22
8680	778.01	-	-	2.14	-12.75	19.36
3783	247.55	CHA112	Gabbro-diorite	-	-11.27	21.55
5655	411.55	CHA212	Leucotonalite	-	-10.37	21.76
5098a	225.81	-	Tonalite	0.64	-12.21	21.88
5399	248.88	-	-	0.16	-12.02	23.70
5098	226.59	-	Altered tonalite	-	-11.78	24.03
8653	666.94	-	Leucotonalite	2.17	-10.49	24.56
5096a	221.62	-	Tonalite	1.77	-13.29	25.55
5096	221.72	-	Altered tonalite	3.89	-14.04	25.60
8581	564.38	-	Tonalite	2.74	-11.80	25.92
5648	494.60	-	-	0.085	-8.97	28.78
Limestones			Rock type			
7251	22.60	CHA118	Bathonian limestone		1.89	26.84
7253	23.10	-	-		2.15	27.47
7248	24.80	-	-		2.00	27.29
7243	72.75	CHA118	Bajocian limestone		2.35	27.93
2459	87.30	CHA110	Toarcian marl		1.83	31.85
7271	116.00	CHA312	Infra-Toarcian dolomite		0.84	26.62

Table 4.4. Stable isotope ($\delta^{13}C$ (PDB) and $\delta^{18}O$ (SMOW)) data of investigated disseminated carbonates in granitoids and of bulk limestones of sedimentary cover.
(see Table 4.1 caption for more details and abbreviation descriptions).

4.4 Discussion

4.4.1 Possible origin of the fluids and elements

The origin of the different fluids may be approached by estimating their O isotopic composition from those of the related mineral phases. For that purpose, we assumed isotopic equilibrium between the carbonate or quartz phases and the parent fluids in the temperature ranges obtained from fluid inclusions studies. For the calcite-water and dolomite-water systems, we used the fractionation equation of O'Neil et al. (1969) combined with the calcite-dolomite fractionations proposed by Sheppard and Schwarcz (1970) and for the quartz-water system, we used the fractionation equations of Zheng (1993).

- The Hercynian fluids

Stage-I_A: Combined with their moderate salinities and their relatively high temperatures of circulation, the calculated $\delta^{18}O$ fluid compositions of early (I_A type) Hercynian fluids leaves no real doubt on their nature despite large uncertainties in the size of the fractionation coefficient (±4‰ for calcite, ± 4.7‰ for dolomite) due to the poor knowledge of the equilibration temperatures (Trapping temperatures of the early stage carbonates were not constrained using FI studies). As they are considered to be synchronous or slightly anterior to the deformation and to the thermal stage related to the peraluminous intrusion, they can be formed in between the lowest temperature of prehnite-pumpellyite stage reached prior to the

leucogranite intrusion, and the temperatures reached at the intrusion stage, i.e., in between 250 to 450°C. Accordingly, most samples of calcite and dolomite yield fluid $\delta^{18}O$ values of 6 to 11 ‰, or 10 to 15 ‰ for equilibrium temperatures taken at the two extrema. These are the isotopic signatures of fluids equilibrated at relatively high temperatures with basement lithologies, i.e. metamorphic or magmatic fluids. Fluids calculated from deformed quartz have also a metamorphic or magmatic origin but they are found to be relatively lighter with $\delta^{18}O$ values ranging from +2.5 to + 6‰ (350°C) and from +3.5 to +7‰ (400°C).

Stage I_B: late Hercynian fluids calculated for carbonates have O isotopic compositions ($\delta^{18}O$ *c.* - 7 to +2‰) characteristic of surface-derived fluids (presumably meteoric water), which were only partly equilibrated with basement rocks. Fluid isotopic characteristics calculated from the 3 types of late quartz, which was more or less coeval with this episode of carbonitization are in the same range (fluid $\delta^{18}O$ *c.* -7 to +2.5‰) with a majority of values around 0 ±2‰. A meteoric origin is consistent with the low salinities recorded in fluid inclusions from both stage IB carbonates and quartz.

The very contrasted properties of stages I_A and I_B Hercynian fluids are well documented in the north-western part of the French Massif Central basement and in other areas of the Variscan belt (Boiron et al., 2000; Essaraj et al., 2000; Fourcade et al., 2000; Marignac et al., 2000, Vallance et al., submitted). They characterize the uplift history of the Variscan basement with i) a first stage involving, at relatively high temperatures (300 - 450°C), aqueous-carbonic fluids which were isotopically equilibrated with the basement (metamorphic or " pseudometamorphic " fluids), ii) a second stage characterized by a drop of temperatures down to *c.* 150-220°C, during which the basement is invaded by low salinities, H_2O-dominated, low-^{18}O fluids, stage which corresponds to an extensional epithermal regime, iii) the production of Au/Sb mineralisations during the switch between the two stages.

Disseminated carbonates contained in " fresh " rocks have O isotopic compositions intermediate between those of stages I_A and I_B vein carbonates (mixed population) and therefore, we can conclude that the circulation of the Hercynian fluids was relatively pervasive.

- Stage II Mesozoic fluids

The fluid O isotopic composition is estimated in the range + 4.5 to 8.5‰ (80°C). Similar estimates of the fluids isotopic signatures (6 to 10‰, 100°C) are obtained from the few quartz associated with these carbonate veins as well as from clay minerals reset by this event (O isotopes, K-Ar dates) within the basement fractures (Cathelineau et al., submitted). Together with their very high salinities, their chemistry and a few determinations of D/H ratios on the fluid inclusions contained in stage-II quartz and carbonates (δD between -30 and -50‰), these fluids correspond to brines of complex derivation interpreted as issued from the nearby Aquitanian Basin and circulating laterally along the basement/cover interface (Boiron et al., submitted).

Disseminated carbonates from more altered plutonites have C/O isotopic compositions very similar to those of stages-II vein carbonates. We can infer that the circulation of the Mesozoic fluids was relatively pervasive, as that of the late Hercynian fluids.

- Late (Stage III) fluids:

Fluids in equilibrium with late calcites had a $\delta^{18}O$ value of -1.2 to -2.1‰, when calculated for the deep-seated samples (CHA 103/2424, 615.05 m; CHA 212/8600, 743.48m) using their O isotopic composition and the temperature derived from fluid inclusions (50 and 55°C, respectively). In the other late calcites found in plutonites, fluid inclusions are scarce. If we use 50°C for the whole set of the late calcites samples, the calculated range of fluid $\delta^{18}O$ values is +2 to -3‰. The reliability of carbonate cements to provide information on the past isotopic composition of sea water is a matter of debate and it is often difficult to identify what fraction of these cements is of pristine marine derivation, recrystallized in closed-system during diagenesis in the presence of marine pore waters, or resulting from open-system late diagenesis (see for example, Frank and Lohmann, 1996, and references therein). Nevertheless, we state that such a range of isotopic signatures is globally consistent with sea water-dominated diagenetic environments. The salinities of FI in the most deep seated vein calcites (*c.* 4% eq. NaCl) agree with this conclusion but not in the case of vein calcites found at the top of the plutonic rocks (*c.* 1wt % eq. NaCl). For those veins, considering lower crystallization temperatures may reconcile the O isotopic signature (fluid $\delta^{18}O < 0$ in that case) with low-salinities. Actually, we have no precise constraints on these temperatures because the period of late vein crystallization is unknown (and thus the thickness of the overlying cover). However, their monophase characteristics argue that they were lower than *c.* 50°C (Goldstein et Reynolds, 1994). It is worth noting that because they share similar O isotopic compositions, late calcites in plutonites and geodic calcites found in the limestones probably crystallized from the same fluid type (see below for the different C origin).

Pervasive carbonitization in " altered " rocks appears to be dominated by stage II and stage III carbonate types.

4.4.2 Redistribution of the early stock of carbon.

An overwhelming majority of early (Hercynian) carbonates in the Vienne plutonites has a $\delta^{13}C$ value between -10 and -14‰. Because the thermal and fluid history of the Vienne plutonites is very complex since their emplacement *c.* 350 Ma ago (Freiberger et al., 2001 and submitted) and by considering the temperature effects on the isotopic fractionation from oxidized fluid systems (e.g., Rye and Williams, 1981), such a C isotopic composition may have had a variety of possible origins. Despite this difficulty, considering the oxidized nature of the late Hercynian fluids (lack of CH_4 in H_2O-(CO_2) fluid inclusions, paragenetic associations), we may rule out some of these possibilities. Direct oxidization of organic material or products derived from it (oil, methane) is unlikely because it is expected to produce a more ^{13}C-depleted carbon (e.g., Irwin et al., 1977; Wallin and Peterman, 1999). Decarbonation of carbonated sediments would release a CO_2 with nearly null or positive $\delta^{13}C$ values. In principle, CO_2 isotopically equilibrated with graphite in metamorphic conditions should have (organic matter with a common $\delta^{13}C$ of *c.* -25‰) the required isotopic signature at temperatures of 350 to 450°C (e.g., Taylor, 1987 and references therein), but the presence of methane corresponding to the $C/H_2O/CH_4/CO_2$ equilibrium is not detected in the present case. Again, oxidization of the methane

fraction would contribute to decrease the fluid $^{13}C/^{12}C$ ratio. Degassing of deep-seated sources (including the mantle or mantle-derived magmas) would require ad hoc conditions to produce such low $\delta^{13}C$ carbonates (^{13}C-depletion of the source through prior CO_2 outgassing; e.g., Javoy and Pineau, 1991; Pineau and Javoy, 1994).

The groups of solutions which may explain the intermediate C isotopic signatures of the Hercynian carbonates call for a mix source of carbon (*local* mean crustal carbon), with a contribution of both sedimentary carbonates and reduced carbon (see Kyser and Kerrich, 1990, and references therein). Circulation of metamorphic fluids (i.e., including fluids of surface derivation strongly equilibrated with basement rocks) coeval with the cooling of plutons is the most likely process by which externally derived C could be introduced in the plutonites synchronously with the breakdown of hornblende, biotite and Ca-plagioclase into carbonate-bearing assemblages (Freiberger et al., 2001). The temperature range of the crystallization of the late Hercynian carbonates (170-200°C) can explain the dispersion of C and O composition as shown by the fractionation curve of dolomite for an arbitrary constant fluid (Fig. 4.5.A). Indeed, from a only type of fluid decreasing in temperature could precipitate carbonates with weakly different isotopic signatures.

The fluid release linked to the emplacement of a large body of late leucogranite underneath the Charroux-Civray site (Freiberger et al., submitted) may also a priori correspond to this episode because the mean crustal carbon isotopic signature may also be acquired during anatexis of metasedimentary series. Nevertheless, we reject this hypothesis since FI do not contain any record (salinities, K/Na ratios, Li content...) of magmatic fluids. It is worth noting that the production of a reservoir of mean crustal carbon is probably a poly-cyclic process and that recycling of more ancient stocks of carbonates disseminated in basement rocks may be easily realized through successive events of fluids circulation (see below).

The recurring similarity in the range of C isotopic compositions for the successive fluid events characterized by extremely distinct sources, chemistries and temperatures (late Hercynian veins I_B, brines-related veins, deep-seated late calcitic veins, pervasive carbonitizations) is very difficult to envision if we admit that each fluid acquired that specific C isotopic signature in different environments. For example, the recurrence of the C isotopic signature in the brines, which were of lateral derivation would be a noticeable coincidence, but the coincidence would still become more troublesome if we consider deep-seated late calcites which were deposited from a totally different fluid at much lower (*c.* 50°C) temperatures. Following the Ockham's razor rule, the most likely explanation for the relative constancy of the carbon isotopic compositions through time is recycling of the stock of carbonates introduced within the plutonites by the early Hercynian alteration event.

In the light of this explanation, the effect of brines traveling laterally through the permeable upper part of the plutonites, weathered during the emersion period (down to a few hundred of meters), was to redistribute a stock of elements initially contained in the basement: Ba (likely extracted from feldspars and biotite), F (from biotite ?) and carbonates. The late calcites represent the youngest redistribution of the stock of basement-hosted carbonates and only in the shallowest part of the plutons, the influence of the overlying stock of seawater-derived carbon is noticeable: shallow late calcite present indeed an evolution of their $\delta^{13}C$ values towards those of limestones-

hosted geodic calcites, which obviously correspond to a recrystallization of marine carbonates.

4.5 Concluding remarks

Several conclusions may be inferred from the present study.

In the present work, we argue that a primeval stock of carbon was introduced in the early stages of the retrograde Hercynian metamorphism and systematically reworked by fluids afterwards, without significant carbon introduction by the subsequent percolating fluids. The exception corresponds to the latest, low-temperature calcite veins which are located in the upper sections of the cores, at a depth reaching no more than 350 m beneath the basement/cover boundary. These latest, shallow-seated calcites display isotopically heavier carbon ($\delta^{13}C$ up to -5‰/PDB) probably derived from the interaction between diagenetic fluids and the overlying Mesozoic limestones. Such carbonates are thus the only witnesses of element transfer from the sediments towards the basement.

Thus, we state that the early carbonated alteration products formed in a basement during its retrograde thermal evolution (during the late Hercynian in the present case) constitutes a huge amount of easily movable material, available for redistribution and for reducing the porosity present or created at each stage of fluid circulation. It is not surprising to observe a considerable amount of carbonated vein infillings in the Vienne plutonites precisely because an important proportion of these rocks are made of Ca-bearing rocks, such as tonalites. Initial trapping of disseminated and vein carbonates related to high Ca contents confers a kind of further self-sealing capacity on the plutonites. In this respect, it is worth noting that, in the Vienne plutonites, the less calcic rock types (leucogranites) are significantly poorer in carbonate infillings.

On the other hand, the C-O isotopic systematic of vein carbonates and O for quartz in basement rocks may be used to assess whether the vein infillings are in equilibrium or not with the past or present-day hydrological systems and to decipher the origin of carbon. The O isotopic composition of carbonates may be a useful tool for that purpose provided that a reliable estimate of (re)crystallization temperatures is available (e.g., Balderer et al., 1987). Nevertheless, we stress the point that, when remobilization of early stocks of carbonates occurs, the information brought by the C isotopic composition is not reliable as concerns the ultimate origin of the later generations of fluids. A very detailed investigation of the successions of carbonate and quartz infillings and of the related fluids chemistry is needed before assessing the fluids provenance.

The observations made in the Vienne granitoids can be possibly extended to a great part of the Hercynian crystalline basement, with or without sedimentary cover. Indeed, over the 4 km deep KTB pilot borehole, an overwhelming majority of the C isotopic compositions in crack-filling calcite are relatively constant and comparable to those of the Vienne basement (Komor, 1995).

Finally, we state that fluid circulation within the Vienne granitoids obviously occurred through the main mechanical discontinuities (fractures and faults) but also more

intimately, within the granitoid matrix, because early disseminated carbonates were scavenged and redistributed. This was particularly the case for the major post-Hercynian fluid event (Mesozoic brines), which induced barite and fluorite deposition and to which are attributed 70% of carbonate fracture fillings in the basement.

ACKNOWLEDGMENTS

This article is a synthesis of studies either supported directly by Andra or by GdR FORPRO - Action 98-III (contribution paper FORPRO No 2001/09 A), a National Research Program between CNRS and Andra (French Nuclear Waste Management Company). Andra is acknowledged for the facilities and permission of sampling the drill cores. Stephane Buschaert benefits of a grant from Andra for completion of his PhD.

REFERENCES

Balderer, W., Fontes, J.-Ch., Michelot, J-L., and Elmore, D., 1987. Isotopic investigations of the water-rock system in the deep crystalline rock of northern Switzerland. In "Saline water and gasses in crystalline rocks" (Fritz P., and Frape, S.K., eds.), GAC Spec. paper n°33, 175-195.

Bertrand, J.M., Leterrier, J. and Delaperrière, E., 1996. Géochronologie U-Pb de granitoïdes du Confolentais, de Vendée et des forages de Charroux-Civray. 17ème Réunion des Sciences de la Terre, Brest, Soc. Géol. Fr., p. 74 (Abstract).

Blyth, A., Frape, S., Blomqvist, R. and Nissinen, P., 2000. Assessing the past thermal and chemical history of fluids in crystalline rocks by combining fluid inclusion and isotopic investigations on fracture calcite. Applied Geochem. 15, (10), 1417-1437.

Boiron, M.C., Cathelineau, M., Banks, D., Vallance, J., Fourcade, S. and Marignac, Ch., 2000. Behaviour of fluids in Variscan crust during the late carboniferous uplifting and fluid mixing, and their consequences on metal transfer and deposition. In " Orogenic gold deposits in Europe ", Geode-GeoFrance 3D workshop (Bouchot, V. and Moritz, R., eds.), Doc. BRGM 297, ext. abstr., 56-57.

Boiron, M.C., Cathelineau, M., Banks, D., Buschaert, S., Fourcade, S., Coulibaly, Y., Boyce, A., and Michelot, J.L. (submitted). Penetration of brines into a crystalline basement during extensional tectonics: role on fracture sealing and mass transfer.

Capdevila, R. 1997. Les suites plutoniques metalumineuses recoupées par les forages Andra de la Vienne: caractérisation, mode de mise en place et discussion du contexte géodynamique. Andra Sci. Meeting, Poitiers, Posters Atlas, p. 13.

Capdevila, R., 1998. Les suites orogéniques dévoniennes du batholite de Charroux-Civray (Vienne) et leur contexte géodynamique. 17ème Réunion des Sciences de la Terre, Brest, Soc. Géol. Fr., p. 86 (Abstract).

Cathelineau, M., Cuney, M., Boiron, M.-C., Coulibaly, A., and Ayt Ougougdal, M., 1999. Paléopercolations et paléointeractions fluides/roches dans les plutonites de Charroux-Civray. Proceedings of the Andra Sci. Meeting Poitiers, EDP Sciences Publ., 159-180.

Cathelineau, M., Fourcade, S., Clauer, N., Buschaert, S., Rousset, D., Boiron, M.C., Martineau, F., Meunier, A., Javoy, M., Nitjchoua, R., 2001. Multistage paleofluid percolations in granites: A stable isotope and K-Ar study of fracture illite from Vienne plutonites (N.W. of the french Massif Central). Clay Min., submitted.

Clauer, N., Frape, S.K., and Fritz, B., 1989. Calcite veins in the Stripa granite (Sweden) as records of the origin of ground waters and their interactions with the granitic body. Geochim. Cosmochim. Acta 53,1777-1782.

Coulibaly, Y, 1998. Recherches des traces de circulations récentes en milieu cristallin : une approche analytique sur les cristallisations dans les fractures et les paléofluides. PhD Thesis, INPL Nancy.

Cuney, M., Brouand, M., Stussi, J.-M., and Gagny, C., 1999. Le massif de Charroux-Civray: un exemple caractéristique des premières manifestations plutoniques de la chaîne hercynienne. Proceedings of the Andra Sci. Meeting Poitiers, EDP Sciences Publ., 63-104.

Essaraj, S., Boiron, M.-C., Cathelineau, M., and Fourcade, S., 2000. Multistage deformation of Au-Quartz veins: evidence for late gold introduction from microstructural, isotopic and fluid inclusions studies. Tectonophysics, in press.

Fourcade, S., Boiron, M.C., Cathelineau, M., Guerrot, C., Lerouge, C., Marignac, C., Martineau, F. and Vallance, J., 2000. Fluids and late carboniferous Variscan gold mineralizations in the French Massif Central. The bearing of stable isotopes. In

" Orogenic gold deposits in Europe ", Geode-GeoFrance 3D workshop (Bouchot, V. and Moritz, R., eds.), Doc. BRGM 297, ext. abstr., 58-59.

Franck, T.D. and Lohmann, K.C., 1996. Diagenesis of fibrous magnesian calcite marine cement: implications for the interpretation of $\delta^{18}O$ and $\delta^{13}C$ values of ancient equivalents. Geochim. Cosmochim. Acta 60, 2427-2436.

Freiberger, R., Hecht, L., Cuney, M. and Morteani, G., 2001. Secondary Ca-Al-silicates from Mid-European Hercynian granitoids: Implications for the cooling history of granitic plutons. Contributions to Mineralogy and Petrology (in press).

Freiberger, R., Boiron, M.C., Cathelineau, M., Cuney, M., Buschaert, S. (submitted). Retrograde P-T evolution and high temperature – low pressure fluid circulation in relation to late Hercynian intrusions: a mineralogical and fluid inclusion study of the Charroux-Civray granitoids (NW Massif Central, France).

Frey, M., de Capitani, C. and Liou, J.G., 1991. A new petrogenetic grid for low-grade metabasites. J. of Metamorphic Geology 9, 497-509.

Friedman, I. and O'Neil, J.R., 1977. Compilation of stable isotope fractionation factors of geochemical interest. In " Data of Geochemistry, 6th ed. (Fleischer, M., ed.), U.S. Gov. Printing Office, Washington, D.C.

Goldstein, R.H. and Reynolds, T.J., 1994. Systematics of fluid inclusions in diagenetic minerals. SEPM short course 31, 212 pp.

Irwin, H., Curtis, C. and Coleman, M., 1977. Isotopic evidence for source of diagenetic carbonates formed during burial of organic-rich sediments. Nature 269, 209-213.

Javoy, M. and Pineau, F., 1991. The volatiles record of a " popping " rock from the Mid-Atlantic Ridge at 14°N: chemical and isotopic composition of the gas trapped in the vesicles. Earth Planet. Sci. Letters 107, 598-611.

Jendrzejewski, N., Javoy, M., and Trull, T., 1996. Mesure quantitative de carbone et d'eau dans les verres basaltiques naturels par spectroscopie infrarouge. Partie I : Le carbone, C. R. Acad. Sci., Paris 322, série IIa, 645-652.

Komor, S.C., 1995. Chemistry and petrography of calcite in the KTB pilot borehole, Bavarian Oberpfalz, Germany. Chem. Geol. 124, 199-215.

Kyser, T.K., and Kerrich, R., 1990. Geochemistry of fluids in tectonically active crustal regions. In " Short Course on Fluids in Tectonically Active Regimes of the Continental Crust ", Vol. 18 (Nesbitt, B.E., ed.), Min. Assoc. Canada, Vancouver, 133-230.

McCrea, J.M., 1950. On the isotope chemistry of carbonates and a paleotemperature scale. J. Chem. Phys. 18, 849-857.

Macpherson, C.G., Hilton, D.R., Newman, S. and Mattey, D.V., 1999. CO_2, $^{13}C/^{12}C$ and H_2O variability in natural basaltic glasses: A study comparing steeped heating and FTIR spectroscopic techniques. Geochim. Cosmochim. Acta 63, 1805-1813.

Marignac, C., Cathelineau, M., Boiron, M.C., Fourcade, S., Vallance, J. and Souhassou, M., 2000. The Q-Au lodes of W Europe: towards the definition of a Variscan-type of shear-zone hosted gold deposits. In " Orogenic gold deposits in Europe ", Geode-GeoFrance 3D workshop (Bouchot, V. and Moritz, R., eds.), Doc. BRGM 297, ext. abstr., 82-85.

Muchez, P., Sintubin, M. and Swennen, R., 2000. Origin and migration pattern of palaeofluids during orogeny: discussion on the Variscides of Belgium and northern France. Journal of Geochemical Exploration, 69-70: 47-51.

Ohmoto, H., 1972. Systematics of sulfur and carbon isotopes in hydrothermal ore deposits. Econ. Geol., 67, 551-579.

Ohmoto, H.; and Rye, R.O. 1979. Isotopes of sulfur and carbon; In H.L. Barnes (Ed.) Geochemistry of hydrothermal ore deposits. John Whiley & Sons. 509-561.

O'Neil, J.R., Clayton, R.N. and Mayeda, T.K., 1969. Oxygen isotope exchange in divalent metal carbonates. J. Chem. Phys. 51, 5547-5558.

Peiffer, M.-T., 1986. La signification de la ligne tonalitique du Limousin. Son implication dans la structuration varisque du Massif Central français. C.R. Acad. Sci. Paris 303, sér. II, 305-310.

Pineau, F. and Javoy, M., 1994. Strong degassing at ridge crests: The behaviour of dissolved carbon and water in basaltic glasses at 14°N, Mid-Atlantic Ridge, Earth and Planet. Sci. Letters 123, 179-198.

Rye, D.M., and Williams, N., 1981. Studies of the base metal sulfide deposits at McArthur River, Northern Territory, Australia: III. The stable isotope geochemistry of the H.Y.C., Ridge, and Cooley deposits. Econ. Geol. 76, 1, 1-26.

Sacchi, E. and Michelot, J.L., 1996. Etude des cristallisations dans les fractures. Applications au site Andra Vienne-Sud. Int. Report Andra, contract n° 315747 AO, 34 p.

Suchy, V., Heijlen, W., Sykorova, I., Muchez, P., Dobes, P., Hladikova, J., Jackova, I., Safanda, J. and Zeman, A., 2000. Geochemical study of calcite veins in the Silurian and Devonian of the Barrandian Basin, (Czech Republic): evidence for widespread post-Variscan fluid flow in the central part of the Bohemian Massif. Sed. Geol. 131, 3-4, 201-219.

Shaw, A., Downes, H., and Thirlwall, M.F., 1993. The quartz diorites of Limousin: elemental and isotopic evidence for Devono-Carboniferous subduction in the Hercynian belt of the French Massif Central. Chem. Geol. 107, 1-18.

Sheppard, S.M.F., and Schwarcz, H.P., 1970. Fractionation of C and O isotopes and magnesium between coexisting metamorphic calcite and dolomite. Contrib. Mineral. Petrol. 26, 161-198.

Taylor, B.E., 1987. Stable isotope geochemistry of ore-forming fluids. In " Short Course in Stable Isotope Geochemistry of Low Temperature Fluids ", Vol. 13 (Kyser, T.K., ed.), Min. Assoc. Canada, Saskatoon, 337-345.

Trave, A., Calvet, F., Sans, M., Verges, J. and Thirlwall, M., 2000. Fluid history related to the Alpine compression at the margin of the south-Pyrenean Foreland basin: the El Guix anticline. Tectonophysics, 321(1): 73-102.

Vallance, J, M.C. Boiron, M. Cathelineau, S. Fourcade and C. Marignac. (submitted to Mineralium Deposita). High T-low P fluid rock interaction and early As introduction in the granite hosted Au deposit of Moulin de Cheni (St Yrieix District, french massif central).

Valley, J.W., Komor, S.C., Baker, K., Jeffrey, A.W.A., Kaplan, I.R., and Raheim, A., 1988. Calcite crack cements in granite from the Siljan Ring, Sweden: stable isotope results. In " Deep drilling in crystalline bedrock ", (Bode, A. and Erikkson, K.G., eds.), Vol. 1, Springer, Berlin, 156-179.

Virlogeux, D., Roux, J and Guillemot, D., 1999. Apports de la géophysique à la connaissance géologique du massif de Civray-Charroux et du socle poitevin. Proceedings of the Andra Sci. Meeting Poitiers, EDP Sciences Publ., 33-61.

Wallin, B. and Peterman, Z., 1999. Calcite fractures as indicators of paleohydrology at Laxemar at the Äspö Hard Rock Laboratory, southern Sweden. Applied Geochem. 14, 953-962.

White, A.F., Bullen, T.D., Vivit, D.V., Schulz, M. and Clow, D.W., 1999. The role of disseminated calcite in the chemical weathering of granitoid rocks. Geochim. Cosmochim. Acta 63, 1939-1953.

Winter, B.L., Valley, J.W., Simo, J.A., Nadon, G.C. and Johnson, C.M., 1995. Hydraulic seals and their origins: evidence from the stable isotope geochemistry of dolomites in the Middle Ordovician St. Peter Sandstone, Michigan Basin. Am. Ass. Petrol. Geol. Bull. 79, 1, 30-48.

Zheng, Y.-F., 1993. Calculation of oxygen isotope fractionation in anhydrous silicate minerals. Geochim. Cosmochim. Acta, 57, 1079-1091.

B. LES ENSEMBLES SEDIMENTAIRES DU GARD RHODANIEN ET DE L'EST DU BASSIN DE PARIS

INTRODUCTION

Les siltites du Gard Rhodanien et les ensembles carbonatés encadrant les argilites de la Meuse-Haute-Marne (MHM, ou site de l'Est) appartiennent à deux contextes sédimentaires présentant des analogies. Ces niveaux assez compétents présentent un certain nombre de fissures ou de cavités fractures tapissées ou parfois remplies de carbonates, qui impliquent des transferts de matière via des fluides percolants ou statiques, à certains stades de l'histoire des sédiments, depuis leur dépôt jusqu'à des stades "diagenétiques", voire post-diagenétiques dont l'âge est inconnu.

L'évolution dans le temps et l'espace des principaux événements de percolation, l'origine de la circulation des fluides anciens à récents (fluides d'origine externe ou strictement intra-formationnelles diagénétiques) et la géométrie des systèmes d'interaction fluide-roche autour de ces fissures constituent un enjeu important dans la compréhension du comportement hydrologique et hydrogéochimique des systèmes actuels.

Cependant, l'histoire des circulations fluides semble différente entre les deux sites. De nombreuses études concluent trop souvent sur une base pétrographique uniquement, à une diagenèse précoce des calcaires sans effectuer une caractérisation isotopique rigoureuse. Dans le cas de l'Est, un événement majeur a été reconnu et bien que les signatures isotopiques en carbone et en Sr (P. Maes, 2001) des calcites sparitiques reflètent celles de l'encaissant calcaire qui a tamponné le fluide percolant, les valeurs en oxygène sont très différentes. Il est donc nécessaire d'identifier l'origine de ce fluide tardif et son extension géographique dans l'Est du bassin de Paris. Quant au Gard, la précipitation de carbonates dans les pores et dans les fractures des siltites et des encaissants gréseux est créée par la circulation de fluides de tendance marine, lors d'une diagenèse de basse température, mais produisant à une histoire assez complexe et d'intensité très variable en fonction des lithologies. Il est essentiel d'identifier les processus ayant créé cette particularité, assez inattendue pour une série sédimentaire en contexte thermique faible et aux caractéristiques géochimiques assez immatures.

RESULTATS SYNTHETIQUES

Ce chapitre étant présenté sous forme d'articles, il a été choisi de synthétiser les problématiques et les principaux résultats ci-après.

a. Origine des circulations fluides dans les formations de Marcoule

Objectifs et moyens

Le secteur de Marcoule étudié par l'Andra fait partie du bassin sédimentaire plissé du Sud-Est de la France. Ce bassin est limité par des accidents majeurs tardi-Hercyniens de direction NE-SW, à l'Ouest par la faille des Cévennes, au Sud-Est par la faille de Nîmes et au Sud par le prolongement de la zone axiale pyrénéenne. Elles ont contrôlé la subsidence du bassin et la puissance des sédiments déposés. D'autres failles de direction E-W, reliées aux directions d'ouverture des bassins stéphano-permiens, ont imposé leur contrôle sur la géométrie du bassin.

Le domaine étudié, à l'aplomb du canton de Bagnol-sur-Cèze, a fait l'objet d'une campagne de sondages (forages Andra MAR501, 203, 401) qui permettent de disposer d'une coupe assez complète du Crétacé de l'Est du Gard de l'Aptien au Coniacien. L'épaisseur totale des sédiments est estimée à cet endroit à 8000 m. La couche silteuse de Marcoule (CSM), d'âge Vracono-Tavien (Albien terminal, Cénomanien basal), est encadrée par des ensembles à dominance gréseuse en alternance avec des marnes et calcaires (Ferry, 1999). Elle repose en profondeur sur une dalle calcaire Urgonienne (ou Bédoulienne) affleurante au nord-ouest dans la vallée de l'Ardèche. Lors des reconnaissances géologiques, la CSM a démontré une grande homogénéité de composition et de texture, ainsi qu'une faible perméabilité.

Il a été choisi de travailler sur des séries représentatives de fractures (ou systèmes de fractures) du Gard où l'on recherchera l'origine du fluide associé aux cicatrisations de fractures macroscopiques à carbonates (± célestine + pyrite) ainsi que leur emprise éventuelle dans leurs épontes.

Principaux résultats

L'analyse de la séquence diagenétique a permis de mettre en évidence les stades suivants de cimentation des lits gréseux:

i) formation de grains de glauconite soit en néoformation, soit en épigénie (pellets fécales, épigénie de minéraux ferro-magnésiens comme des chlorites ou des biotites), probablement très précoces car entièrement cimentés par les stades suivants,

ii) néoformation de cristaux automorphes de calcite (I) englobant les grains de quartz détritiques dans les lits gréseux, puis de cristaux automorphes de dolomite, notamment à l'interface entre les lits silteux et gréseux, stade suivi d'une cristallisation épitaxique d'une frange d'ankérite sur la dolomite. La sidérite est rencontrée exceptionnellement dans certaines fissures; les bioclastes sont épigénisés en calcite II. Des interstratifiés illite/smectite sont observés en intime association avec la calcite II, en remplissage des loges de foraminifères ou de gastéropodes et sont interprétés comme néoformés à ce stade.

iii) formation d'un ciment de calcite III xénomorphe remplissant toute la porosité résiduelle de la roche, ceci expliquant la très faible perméabilité des siltites.

Les échantillons de la couche silteuse sont constitués par des alternances de lits argileux (siltite gréseuse) constitués de minéraux détritiques phyllosilicatés et de lits grèseux à ciment carbonaté riches en bioclastes. Les siltites sont également cimentées, à un moindre degré que les grès, par de la calcite.

La cimentation précoce des roches a induit une forte diminution de la perméabilité, ce qui a favorisé la formation de fissures dans ces niveaux compétents. Les nombreuses fissures sub-verticales à remplissage carbonaté sont interprétées comme liées à la fracturation préférentielle des lits gréseux plus compétents lors de l'enfouissement et lors phases tectoniques Eocène et Oligocène. Certaines fractures se sont probablement formées à partir de discontinuités syn-sédimentaires, car les bords des fractures ne sont pas toujours francs et rectilignes, et sont tapissés d'un liseré de glauconite dont l'origine semble précoce. Le remplissage des fractures, lors

de circulations plus tardives, est à calcite seule (± pyrite, ± barytine et celestine) et ne comporte aucune néoformation d'argiles. Cependant, l'histoire des colmatages dans les fractures s'est révélée très complexe au regard des résultats isotopiques et de la typologie des fractures.

Dans l'intervalle Aptien-Albien, les calcites des fractures montrent des $\delta^{18}O$ très variables allant de 17 à 27 ‰ SMOW, ce qui correspond également aux valeurs globales des ciments analysés dans les roches adjacentes (18 à 29 ‰). Dans les formations sous jacentes, les calcaires montrent des valeurs marines ($\delta^{18}O$ de 25.5 à 29 ‰), alors que les calcites de fractures présentent des $\delta^{18}O$ inférieurs à 21 ‰.

La cimentation de la microporosité des roches apparaît comme relativement précoce sous l'effet de fluides diagénétiques, sous des conditions de diagenèse très modérée (température faible < 50°C), ce qui explique la préservation des argiles néoformées (I/S riches en smectite) et des matières organiques (totale immaturité thermique attestée par l'étude des biomarqueurs, Fleck, 2000).

Le colmatage des fractures, plus complexe, a lieu en fonction des niveaux, soit en système clos avec redistribution locale de matière, l'identité en C et O étant souvent conservée entre les calcites de fracture et l'encaissant suivant le niveau stratigraphique, soit en système plus ouvert avec introduction de C et O par des sources externes. Dans ce second cas, la participation d'eaux météoriques mélangées aux eaux d'origine marine dans le colmatage des fissures ou des macropores des sédiments est suspectée pour certaines fractures du Gard, notamment dans les niveaux aquifères grèseux et calcaires.

Les résultats sont présentés dans l'article *'Local paleo-fluid infiltration and fracture sealing in low permeability Cretaceous siltites (South-eastern Basin, France): an isotopic study of diagenetic fractures and rock cements'.*

b. Origine des circulations fluides dans les formations de l'Est

Objectifs et moyens

Les recherches de l'Andra dans l'Est du bassin de Paris se sont focalisées sur une couche d'argillites du Callovo-Oxfordien très imperméables et de 150 m d'épaisseur. Elle est encadrée par deux grands ensembles calcaires très cimentés : en dessous par les calcaires du Dogger, et au dessus par les ensembles calcaires Oxfordiens, eux mêmes surmontés par les marnes Kimméridgiennes et les calcaires du Barrois (Tithonien ou Portlandien). Le site choisi est situé sur la limite des départements de Meuse et de Haute Marne, à proximité des communes de Bure et de Saudron. Il est délimité par deux grandes zones faillées, à l'Ouest par la faille de la Marne (NNW-SSE) et à l'Est par le fossé de Gondrecourt (NNE-SSW). Plus à l'Est, vers Neufchateau, on retrouve une autre zone de faille orientée N010.

Dans les calcaires mésozoïques du site Andra de la Haute-Marne, des carbonates d'âge inconnu colmatent des fissures et tapissent des cavités de dissolution. L'objectif est d'identifier les mécanismes à l'origine de ces colmatages. De plus, les calcaires sont assez souvent fortement recristallisés par des sparites obturant la

porosité. Le couplage réalisé entre les études pétrographiques des ciments, les contraintes de paléothermicité (microthermométrie des inclusions fluides) et l'acquisition des données isotopiques, d'abord globales (à Rennes), puis ponctuelles (IMS1270 au CRPG) sont nécessaires pour évaluer la nature et la source des fluides à l'origine à la fois des cimentations dans la porosité (micropores et géodes) et dans les fractures. L'étude des ciments carbonatés présents dans les discontinuités (microfissures, cavités à colmatage imparfait) du site de l'Est a été réalisée et comparée aux référentiels que constituent les ensembles carbonatés sus- et sous-jacents, ainsi que la fraction carbonatée de l'ensemble argileux du Callovo-Oxfordien.

Principaux résultats

1. Sur les forages étudiés, la fraction carbonatée globale des calcaires et argilites présente des valeurs de $\delta^{18}O$ relativement proches de celles qui sont attendues au cours d'une sédimentation en milieu marin (28-29 ‰ SMOW), bien qu'un peu plus faible (25 à 27 ‰ SMOW). Par contre, les données sur les calcites de géodes et fractures ($\delta^{18}O$ de 21±1 ‰ SMOW) permettent de calculer, pour une température de précipitation de 35 à 40°C déterminée par l'étude des inclusions fluides, un $\delta^{18}O$ d'environ -4 à - 6 ‰ SMOW pour l'eau correspondante. Ce fluide est interprété comme un fluide d'origine continentale avec une composante météorique.

Les analyses isotopiques ponctuelles en oxygène étaient nécessaires pour nous permettre de caractériser les différents types de ciments carbonatés obturant la porosité et de les comparer aux ciments de géodes et de fractures. En effet, leur étude pétrographique, couplée à la cathodoluminescence, a permis d'établir une chronologie de cristallisation.

Les résultats montrent que les éléments calcaires présentent des valeurs en $\delta^{18}O$ comprises entre 24 et 28 ‰ (SMOW), ce qui était attendu par rapport aux analyses globales des calcaires (de 25 à 28.5 ‰). Les premiers ciments calcitiques, qui se présentent par une fine frange accolée aux éléments calcaires, ont des valeurs similaires allant de 24.5 à 27 ‰. Ceci confirme leur origine phréatique marine précoce.

Par contre, les ciments de type sparitique qui obturent la porosité, présentent des valeurs (20 à 21.5 ‰) tout à fait comparables à celles obtenues sur les ciments carbonatés des géodes et des fractures par analyses ponctuelles (19 à 23 ‰) et globales (21 ‰). Ces données confirment le caractère continental des eaux à l'origine des derniers ciments aussi bien au niveau des pores que dans les fractures.

Les échantillons étudiés de fractures/géodes de l'Est sont liés à un épisode relativement tardif de percolation des fluides d'origine continentale d'âge indéterminé sous un régime de températures relativement faibles. Ce fluide a aussi permis la recristallisation de sparite dans la porosité de la plupart des calcaires.

Les résultats sont présentés dans l'article *'Widespread cementation induced by inflow of continental water in the eastern part of the Paris basin: O and C isotopic study of carbonate cements'*.

2. L'origine de la recharge a été envisagée par l'échantillonnage des calcites de fractures et fentes de tension régionales. Les résultats en $\delta^{18}O$ sur ces calcites (20-21 ‰ SMOW) sont similaires aux résultats donnés précédemment sur les calcites géodiques et de fractures des forages, et cela quelle que soit l'orientation des fractures ou fentes. Aux températures de cristallisations considérées (T<45°C), le fluide calculé pour ces calcites régionales a une valeur moyenne autour de -5 ‰, soit une valeur comparable au fluide reconstitué au niveau des forages. Ceci montre que l'origine des calcites dans les géodes, fractures et pores des ensembles sédimentaires du site est bien liée à la présence de grands fossés distensifs (Gondrecourt, Neufchateau), généralement interprétés comme d'âge Oligocène (en liaison avec l'ouverture du fossé Rhénan). De plus, les valeurs isotopiques en C prouvent que ces fluides ont remonté verticalement le long de ces accidents. Cependant, l'âge des circulations reste indéfini, mais estimé plutôt situé comme Tertiaire (Oligocène, Miocène).

La percolation de ce fluide continental dans les roches mésozoïques du site de l'Est, latéralement à ces accidents, est à l'origine de la cimentation / recristallisation intense des calcaires oolitiques à grande porosité initiale (cavités dans les biohermes, pores dans les calcaires oolitiques et oncholitiques) et a contribué aux faibles valeurs de perméabilités actuelles.

Ces derniers résultats sont présentés dans l'article *'Fracture sealing in Mesozoic limestones (eastern Paris Basin, France): continental waters drainage in the vicinity of fault zones'.*

5 LOCAL PALEO-FLUID INFILTRATION AND FRACTURE SEALING IN LOW PERMEABILITY CRETACEOUS SILTITES (SOUTH-EASTERN BASIN, FRANCE): AN ISOTOPIC AND DIAGENETIC STUDY OF FRACTURE AND ROCK CEMENTS

S. Buschaert[a,e], M. Cathelineau[a] ,S. Fourcade[b], J.L. Michelot [c], J. Lancelot[d]

[a] UMR G2R 7566- CREGU, BP23, 54501 Vandoeuvre-lès-Nancy, France
[b] Géosciences Rennes UMR 6118, Univ. Rennes 1, 35042 Rennes Cédex, France
[c] UMR-CNRS-UPS Orsay Terre, Laboratoire d'hydrologie et de Géochimie isotopique, Université de Paris Sud, Bat 504, 91405 Orsay, France
[d] ISTEEM, Univ. Montpellier, Place E. Bataillon, Montpellier, France
[e] Andra, French Agency for Nuclear Waste Management, 92298 Châtenay-Malabry

In preparation

Figure captions ***5-152***
Table captions ***5-152***
Abstract ***5-153***

5.1 INTRODUCTION ***5-155***

5.2 GEOLOGICAL BACKGOUND AND SAMPLING ***5-157***
5.2.1 Sampling 5-159
5.2.2 Petrography of fracture and host rocks 5-159

5.3 ANALYTICAL TECHNIQUES ***5-161***

5.4 RESULTS ***5-162***
5.4.1 Isotopic data 5-162
- Albian siltstone series and Urgonian limestones 5-162
- Calcite fractures and relationships with host rocks 5-163

5.4.2 Temperatures of diagenesis and fracture formation 5-168

5.5 INTERPRETATION OF THE FLUID ORIGIN ***5-169***
5.5.1 Isotopic signature of fluid 5-169
5.5.2 The case study of the fault zone from MAR 501 5-170

5.6 CONCLUDING REMARKS ***5-171***
Acknowledgements ***5-172***
References ***5-173***

FIGURE CAPTIONS

Fig. 5.1. A: Structural map showing the location of the study site within the south-eastern basin, in the area bounded to the west by the Cévennes fault and to the east by the Nimes fault, with indication of the main deformational structures: EW folds, and NS fault systems, especially in the Bagnols/Cèze area, B: Geological map with location of the three studied drill-holes, and main structures (dip of the main anticline, and faults)..... 5-156

Fig. 5.2. Cross-section showing the stratigraphy of the studied area and location of the Albian-Aptian silt within the Cretaceous series..... 5-158

Fig. 5.3. Stratigraphy of the studied drill-holes with indication of the location of the main fault zones. Dotted box on MAR501 borehole corresponds to the series isotopically studied. For isotopic logging (Fig. 5.7), samples from MAR401/2 and 203 are stratigraphically correlated to MAR501. 5-158

Fig. 5.4. Sketch drawing showing the textures of the studied fracture infillings and their relationships with the deformational structures. A: sub-horizontal sliding zones, B and C: sub-vertical faults and related opened structures filled by calcite, D: breccia within the Urgonian limestones. Calcite appears in black..... 5-160

Fig. 5.5. Sketch showing the chronology and relationships between diagenetic minerals..... 5-161

Fig. 5.6. $\delta^{13}C$ (PDB) versus $\delta^{18}O$ (SMOW) for calcite filling in fractures (open symbols), for whole rock samples (black symbols; limestones and the carbonate cements of the silstones / sandstones). The straight lines between dots corresponds to the couple of corresponding fracture calcite, fracture wall and bulk rock of one given sample. The straight dotted line joins 3 calcites sampled at different place in the metric length fracture of the sample 9763..... 5-163

Fig. 5.7. Vertical distribution of $\delta^{13}C$ (PDB) values (A) and of $\delta^{18}O$ (SMOW) values (B) for calcite filling in fractures (circles) and for bulk rock analysis (others symbols; limestones, and carbonate cements of siltstones / sandstones with reference to the stratigraphy (borehole MAR 501, 401/402 and 203 after correction of depth and correlation with MAR 501 after Ferry (1999), Mouroux and Bruhlet (1999) and Lebon (1999). Samples from MAR203 and 401/2 are labeled..... 5-164

Fig. 5.8. A: $\delta^{13}C$ (PDB) of host rock carbonate cement versus $\delta^{13}C$ (PDB) of the fracture calcite; B: $\delta^{18}O$ (SMOW) of host rock carbonate cement versus $\delta^{18}O$ (SMOW) of the fracture calcite..... 5-165

TABLE CAPTIONS

Table 5.1. Ca, Mg, Mn, Fe and Sr contents of calcite cements. Electron microprobe analyses mean values (n= number of analyses)..... 5-161

Table 5.2. Isotopic data of rocks cements in boreholes MAR203, 401/2, 501. For MAR203 & 401/2, depths are corrected with respect to MAR501 on the basis of stratigraphical correlations. Values in brackets correspond to the real depth below surface. fw: fracture wall..... 5-167

Table 5.3. Isotopic data of geode/fracture calcite cements in boreholes MAR203, 401/2, 501. For MAR203 & 401/2, depths are corrected with respect to MAR501 on the basis of stratigraphical correlations. Values in brackets correspond to the real depth below surface..... 5-168

ABSTRACT

Cretaceous siltites (Albian age or Vraconian) from the South-eastern Basin (South France) constitute a rather thick and low permeability formation which display sub-vertical or sub-horizontal micro-veins and veins almost completely filled by calcite. The formation of fractures and veins is related to main types of deformational structures: low angle fault linked to movements in relation with the Eocene EW anticlines, and a NS fault set related to Oligocene distensive tectonics. The wall rocks never display alteration features (stability of diagenetic carbonates and glauconites as well as detrital phyllosilicates). Along faults, calcite is also the main mineral sealing the porosity and related opened microstructures. The main objective of our study was to determine the regime and the source of fluids at the origin of re-crystallized calcite material using stable isotopes (O, C) and fluid inclusion data, and possibly to unravel the possible relationships between fluids circulation and the tectonic history of the South-eastern Basin.

Calcite from fractures in the Albian-Aptian detrital series display a large range of $\delta^{18}O$ values from 17.0 to 27.7‰ SMOW. This range is also recorded in the bulk carbonate cements of the host siltstones series: 18.0 to + 28.9‰. In silex limestones underlying the detrital formation, bulk carbonates display rather pristine marine isotopic signatures ($\delta^{18}O$ values between 25.5 to 28.9‰) whereas the calcitic fracture infilling also record diagenetically modified material ($\delta^{18}O$ down to 20.7‰). Considering reasonable temperature estimates for the diagenesis of the series (35 to 50°C, according to bio-markers, fluid inclusions and clays typology), diagenetic crystallization of whole rock cements occurred in the presence of significant fluxes of seawater-derived fluids, but also required an additional groundwater component, especially in some specific glauconite sandstone layers where the ancient permeability was presumably high. The formation of fracture calcites occurred either by close system redistribution of the nearby host rocks cements or in open system (introduction of O and C from external sources). In open system, carbon of organic derivation was also introduced in most of the newly formed cements. Early cementation induced a strong decrease of permeability which is likely responsible for the crack formation in the most competent layers through the increase of overburden pressures during burial and/or later on during Eocene and Oligocene tectonic phases. The sealing of the fractures led to the very low present day permeability of the series. The complexity and intensity of the diagenetic history in the siltites from the South-eastern Basin were not expected in view of the relatively immature characteristics of that sedimentary material.

Keywords: calcite; stable isotopes; Cretaceous; siltites; diagenesis

5.1 Introduction

Sedimentary rocks, especially silts and sandstones, may be or become efficient reservoirs for water or oil but may also undergo complex evolutions of their porosity and permeability through time as a function of diagenesis, compaction or fluid circulation. When such rocks experience cementation, the role of discontinuities on fluid flow and the connection between pores and minor sets of fractures are critical parameters which affect the hydrological properties and the mechanisms of fluid transfer from reservoirs or aquifers (Wallin and Peterman, 1999, Blyth et al., 2000).

The knowledge of past hydrological systems and their evolution in time and space are of particular importance in understanding and predicting the hydro-dynamics of sedimentary formations The paleo-fluid systems can be investigated through the geochemical and mineralogical study of the materials sealing the fractures or pore spaces after sedimentation.

An interesting case study, never characterized by stable isotopic way, was found recently during the drilling of a thick series of clay-rich silts of Albian - Aptian age (corresponding local names are Bedoulian – Gargasian – Vraconian). In these siltites, localized sets of calcite veins argue, at least on a local scale, for the existence of fluid-induced mass transfers within this rather impermeable formation. The South-Eastern Basin (southern France), bounded to the West by the southern Massif Central (Cévennes fault, Fig. 5.1.A) and to the East by the Alpine mountain belt, constitutes the continental shelf of the Tethys ocean during Jurassic and Cretaceous times and contains more than 8 000 m of accumulated sediments (Baudrimont and Dubois, 1977). Within this basin, the Albian-Aptian formation (especially an homogeneous series of Upper Albian (Vraconian) glauconitic silts, forming the so-called, Marcoule silt layer, MSL) is made of clay-rich silts which overlie Urgonian (Bedoulian) limestones and are overlain by Cenomanian to Coniacian sandstones. The MSL is bounded by two present day aquifers: the upper aquifer is located into the overlying Cenomanian sediments, the second one restricted to a sandstone level located between the MSL and the Urgonian limestones (Fig. 5.2).

The Albian silts display sealed macroscopic fractures and microfractures which are almost completely filled with calcite within the most competent (cemented sandstones) layers. These fractures and whole rock cements were studied using a mineralogical and geochemical ($\delta^{18}O$ and $\delta^{13}C$) approach in order to: i) determine the nature and the source of fluids at the origin of calcite cements and ii) to evaluate the impact and extent of these fluid movements at the scale of a whole sedimentary series.

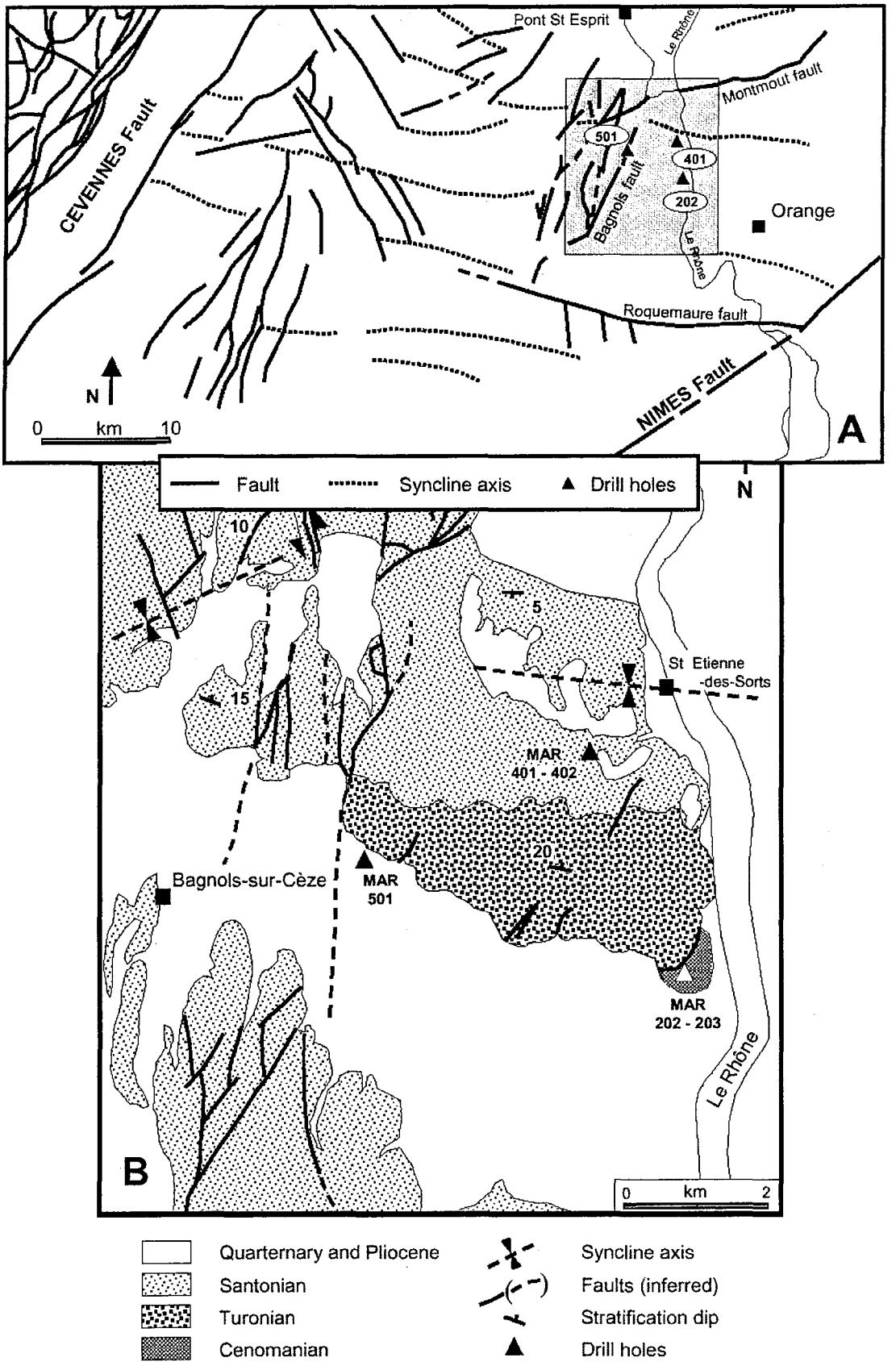

Fig. 5.1. A: Structural map showing the location of the study site within the south-eastern basin, in the area bounded to the west by the Cévennes fault and to the east by the Nimes fault, with indication of the main deformational structures: EW folds, and NS fault systems, especially in the Bagnols/Cèze area, B: Geological map with location of the three studied drill-holes, and main structures (dip of the main anticline, and faults).

5.2 Geological backgound and sampling

Recent deep boreholes were drilled by Andra (French agency for nuclear waste management) into Cretaceous layers of the South - East sedimentary Basin and led to the discovery of the " Marcoule silty-clay layer " (MSL), a Vraconian silto-argillaceous formation (Beaudoin, 1997, Beaudoin et al., 1997, Ferry, 1999). The MSL has been sampled from -400 to -800 m in depth by the Andra boreholes noted MAR 202-203 (Fig. 5.1.A and B, Fig. 5.2 and Fig. 5.3) This formation corresponds to a unique sedimentary cycle dated as Albian (100 Ma old) on the basis of macroscopic bioclasts (ammonites, Amedro and Robasynsky, 1997, Robazinky et al., 1997) and K-Ar ages on syn-sedimentary glauconites (Leclerc, 1999). These marine sediments are sandstones, siltstones and clay-rich silts deposited at rather shallow depths (around a few tens of meters) and affected by a strong bioturbation (annelides) which contributed to mechanical homogenization of the deposits. Although remarkably homogeneous, this formation displays a slight and gradual geochemical evolution from carbonate-rich levels at the bottom, to more detrital sediments upwards. To the NW, close to the basin margin, the MSL becomes thinner (Fig. 5.3; MAR501). To the North, the MSL deepens but its thickness decreases to 150 m, according to stratigraphic logs yielded by MAR 401 and 402 boreholes (Fig. 5.3). Diagenetic carbonated cements have entirely filled the open porosity, which resulted in a very low permeability for the whole MSL ($2{,}6.10^{-14} < K < 5{,}7.10^{-12}$ m/s; Lebon, 1999). The Upper Albian formation (Vraconian in terms of local geology) overlies the Urgonian (Bedoulian) limestones and are overlain by Cenomanian to Coniacian detritic sediments. The MSL silts are constituted of detrital minerals (30-50 % of quartz, phyllosilicates (biotite, muscovite), illite and illite/smectite mixed layered minerals enriched in illite), syn-sedimentary glauconite (30-40 %) and diagenetic carbonated cements, including calcite, dolomite and ankerite (10-20%)). Some glauconite-rich levels are encountered in the upper part of the MSL.

Since Cretaceous times, the studied area underwent tectonic and morphological changes through the onset of the Pyrenean (Eocene Pyrenean compression) and Alpine (s.s.) orogenies (e.g., Roure and Coletta, 1996; Séranne, 1999 and references therein). It is located between the Cévennes fracture zone and the Nîmes fault (Fig. 5.1.A) which is still active today. Such tectonic and morphological events were likely to induce structural discontinuities, fluid flows and water-rock interactions in the MSL. However, the main faults are generally considered as syn-sedimentary (Cretaceous), and reactivated or newly created during the Oligocene distension (e.g., Philip et al., 1984, Clauzon et al., 1996; Beaudouin et al., 1997, and references therein, Combes and Carbon, 1997, Grelet, 1997).

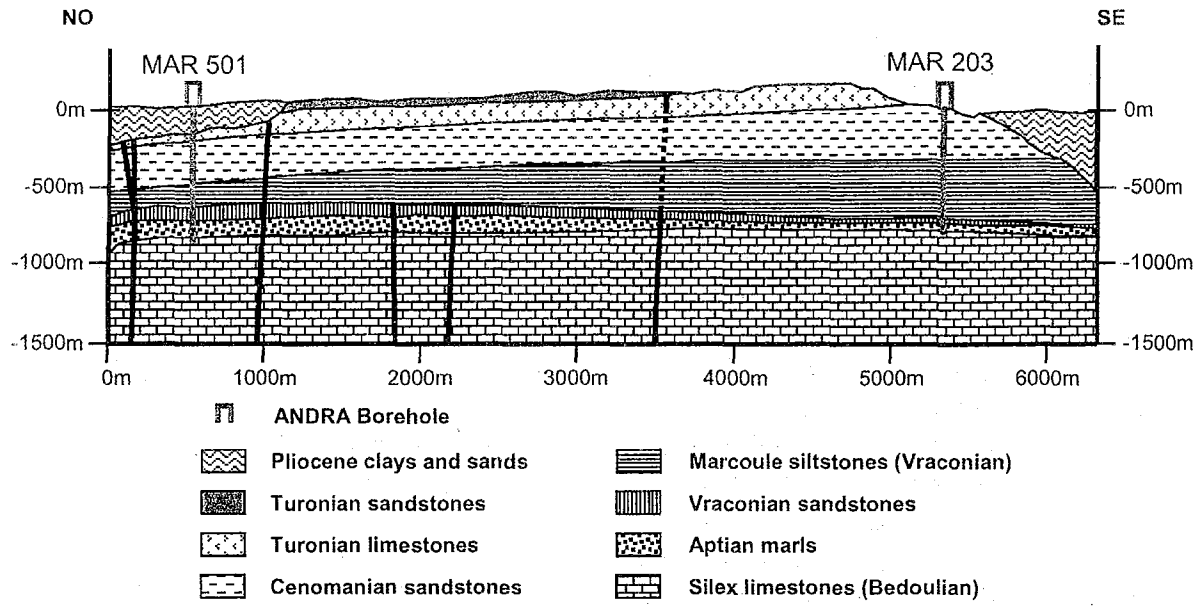

Fig. 5.2. Cross-section showing the stratigraphy of the studied area and location of the Albian-Aptian silt within the Cretaceous series.

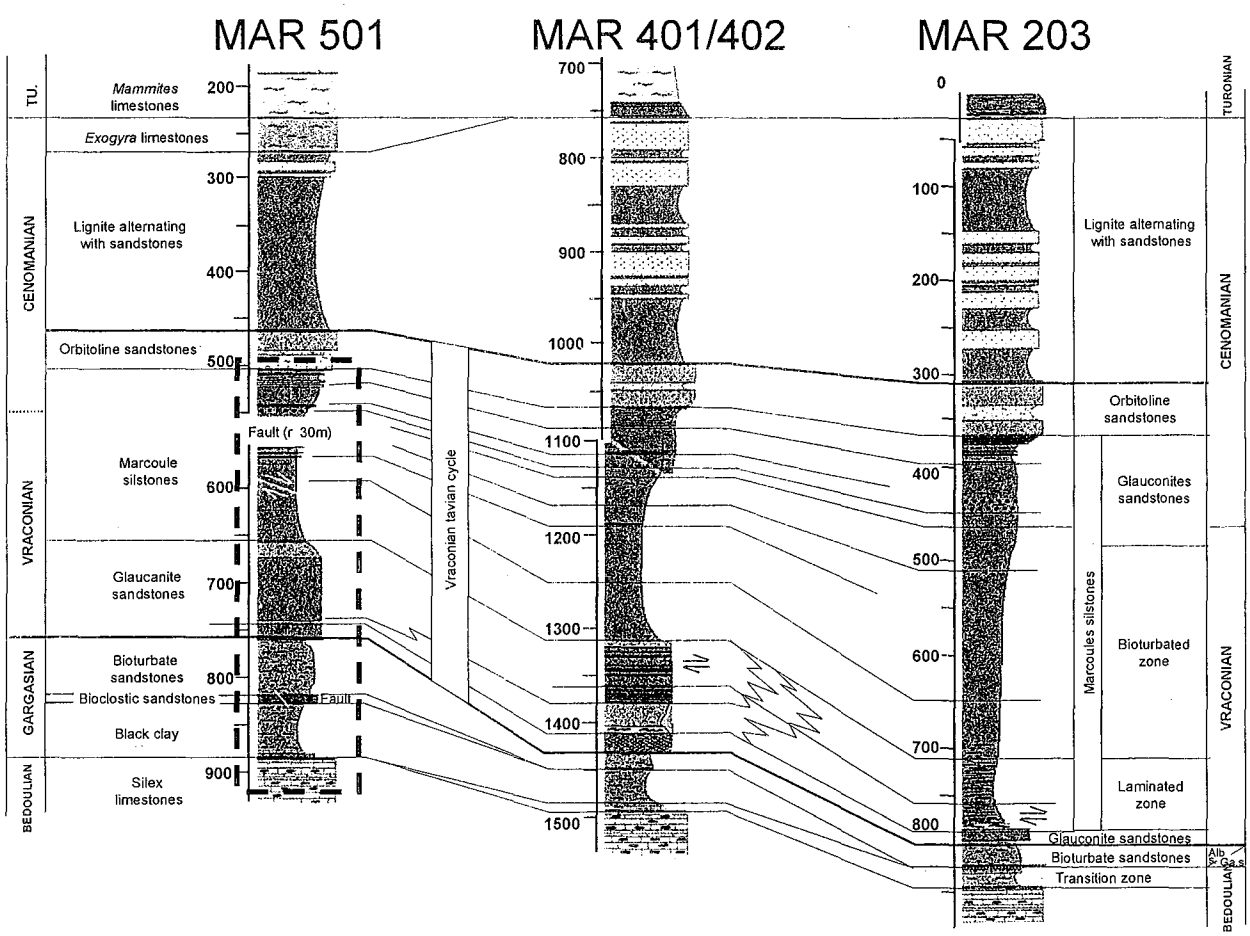

Fig. 5.3. Stratigraphy of the studied drill-holes with indication of the location of the main fault zones. Dotted box on MAR501 borehole corresponds to the series isotopically studied. For isotopic logging (Fig. 5.7), samples from MAR401/2 and 203 are stratigraphically correlated to MAR501.

5.2.1 Sampling

Small fractures and tension gashes mostly filled by calcite were sampled in three boreholes MAR 501, MAR 203 and 401/2 (see cross-section from Fig. 5.3, maps from Fig. 5.1.B and cross-sections from Fig. 5.2). The list of samples with location in the drill-holes is given in Table 5.2 and Table 5.3. Depths are given with respect to the surface level for MAR 501 and corrected for MAR 203 and 401/2 on the basis of stratigraphic correlations (Ferry, 1999).

Although some structural data are available on the studied formation thanks to the wall imaging system in the drill hole (Grelet, 1997), the drill cores are not oriented. Studied calcite may be related to three main types of deformational structures (Fig. 5.4):

1. Scarce and minor inverse/ or normal low angle (less than 25°) faults striking sub-EW were recognized in the drill holes MAR 203 (samples MAR 203 at 774 m and 780 m depth) and 401/2. They correspond to sliding along the stratification planes (Fig. 5.4.A), mostly in the clay rich layers at the basis of the MSL, and interpreted as related to the Pyrenean episode (Eocene compressive stage yielding to folding tectonics).

2. The studied formation is also crosscut also by scarce sub-meridian faults (2 of them being found in the MAR 501 drill hole around 550-555m and 600 m depth), which belong to the sub-parallel set of Bagnols/ Cèze faults . They are either related to the Upper cretaceous distensive episode, or to the Oligocene distension. The normal fault recognized at -600 m depth by the MAR 501 borehole is characterized by a cm thick breccia (Fig. 5.4.B), and calcite cement with normal stria, the fault plane making an angle of around 45° with the drilling axis (this part was not orientated). This fault has been previously studied in details for Pb and Sr isotopes (Verdoux, 1997, Lancelot et al., 1999, Leclerc, 1999). Calcite (±celestite and barite) crystallized in the fault breccia and in its related surrounding tension gashes.

   Breccia and fractures in Urgonian limestones (Fig. 5.4.D) could probably be related to the same fracturing event.

3. Thin sub-vertical structures (Fig. 5.4.C) affect the most competent layer constituted by the cemented silts displaying the highest quartz amounts (metric sandstones layers within the MSL). Examples are given by samples MAR 501 at 538.6 m, 760.9 and 880.4 m depth, and MAR 203 at 1313m depth).

5.2.2 Petrography of fracture and host rocks

Siltstones: In the studied siltstones samples, three main calcite cements are identified as already mentioned by Oberger et al. (2000) (Fig. 5.5): i) micritic and bioclastic calcite I, ii) early sparite crystals (Cc II) as euhedral poecilitic crystals including quartz grains, iii) dissolution/re-crystallization of the micrite producing new generations of cement (Cc III) characterized by slightly higher and heterogeneous Fe contents. Rhombohedral dolomite surrounded by ankerite is found as isolated crystals mostly in the most clay-rich layers or at the interface with the more sandy

layers. It crystallized in one or several stages after the early micrite (Cc I) and before Cc III.

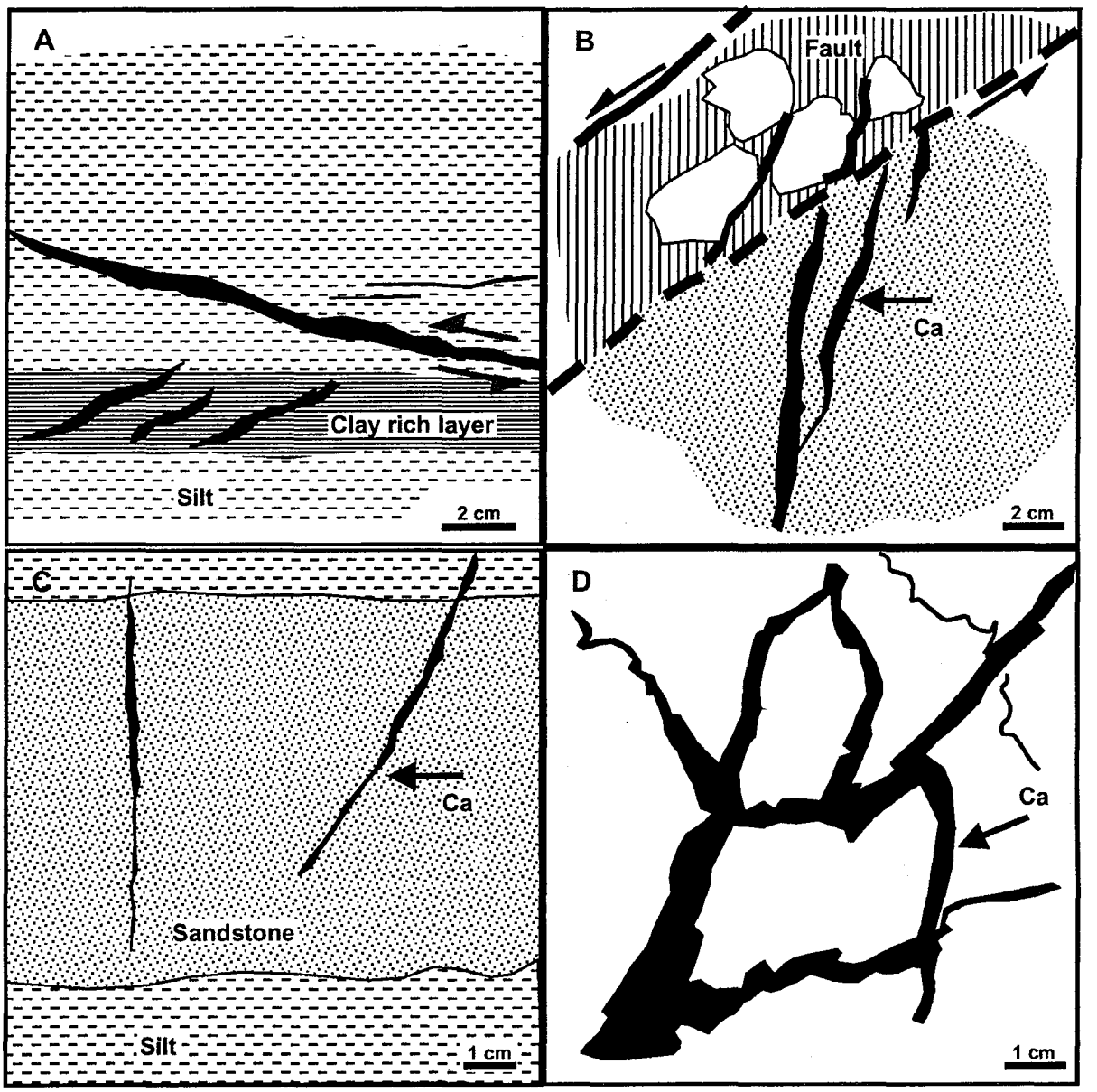

Fig. 5.4. Sketch drawing showing the textures of the studied fracture infillings and their relationships with the deformational structures. A: sub-horizontal sliding zones, B and C: sub-vertical faults and related opened structures filled by calcite, D: breccia within the Urgonian limestones. Calcite appears in black.

Fractures: They are for their most part a few mm - thick and are partially to entirely filled with large crystals of sparite. No early cements were found in macroscopic fractures. These sparites are rather limpid and occur as mosaic-like grains and are nearly pure calcite (very low Fe, Mg, Mn and Sr contents, Table 5.1). This late calcite generation (CcIV) may also been found filling the remaining micro-porosity of limestones (Fig. 5.5), but generally corresponds to a very low proportion of the diagenetic carbonates. Exceptions concern samples from MAR 203 which are rich in

clays with a low carbonate content but display abundant calcite micro-fractures around the low angle fracture zones.

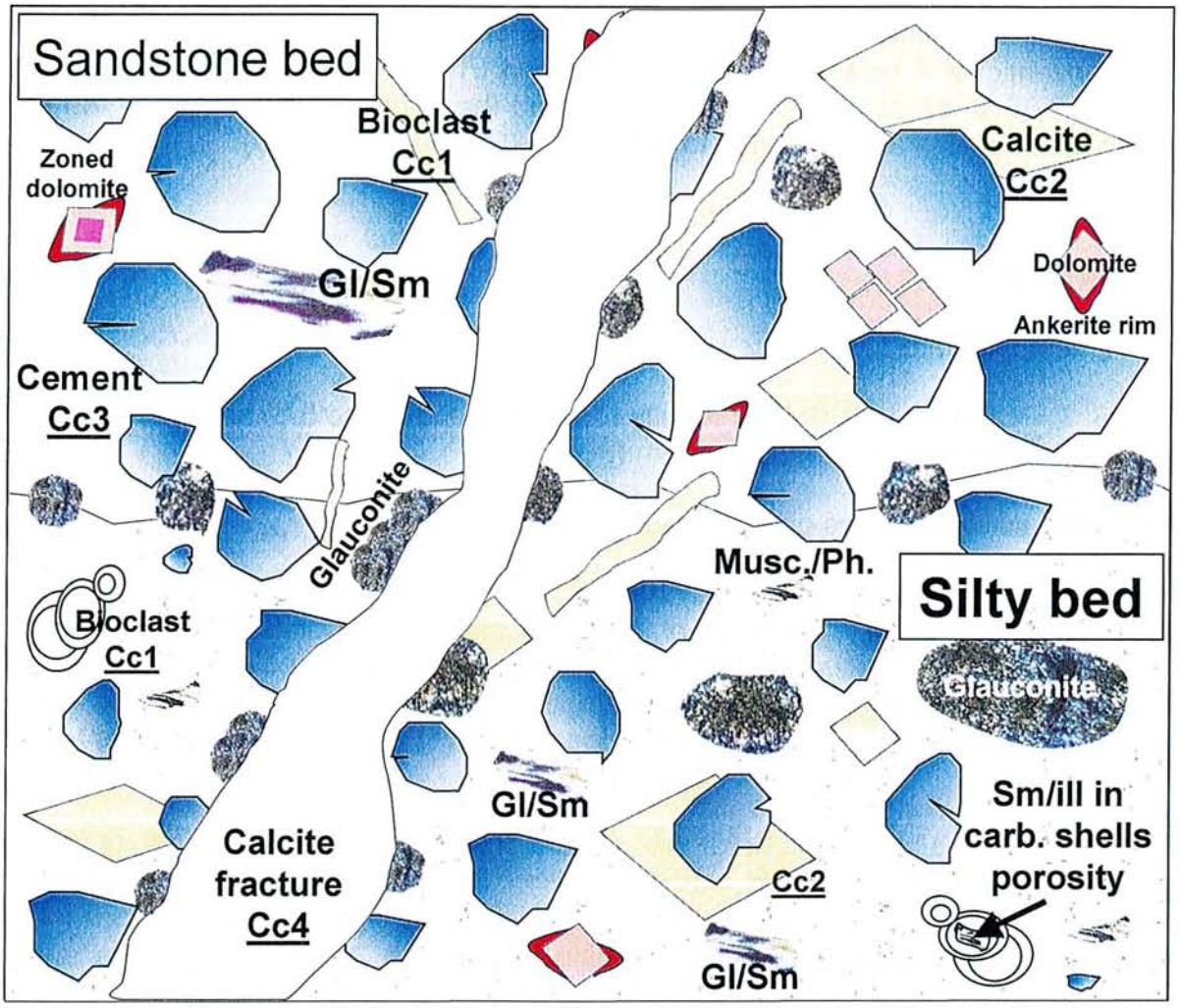

Fig. 5.5. Sketch showing the chronology and relationships between diagenetic minerals.

Type of cement	N	Ca	Mg	Mn	Fe	Sr
Bioclast Ccl	15	1.94	0.04	-	0.02	-
Micritic calcite Ccl	10	1.94	0.03	-	0.03	-
Dolomite	35	1.15	0.80	-	0.05	-
Euhedral calcite CcII	12	1.95	0.01	-	0.03	-
Calcite cement CcIII	10	1.96	0.01	-	0.03	-
Fracture cement CclV	40	1.95	0.01	-	0.03	-

Table 5.1. Ca, Mg, Mn, Fe and Sr contents of calcite cements. Electron microprobe analyses mean values (n= number of analyses).

5.3 Analytical techniques

Calcite was extracted manually from fractures and sometimes directly sampled on the polished wafers used for fluid inclusion studies. When the fractures were very thin (*c.* 1 mm), calcite was collected by micro-sampling using a dental drill. Whole rocks were analyzed in the vicinity of the fault or fractures in order to define the isotopic anomalies generated in the MSL by water-rock interactions. Calcite from fracture infillings and from bulk rocks (limestones and argillites) was finely crushed. The

carbonate fraction (1-10 mg) was reacted with 100% orthophosphoric acid at 25°C (McCrea, 1950) and we used $\alpha(O)$ $CO_2/CaCO_3$ (extraction) = 1.01025. Isotopic analyses were carried out on CO_2 gas using a VG SIRA 10 mass spectrometer and expressed, using internal carbonate standards and NBS 19 reference material, with the conventional δ notation vs. SMOW (O) and PDB (C). The mean precision was around 0.05 ‰ on some replicate samples and the uncertainties related to the PDB and SMOW scales are estimated to be < 0.1‰ (C) and *c.* 0.1‰ (O).

5.4 Results

5.4.1 Isotopic data

The $\delta^{13}C$ PDB and $\delta^{18}O$ SMOW results (Table 5.2 and Table 5.3) are presented on a binary diagram (Fig. 5.6) and vs. depth (Fig. 5.7).

- Albian siltstone series and Urgonian limestones

The upper part of Urgonian limestones have a $\delta^{13}C$ of 2.9± 0.5‰ (Fig. 5.6). Such values are maintained at the basis of the Albian series (glauconite sandy limestones). Above, in the bulk carbonate cements of the Albian detrital sediments (sandstones and siltstones), the $\delta^{13}C$ value is variable and generally lower than in limestones: (0.9 to 2.7‰) with a level (glauconitic sandstones) showing much larger variations (-2.4 to 3.1‰).

All the O isotopic compositions are a little lighter than those typical of marine carbonates (*c.* 29-30‰). Bulk carbonate cements of the Urgonian limestones are mostly found with $\delta^{18}O$ values around 26-28 ‰). Most of the Albian siltstones have $\delta^{18}O$ values (Fig. 5.6 and Fig. 5.7) ranging from 24 to 29 ‰ (mean value around 26‰) with some local exceptions. The sample MAR 203 at -745 m depth is the most noticeable exception ($\delta^{18}O$= 18.04‰).

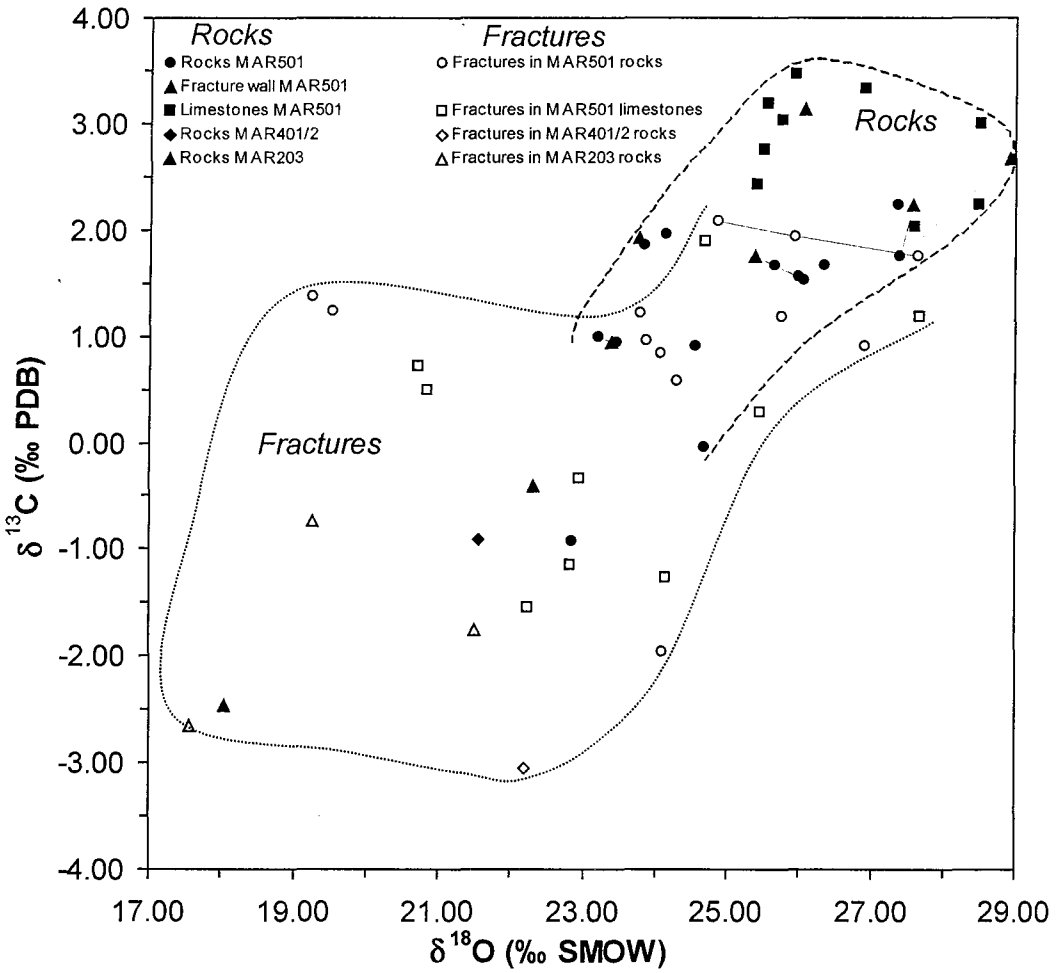

Fig. 5.6. $\delta^{13}C$ (PDB) versus $\delta^{18}O$ (SMOW) for calcite filling in fractures (open symbols), for whole rock samples (black symbols; limestones and the carbonate cements of the silstones / sandstones). The straight lines between dots corresponds to the couple of corresponding fracture calcite, fracture wall and bulk rock of one given sample. The straight dotted line joins 3 calcites sampled at different place in the metric length fracture of the sample 9763.

- Calcite fractures and relationships with host rocks

The calcites from fractures display a rather wide range of $\delta^{13}C$ and $\delta^{18}O$ values (Fig. 5.6, Table 5.2). The $\delta^{13}C$ values ranges from -3.0 to 2.1 ‰ and vary as a function of lithology and host sedimentary layers (Fig. 5.7). Fracture calcites have $\delta^{13}C$ values close to those of host rocks in Albian series, especially in the upper part of the MSL, but are rather distinct in the Urgonian limestones. The largest difference observed between $\delta^{13}C$ from fracture calcites and their corresponding host rocks is less than - 0.5 ‰ in the upper part of the MSL (MAR 501 drill hole), around - 2‰ in the glauconite sandstones, and reaches - 4‰ in the Urgonian limestones.

The $\delta^{18}O$ values of fracture calcites cover also a large range: 17.6 to 27.6 ‰. They may be either i) significantly lower than those of the host rock carbonates, the difference being up to *c.* - 6 ‰ in MAR203 at -774 m depth (Fig. 5.7) or ii) nearly similar to those of host rock, for example at -551.3m and -601m in the MSL.

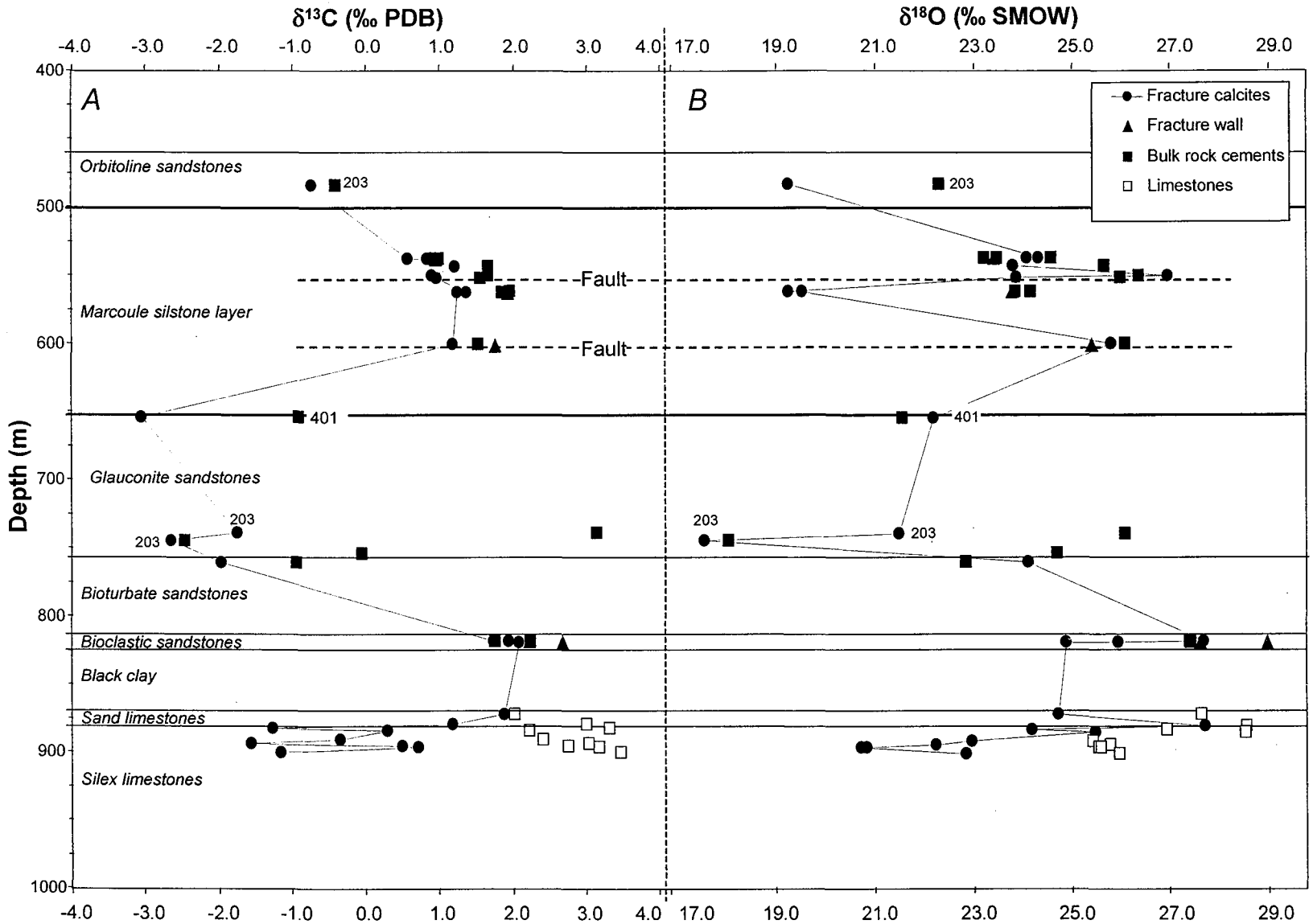

Fig. 5.7. Vertical distribution of $\delta^{13}C$ (PDB) values (A) and of $\delta^{18}O$ (SMOW) values (B) for calcite filling in fractures (circles) and for bulk rock analysis (others symbols; limestones, and carbonate cements of siltstones / sandstones with reference to the stratigraphy (borehole MAR 501, 401/402 and 203 after correction of depth and correlation with MAR 501 after Ferry (1999), Mouroux and Bruhlet (1999) and Lebon (1999). Samples from MAR203 and 401/2 are labeled.

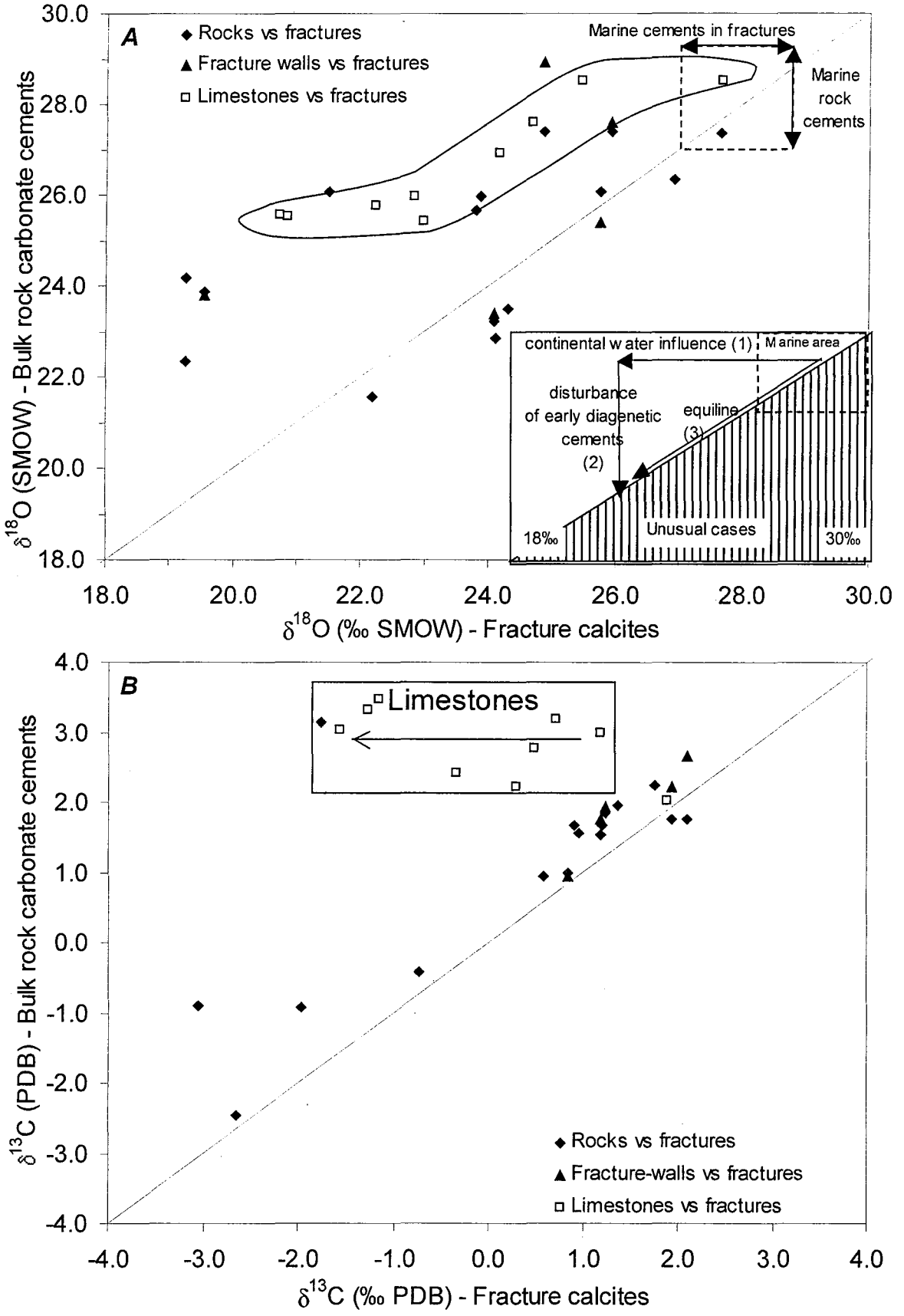

Fig. 5.8. A: $\delta^{13}C$ (PDB) of host rock carbonate cement versus $\delta^{13}C$ (PDB) of the fracture calcite; B: $\delta^{18}O$ (SMOW) of host rock carbonate cement versus $\delta^{18}O$ (SMOW) of the fracture calcite.

Fig. 5.8.A and B illustrate the variations of the isotopic compositions of fractures as a function of their host rocks or wall rocks (the later are portions of the host rocks immediately adjacent to the veins over a thickness of *c.* 1 cm). The lines with a slope of 1 (equilines) represent those fracture/host rock pairs displaying equivalent isotopic signatures. Conversely, a total decoupling between the compositions of fractures and host rocks would appear as horizontal lines in those diagrams, provided that the initial host rocks have a constant primary isotopic signature. Accordingly, in Fig. 5.8, we give the approximate field corresponding to such a situation, using the classical $\delta^{18}O$ composition range of pristine marine limestones and the $\delta^{13}C$ range measured in our Urgonian limestones. Taking into account the fact that we paid much attention during the rocks samples preparation to avoid contamination by material of fractures, analytical data (Fig. 5.8) enlighten two types of behaviors:

i) Some fracture/host rock pairs plot near the equiline (Fig. 5.8.A) which is consistent with two explanations:

a. The O isotopic composition of a given fracture and its carbonated cements of host rock were both controlled by a fluid of external derivation. This hypothesis must be ruled out considering the size of the O isotopic variations: $\delta^{18}O$ of whole rocks plotting along the equiline vary from 28.5 to 18.05‰. Indeed, in a open fluid system, this hypothesis would imply variable fluid/rock ratios during interaction. In such a case, the newly formed calcite in the fracture is expected to be systematically controlled by the fluid whereas the host rock should display decreasing degrees of (pervasive) alteration for decreasing fluid/rock ratios. In this event, one may even consider the host rocks as mixture of newly formed material (poral (re)-crystallized carbonate similar in composition to the vein) and pristine marine calcite (bioclasts, micrite): this type of mixing process (related to variable fluid/rock ratios would be represented by a vertical trend (Fig. 5.8.A inset, trend n°(2)), not by the equiline in the diagram.

Consequently, we preferably conclude that pairs plotting along the equiline behave more or less in close systems by the redistribution in the adjacent fractures by later fluid flow event(s) of the O isotopic variations of the whole rocks, which were the result of earlier and more pervasive diagenetic events, .

b. As a result, the carbon of host rocks have also been transferred into the fractures without important isotopic fractionation (dissolution and re-precipitation) and this implies that the fluid filling the local medium (fracture + recharge pore space) was not a significant reservoir of carbon and oxygen (close system behavior).

ii) The other fracture/host rock pairs plot at left of the equiline. We interpret this group of fractures as formed in open system, i.e., crystallized from an external fluid which produced an ^{18}O depletion in vein calcite but left the host rocks isotopically unmodified (keeping the O isotopic variations acquired at the time of fracturation or disturbed by new cements). The fractures/host rocks relationships described here remain consistent with the C isotopic compositions (Fig. 5.8.B). During the fracture formation, the fluids were not a significant isotopic reservoir of C, which was washed in most cases from adjacent rocks and redistributed locally in the veins. The reason is likely that fluids in open system were displaying a low C/O ratio.

By contrast, limestones still preserved nearly pristine marine C isotopic signatures and exhibit a decoupling between the fractures (C/O of external derivation) and host rocks (isotopically unaltered) which is clearly indicative of an open system behavior. Thus, it appears that Urgonian limestones preserved to some extent their primary isotopic signatures despite the introduction of external carbon in their fractures likely because of their high total carbonate content.

Borehole	Sample	Depth (m)	Lithology	$\delta^{13}C$ ‰ PDB	$\delta^{18}O$ ‰ SMOW
MAR203	18803	485 (351)	Cenomanian orbitoline sandstone	-0.41	22.32
MAR501	17380-1	538.6	Albian Marcoule siltsone	0.94	23.48
-	17380-2	538.7	-	0.99	23.21
-	17380-3	538.8	-	0.90	24.57
-	17380-fw	538.9	-	0.95	23.40
-	17399	543.9	-	1.66	25.65
-	17433	551.4	-	1.67	26.34
-	17425	553.0	-	1.56	25.98
-	17483-1	563.1	-	1.96	24.16
-	17483-2	563.2	-	1.85	23.86
-	17483-fw	563.4	-	1.93	23.79
-	11234	601.0	-	1.53	26.07
-	11234-fw	601.5	-	1.76	25.39
MAR402	17145	655 (1313)	Albian glauconite sanstone	-0.90	21.57
MAR203	11369	740 (774)	-	3.14	26.06
-	17167	745 (780)	-	-2.46	18.04
MAR501	17237	754.3	-	-0.05	24.68
-	17232	760.9	Aptian bioturbate sandstone	-0.93	22.85
-	9763-1	818.5	Aptian bioclastic sandstone	2.24	27.36
-	9763-2	818.7	-	1.76	27.39
-	9763-fw1	818.7	-	2.23	27.58
-	9763-fw2	819.5	-	2.67	28.92
-	17222	872.3	Aptian glauconite sand limestone	2.03	27.60
-	9998	880.4	-	3.00	28.52
-	17219	882.9	Urgonian (Bedoulian) silex limestone	3.32	26.91
-	17218	885.3	-	2.23	28.50
-	17207	891.7	-	2.42	25.42
-	17209	894.5	-	3.03	25.77
-	17211	896.2	-	2.76	25.52
-	17213	896.8	-	3.18	25.57
-	17204	901.4	-	3.47	25.95

Table 5.2. Isotopic data of rocks cements in boreholes MAR203, 401/2, 501. For MAR203 & 401/2, depths are corrected with respect to MAR501 on the basis of stratigraphical correlations. Values in brackets correspond to the real depth below surface. fw: fracture wall.

Borehole	Sample	Depth (m)	Lithology	Sample type	$\delta^{13}C$ ‰ PDB	$\delta^{18}O$ ‰ SMOW
MAR203	18803	485 (351)	Cenomanian orbitoline sandstone	Epigenetic calcite replacing bioclasts	-0.73	19.26
MAR501	17380-1	538.6	Albian Marcoule siltsone	Subvertical tension gashes in sand silt	0.58	24.31
-	17380-2	538.7	-	-	0.84	24.09
-	17399	543.9	-	Fracture in clay rich silt	1.21	23.81
-	17433	551.4	-	-	0.90	26.92
-	17425	553.0	-	NS normal fault zone: Breccia infillings	0.96	23.87
-	17483-1	563.1	-	NS normal fault zone: Striated 'fault' plane	1.37	19.26
-	17483-2	563.2	-	NS normal fault zone: -	1.24	19.54
-	11234	601.0	-	NS normal fault zone: NS normal fault	1.19	25.78
MAR402	17145	655 (1313)	Albian glauconite sanstone	Subvertical tension gashes in sandstone	-3.05	22.19
MAR203	11369	740 (774)	-	Subhorizontal opened structures	-1.75	21.51
MAR203	17167	745 (780)	-	Subhorizontal micro-cracks	-2.65	17.57
MAR501	17232	760.9	Aptian bioturbate sandstone	Subvertical micro-crack in sandstone	-1.96	24.12
-	9763	818.6	Aptian bioclastic sandstone	Subvertical wavy fracture	1.75	27.65
-	9763-1	818.7	-	-	1.94	25.93
-	9763-2	819.5	-	-	2.09	24.88
-	17222	872.3	Aptian glauconite sand limestone	Geode connected with subvertical fissure	1.89	24.70
-	9998	880.4		Subvertical microfissure in sand limestone	1.19	27.68
-	17219	882.9	Urgonian (Bedoulian) silex limestone	Sets of subvertical fractures	-1.26	24.17
-	17218	885.3		Stylolitic structure with clays & calcite	0.29	25.47
-	17207	891.7	-	Euhedral calcite in geode connected fissure	-0.34	22.97
-	17209	894.5	-	Breccia fracture	-1.55	22.24
-	17211	896.2	-	Breccia fracture	0.49	20.85
-	17213	896.8	-	Euhedral calcite in geodes (breccia)	0.72	20.72
-	17204	901.4	-	Geodes (post stylolites) in brecciated zone	-1.16	22.84

Table 5.3. Isotopic data of geode/fracture calcite cements in boreholes MAR203, 401/2, 501. For MAR203 & 401/2, depths are corrected with respect to MAR501 on the basis of stratigraphical correlations. Values in brackets correspond to the real depth below surface.

5.4.2 Temperatures of diagenesis and fracture formation

Interpretation of the isotopic data in terms of fluid sources requires independent temperature estimates on the conditions of calcite crystallization. Fluid inclusions study is one of the most powerful techniques available to evaluate the thermal conditions of minerals growth. Fluid inclusions (FI) found in calcite are scarce, of very small size (< 10 µm) and mostly found in calcites from geodes and fractures, rarely in the sparitic cement. FI are primary, coeval with calcite crystallization and all of them are aqueous and one-phase. UV-excitation fluorescence indicates that FI are free of hydrocarbon compounds. Thermal pulses (successive cooling and heating) were performed on calcite crystals in order to nucleate a vapour phase in one-phase FI. The meta-stability of the one-phase entity could not be broken down, as no nucleation was obtained. Therefore, the one-phase FI were formed at low temperatures, probably lower than 45-50°C (Goldstein and Reynolds, 1994). These temperature estimates are in total agreement with the other geothermometric considerations as:

i) the clay mineralogy data, especially the suspected formation of smectite after glauconite, smectite identified and analyzed by TEM studies (Roubeuf, 2000)

ii) the specific bio-markers indicating that the Albian organic matters are fully immature and did not experience a temperature higher than 50°C, if the burial duration was about some tens of million years (Fleck, 2001).

On the other hand, an upper limit to the temperature experienced by the MSL may be estimated considering that it underwent a maximum burial of 1500 to 2000m (i.e., *c.* 1000 to 1400m deeper than today) according to Mouroux and Bruhlet (1999) and that the present day geothermal gradient is around 30°C/km. Thus, a temperature range bracketed between 34 ± 2°C (present day temperature) and 65°C is inferred for the (re)crystallization of whole rocks and fracture calcite (i.e., 30°C higher than present day measured temperatures of 32 and 36°C at 660 and 860 m depths, respectively). However, 50°C is likely a maximum taking into account the stability of bio-markers and the total lack of two-phase FI.

5.5 Interpretation of the fluid origin

5.5.1 Isotopic signature of fluid

The oxygen isotopic composition of the diagenetic fluids was calculated using the isotopic fractionation coefficients of Kim and O'Neil (1997) for the calcite-water system. Since the history of altered whole rocks and fractures is not identical, the two kinds of materials must be treated separately. The most extreme compositions recorded in whole rocks and in fractures would a priori be the most appropriate to provide information on fluid characteristics.

The lowest $\delta^{18}O$ value recorded in whole rocks of the MSL is 18.04‰. The calculated fluid $\delta^{18}O$ values are -8‰ and -5.5‰ for temperatures of 35 and 50°C, respectively. This value is not compatible with a seawater derivation and implies the pervasive penetration of groundwaters at that level. With this exception, the O isotopic composition of all the other whole rock cements are consistent, within uncertainties, with marine diagenesis at the maximum estimated temperature (50°C), as well as with the development of glauconite in the MSL. K-Ar dating of glauconite in that section shows that this mineral developed soon after sedimentation which is considered to be rapid in the MSL (Clauer et al., 2001). Decreases of the $^{13}C/^{12}C$ ratios in the whole rocks of the MSL sympathetically with a decrease of $^{18}O/^{16}O$ ratios may be linked to the introduction of oxidized organic carbon by the diagenetic fluid in the most porous levels of the MSL in the way described (at higher diagenetic conditions) by Winter et al. (1995). Large water fluxes are necessary to induce the isotopic variations introduced during this diagenetic event.

Fractures calcite with the lowest $\delta^{18}O$ value (17.57‰, sample 17167 of MAR 203) may be produced in a seawater-dominated medium provided that crystallization temperatures were in the order of 80± 5°C, a temperature level which is incompatible with all the available thermometrical estimates (bio-markers, clays, FI). Moreover, to reconcile the large O isotopic variations observed among the group of fracture calcites with the seawater hypothesis, it would be necessary to call for unreasonable assumptions, i.e., significant differences in the crystallization temperatures of fractures calcites (30 to 80°C) over short depths intervals (e.g., samples 11369 and 17167 of MAR 203). Consequently, the fluid $\delta^{18}O$ composition corresponding to

sample 17167 of MAR 203 is found in between -8.5 and -6 ‰ for temperatures of 35°C and 50°C, respectively. Noteworthy is the fact that these are limit values corresponding to a fluid acting as an infinite isotopic reservoir. If that was not the case, the fluid isotopic composition could have been lighter. On the basis of this $\delta^{18}O_{fluid}$ value, the corresponding fluids at the origin of the late calcite cannot be pristine marine waters. Such extreme isotopic signatures may be those of meteoric water or may be achieved through mixing between marine and meteoric water.

Still lighter isotopic compositions (-11.5 to -10.5‰) are calculated if fracture formation occurred in early sedimentary conditions (e.g., 20-25°C). Fluid mixing is a common process in sedimentary basins in coastal zones such as those linked the output of large continental watersheds (Lynn Ingram et al., 1996), and to the submarine infiltration of groundwater issued from the neighboring emerged areas in shallow-seated sediments (Li et al., 1999; Moore, 1996). Nevertheless, we rule out the input of meteoric water at the time of sediments deposition or during early diagenesis at shallow depth because sedimentation in the MSL appears to be rapid and the development of fracturation seems to occur slightly later than bulk diagenesis around the maximum of compaction during Tertiary tectonic phases.

5.5.2 The case study of the fault zone from MAR 501

Fluid flow through the MSL in the vicinity of the fault at -600 m (sample 11234) was investigated using a combined C, O and Sr isotopic approach on whole rock carbonate cements and calcite infilling the fault. Sr isotopic compositions were also studied on calcite (and locally celestite) from proximal tension gashes (up to 20 cm away from the fault limbs). Previous data on Pb isotopes were acquired on pyrite from the fault infillings and on whole rock samples collected in the vicinity of the fault (Lancelot et al., 1999).

Calcite from the fault infillings, from the fault wall-rock and the nearby silt sample (1 m away from the fault limb), share similar $\delta^{18}O$ and $\delta^{13}C$ values. Moreover, the $\delta^{18}O$ in the fault calcite (25.78‰) is one of the highest found among the fracture carbonates. These data argue that the calcitic fault infillings were produced by redistribution of the carbonate cements from the host zone, i.e. that the fluid present during that redistribution was isotopically buffered by those cements (low mobility). This conclusion agrees with the Sr isotopic data obtained around the same fault zone (Verdoux, 1997, Lancelot et al., 1999). MSL whole rocks, sampled at 5 to 25 m away from the fault, does not show any significant change of $^{87}Sr/^{86}Sr$ ratios (0.70902 to 0.70973). This isotopic signature is still preserved in calcite from one MSL whole rock sampled at few centimetres above the upper limb of the fault: $^{87}Sr/^{86}Sr$ = 0.70929. These features are consistent with the remarkable homogeneity of chemical and mineralogical compositions within the MSL (attributable to mechanical mixing by bioturbation). Celestite and calcite fractions extracted from the cement of the fault breccia and from tension gashes show lower Sr isotopic compositions (0.70749 to 0.70768). Comparison of these isotopic signatures with those of the local Cretaceous diagenetic carbonates (values obtained only on carbonate leachates: 0.70741 ± 0.00002) suggests that the sealing fluid was isotopically equilibrated for strontium with the whole diagenetic/marine carbonates (Clauer, 1981a/b, Burke et al., 1982, Clauer et al., 1989) present in the host siltstones. The slight difference could reflect that the fluids may have scavenged and washed some more radiogenic strontium from the clay particles (glauconite, or detrital phyllosilicates). By contrast, $^{206}Pb/^{204}Pb$

ratios of authigenic pyrites, disseminated within the MSL, are distinctly less radiogenic than those of pyrites present in tension gashes and in the tectonic breccia of the fault zone (Verdoux, 1995, Lancelot, 1999). This indicates that some Pb transfer has occurred after the sealing of the tension gashes around or within the fault. The latter event is not significantly recorded by stable isotopes. Calcite in the fault zone (pore cement, tension gashes) has thus the same C, O isotopic compositions than the carbonate cements, this indicating element transfer along rather short distances.

5.6 Concluding remarks

Several conclusions can be put forward from this study:

- Despite being very immature (bio-markers, clays typology) the sedimentary formation studied experienced intense diagenetic events linked to two main types of fluid. The first type likely corresponds to diagenetic re-crystallization in the presence of significant fluxes of seawater-derived fluids. Superimposed to these effects, localized infiltration of groundwaters also induced rock re-crystallizations.

- Some fractures were filled in with carbonate material issued from the immediate surroundings and this implies that the resident fluid was rather static (close system behavior of crack-seal type). Some other fractures were filled by material of more remote provenance (open system behavior) and this is the case of all the fractures studied in the Urgonian limestones. In some instances (e.g., glauconite sandstone and associated fracture), the influence of groundwater circulation is very marked. These aquifer levels were likely characterized by high permeabilities.

- Groundwater entering the main aquifers (Urgonian, and may be sandstones) travelled laterally and penetrated then throughout the localized micro-fracture permeability affecting the Albian-Aptian formation and likely mixed with the residual pore fluids (marine waters). The degree of mixing is probably highly variable from one sedimentary layer to the other due to the low whole permeability of the formations, the discontinuous nature and the low conductivity of many fractures (which show carbonate redistribution of a local scale). This could explain the lack of homogeneity in the analyzed $\delta^{18}O$ values. No specific differences characterize the sets of horizontal micro-fractures linked to Eocene folds, and sub-vertical microfractures in relation with the NS faulting of the series during the Oligocene distensive tectonics.

- Early diagenesis in the presence of seawater-derived fluids is apparently linked to the burial of sediments. However, deciphering remnants of the paleo-environmental histories (if still present) in the MSL would require a very detailed microanalysis approach. Their fracturation is linked to the role of overburden pressures and deformational events linked to the folding and the faulting of the series during Eocene and Oligocene. So the fracturing occurs after the considerable decrease of the initial porosity through the preceding cementation stage. Further sealing process have cancelled the permeability of the sets of fractures and so, the present-day global permeability of the rocks, which is very low.

ACKNOWLEDGEMENTS

This study was supported by GdR FORPRO - Action 98-III (paper FORPRO n° 2001/13 A), a National Research Program between CNRS and Andra (French Nuclear Waste Management Company). Andra is acknowledged for the facilities and permission of sampling the drill cores. Stéphane Buschaert benefited of a grant from Andra for completion of his PhD.

REFERENCES

Amedro, F., Robaszynski, F., 1997. Datations précises en forages à l'aide des ammonites. J. Sci. Andra, 20-21 oct. 97, Bagnols/Cèze, abstract, p.7-8.

Baudrimont, A.F., Dubois P., 1977. Un bassin mésogéen du domaine péri-alpin : le Sud-Est de la France. Bulletin du Centre de Recherche d'Exploitation et Production d'Elf Aquitaine, 1, 1, 261-308.

Beaudoin, B., 1997. Stratigraphie de l'Albien et calibrage temps de la série de Marcoule. J. Sci. Andra, 20-21 oct. 97, Bagnols/Cèze, abstract, p.10

Beaudouin, B., Accarie, H., Berger, E., Brulhet, J., Cojan, I., Haccard, D., Mercier, D., and Mouroux, B., 1999. Les enseignements de la crise " fini-messinienne ". Proceedings of the Andra Sci. Meeting Bagnols-sur-Cèze, EDP Sciences Publ., 115-135.

Blyth, A., Frape, S., Blomqvist, R. and Nissinen, P., 2000. Assessing the past thermal and chemical history of fluids in crystalline rock by conbining fluid inclusion and isotopic investigations of fracture calcite. Appl. Geochem., 15: 1417-1437.

Burke, W.H., Denison, R.E., Hetherington, E.A., Koepnick R.B., Nelson N.F. and Otto J.B., 1982. Variation of seawater $^{87}Sr/^{86}Sr$ throughout phanerozoic time. Geology, 10, 516-519.

Clauer, N., 1981a. 87Sr/86Sr ratios of the Barremian and early Aptian seas. In : thiede J., Vallier T.L. et al., initial reports of the deep sea drilling project. U.S. Government Printing Office, 62, 781-783.

Clauer, N., 1981b. Rb-Sr and K-Ar dating of precambrian clays and glauconies. Precambrian Research, 15, 331-352.

Clauer, N., Chaudhuri, S., Subramanium, R., 1989. Strontium isotopes as indicators of diagenetic recrystallization scales with carbonate rocks. Chem. Geol., 80, 27-34.

Clauer, N., et al. (17 co-authors), 2001, Evolution diagénétique des formations argileuses très imperméables de l'Est et du Gard, FORPRO report no 2001/04 Rf (action 98-VI).

Clauzon, G;, Suc, J.-P., Gautier, F., Berger, A. and Loutre, M.-F., 1996. Alternate interpretation of the Messinian salinity crisis: controversy resolved? Geology, 24, 4, 363-366.

Combes, Ph. and Carbon, D., 1997. Néotectonique et sismicité du Gard Rhodanien. Proceedings of the Andra Sci. Meeting Bagnos-sur-Cèze, EDP Sciences Publ., 93-114.

Ferry, S., 1999. Apport des forages Andra à la connaissance de la marge crétacée rhodanienne. Proceedings of the Andra Sci. Meeting Bagnols-sur-Cèze, EDP Sciences Publ., 63-91.

Fleck, S, 2001. Corrélation entre géochimie organique, sédimentologie et stratigraphie séquentielle pour la caractérisation des environnements de dépôt. PhD Thesis Univ. Nancy I.

Goldstein, R.H. and Reynolds, T.J., 1994. Systematics of fluid inclusions in diagenetic minerals. SEPM short course 31, 212 pp.

Grelet, B., 1997. Analyse de la fracturation en forages. J. Sci. Andra, 20-21 oct. 97, Bagnols/Cèze, abstract, p.17.

Kim, S.T. and O'Neil, J.R., 1997. Equilibrium and nonequilibrium oxygen isotope effects in synthetic carbonates. Geochim. Cosmochim. Acta, 61: 3461-3475.

Lancelot, Leclerc, S., Verdoux, P., and Aranyossy J.F., 1999. A strontium and lead isotopic study of the Marcoule silty-clay layer (Gard, France) and implications for charcaterization of water-rock intercations in low permeability argillaceous media.

OCDE Proc. NEA/ EC Workshop "Fluid flow through faults and fractures in argillaceous formations" Berne, 223-242.

Lancelot, J., 1999. Discussion de l'évolution des isotopes radiogéniques dans la couche silteuse de Marcoule en domaines non fracturés et fracturés. Proceedings of the Andra Sci. Meeting Bagnols-sur-Cèze, EDP Sciences Publ., 139-166.

Lebon, P., 1999. La couche silteuse de Marcoule : des propriétés exceptionnelles. Proceedings of the Andra Sci. Meeting Bagnols-sur-Cèze, EDP Sciences Publ., 3-13.

Leclerc, S., 1999. Contribution de la méthode Rb/ Sr à la démontsration de la qualité de confinement de la couche silteuse de marcoule (Gard Rhodanien). Thesis, Montpellier Univ., 208.

Li, L., Barry, D.A., Stagnitti, F. and Parlange, J.-Y., 1999. Submarine groundwater discharge and associated chemical input to a coastal area. Water Res. Res., 35: 3253-3259.

Lynn Ingram, B., Conrad, M.E. and Ingle, J.C., 1996. Stable isotope and salinity systematics in estuarine waters and carbonates: San Francisco Bay. Geochim. Cosmochim. Acta, 60(3): 455-467.

McCrea, J.M., 1950. On the isotope chemistry of carbonates and a paleotemperature scale. J. Chem. Phys., 18: 849-857.

Moore, W.S., 1996. Large groundwater inputs to coastal waters revealed by ^{226}Ra enrichments. Nature, 380: 612-614.

Mouroux, B., Brulhet, J., 1999, La démarche scientifique de l'Andra : site du Gard. Proceedings of the Andra Sci. Meeting Bagnols-sur-Cèze, EDP Sciences Publ., 13-33.

Orberger, B. & Pagel, M., 2000. Diagenetic evolution of Cretaceous siltstones from drill hole MAR 501 (South-Eastern France). Journal of Geochemical Exploration, 69-70, 115-118.

Philip, J., 1984. Tectonique méso-crétacée en Provence « Synthèse géologique du Sud-Est de la France ». Edité par Debrand-Passard et al. Mém. BRGM, n° 125, pp. 384-386.

Robaszynski, F., Amedro, F., Devalque, C., 1997. Positionnement de la limite stratigraphique entre les étages cénomanien et turonien dans les sondages de Marcoule. J. Sci. Andra, 20-21 oct. 97, Bagnols/Cèze, abstract, p. 9.

Roubeuf, V., 2000. Interactions entre fluides et sédiments argileux naturels : Étude expérimentale dans des conditions simulant un stockage souterrain de déchets radioactifs. Thesis Univ. Nancy I.

Roure, F. and Colletta, B., 1996. Cenozoic inversion structures in the foreland of the Pyrénées and the Alps. In: "Peri-tethys Memoir 2: Structure and aspects of Alpine basins and forelands " (Ziegler, P.A. and Horvàth, F., eds.), Mém. Mus. Hist. Nat., 170, 173-209.

Séranne, M., 1999. The Gulf of Lion continental margin (NW Mediterranean) revisited by IBS: an overview. In: " The Mediterranean Basins: Tertiary Extension within the Alpine Orogen " (Durand, B., Jolivet, L., Horvàth, F and Séranne, M., eds.), Geol. Soc. London Spec. Publ. 156, 15-36.

Verdoux, P., 1997. Contribution des systèmes Rb/Sr et U/Pb à la charactérisation des circulations et des paléocirculations de fluides en domaine continental entre 0 et 2000 m de profondeur. Conséquences sur les ressources en eaux et le stockage des déchets radioactifs en profondeur. Thèse de doctorat, Université de Montpellier, 342 pp.

Wallin, B. and Peterman, Z., 1999. Calcite fracture fillings as indicators of paleohydrology at Laxemar at the Aspö Hard Rock Laboratory, southern Sweden. Appl. Geochem., 14: 953-962.

Winter, B.L., Valley, J.W., Simo, J.A., Nadon, G.C., Johnson, C.M., 1995. Hydraulic seals and their origins: evidence from the stable isotope geochemistry of dolomites in the Middle Ordovician St. Peter Sandstone, Michigan Basin. Am. Ass. Petrol. Geol. Bull. 79, 1, 30-48.

6 WIDESPREAD CEMENTATION INDUCED BY INFLOW OF CONTINENTAL WATER IN THE EASTERN PART OF THE PARIS BASIN: O AND C ISOTOPIC STUDY OF CARBONATE CEMENTS

S. Buschaert[a,d], S. Fourcade[b], M. Cathelineau[a], E. Deloule[c], F. Martineau[b], M. Ayt Ougougdal[a], A. Trouiller[d]

[a] CREGU - UMR G2R 7566, BP23, 54501 Vandoeuvre-lès-Nancy, France
[b] Géosciences Rennes – UMR CNRS 6118, 35042 Rennes cedex, France
[c] CRPG-CNRS, 54501 Vandoeuvre-lès-Nancy, France
[d] Andra, French Agency for Nuclear Waste Management, 92298 Châtenay-Malabry

Submitted to Applied Geochemistry

Figure captions ***6-180***
Table captions ***6-180***
Abstract ***6-181***

6.1 INTRODUCTION ***6-183***

6.2 GEOLOGICAL BACKGROUND OF THE EASTERN FLANK OF THE PARIS BASIN ***6-184***

6.3 LATE SPARITE CRYSTALLISATION STAGE ***6-185***

6.4 ANALYTICAL METHODS ***6-188***
6.4.1 Fluid inclusions 6-188
6.4.2 Conventional C and O isotope analysis 6-188
6.4.3 Oxygen isotope microanalysis by SIMS 6-188

6.5 RESULTS ***6-189***
6.5.1 Isotopic data 6-189
- Limestones and clay-rich formation 6-189
- Calcite in geodes and fractures 6-190
- Relationships with stratigraphy 6-191
- Calcite of cements: SIMS analysis 6-194

6.5.2 Formation temperatures of late sparite 6-196

6.6 INTERPRETATION OF THE FLUID SOURCE ***6-197***
6.6.1 Isotopic signature of fluid 6-197
6.6.2 Discussion on the possible pathways and timing of fluid circulation 6-198

6.7 CONCLUDING REMARKS ***6-200***
Acknowledgements ***6-202***
References ***6-203***

FIGURE CAPTIONS

Fig. 6.1. Schematic geological map showing the regional location of the studied site and related boreholes. *6-184*

Fig. 6.2. A: macroscopic cavities partially filled by calcite (HTM102-331: 141 m). This type of voids is usually created during sedimentation in reef environment. B: small vertical tension gashes filled by calcite crosscutting or crosscut by thin sub-horizontal stylolites as an example of complex relationship between stylolites and fissures (HTM102-2523: 111 m). C. microphotographs of petrography showing the intensive recrystallisation of limestones by the new sparite (HTM102-2509: 86 m). D: Microphotographs of petrography showing the scarce case of coexistence of pellets cemented by early micrite with the new sparite often replacing the early cements in porosity (as in photograph C) and filling also the fracture (HTM102-2184: 483 m) *6-187*

Fig. 6.3. $\delta^{13}C$ (PDB) versus $\delta^{18}O$ (SMOW) for calcite from geodes and fractures (open symbols), for whole rock samples (limestones) and for the micrite cement of the argillites with distinction of the main stratigraphic layers. Bath.: Bathonian, Call.: Callovian, Low Oxf.: lower Oxfordian, Mid. Oxf.: Middle Oxfordian, Up. Oxf.: Upper Oxfordian, Kimm.: Kimmeridgian. F refers to vertical tension gashes. *6-191*

Fig. 6.4. Vertical distribution of $\delta^{13}C$ (PDB) values (A) and $\delta^{18}O$ (SMOW) values (B) for calcites from geodes and fractures (F) and bulk rocks analysis (limestones and argillites (micrite cement)) with reference to the stratigraphy (borehole HTM 102, and EST 103 after correction of depth and correlation with HTM 102 after Trouiller and Lebon, 1999) *6-192*

Fig. 6.5. Abundance (volume estimate by petrographic image analysis) of late sparite in limestones versus $\delta^{18}O$ (SMOW) values of the bulk rock *6-193*

Fig. 6.6. In situ SIMS $\delta^{18}O$ analyses of the primary constituents (ooliths, pellets, early cements), and of the late sparite found in the micropores and in a geode of limestone HTM2509. Conventional analysis results are also presented for reference (black dots) *6-194*

Fig. 6.7. $\delta^{18}O$ (SMOW) values of the fluid vs. temperature. Calcite/water fractionation curves are reported. The calculated fluid O isotopic compositions are presented for an assumed formation temperature of 20-25°C (marine carbonates), and for 3 ranges of hypothetical recrystallisation temperatures (sparite from geodes and fractures): ① subsurface temperature conditions, ② higher temperature (60-70°C) required to obtain a fluid of marine derivation, and ③ the most reliable estimated growth temperature (32-42°C; derived from fluid inclusion study). *6-198*

TABLE CAPTIONS

Table 6.1. Ca, Mg, Mn, Fe and Sr contents of calcite cements. Electron microprobe analyses mean values (n= number of analyses). Sr values in brackets given for geodes have been obtained by ICP-MS (range for 5 samples). *6-187*

Table 6.2. Depth and $\delta^{13}C$ (PDB)-$\delta^{18}O$ (SMOW) data of studied limestones and argillites in boreholes HTM102 and EST103/106. ..... *6-189*

Table 6.3. Depth, host rock lithology, and $\delta^{13}C$-$\delta^{18}O$ data of calcites from geodes and fractures in boreholes HTM102 and EST103/106. ..... *6-190*

Table 6.4. SIMS oxygen isotope microanalyses of calcite cements. *6-195*

ABSTRACT

Mesozoic limestones from the eastern part of the Paris Basin display, mostly in strata rich in bioherms, abundant macro-cavities and some connected micro-fractures almost completely filled with euhedral calcite crystals (late sparite). The micro-porosity of limestones is also recrystallised into euhedral calcite cements and rarely displays the preservation of the structures typical of early marine cements. These sparitic calcites (both from cavities infillings and cements) were studied in drilled cores crosscutting the Kimmeridgian to Bathonian series with the main objective of determining the nature and flow regime of the fluids responsible for the porosity reduction in that part of the Paris Basin. The approach combined the mineralogical and geochemical study (O and C stable isotopic compositions measured by conventional and SIMS method) and the fluid inclusion data.

The $\delta^{13}C$ values of late calcite are close to those of the host limestones and correlated with the $\delta^{13}C$ changes in host rocks, indicating a proximal origin of carbon. By contrast, late calcites from geodes, fractures and also in the microporosity of limestones have $\delta^{18}O$ values around + 21‰/SMOW, values which are very distinct from those of bulk host limestones (+ 25 to + 27‰). The $\delta^{18}O$ value of the fluid is estimated to be -5.5 to -3.5 ‰ for a crystallisation temperature comprised between 32 to 42°C according to fluid inclusion data. Thus, the fluid parent of recrystallised cements, geodes and fractures infillings likely contained a component of continental derivation, contrarily to the previous belief that the reduction of porosity in those series was related to early marine diagenesis. Possible situations allowing percolation of such a low ^{18}O fluid may correspond to i) a stage of undefined age connecting the limestone aquifers to surface, and/or ii) a fluid input from deeper zones of the basin throughout the channelling regional fault systems.

The O isotopic compositions of the calcitic cements in the underlying 140 m - thick Callovo-Oxfordian argillites and those of the less recrystallised Bathonian to Kimmeridgian limestones are those expected for unmodified marine calcite: $\delta^{18}O$ = ca. +28 ‰/SMOW. Therefore, from the isotopic point of view, the Callovo-Oxfordian argillites remained essentially unaffected by the paleo-fluid circulation which is documented in the adjacent limestone series and this level acted as an efficient permeability barrier in the past.

Keywords: calcite; stable isotopes; SIMS analyses, Mesozoic limestones; calcite crystallisation; Eastern Paris basin

S.C.D. - U.H.P. NANCY 1
BIBLIOTHÈQUE DES SCIENCES
Rue du Jardin Botanique - BP 11
54601 VILLERS-LES-NANCY Cédex

6.1 Introduction

The knowledge of past hydrological systems and their evolution in time and space are of particular importance in understanding and predicting the hydrodynamic behaviour of low-permeability rocks. The role of discontinuities on fluid flow and the connection between pores and minor fractures or cavities are critical parameters to evaluate the past hydrological properties of geological formations (Blyth et al., 2000; Wallin and Peterman, 1999).

In order to prepare experiments in an underground laboratory to study the feasibility of nuclear waste disposal, the French government has selected an area characterised by a low seismicity and the presence of a clay-rich formation at accessible depth between two limestone sequences in the Eastern part of the Paris Basin (Fig. 6.1). Andra (French Agency for Nuclear Waste Management) is in charge of the site investigations and has selected a zone of study near Bure (near EST103 borehole). The target formation is a thick (130 - 145 m) sequence of detrital clay-rich rocks, Callovo-Oxfordian in age, located in between two limestone sequences: Bajocian/Bathonian age underneath the argillite formation, Oxfordian to Kimmeridgian, above it.

Andra prospecting drillings (HTM102 and EST103/106) in eastern part of Paris basin have provided the opportunity to get a cross-section within the whole series from Bathonian to Kimmeridgian sediments. The system made up of aquifers and aquitards (limestones and argillites) have never undergone a burial at more than 2 km (Cathelineau et al., 1997; Landais and Elie, 1999). The past and recent hydrological behaviour of this formation as a potential repository site for nuclear wastes is of special interest to investigate the (self)-sealing properties and the possible re-crystallisation phenomenon of limestones surrounding the argillites. Indeed, the present-day hydrological properties are in part inherited from the result of past fluid circulation, which may have considerably affected the permeability/porosity of rocks through time. The main record of these events is the presence of minerals deposited in the open spaces and the reduction of the permeability by paleo-cements. The paleo-fluid systems are therefore important to consider and this point can be addressed through the geochemical and mineralogical study of the fracture or open space infillings (pores, macro-cavities), which were cemented after sedimentation.

In this studied site, limestones display macroscopic cavities, mostly of sedimentary origin (zones of bioherm accumulation), and some geode-connected microfractures, almost completely filled with euhedral calcite crystals (late sparite). Such type of infillings is often attributed to the early marine diagenetic history without isotopic considerations. These cavities and microfractures were thus studied in comparison with host rocks using a mineralogical and a geochemical ($\delta^{18}O$ and $\delta^{13}C$) approach in order to: i) determine the nature and flow regime of the fluids responsible for the porosity reduction in that part of the Paris Basin, ii) evaluate the impact of these fluids on the argillitic formation, and iii) to discuss the possible geodynamic context in which the recrystallisation took place.

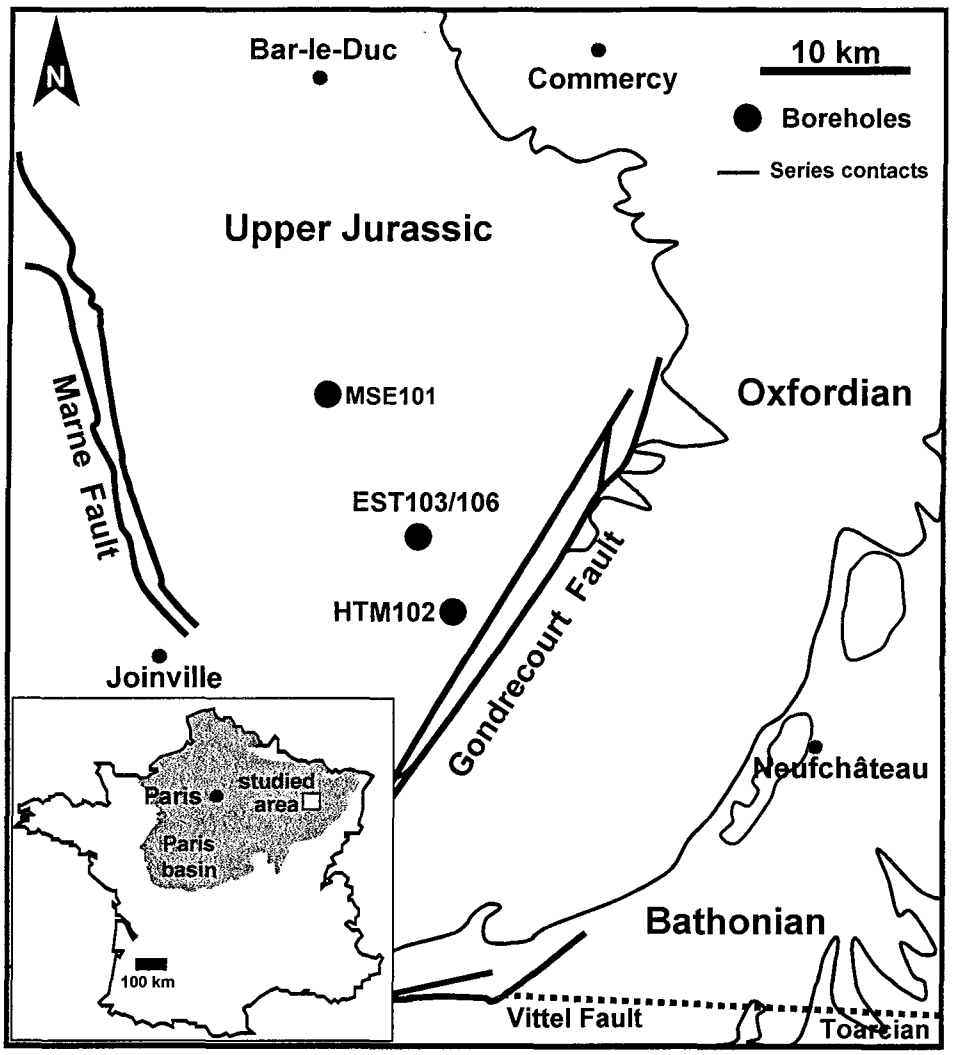

Fig. 6.1. Schematic geological map showing the regional location of the studied site and related boreholes.

6.2 Geological background of the eastern flank of the Paris Basin

The Paris Basin is a large subsiding zone initiated after the Variscan orogeny in northern Europe. Lithospheric cooling and gravitational loading mechanisms triggered the subsidence during the Permo-Trias (Pommerol, 1989). The basin is filled by a thick accumulation of Mesozoic and Cenozoic sediments and is almost devoid of tectonic activity with the exception of epirogenic movements. The eastern Paris Basin sedimentary formations slightly dip to the West, within a simple monocline related to subsidence of the central part of the Paris Basin. Except major regional fault zones, such as the Bray, Vittel and Metz faults (Lamiraux and Mascle, 1998) and the faults of Gondrecourt and of Marne which delimit the investigated area, there is little evidence of deformation in the formations.

The studied formation (cf. log of Fig. 6.4) corresponds to the transgression-regression cycle of Callovo-Portlandian (Guillocheau, 1991). The Lower Callovian, dominated by limestones, is in continuity of the Bathonian series, both corresponding to a limestone platform. Above, occurs a clay-rich formation from middle and late Callovian age. This is a detrital clay-rich rock (illite, ordered mixed-layered illite-smectite minerals dominated by illite, kaolinite, minor amounts of chlorite) cemented

by c. 25-30 wt. % of micrite. The transitional Lower Oxfordian displays a new sequence indicative of a globally high sea level. The Lower Oxfordian is also characterised by a significant change in clay mineralogy (occurring at a depth of c. 420 m in the borehole), namely the disappearance of kaolinite and chlorite and the appearance of a significant amount of disordered mixed-layered mineral (illite/smectite of R0 type with more than 60% smectite; Pellenard et al., 1999; Ruck-Mosser et al., 1999). This transition, which occurs within a few meters, corresponds to a maximal flooding surface which is marked by a shift in the nature and source of the organic matter (Landais and Elie, 1999) and of the pollen (Huault, 1994). It does not result from a temperature increase during burial. In the clay-rich formation, the carbonate cement is dominantly a micritic calcite. Scarce euhedral dolomite crystals with an ankeritic rim are also dispersed within the sediment. Re-crystallisation of bioclasts into sparitic calcite is observed. The Oxfordian consists of series of oolitic/oncholitic shelf limestones and bioherms.

6.3 Late sparite crystallisation stage

Oolitic/oncholitic shelf limestones and bioherms are characterised by a series of early cements: i) an early micro-crystalline cement (micrite) observed between the oolites; ii) a fringe of small euhedral crystals of microspar (less than 50 micrometers thickness) observed around bioclasts and oolith. These scarce cements, display similarities with those formed by marine phreatic processes (e.g., coatings of high magnesium calcite, Bricker, 1971; Milliman, 1975; Berner, 1980). Nevertheless, the major part of cement in limestones is constituted by sparitic calcite.

A series of macroscopic cavities (Fig. 6.2.A), up to a few centimetres, and fissures (Fig. 6.2.B), a few mm thick, partially to entirely filled in by carbonate are found mostly in the Oxfordian limestones, in metric-size zones rich in bioherms. Some of these cavities represent early voids usually created during sedimentation in coral reef environments. Cavities may have also been enlarged by dissolution stage(s) as shown by the replacement textures and relicts of ooliths at the margin of the cavities. All microfractures and cavities are partially to totally filled in by large crystals of calcite (late sparite type). No early cements were found in macroscopic geodes and cavities and in microfractures.

The late sparite crystals (Fig. 6.2.A-B) display similar textural features to those of the late cements observed elsewhere (younger ferroan cements, Meyers, 1991), found for instance in the Bajocian series from Burgundy (Durlet, 1996; Durlet and Loreau, 1996). However, our late sparites are rather clear and pure with very low Fe, Mg, Mn and Sr contents (Table 6.1). ICP-MS analyses (37 elements) confirm a great purity of these calcites, with a very low content in most trace elements, including REE which contents are very close to the detection limits of the method (a few ppm). They display under cathodoluminescence a dark red colour that reveals a great chemical homogeneity, and some scarce fluctuations in luminescence properties in the series of growth bands.

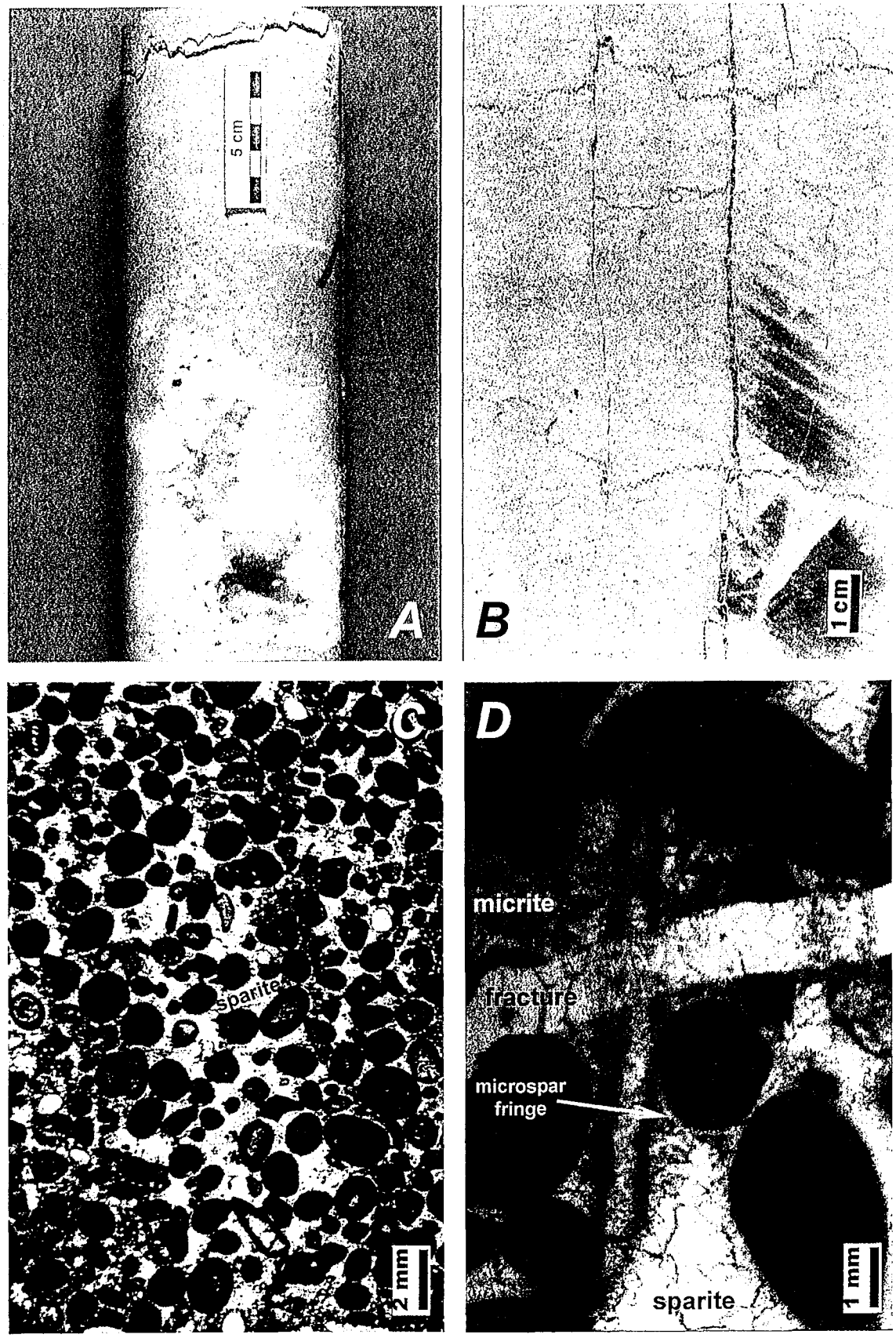
5 cm
A
B
1 cm
C
sparite
2 mm
D
micrite
fracture
microspar
fringe
sparite
1 mm

Fig. 6.2. A: macroscopic cavities partially filled by calcite (HTM102-331: 141 m). This type of voids is usually created during sedimentation in reef environment. B: small vertical tension gashes filled by calcite crosscutting or crosscut by thin sub-horizontal stylolites as an example of complex relationship between stylolites and fissures (HTM102-2523: 111 m). C. microphotographs of petrography showing the intensive recrystallisation of limestones by the new sparite (HTM102-2509: 86 m). D: Microphotographs of petrography showing the scarce case of coexistence of pellets cemented by early micrite with the new sparite often replacing the early cements in porosity (as in photograph C) and filling also the fracture (HTM102-2184: 483 m).

This late generation of calcite cement constitutes the filling of all macroscopic cavities and fills the remaining micro-porosity in limestones (Fig. 6.2.C-D). Actually, in most of the studied limestone samples, sparite partly replaces the earlier cements (micrite, or one of the earliest cement) and, in some instances, the ooliths (Fig. 6.2.C). Two types of carbonates can be thus distinguished (Fig. 6.2.D): i) the inherited part composed of ooliths, oncholiths and bioclasts, and the early cements (micrite, fringe of early calcites), and ii) the new cements (late sparite), which represent the majority of porosity cements and are easily identified by their clearness even under binocular observation, sometimes replacing the early cements (also called pseudo-sparite).

Sub-vertical tension gashes are filled with the same kind of sparite as those of geodes (Table 6.1). These microfractures, which are linked to the opening of extensional fractures, crosscut or are crosscut by sub-horizontal stylolites (Fig. 6.2.B) implicating a formation of fractures more or less associated, either with the increased overburden pressure, and/or with tectonic activities at different epochs from Jurassic, Cretaceous, Oligocene, Miocene up to the present day times (Guillocheau et al., 2000). Their orientations (N30° ± 10°E, and 140°E ± 10°) are compatible with the orientation of the major direction of stress inferred for the Oligocene extensive movements, and the Miocene to present day compressive stress linked to alpine tectonics known in the Paris basin (Guillocheau et al., 2000).

Micro-porosity (late sparite in limestones), macroporosity and fractures are connected and seem to be filled by only one type of sparitic calcite on the basis of petrographic and mineralogical similarities (Fig. 6.2).

Type of cement	n	Ca	Mg	Mn	Fe	Sr
Calcite cement in limestones						
Earliest pseudo-sparite	16	1.987	0.011	0.000	0.002	0.000
Sparite (main fillings)	93	1.979	0.018	0.000	0.002	0.001
Calcite cement in fractures and geodes						
Fracture	12	1.979	0.016	0.001	0.004	0.001
Geodes	18	1.986	0.013	0.000	0.000	0.001 (150-450 ppm)

Table 6.1. Ca, Mg, Mn, Fe and Sr contents of calcite cements. Electron microprobe analyses mean values (n= number of analyses). Sr values in brackets given for geodes have been obtained by ICP-MS (range for 5 samples).

6.4 Analytical methods

6.4.1 Fluid inclusions

The fluid inclusion (FI) study was performed on doubly polished thick sections made on the same samples (geodes, fractures and rocks) also used for isotopic studies. Microthermometric measurements were conducted on wafers using a Fluid inc. heating-freezing stage, calibrated using international standards, providing errors on measurements of ±1°C within the used range of temperature. Trapping temperatures of primary FI, which correspond to the crystallisation temperature of late sparite, are essential for the reconstitution of sparite-forming fluids.

6.4.2 Conventional C and O isotope analysis

All the calcite cements found at different depths in the macroscopic geodes and fractures within the limestones (mainly from the HTM102 borehole and a few from the EST103/106 drilling; Fig. 6.1) were systematically sampled, directly on the cores or on the polished thick sections (used for fluid inclusion studies) and analysed for stable isotopes. When the fractures were very thin (c. 1 mm thick), calcite was collected by micro-sampling using a dental drill. Additionally, bulk host limestones were sampled at the corresponding level of most studied cavities or fractures, at a distance of 5-10 cm from them. The bulk-carbonated fraction of a representative series from the Callovian to Oxfordian clay-rich sequence has also been analysed.

The sparitic calcites from fracture and geode infillings and the bulk rocks (limestones and argillites) were finely crushed. The carbonate fraction (5-10 mg) was reacted with 100% orthophosphoric acid at 25°C (McCrea, 1950) assuming $\alpha(O)$ $CO_2/CaCO_3$ (extraction) = 1.01025. Isotopic analyses were carried out on CO2 gas using a VG SIRA 10 mass spectrometer at Géosciences Rennes and expressed, using internal carbonate standards and NBS 19 reference material, with the conventional δ notation vs. SMOW (O) and PDB (C). The average precisions for C and O analysis were respectively 0.04 ‰ and 0.09 ‰ by duplicating 5 samples and the uncertainties related to the PDB and SMOW scales are estimated to be < 0.1‰ (C) and c. 0.1‰ (O).

Location and list of samples are given in Table 2 and 3. We analysed: i) 28 samples of fracture and geode calcites and 18 bulk limestones from Oxfordian and Kimmeridgian levels, ii) 5 samples of calcite fillings and 2 limestones from the Bathonian series, and iii) 9 samples of argillites.

6.4.3 Oxygen isotope microanalysis by SIMS

In situ oxygen analysis of late calcite cements in the microscopic porosity were performed by secondary ion mass spectroscopy (SIMS). This work was carried out on the CAMECA IMS1270 at CRPG, Nancy (France). Measurements were done on standard polished thin sections coated with gold by use of ≈ 0.5 nA defocused primary ion beam of Cs+ (impact energy of 10 keV) following the method of Rollion-Bard (2001) and on the basis of previous work on synthetic calcites (Reeder et al, 1997). Sub-circular ablation craters of 10-20 µm were produced by analysis. The external reproducibility estimated by different analyses on a single grain of internal standards (calcite) during a single session with the same instrumental settings is

around 0.5 ‰ for $\delta^{18}O$ measurements. Instrumental mass fractionation was corrected considering the isotopic values of the calcite standards known by conventional analysis.

6.5 Results

6.5.1 Isotopic data

The $\delta^{13}C$ and $\delta^{18}O$ results (Table 2 and 3) are presented on a binary diagram (Fig. 6.3) as well as on a logging diagram (Fig. 6.4).

- Limestones and clay-rich formation

Fig. 6.4 displays the vertical variation of $\delta^{13}C$ values in the Oxfordian limestones. Limestones from the upper part of Middle Oxfordian and the Upper Oxfordian have a $\delta^{13}C$ c. 3 ‰/PDB. In the lower part of Middle Oxfordian, limestones have a $\delta^{13}C$ around 2.5 ‰. The $\delta^{13}C$ value of the micritic cement in the clay-rich formation is variable and generally lower than that of limestones: c. 2 ‰ in the Lower Oxfordian and 1.25 ‰ in the Callovian.

Borehole	Sample	Stage/Lithology	Depth (m)	$\delta^{18}O$ (‰ SMOW)	$\delta^{13}C$ (‰ PDB)
EST106/103	133C	Lower Kimmeridgian	55 (133)	26.75	2.30
HTM 102	2502	Upper	75	27.71	3.10
-	2509	Oxfordian	86	25.95	3.02
-	0225	limestones	87	27.76	3.39
-	2522	-	111	26.32	3.02
-	2523	-	112	26.59	3.05
-	0274	-	116	28.34	3.07
-	2158	-	135	26.22	2.82
-	331	-	141	25.58	2.71
HTM102	2540	Middle	218	25.63	2.66
-	2160	Oxfordian	226	24.48	2.85
-	2164	limestones	251	25.46	3.13
-	2166	-	265	24.88	2.77
-	2171	-	289	26.91	2.10
EST 103	3200	-	315 (396)	26.32	2.24
HTM 102	2180	-	322	28.16	2.46
EST 103	3196	-	326 (407)	28.04	2.47
HTM 102	2182	-	327	28.16	2.04
HTM 102	0801	Callovo-	357	26.86	2.14
-	0854	Oxfordian	371	26.75	2.24
-	0946	argillites	392	28.17	2.04
-	1001	-	405	27.13	1.89
-	1055	-	417	26.96	2.02
-	1075	-	423	28.11	1.73
-	2156	-	439	28.26	0.56
-	1185	-	451	27.33	1.17
-	1227	-	463	26.97	1.29
HTM 102	2565	Bathonian	480	26.68	2.02
-	2186	limestones	485	26.24	1.17

Table 6.2. Depth and $\delta^{13}C$ (PDB)-$\delta^{18}O$ (SMOW) data of studied limestones and argillites in boreholes HTM102 and EST103/106.
For EST103/106, depths are corrected with respect to HTM102 on the basis of stratigraphical correlations. Values given in brackets correspond to the depth below surface.

The limestones and the cements in the clay-rich formation have $\delta^{18}O$ values (Fig. 6.3 and Fig. 6.4) ranging mostly from 26 to 28 ‰/SMOW, with a mean around 26.5 ‰. A few values around 25 ‰ were found in some Callovian limestones. Micrite in the clay-rich formation has $\delta^{18}O$ values around 27.5‰. All O isotopic compositions are lighter than those typical of marine carbonates (*c.* 29-30 ‰/SMOW).

- Calcite in geodes and fractures

Calcites from fractures and geodic cavities display a marked homogeneity in both $\delta^{13}C$ and $\delta^{18}O$ values (Fig. 6.3). The $\delta^{13}C$ values range from 2.3 to 3.1‰ and are around 1.5 ± 0.3 ‰ PDB, respectively in the Oxfordian and in the Bathonian (Fig. 6.3 and Fig. 6.4). The $\delta^{18}O$ values of geode and fracture calcites (21 ± 1 ‰/SMOW) are significantly distinct from those of host rock carbonate (26 to 28 ‰), the difference being c. 6 ‰ (Fig. 6.4), whatever the borehole, with the exception of 4 samples. One sample of geodic calcite found in the lower part of the Middle Oxfordian limestones corresponds to a well-preserved coral structure. Three other particular Bathonian calcites, located near the interface with the clay-rich formation, display $\delta^{18}O$ values similar to those of host limestones.

Borehole	Sample	Stage	Sample type	Host lithology	Depth (m)	$\delta^{18}O$ (‰ SMOW)	$\delta^{13}C$ (‰ PDB)
EST106/103	133G1	Lower	geode	micritic limestones	55 (133)	22.26	1.98
-	133G2	Kimmeridgian	geode	micritic limestones	55 (133)	21.46	2.03
HTM 102	2509	Upper	geode	bioclastic limestone	86	21.82	3.01
-	2513	Oxfordian	geode	oolitic limestone	91	20.42	2.91
-	2518	-	micro-fracture	oolitic limestone	101	20.55	2.59
-	2523	-	fracture	oolitic limestone	111	21.10	2.98
-	2158	-	geode	polyp limestone	135	20.55	2.61
-	2159	-	geode	polyp limestone	136	20.64	2.99
-	0331	-	geode	oolitic limestone	141	21.80	3.09
-	2533	-	geode	bioclastic limestone	164	20.44	2.86
-	2536	-	micro-fracture	oolitic limestone	196	20.22	3.18
HTM 102	2540	Middle	fracture	oolitic limestone	218	21.66	2.95
-	2160	Oxfordian	geode	oolitic limestone	226	21.92	2.91
-	2164	-	geode	bioclastic reef limestone	251	21.45	2.96
-	2166	-	geode	bioclastic limestone	265	21.76	2.73
-	2169	-	geode	polyp limestone	277	20.64	2.51
-	2546	-	geode	bioclastic oolitic limestone	288	20.93	2.39
-	2171	-	geode	bioclastic oolitic limestone	289	22.08	2.32
-	0607	-	geode	bioclastic oolitic limestone	289	20.98	2.51
-	2173	-	geode	boundstone	294	21.87	2.61
-	2176	-	geode	reef limestone	297	21.19	2.56
-	2178	-	geode	reef limestone	299	21.43	2.56
-	2547	-	geode	reef limestone	304	21.52	2.53
EST 103	3200	-	geode	reef limestone	315 (396)	27.68	2.32
-	3198	-	geode	reef limestone	318 (399)	21.91	2.64
HTM 102	2180	-	geode	argillaceous reef limestone	324	20.70	2.76
EST 103	3196	-	geode	argillaceous limestone	326 (407)	22.26	2.57
HTM 102	2182	-	geode	argillaceous reef limestone	327	20.79	2.62
HTM 102	2184	Bathonian	micro-fracture	oolitic limestone	483	25.60	1.76
-	2563	-	micro-fracture	oolitic limestone	484	20.42	1.56
-	2186	-	fracture	oolitic limestone	485	20.05	1.50
-	2188	-	fracture	oolitic limestone	490	25.34	1.80
-	2193	-	geode	oolitic limestone	496	25.30	1.62

Table 6.3. Depth, host rock lithology, and $\delta^{13}C$-$\delta^{18}O$ data of calcites from geodes and fractures in boreholes HTM102 and EST103/106.
For EST103/106, depths are corrected with respect to HTM102 on the basis of stratigraphical correlations. Values given in brackets correspond to the depths below surface.

Fractures and geodic calcites have $\delta^{13}C$ values nearly equal to those of the host rock carbonate. The largest difference observed between $\delta^{13}C$ from geodic calcites and their corresponding nearby limestones is less than 0.35 ‰.

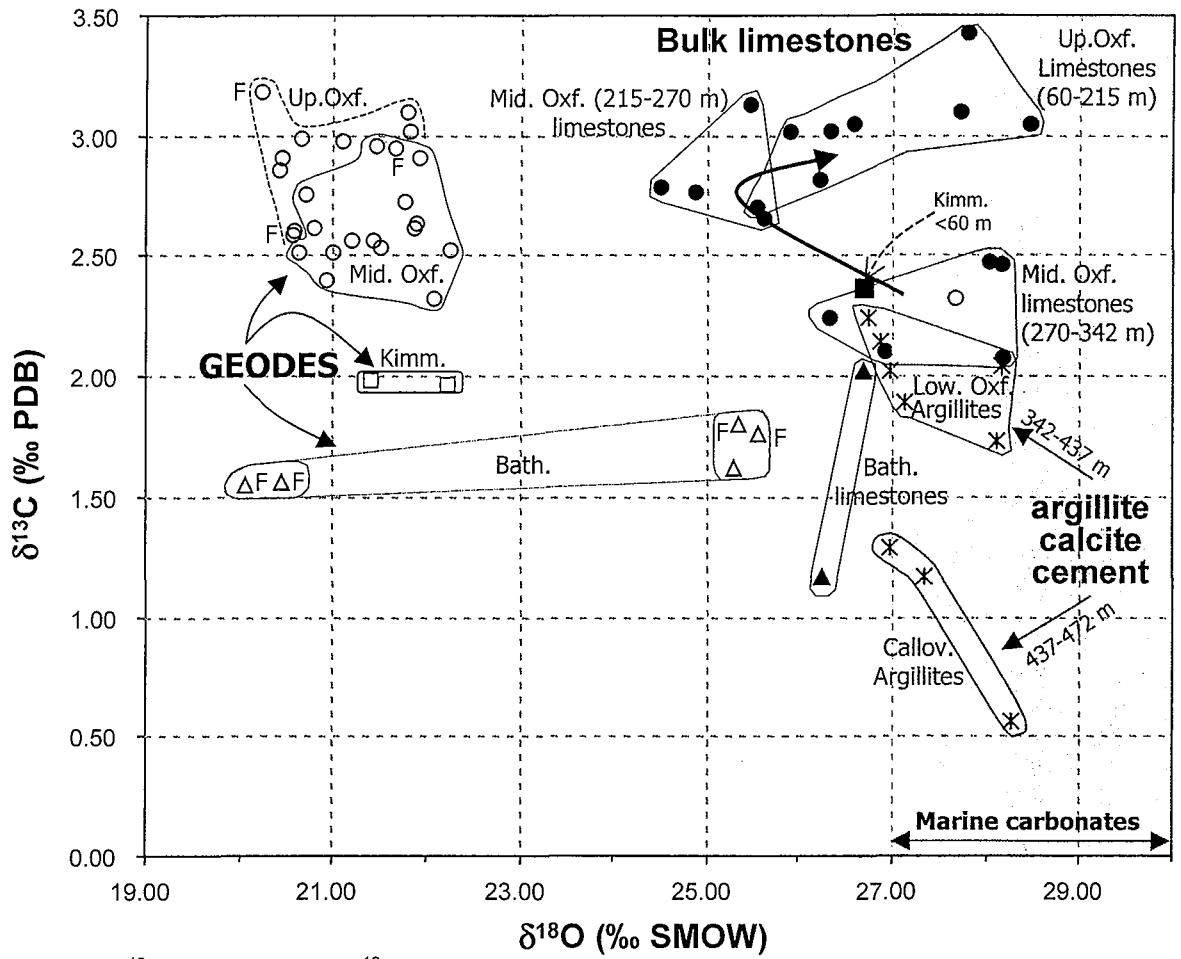

Fig. 6.3. $\delta^{13}C$ (PDB) versus $\delta^{18}O$ (SMOW) for calcite from geodes and fractures (open symbols), for whole rock samples (limestones) and for the micrite cement of the argillites with distinction of the main stratigraphic layers. Bath.: Bathonian, Call.: Callovian, Low Oxf.: lower Oxfordian, Mid. Oxf.: Middle Oxfordian, Up. Oxf.: Upper Oxfordian, Kimm.: Kimmeridgian. F refers to vertical tension gashes.

- Relationships with stratigraphy

The overall evolution of $\delta^{13}C$ with decreasing depth and age of sediments is an increase from 1 to 3‰/PDB. However, drastic changes of $\delta^{13}C$ values are found at the stratigraphic boundary between Callovian and Oxfordian in the clay-rich formation (around 440 m depth), which corresponds to a minimum sea level probably associated to a low sedimentation rate, and between the Oxfordian clay-rich rocks and the overlying limestones (340-345 m). Between 440 and 415 m, the $\delta^{13}C$ increase corresponds exactly to the sea level rise documented by Trouiller and Lebon, (1999). Because the present work was devoted to unravel the causes of porosity reduction, a detailed investigation of the "isotopic stratigraphy" within the clay-rich formation with potential information on sedimentology or global changes was not performed.

The variations of $\delta^{13}C$ values in the geodic calcites are in continuity to those of the Oxfordian limestones, which implies a rather proximal source of the geodic carbon (Fig. 6.4). This means that C was transferred from the adjacent limestone to a given cavity without isotopic fractionation. The most likely explanation for this fact is that i) the fluid filling the local medium (cavity + recharge pore space) was not a significant reservoir of externally derived carbon, ii) the effects of the isotopic fractionation related to dissolution was cancelled by a reverse one during crystallisation.

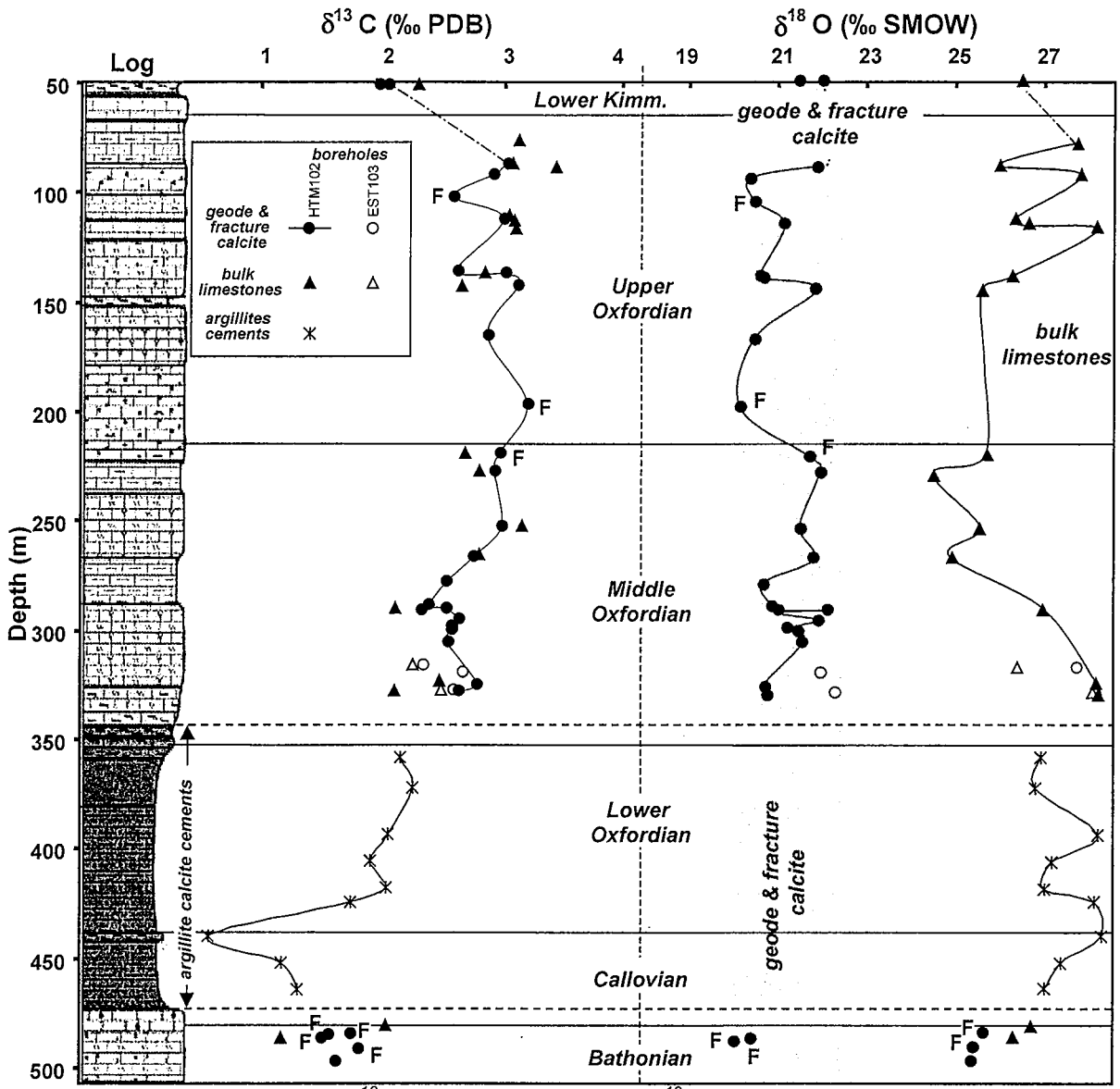

Fig. 6.4. Vertical distribution of $\delta^{13}C$ (PDB) values (A) and $\delta^{18}O$ (SMOW) values (B) for calcites from geodes and fractures (F) and bulk rocks analysis (limestones and argillites (micrite cement)) with reference to the stratigraphy (borehole HTM 102, and EST 103 after correction of depth and correlation with HTM 102 after Trouiller and Lebon, 1999).

Conversely, the decrease of $\delta^{18}O$ values (down to 25‰) observed in most limestones with respect to typical primary marine signatures (c. 28-30 ‰) may be due to a minor extent to environmental parameters in the oceanic deposition medium (temperature, isotopic composition of the ocean) and mostly to a mechanical mixing between a late

sparite component and an inherited marine carbonate component (ooliths, pellets, micritic cements...). Owing to the relatively large size of the isotopic bias, a mechanical mixing contribution of small fractures and geodes to the analysed bulk rocks is unlikely because attention was paid to that point during samples preparation.

The most likely explanation for this isotopic bias is that the low 18O carbonate component is contained in the limestone porosity itself as late sparite. The fact that petrographic and mineralogical properties of late sparite are similar in cements, geodic cavities and fractures (Table 6.1) is consistent with this explanation.

Additional support to this interpretation is furnished by the correlation between the percentage of late sparite cement in the porosity (quantitatively discriminated from early cements by using image analysis software on thin sections photographs) and the $\delta^{18}O$ values of the corresponding bulk limestones (Fig. 6.5). A shift towards low $\delta^{18}O$ values is observed for coarse-grained limestones with high percentages of late cements. Typical marine values (28-30 ‰) are preserved in the weakly cemented limestones. Thus, the whole variations of O isotopic compositions in the limestones may be explained in terms of variations in the relative proportions of early and late cements, the later having $\delta^{18}O$ values comparable to those of the sparite contained in the infillings of the macroscopic porosity (geodes and fractures). A test of that interpretation requires direct O isotopic analysis of the cements on a small scale.

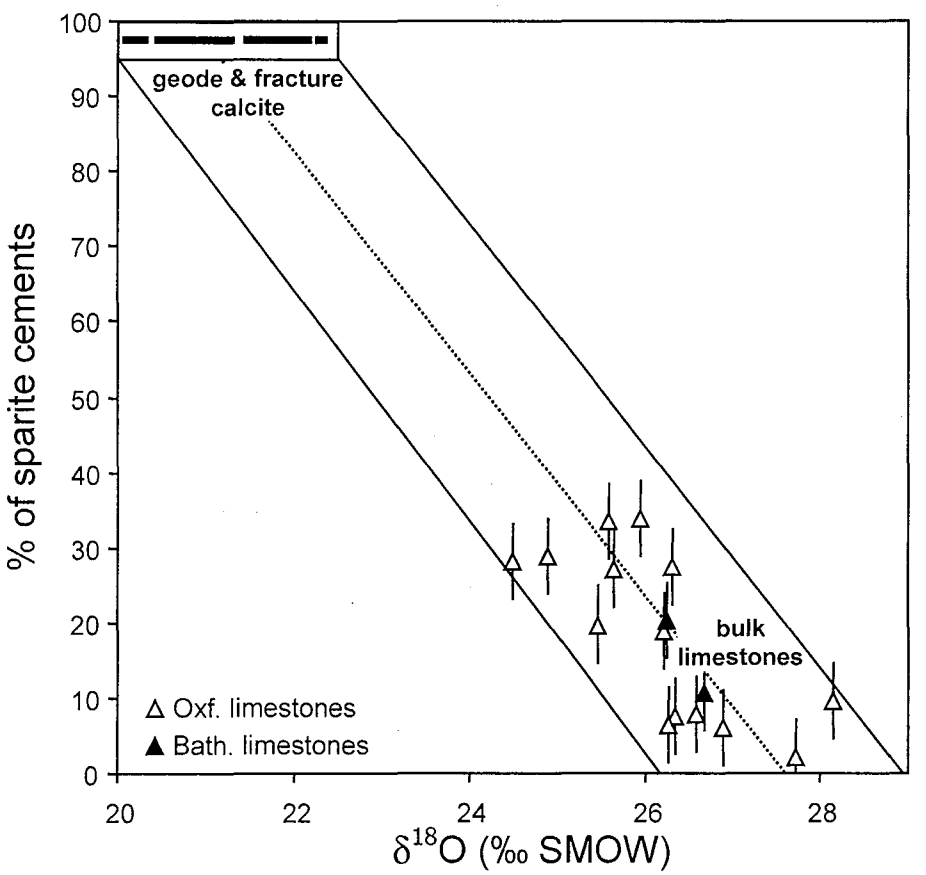

Fig. 6.5. Abundance (volume estimate by petrographic image analysis) of late sparite in limestones versus $\delta^{18}O$ (SMOW) values of the bulk rock.
The diagram shows that the shift of bulk rocks $\delta^{18}O$ values can be attributed essentially to the amount of late sparite filling the remaining porosity, or replacing the early cements, as most analytical points

distribute along the correlation line between two end-members, namely i) the early marine cements and inherited components of the sediments, and ii) the geode/ fracture sparite.

- Calcite of cements: SIMS analysis

To confirm the similarity of late sparitic cements contained both in the macroporosity infillings and in the intimate cements by means of isotopic compositions, in situ oxygen isotopic analysis (Table 6.4) were performed on sparite filling the ancient microporosity as well as on components supposed to be of marine origin in limestones (early cements, pellets and ooliths). The five samples studied are distributed either in the Oxfordian limestones or in the underlying clay-rich formation.

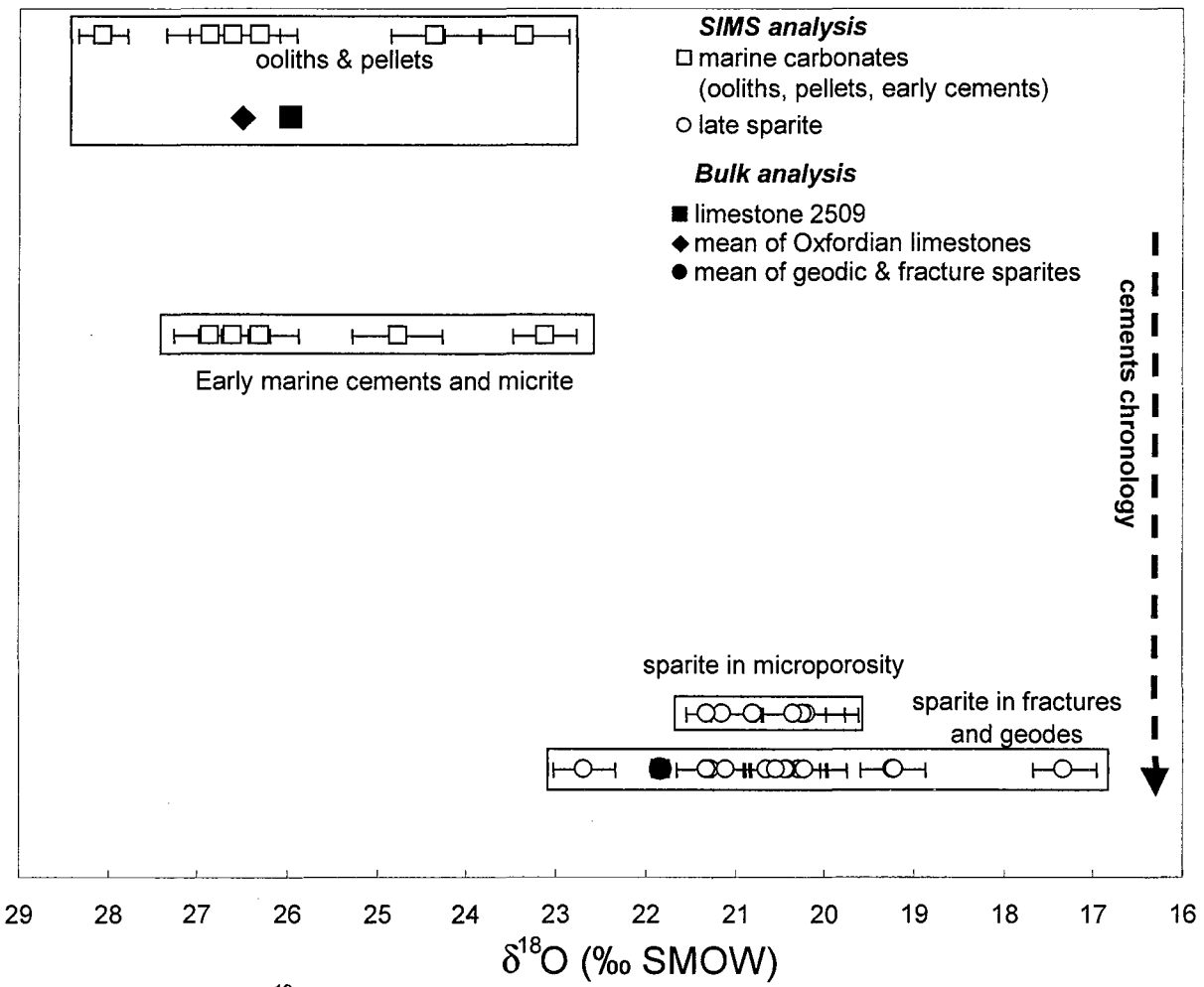

Fig. 6.6. In situ SIMS $\delta^{18}O$ analyses of the primary constituents (ooliths, pellets, early cements), and of the late sparite found in the micropores and in a geode of limestone HTM2509. Conventional analysis results are also presented for reference (black dots).

Oxfordian limestones: Sample HTM2509 located at 86 m depth is a coarse-grained limestone displaying a rather complete sequence of cements. Early marine cements, sometimes preserved from dissolution, present typical marine O isotopic signatures as the pellets and ooliths. However, sparites from intimate cements and the geodic infillings (bulk $\delta^{18}O$ value of the latter: 21.8 ‰) share similarly lower $\delta^{18}O$ values, in between 17.5 and 22 ‰ (Fig. 6.6). Thus, O isotopic ratios confirm the idea suggested

by petrographic and mineralogical data, that late sparitic cements in the limestones had a common history, whatever the type of porosity they are filling.

Sample	Host lithology	Type and localisation of analysed grain	$\delta^{18}O$ (‰ SMOW)
HTM2509/86 m microporosity	Upper Oxfordian bioclastic limestone	oolith	26.30
		-	26.59
		-	26.85
		-	28.06
		-	23.35
		-	24.34
		micrite cement	26.30
		-	26.85
		-	26.30
		-	23.11
		early marine cement	24.76
		sparite cement in microporosity	20.80
		-	20.20
		-	21.13
		-	20.23
		-	20.34
HTM2509/86 m geode		geode	17.32
		-	19.23
		-	20.29
		-	20.40
		-	20.43
		-	20.65
		-	21.27
		-	22.68
		-	21.09
		-	19.21
		-	20.54
		-	21.30
		-	20.21
HTM2526/134 m	Upper Oxfordian polyp limestone	fissure	17.46
		-	20.09
		-	16.12
		-	16.20
		-	18.66
		microgeode of calcite	20.62
HTM2536/196 m	Upper Oxfordian oolitic limestone	fissure	19.26
		-	20.80
		-	22.39
		narrow late micro-fissure (<< 1 mm)	15.66
HTM2343/356.2 m	Callovo-Oxfordian argillites	micro-fissure	22.20
		-	22.54
		-	20.88
HTM854/371 m	Callovo-Oxfordian argillites	microgeode of calcite	22.31
		recrystallised fossils	23.09
		-	23.74

Table 6.4. SIMS oxygen isotope microanalyses of calcite cements.

Calcite filling thin microcracks was analysed in other limestones situated at 135 and at 195 m depth and confirm the previous data. $\delta^{18}O$ values are ranging from 19 to 16 ‰ (Table 6.4), the lowest value being found in a late fissure crosscutting a micro-crack.

Oxfordian clay-rich formation: No macroscopic cavity filled by sparite was found in the clay-rich formation. The only objects which were identified for our purpose are i) at 356 m depth, a tiny fracture (a few tens of microns thick) not commensurate with

the possibilities of bulk analysis, which gave a $\delta^{18}O$ value of 21.8‰ by SIMS and ii) microscopic cavities filled with calcite in a second sample, with similar isotopic results (Table 4). These data imply that although the whole carbonate fraction (25 to 30 weight percent of the rocks) in the clay-rich formation remained isotopically unaffected by the late recrystallisation event, subtle footprints of that event are locally present.

6.5.2 Formation temperatures of late sparite

Interpretation of the isotopic data in terms of fluid sources requires independent temperature estimates on the conditions of sparitic calcite crystallisation. Fluid inclusions (FI) study is one of the most powerful techniques available to evaluate the thermal conditions of minerals growth or recrystallisation. Fluid inclusions observed in calcite cements from Oxfordian and Bathonian limestones are scarce, of very small size (< 10 µm) and were mostly found in calcites from geodes and fractures, sometimes in the sparitic cement. Inclusions are isolated, primary, and are thus contemporaneous to the calcite growth. They are for their most part, one-phase fluid inclusions and all aqueous as hydrocarbon FI were not detected under UV-excitation fluorescence. Because all our sparitic minerals are strongly fluorescent under Raman excitation spectroscopy, further FI investigations (salts, gas as methane or other dissolved hydrocarbon compounds) were impossible to realise.

Among the numerous thick sections studied, only 6 were found to be two-phase aqueous FI and were used to determine the salinity and the homogenisation temperature corresponding to the minimal entrapment temperature. The vapour filling percentage of inclusions is always less than 10 %. The six homogenisation temperatures (Th) range from 31° to 37.9°C and ice melting temperatures are c. -1.5°C, yielding a salinity of 2.6 % wt. eq. NaCl. Thermal pulses (successive cycles of cooling and heating) were performed on calcite crystals in order to nucleate a vapour phase in the dominant one-phase fluid inclusions. The meta-stability of the one-phase entity could not be broken down, as no nucleation of a vapour phase was obtained. Therefore, the one-phase fluid inclusions were considered to be formed under low temperatures conditions, likely lower than 45-50°C. This is in agreement with the observation of the 6 fluid inclusions homogenising at temperatures between 31 and 38°C. Considering usual geothermal gradients between 27° and 33°C/km, an hydrostatic pressure and putative surface temperatures of 10° and 20°C, the trapping temperatures for sparites in limestones are estimated to be in the range 32° to 42°C. Such temperature estimates agree with the other geothermometric data obtained on the clay-rich Callovian-Oxfordian formation, i.e.:

i) The clay mineralogy data, especially the lack of conversion of smectite into illite in I/S (Ruck-Mosser et al., 1999),

ii) The presence of specific bio-markers in the organic matter which indicate, in modelling extreme burial scenario, that the formation did not experience a temperature higher than 37°C or 48°C, if the duration of burial was 160 My or 10 My, respectively (Landais and Elie, 1999). It can be noted that the clay-rich formation occurs around 100-200 m deeper than the limestones and may have underwent

temperatures around 3-6°C higher than those recorded by fluid inclusions in the geodes from limestones assuming a mean thermal gradient of 30°C/km.

6.6 Interpretation of the fluid source

6.6.1 Isotopic signature of fluid

The isotopic composition of the fluid present during the formation of late sparite was calculated using the crystallisation temperatures estimated from fluid inclusions and the isotopic fractionation coefficients of Kim and O'Neil (1997).

Fig. 6.7 displays the spatial distribution of $\delta^{18}O$ values calculated for fluids ($\delta^{18}Of$). Estimated temperatures are 20-25°C for the formation of limestones, 32 and 42°C bracketing the growth temperature of geode calcite. Bulk rock affected by sparite recrystallisation cannot provide meaningful $\delta^{18}Of$ values but a seawater-type isotopic signature is obtained by considering bulk rock displaying less than 5% contamination by sparite. From calcite in fractures and geodes, $\delta^{18}Of$ values are calculated in the range -6.8 ‰ to -2.4 ‰ for temperatures of 32°C and 42°C, respectively. These are limit values corresponding to a fluid acting as an infinite isotopic reservoir. If that was not the case, the isotopic composition of fluid could have been lighter. Consideration of higher temperatures for the formation of sparites (for instance, 60-70°C) would yield $\delta^{18}Of$ values compatible with marine waters but such conditions are not consistent with all the thermometric data so far available in that series (bio-markers, clays, fluid inclusions).

On the basis of our estimated $\delta^{18}Of$ value, the corresponding fluids at the origin of the late calcite are not pristine marine waters. Such isotopic signatures may be those of meteoric water infiltrated from the surface, which is a widespread feature in continental rocks until those depths. This may also be achieved through mixing between marine and meteoritic water. Fluid mixing is a common process in sedimentary basins in coastal zones such as those linked to the output of large continental watersheds (Linn Ingram et al., 1996), or when the submarine groundwaters issued from the neighbouring emerged areas infiltrate shallow-seated sediments (Li et al., 1999; Moore, 1996). However, dilution of groundwater at the time of sediment deposition or during early diagenesis at shallow depth is not compatible with the present data on the temperatures recorded by fluid inclusions in geodic calcite (around 40°C) for a seawater environment and no textural data is in favour to re-equilibration of inclusion density after their formation (post-trapping changes).

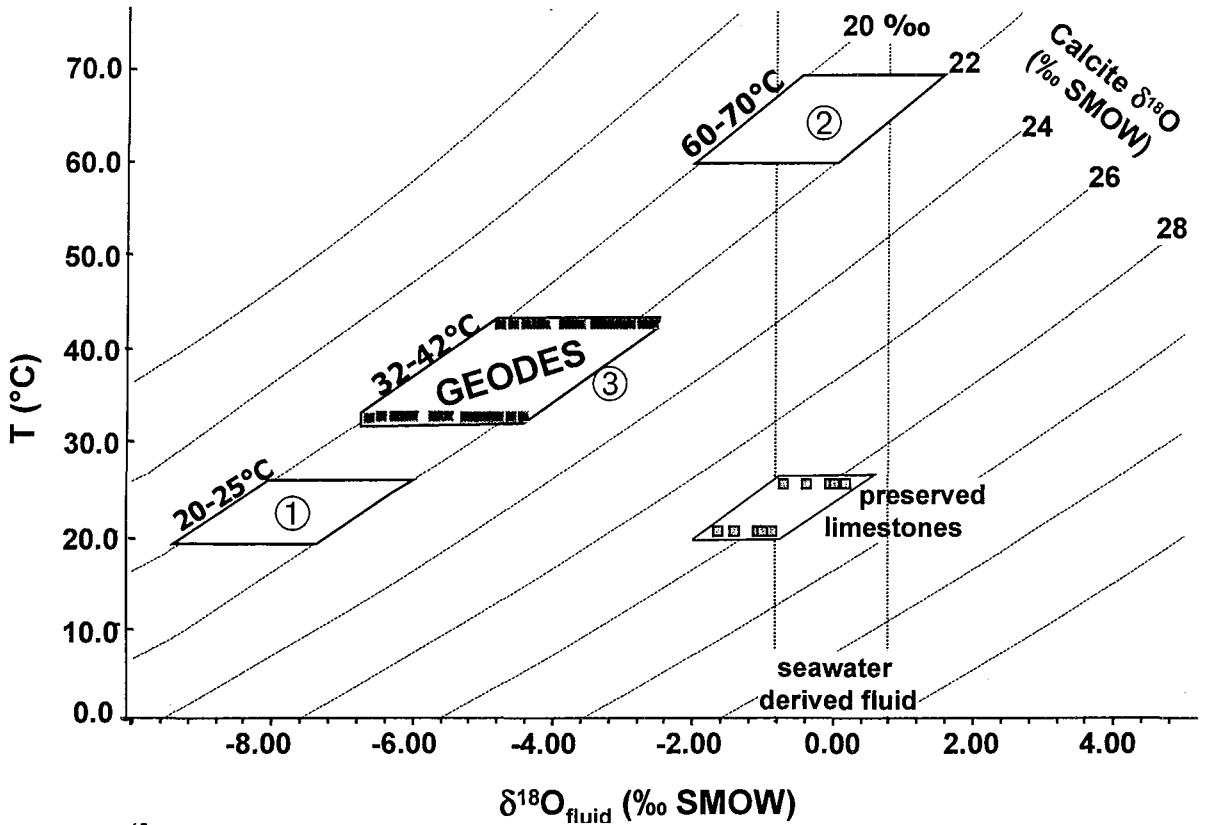

Fig. 6.7. $\delta^{18}O$ (SMOW) values of the fluid vs. temperature. Calcite/water fractionation curves are reported. The calculated fluid O isotopic compositions are presented for an assumed formation temperature of 20-25°C (marine carbonates), and for 3 ranges of hypothetical recrystallisation temperatures (sparite from geodes and fractures): ① subsurface temperature conditions, ② higher temperature (60-70°C) required to obtain a fluid of marine derivation, and ③ the most reliable estimated growth temperature (32-42°C; derived from fluid inclusion study).

6.6.2 Discussion on the possible pathways and timing of fluid circulation

At first glance, the meteoric water hypothesis is at variance with salinity data from fluid inclusions (2.6% wt. eq. NaCl). Moreover, assuming that the salinity measured in fluid inclusions is representative of a mixed (oceanic/meteoric) water medium, it implies that the isotopic composition of the groundwater should range in between -15 to -20‰, a very unrealistic composition for rainfall during Upper Jurassic/Lower Cretaceous times in that part of Western Europe. To overcome this contradiction, it is necessary to call for salt dissolution and other periods of fluids circulation. Two levels in the Paris Basin contain salts of marine derivation.

The first level is located at the bottom of the sedimentary pile (Keuper). Salted fluids of complex derivation, involving a meteoric water component mixed with a seawater or groundwater component that has dissolved Triassic halite or with brines, are well documented in the lower sections of eastern Paris Basin. They have isotopic compositions similar to those discussed in the present case (e.g., Fontes and Matray, 1993). Those fluids are found in the Keuper and Rhaetian as well as occasionally in the Dogger (Fontes and Matray, 1993; Matray et al., 1994; Demars, 1994; Worden and Matray, 1995; Worden et al., 1999). In such a case, the fluid migration responsible for calcite neoformation is globally vertical, in relation with compaction or tectonic activity. However, a few geodic cavities and fracture cements analysed in the

vicinity of the Callovo-Oxfordian clay-rich formation do not display such low 18O signatures recorded in the other samples. Nevertheless, several reasons could explain their signature. Bioclastic structures and earlier cements are best preserved in most of these particular geodic samples. Moreover, these samples are basically located near the low-permeability clay-rich layer, where no macroscopic cavities have been observed. Thus the most likely way for salted fluids of deep origin (Keuper) to reach the upper part of the series is to travel through the by-pass structures, constituted by the regional fault systems. It implies that these fluids would have probably flowed laterally outside the faults. The cause and the timing of an upward circulation are not well known. It could have occurred during the maximum of compaction in that part of the basin, which may have happened during or slightly after the Cretaceous chalk deposition in this area, which is still under debate. On the other hand, tectonic forcing of the upward fluid migration may have also occurred when the Paris Basin was experiencing extension tectonics (Cretaceous, Late Eocene - Oligocene) or compression tectonics (Paleocene – Late Eocene) or both (Neogene) (Guillocheau et al., 2000; Mégnien, 1980a; Mégnien, 1980b).

The second type of salted levels in the Paris Basin are found within the Oxfordian-Kimmeridgian limestones It consists of horizons characterised by anhydrite nodules typical of emerged supratidal zones. The paleogeographical reconstructions of the eastern Paris basin also indicate that emersion gaps exist during the Lower Cretaceous. One is known for the discovery of terrestrial faunas including a dinosaur skeleton (Iguanodon) near St Dizier, at the West of the studied zone. These formations (Purbeckian - Lower Berriasian) located at the beginning of the first emersion event contain salt deposits (Guillocheau et al., 2000). In that case, the salinity is disconnected from the isotopic composition and the meteoric fluid flow could have occurred downward, throughout the whole macro and micro-porosity.

It is worth noting here that if sparite recrystallisation took place after the maximum of burial, the temperatures estimated from fluid inclusions and from the maturation state of biomarkers imply that the present erosion level was not reached, if we accept the idea of thermal equilibrium between the fluids and the material they infiltrate. Therefore, time solutions for the circulation of the fluids should be located in between the age of the maximum burial and that corresponding to the removal of the sedimentary pile which was existing above the present-day surface, i.e., in a time period starting at the Upper Cretaceous. On the other hand, fluid circulation could have also occurred during or after the denudation stage if the recrystallisation temperatures were not those corresponding to burial in a normal temperature gradient, i.e., corresponded to a thermal crisis affecting that part of the basin. Actually, the existence of a high thermal regime in the easternmost part of the Paris Basin is possible in relation to the alkaline magmatic activity spatially associated with the Rhinegraben and crosscutting Jurassic series of its western shoulder (e.g., Maury and Varet, 1980; Keller, 1999 and references therein). Although not precisely dated yet, this magmatism is likely Cenozoic in age (ancient attempts to date altered samples of that magmatism furnished apparent Lower Paleocene to Late Oligocene ages; Lippolt et al., 1974; Illies and Fuchs, 1974; Baranyl et al, 1976).

In the present stage of knowledge, no strong argument is available to demonstrate one of the possibilities. A possible way of solving the problem would be to perform a detailed study of paleo-fluid circulation in and around the major faulted systems of that area. In any case, the net result of that fluid circulation event, of unknown age,

but necessarily younger than Kimmeridgian, was to induce a considerable reduction of the limestones porosity.

6.7 Concluding remarks

Several conclusions can be put forward from this study:

i) The $\delta^{13}C$ values of geode/fracture calcite are close to those of host limestones and vary accordingly to the $\delta^{13}C$ variations in the host rocks, indicating a proximal origin of carbon. Therefore, the main process involved in the formation of geode or fracture infillings is likely a dissolution - recrystallisation process, by fluids originally under-saturated with respect to calcite and displaying pH-pCO2 pairs distinct from those of the limestone aquifers.

ii) Geodes and fracture calcites have $\delta^{18}O$ values around + 21‰, rather distinct to those of bulk host limestones which range from + 25 to + 27‰. This light O isotopic signature is also found in the intimate sparitic cements within the limestones and is attributed to recrystallisation in the presence of a fluid of meteoric derivation ($\delta^{18}O$ = -5.5 to -3.5‰) for crystallisation temperatures, deduced from a fluid inclusion study, in between 32° and 42°C. This fluid could be ground water flowing downward during emersion periods or could be released from deeper zones of the Paris Basin through a few by-pass mechanical discontinuities (faults).

iii) The age of the process remains unknown. Nevertheless, the homogeneity of the calcite characteristics all over the studied series, their crosscutting relationships with other cements and their crystallisation temperatures confirm that the process is younger than Kimmeridgian. Several time periods could be possible for that fluid flow but we believe that the intense cementation process involving fluids containing a groundwater component should correspond to a crisis during the basin evolution. Periods of tectonic activity and of high thermal regime are favorable situations in which fluid circulation could be activated and induce cementation. The period at which the Rhine graben and the regional fault systems in the area began to develop (Oligocene) is a good candidate for the onset of fluid flow.

iv) The present day hydrological system made up of aquifers and aquitards (limestones and argillites) have never underwent a burial at more than 2 km (Cathelineau et al., 1997; Landais and Elie, 1999). Indeed, the present-day hydrological properties are in part inherited from the result of past fluid circulation, which may have considerably affected the permeability/porosity of rocks through time. The main record of these events is the presence of minerals deposited in the open spaces and the reduction of the permeability by paleo-cements. The paleo-fluid systems are therefore important to consider and this point can be addressed through the geochemical and mineralogical study of the fracture or open space infillings (pores, macro-cavities), which were cemented after sedimentation. The present study shows that the impact of a fluid circulation event is significant on limestone rocks as the initial porosity, which may have reached 30%, is now almost completely filled by the late sparite calcite. The very low permeabilities presently recognised in most of the Oxfordian to Kimmeridgian limestones during the drillings performed by Andra are likely related to this event. In marked contrast with these limestones, bulk

carbonate cements of the Callovian-Oxfordian clay-rich formation do not record the effects of that major fluid flow event although being a priori more sensitive to fluid–rock interaction because of much lower carbonate contents. This demonstrates that at the corresponding period of fluid flow, the clay-rich formation was already working as a permeability barrier even though it could have been affected locally by the cementing fluid in minute (probably transient) microfratures.

ACKNOWLEDGEMENTS

This study was supported by GdR FORPRO - Action 98-III (paper FORPRO n°2000/12 A), a National Research Program between CNRS and Andra (French Nuclear Waste Management Company). Andra is acknowledged for the facilities and permission of sampling the drill cores. Stephane Buschaert benefited of a grant from Andra for completion of his PhD.

REFERENCES

Baranyl I., Lippolt H.J., Todt W. (1976)- Kalium Argon Altersbestimmunen an tertiären vulkaniten des Oberrheingraben-Gebietes : II die Alterstraverse vom Hegau nach Lothringen. Oberrhein geol. Abh. Karsruhe, 25.

Berner R.A., 1980. Early diagenesis - a theoretical approach. Princeton Univ. Press, 237 pp.

Blyth, A., Frape, S., Blomqvist, R. and Nissinen, P., 2000. Assessing the past thermal and chemical history of fluids in crystalline rock by conbining fluid inclusion and isotopic investigations of fracture calcite. Appl. Geochem. 15, 1417-1437.

Bricker, O.P., 1971. Carbonate cements, 19. John Hopkins Univ. Studies in Geology, 376 pp.

Cathelineau, M., Ayt Ougougdal, M., Elie, M. and Ruck, R., 1997. Mise en évidence d'une diagenèse de basse température dans les séries mésozoïques du site Est: une étude des inclusions fluides, des argiles et de la matière organique, J. Scientif. Andra, Bar-le Duc.

Demars, C., 1994. Evolution diagénétique, paléofluides et paléothermicité dans les réservoirs du Keuper et du Dogger du bassin de Paris. PhD Thesis, INPL, 394 pp.

Durlet, C. and Loreau, J.P., 1996. Séquence diagénétique intrinsèque des surfaces durcies : mise en évidence de surface d'emersion et de leur ablation marine. exemple de la plate-forme bourguignonne, Bajocien (France). C. R. Acad. Sci. Paris 323(5), 389-396.

Durlet, C., 1996. Apports de la diagenèse des discontinuités à l'interprétation paléo-environnementale et séquentielle d'une plate-forme carbonatée. Exemple des "calcaires à entroques" du Seuil de Bourgogne (Aalénien-Bajocien), PhD Thesis, Univ. of Bourgogne, 444 pp.

Fontes, J.C. and Matray, J.M., 1993. Geochemistry and origin of formation brines from the Paris basin, France. 2. Saline solutions associated with oil fields. Chem. Geol. 109, 177-200.

Goldstein, R.H. and Reynolds, T.J., 1994. Systematics of fluid inclusions in diagenetic minerals. SEPM short course 31, 212 pp.

Guillocheau, F. et al., 2000. Meso-cenozoic geodynamic evolution of the Paris Basin: 3D stratigraphic constraints. Geodyn. Acta 13-4, 189-246.

Guillocheau, F., 1991. Mise en évidence de grands cycles transgression-régression d'origine tectonique dans les sédiments mésozoïques du Bassin de Paris. C. R. Acad. Sci. Paris 312, 1587-1593.

Huault, V., 1994. Recherches palynologiques dans le Dogger de la bordure Sud-Est du bassin de Paris. Palynostratigraphie, analyse de l'évolution des assemblages microfloristiques et confrontation avec les variations du niveau marin relatif, PhD Thesis, Univ. of Bourgogne, 253 pp.

Illies J.H., Fuchs K. (1974) - Approach to taphrogenesis. Proc. Int. Rift Symp. Karlsruhe 1972. Int Union Commission on Geodynamics Scientif Report n°8. Schweizerbatt ed. Stuttgart, 460p.

Keller, J., 1999. Primary magmas in the tift valley volcanism of the upper Rhinegraben province. EUG 10, J. of Conf. Abst., Cambridge Pubs. 4, 1, 322.

Kim, S.T. and O'Neil, J.R., 1997. Equilibrium and nonequilibrium oxygen isotope effects in synthetic carbonates. Geochim. Cosmochim. Acta 61; 3461-3475.

Lamiraux, C. and Mascle, A., 1998. Petroleum exploration and production in France. First break 16(4), 109-117.

Landais, P. and Elie, M., 1999. Utilisation de la géochimie organique pour la détermination du paléoenvironnement et de la paléothermicité dans le Callovo-Oxfordien du site de l'Est de la France, Actes de Journées Scientifiques CNRS/Andra, Bar-le Duc, 20 et 21 oc. 1997. EDP Sciences, Paris, pp. 35-58.

Li, L., Barry, D.A., Stagnitti, F. and Parlange, J.-Y., 1999. Submarine groundwater discharge and associated chemical input to a coastal area. Water Res. 35, 3253-3259.

Lippolt H.J., Todt W. and Horn P (1974) - Apparent Potassium-Argon Ages of lower Tertiary Rhine Graben volcanics in (Illies J.H. and Fuchs K.) Proc. Int. Rift Symp. Karlsruhe 1972. Int Union Commission on Geodynamics Scientif Report n°8. Schweizerbatt ed. Stuttgart, 460p.

Lyman, J. and Fleming, R.H., 1940. The composition of seawater. J. Marine Res. 3, 134-146.

Lynn Ingram, B., Conrad, M.E. and Ingle, J.C., 1996. Stable isotope and salinity systematics in estuarine waters and carbonates: San Francisco Bay. Geochim. Cosmochim. Acta 60(3), 455-467.

Matray, J.M., Lambert, M. and Fontes, J.C., 1994. Stable isotope conservation and origin of saline waters from the Middle Jurassic aquifer of the Paris Basin, France. Appl. Geochem. 9, 297-309.

Maury, R.C. and Varet, J., 1980. Le volcanisme tertiaire et quaternaire en France. In: Autran, A. and Dercourt, J (Eds), "Evolutions géologiques de la France", Mem. BRGM 107, pp.137-159.

McCrea, J.M., 1950. On the isotope chemistry of carbonates and a paleotemperature scale. J. Chem. Phys. 18, 849-857.

Mégnien, C., 1980a. Synthèse géologique du Bassin de Paris. Mém. BRGM 101.

Mégnien, C., 1980b. Tectogenèse du Bassin de Paris: étapes de l'évolution du bassin. Bull. Soc. Géol. Fr. 22, 669-680.

Meyers, W.J., 1991. Calcite cement stratigraphy: An Overview, In: Luminescence Microscopy: Quantitative and Qualitative Aspects. SEPM Short Course n°25, pp. 133-147.

Milliman, J.D., 1975. Recent Sedimentary Carbonates 1, Marine Carbonates. Springer-Verlag, Berlin, 375 pp.

Moore, W.S., 1996. Large groundwater inputs to coastal waters revealed by ^{226}Ra enrichments. Nature, 380: 612-614.

Pellenard, P., Deconinck, J. F., Marchand D., Thierry J., Fortwengler, D, Vigneron, G., 1999. Eustatic and volcanic influence during Middle Callovian to Middle Oxfordian clay sedimentation in the eastern part of the Paris Basin. C. R. Acad. Sci. Paris 328(12), 807-813.

Pommerol, C., 1989. L'évolution du Bassin Parisien. In: ASF (Editor), Dynamique et méthodes d'étude des bassins sédimentaires. Editions Technip, Paris, pp. 165-178.

Reeder, R.J., Valley, J.W., Grahamm, C.M., Eiler, J.M. 1997. Ion microprobe study of oxygen isotope compositions of structurally nonequivalent growth surface on synthetic calcite. Geochim. Cosmochim Acta 61(23), 5057-63.

Rollion-Bard, C. 2001. Mesures isotopiques (B, C et O) par sonde ionique sur marqueurs paléoenvironnementaux. PhD Thesis, INPL Nancy, France

Ruck-Mosser, R., Cathelineau, M., Elie, M., Landais, P., Boiron, M.C., Roubeuf, V., 1999. Pétrographie, géochimie et cristallochimie détaillée d'échantillons représentatifs des argilites de la Haute-Marne: Synthèse des données et implications géochimiques sur la diagénèse des sédiments, Rapport Andra-CREGU.

Trouiller, A. and Lebon, P., 1999. La démarche scientifique de l'Andra dans l'Est de la France., Actes de Journées Scientifiques CNRS/Andra, Bar-le Duc, 20 et 21 oc. 1997. EDP Sciences, Paris, pp. 35-58.

Wallin, B. and Peterman, Z., 1999. Calcite fracture fillings as indicators of paleohydrology at Laxemar at the Aspö Hard Rock Laboratory, southern Sweden. Appl. Geochem. 14, 953-962.

Worden, R.H. and Matray, J.-M., 1995. Cross formational flow in the Paris Basin. Basin Res. 7, 53-66.

Worden, R.H., Coleman, M.L. and Matray, J.-M., 1999. Basin scale evolution of formation waters: a diagenetic and formation water study of the Triassic Chaunoy Formation, Paris Basin. Geochim. Cosmochim Acta 63(17), 2513-28.

7 FRACTURE SEALING IN MESOZOIC LIMESTONES (EASTERN PARIS BASIN, FRANCE): CONTINENTAL WATERS DRAINAGE IN THE VICINITY OF FAULT ZONES

S. Buschaert [a], S. Fourcade [b], M. Cathelineau [a], C. Hibsch [a], G. André [a], A. Trouiller [c], R. Njitchoua [c]

[a] *CREGU - UMR G2R 7566, BP23, 54501 Vandoeuvre-lès-Nancy, France*
[b] *Géosciences Rennes - UMR 6118, Univ. Rennes 1, 35042 Rennes Cédex, France*
[c] *Andra, French Agency for Nuclear Waste Management, 92298 Châtenay-Malabry*

In preparation for Applied Geochemistry

Figure captions ***7-210***
Table captions ***7-210***
Abstract ***7-211***

7.1 INTRODUCTION ***7-213***

7.2 GEOLOGICAL BACKGROUND OF THE EASTERN FLANK OF THE PARIS BASIN ***7-213***

7.3 SAMPLE COLLECTION ***7-215***

7.4 ANALYTICAL TECHNIQUES ***7-218***

7.5 ISOTOPIC RESULTS ***7-220***
7.5.1 Calcite from tension gashes 7-220
7.5.2 Main fault zones 7-221

7.6 INTERPRETATION OF FLUID ORIGIN ***7-221***
7.6.1 Carbon source 7-221
7.6.2 Source of calcite-forming fluid 7-222

7.7 SUMMARY AND CONCLUSIONS ***7-224***
Acknowledgements ***7-226***
References ***7-227***

FIGURE CAPTIONS

Fig. 7.1. Maps of deformation field in the Eastern Part of Paris Basin from Guillocheau (2000) with study area (dashed zone). A: Late Miocene, B: Lower Oligocene. 7-215

Fig. 7.2. Map showing the location of the study area, and sampling sites with corresponding schematic orientation diagram representation of relative length roughly proportional to the abundance of main fractures and fissures in sampling site. 7-216

Fig. 7.3. Schematic stratigraphy of the studied series in the eastern part of Paris basin. 7-217

Fig. 7.4. A: small vertical fissure filled by calcite crosscuting thin subhorizontal stylolites from middle Oxfordian limestones in borehole HTM102 (2540: 218m). B: fissures (N30 strike) from N11 site (Bathonian-Bajocian limestones) filled by calcite. C-D: microphotographs thin calcite fissures crosscutting: C: mudstone (HTM102-2523: 111m) and D: oolitic limestones (HTM102-2536: 196m) cemented by pervasive calcite similar to that one of the thickest fissure (HTM102-2536: 196m). 7-219

*Fig. 7.5. $\delta^{13}C$ (PDB) versus $\delta^{18}O$ (SMOW) diagram for calcites from Eastern Paris Basin fractures. The sampling site references are written near values. Oxf.: Oxfordian, Kimm.: Kimmeridgian; Tith.: Tithonian. Small dotscorrespond to geodic calcites from Oxfordian limestones (HTM102 drillhole). *: Rocks fields are indicated using data from previous studies (Buschaert et al., 2001; Demars, 1994). 7-220*

Fig. 7.6. $\delta^{13}C$ (PDB) versus $\delta^{18}O$ (SMOW) diagram for diagenetic calcites from the Paris Basin: i) data from this study (regional and HTM102 borehole sampling: black dots), and ii) from previous studies of sparite cements from central part of Paris Basin: (1) calcite cements from lower Callovian limestones at depths ranging from 1600 to 1850 m (Demars, 1994), (2) carbonate cements from Triassic sandstones (Worden et al., 1999). 7-222

Fig. 7.7. Schematic drawing of fluid circulation along major faults and in microporosity (pores & microfractures) of the limestones. 7-224

TABLE CAPTIONS

Table 7.1. Location (sampling sites), main features (host formation, direction of fault or tension gashes), and $\delta^{13}C$-$\delta^{18}O$ data of the HTM102 fracture calcites and of the regional fracture samples. Values in brackets correspond to host limestone rock analysis. 7-217

ABSTRACT

Mesozoic limestones (Bathonian to Tithonian) from the eastern part of the Paris basin display sets of fractures and microfractures interpreted as tension gashes the geometry of which (subvertical, striking N30 to 170°E) is in agreement with regional stresses determined either for post-Cretaceous or for present day tectonics. Fractures are in general almost completely filled with euhedral calcite crystals. Along the main regional faults, calcite is also found in the fracture porosity as the main mineral sealing. The main objective of our study was to determine the regime and the source of fluids at the origin of calcite cements using stable isotopes (O, C), fluid inclusion data in the framework of the regional tectonic context of the eastern part of the Paris Basin.

Calcite from fractures have $\delta^{18}O$ values around + 20-21 ‰ SMOW which are distinct from those of bulk host limestones (+ 25 to + 27‰). The calculated fluid $\delta^{18}O$ signature ranges between -7.6 ‰ and -2 ‰ (mean values: -6 ‰ and -4 ‰) for respective crystallization temperatures of 35°C and 45°C according to the fluid inclusion data. Thus, the fluid parent of fractures infillings likely contained a component of continental derivation. The past hydraulic system, which is responsible of the cementation, was a circulation of continental water infiltrated in the basin through faults zones and travelling laterally through microfracturation sets or direct infiltration of groundwater into the macro and microporosity of limestones. The age of the process is unknown but the homogeneity of the calcite features, their crosscutting relationships with other cements (Buschaert et al., 2001) argues that the fluid circulation is younger than Tithonian. It may have occurred: i) during the Oligocene, the epoch at which the Rhine Graben began to develop as well as the probably linked local fault systems, or ii) later on, during the Tertiary (Miocene), when the Paris Basin was submitted to a significant compressive tectonic episode in which the stress state appears compatible with the observed orientation of the tension gashes. Fluids migrating through fault systems can be considered as responsible for significant permeability decreases in the Dogger/Malm limestones through the sealing of tension gashes and macroscopic cavities, combined with the final cementation of the microporosity.

Keywords: calcite; stable isotopes; cementation; Paris basin; fault; fluid; Mesozoic limestones

7.1 Introduction

Understanding the past hydrological systems and their evolution in time and space are of particular importance in predicting the hydrodynamic behavior of low-temperature and low-permeability rock systems. In fact, the present-day hydrological properties are in part inherited from past fluid circulation, which may have increased or decreased the permeability through dissolution or cementation. Moreover, critical levels acting as permeability barriers or as major drains may have controlled the past fluid flow and such features may be recurring in the present day or future hydrological behaviors of a given rock system (e.g., Blyth et al., 2000).

The most obvious record of ancient flow events is the presence of minerals deposited in the open spaces and thus, the knowledge of paleofluid systems may be obtained from the geochemical and mineralogical study of the fracture infillings, which were cemented after sedimentation. The main difficulties found in most sedimentary formations dominated by limestones and clay-rich lithologies come from the low information potential of fracture infillings: quasi-monomineralic nature (calcite), poor discrimination of the genetic conditions linked to the scarcity of fluid inclusions, lack of discriminating trace element contents. It is particularly difficult to evaluate a priori from standard macroscopic and microscopic observations the epoch and the duration of fluid migration, the evolution of the physico-chemical properties of fluids during crystallization as well as their origins. A possible way is to link field observations (especially the structural analysis of the fracturation system) to the geochemical information, which can be obtained on the fracture infillings themselves.

Accordingly, calcite infillings were sampled in fissures from a deep borehole, devoted to study the feasibility of an underground site for nuclear waste repository and located in the eastern Paris Basin as well as regionally, in major faults or in minor fractures from the neighbouring areas. The aim of the present study was to precise the origin, the geometry and the regional/vertical extension of past fluid circulations in the eastern part of the Paris Basin.

7.2 Geological background of the eastern flank of the Paris Basin

The Paris Basin is a large subsiding zone initiated after the Variscan orogeny in northern Europe. Lithospheric cooling and gravitational loading mechanisms emphasized the subsidence during the Permo-Trias (Pommerol, 1989). The basin is filled by a thick accumulation of Mesozoic and Cenozoic sediments and is slightly affected by tectonics with the exception of epirogenic movements.

During the Jurassic, a series of transgression and regression cycles are registered by the alternating series of limestones and clay-rich detrital sediments. Callovo-Portlandian series describe a first order cycle of transgression-regressions (Guillocheau, 1991). The Lower Callovian, dominated by limestones, is in continuity to underlying Bathonian series, both corresponding to a limestone platform. Above, two second order regressive/ transgressive cycles characterize the middle to the Upper Callovian sedimentation (limestones and marls) and the Lower Oxfordian series (detrital clay-rich formations). The lower part of the Middle Oxfordian is made of reef and oolitic limestones.

Regional tectonics: Eastern Paris Basin formations occur as series slightly dipping to the West forming a simple monocline due to subsidence of the central part of the Paris Basin. Major regional fault zones, such as the Bray, Vittel and Metz faults (Lamiraux and Mascle, 1998) affect the Paris Basin and the faults of Gondrecourt (N030-040) and Neufchateau (N130-140) which delimit the investigated area, are parts of that system. In the studied formations, there is little evidence of intrinsic deformation attributable to tectonic activity. The only noticeable deformation features are found in the most competent formations (limestones mainly): they are the nearly vertical calcitic veins observed in the boreholes and interpreted as tension gashes as well as some fissures and fractures generally filled by calcite on the outcrop scale. Calcitic veins from the HTM102 borehole show orientation distributions similar to those identified for the studied regional fault system (Gondrecourt graben and Neufchateau fault; Andra, 1999) and compatible with the regional stresses determined for both post-Cretaceous and present day tectonics contexts.

The extensional tectonic activity which characterized the Paris Basin during the Triassic and Jurassic progressively evolve into a compressional tectonic context in several steps (Guillocheau, 2000; Maurin and Nivière, 2000): i) a NE-SW compressional regime existed during the Lower Berriasian to Late Aptian, ii) compressional regimes prevailed also from the Late Turonian to present day (Fig. 7.1), but may be subdivided into three periods: - in the Late Cretaceous, compression directions are NE-SW; - from the Lutetian to Lower Oligocene, both N-S compression and correlated E-W extension occurred; - At last, during Miocene, compression directions are NE-SW (Burdigalian) and move into NW-SE (Late Miocene).

The studied area is located in the eastern Paris Basin, which is also the western shoulder of the Rhine Graben, initiated during the Latest Eocene (Priabonian) - Early Oligocene. Neither the exact chronology of the graben development nor the extent of its tectonic influence onto the eastern Paris Basin, and nor its relationships with the regional faults are well known. This is due to the lack of sediment conservation after the Late Jurassic. Most authors guess that the extension, which probably created NE-SW trending-type faults (e.g. the Omey-Luxemburg, Metz and Gondrecourt faults) is younger than Priabonian and probably active during Oligocene. Nevertheless, we emphasize the fact that, in the lack of firm constraints on tectonic activities during this period of time, the development of the Gondrecourt and Neufchateau fault systems remains compatible with later stress regimes such as those prevailing during the Miocene (beginning by NE-SW trending compression and ending by NW-SE trending at Late Miocene).

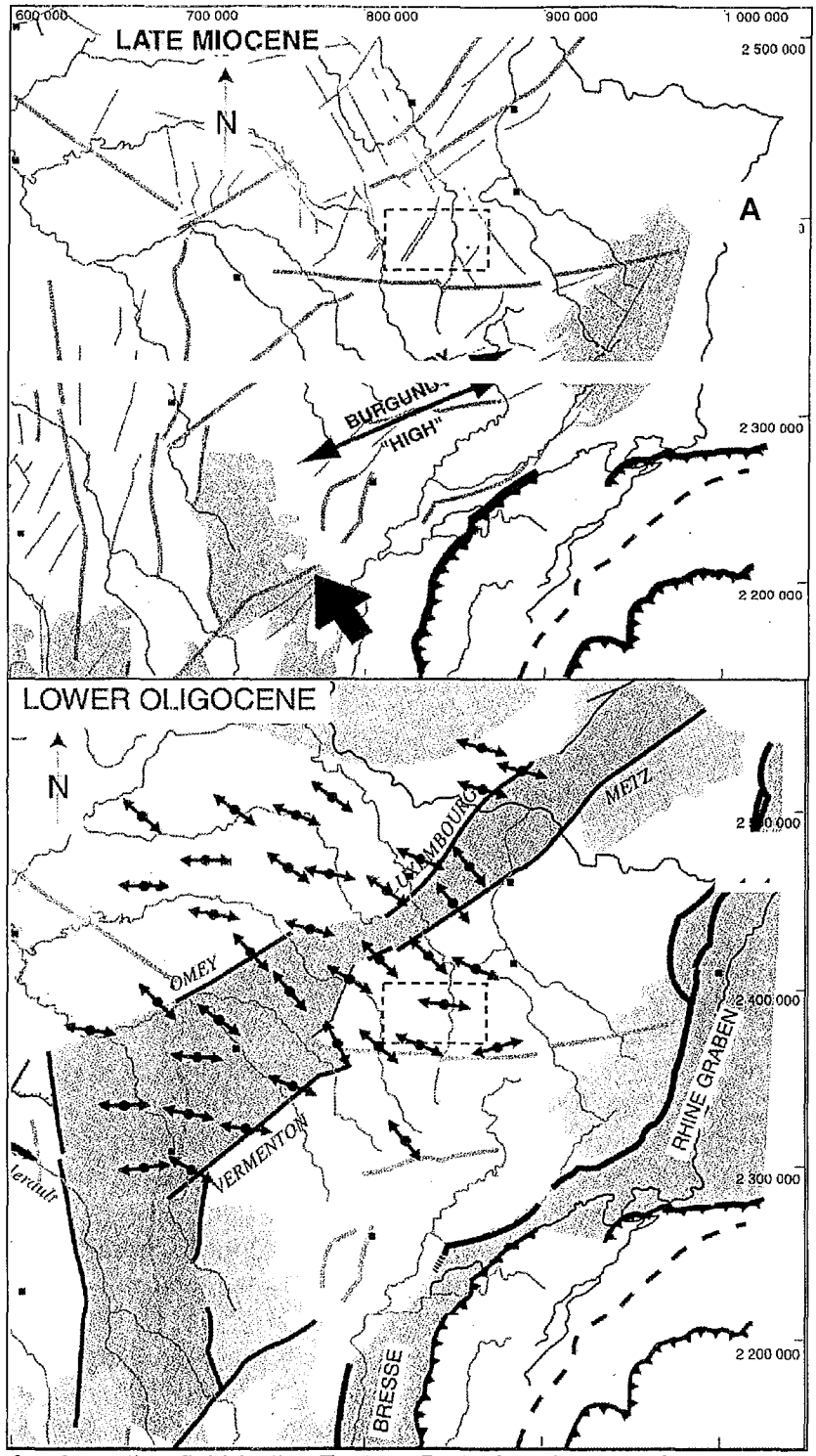

Fig. 7.1. Maps of deformation field in the Eastern Part of Paris Basin from Guillocheau (2000) with study area (dashed zone). A: Late Miocene, B: Lower Oligocene.

7.3 Sample collection

Vein calcite was sampled throughout the limestones formations outcropping between the Gondrecourt ditch and the Neufchateau fault (Fig. 7.2) in order to give a representative picture of the recrystallized material in the Bajocian/Bathonian to Kimmeridgian/Tithonian series of the area. Additionally, borehole HTM102 performed by Andra (French Nuclear Waste Management Company) provided the access to

numerous samples (calcitic veins and their host limestones) over the whole Bajocian to Kimmeridgian sequence at depths ranging from c. 100 to 485 m (Fig. 7.3). The locations and a brief description of the studied samples (host formation, orientation of fault or fractures) are given in Table 7.1 and Fig. 7.2, respectively.

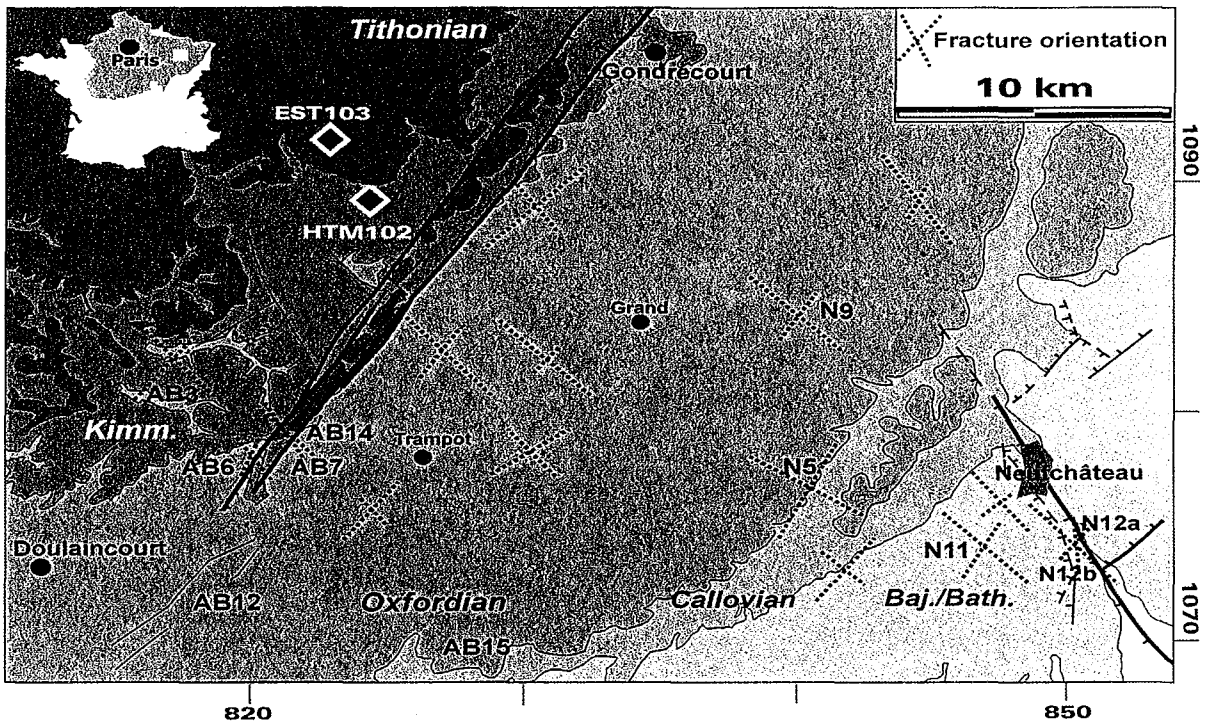

Fig. 7.2. Map showing the location of the study area, and sampling sites with corresponding schematic orientation diagram representation of relative length roughly proportional to the abundance of main fractures and fissures in sampling site.

Samples were obtained from isolated fractures or from fractures located in the vicinity of major faults. Fractures and fissures (width varying from 1mm to 1 dcm, length from a few cm to 20 cm; Fig. 7.4) similar as tension gashes are generally entirely filled with calcite cements (sparite). In the cavities of reef limestones, the sparitic calcite infillings (more or less total) present petrographic habits, mineralogical and chemical properties (limpidity, low Fe, Mg, Mn and Sr contents) similar to those of calcite found in the veins and even in the rocks microporosity from the HTM 102 borehole samples (Buschaert et al., 2001) where it partly replaces the earlier cements and, in some instances, the oolites. No cements of an earlier type or other minerals were found in the whole group of calcite infillings. The microporosity, cavities and fractures appear connected and all these features strongly suggest that the whole porosity was filled by the same generation of calcite.

Sample ref.	Host lithology	Orientation & type	$\delta^{13}C$ ‰ PDB	$\delta^{18}O$ ‰ SMOW
AB14-F	Tithonian limestones	Gondrecourt fault (N052 fracture)	1.66	21.72
AB7-F1	Kimmeridgian marls	Gondrecourt fault	2.65	21.84
AB7-F2	-	-	1.82	21.10
AB7-F3	-	-	1.11	21.54
AB7-F4	-	-	1.90	21.47
AB3-F	Upper Oxfordian limestones	fissure	2.47	22.22
N9-F	-	N030,85°W	3.08	20.63
AB12-F	-	N160	1.55	21.79
AB6 F N040	Upper Oxfordian limestones	N040 fissure near the Gondrecourt fault	1.03	22.08
AB6 F N140	-	N140 fissure -	0.68	21.76
AB6 F N170	-	N170 fissure -	0.67	21.99
HTM102-2518 (101 m)	-	micro-fissure	2.59	20.55
HTM102-2523 (111 m)	-	fracture	2.98	21.10
			*3.05**	*26.59**
HTM102-2536 (196 m)	-	micro-fissure	3.18	20.22
HTM102-2540 (218 m)	Middle Oxfordian limestones	fracture	2.95	21.66
			*2.66**	*26.63**
AB15-F	Lower Oxfordian limestones	N025 fissure	2.70	22.02
N5-F	-	N025-N030 fracture	2.85	20.84
HTM102-2563 (484 m)	Bathonian limestones	micro-fracture	1.56	20.42
HTM102-2186 (485 m)	-	fracture	1.54	20.05
			*1.17**	*26.24**
N11-F	Bath./Bajocian limestones	N030 fissure	1.22	18.51
N12b-F1	Bath./Bajocian limestones	N010, 80-85°E fault	0.99	21.39
N12b-F2	-	-	1.31	20.84
N12b-F3	-	-	1.07	20.90
N12b-F4	-	-	1.42	20.88
N12a-F1	Bath./Bajocian limestones	N032, 60° SE fault	1.05	19.31
N12a-F2	-	-	1.06	19.83
N12a-F3	-	-	1.26	19.43
N12a-F4	-	-	1.84	20.49
N12a-F5	-	-	1.02	19.89
N12a-F6	-	-	1.43	21.02

Table 7.1. Location (sampling sites), main features (host formation, direction of fault or tension gashes), and $\delta^{13}C$-$\delta^{18}O$ data of the HTM102 fracture calcites and of the regional fracture samples. Values in brackets correspond to host limestone rock analysis.

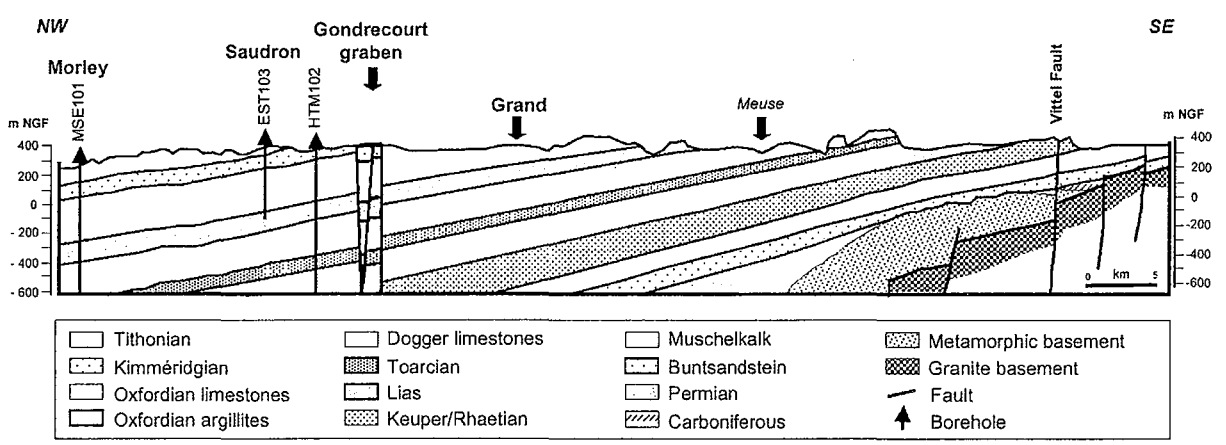

Fig. 7.3. Schematic stratigraphy of the studied series in the eastern part of Paris basin.

Sampling sites N11, N12 a and b are located in Bathonian limestones in faults adjacent to the Neufchateau major fault (Fig. 7.2). Both N12 a and N12 b faults are decimetre-wide fractures which present several distinct generations of calcite infillings numbered F1 to Fn (Table 7.1). The N12 a and N12 b faults are oriented

N032, 60° SE and N010, 80-85°E, respectively. A thin (width: 2-4 mm, Fig. 7.4.B) vertical microfissure oriented N030 was sampled at the N11 site. In the lower and upper Oxfordian limestones (N5, N9 and AB3 sites), others microfissures were found. Only one (N5) could be oriented and shows a N030, 85°W trending.

Fractures in Kimmeridgian marls and Tithonian limestones (AB7 and AB14 sites, respectively) were sampled in the Gondrecourt graben and they display orientations grossly similar to those of the graben faults. Several generations of calcite infillings were found in AB7 fractures and three of them were sampled.

HTM102 borehole fissures are a few mm-thick and sub-vertical (Fig. 7.4.B). They could be interpreted as linked to the opening of extensional fractures during burial, but could also have been created during later stresses. These fractures crosscut or are crosscut by sub-horizontal stylolites, demonstrating that the formation of fractures and their infillings are associated either with the increased overburden pressure or, later, under other stress conditions. These small fractures were systematically sampled at different depths within the limestones in drill cores from the HTM102 borehole (Table 7.1).

7.4 Analytical techniques

Calcite was hand-picked in fractures and sometimes directly sampled on the polished wafers used for fluid inclusion studies. When the fractures were very thin, especially in borehole samples (*c.* 1 mm), calcite was collected by micro-sampling using a dental drill.

Calcite from fracture infillings was finely crushed, reacted (5-10 mg) with 100% orthophosphoric acid at 25°C (McCrea, 1950) and we used $\alpha(O)$ $CO_2/CaCO_3$ (extraction) = 1.01025. Isotopic analyses were carried out on CO_2 gas using a VG SIRA 10 mass spectrometer at Géosciences Rennes and expressed, using internal carbonate standards and NBS 19 reference material, with the conventional δ notation vs. SMOW (O) and PDB (C). The mean precision was about 0.04 ‰ on replicate samples and the uncertainties related to the PDB and SMOW scales are considered to be < 0.1‰ (C) and *c.* 0.1‰ (O).

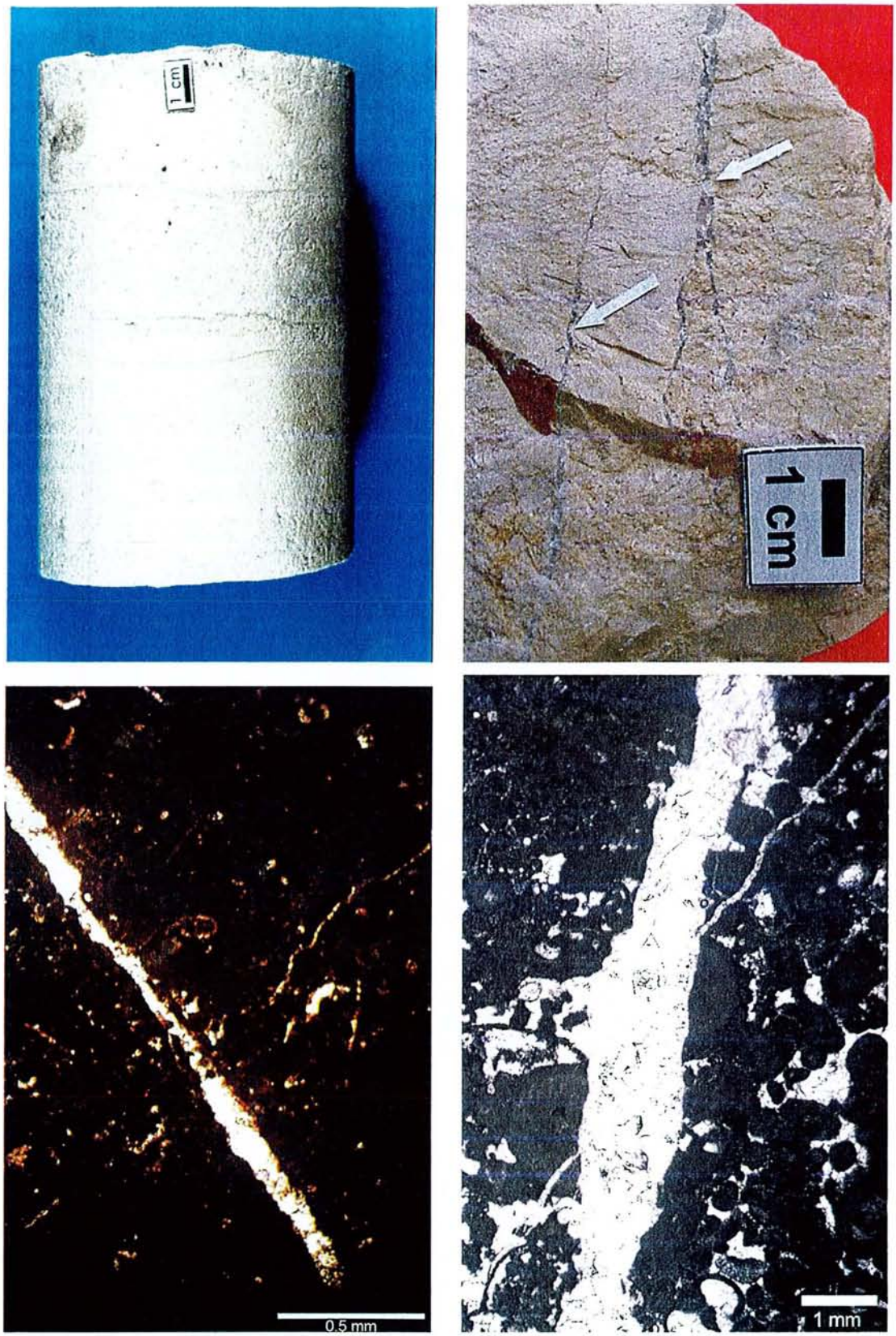

Fig. 7.4. A: small vertical fissure filled by calcite crosscuting thin subhorizontal stylolites from middle Oxfordian limestones in borehole HTM102 (2540: 218m). B: fissures (N30 strike) from N11 site (Bathonian-Bajocian limestones) filled by calcite. C-D: microphotographs thin calcite fissures crosscutting: C: mudstone (HTM102-2523: 111m) and D: oolitic limestones (HTM102-2536: 196m) cemented by pervasive calcite similar to that one of the thickest fissure (HTM102-2536: 196m).

7.5 Isotopic results

The $\delta^{13}C$ and $\delta^{18}O$ results (Table 7.1) are presented in a binary diagram (Fig. 7.5).

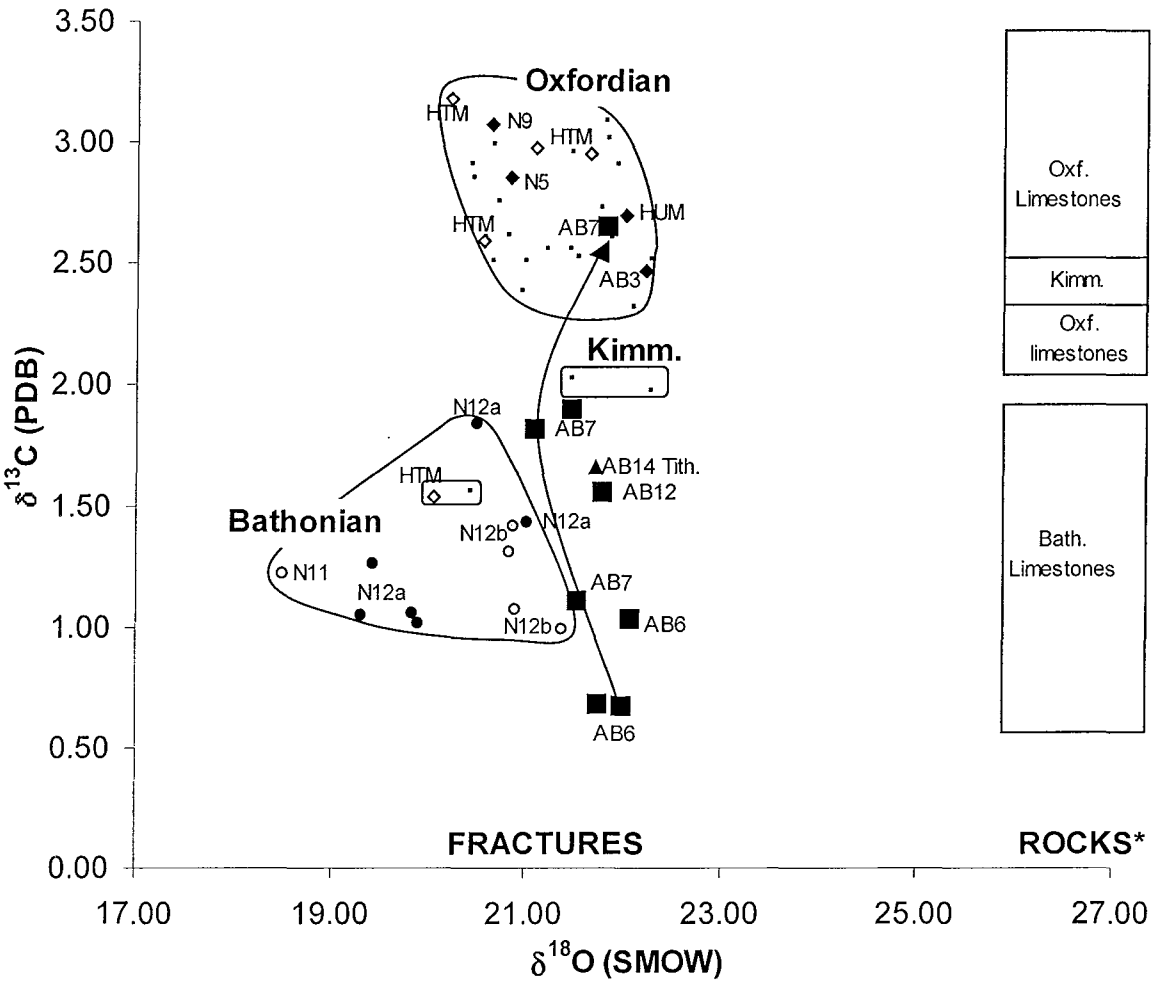

*Fig. 7.5. $\delta^{13}C$ (PDB) versus $\delta^{18}O$ (SMOW) diagram for calcites from Eastern Paris Basin fractures. The sampling site references are written near values. Oxf.: Oxfordian, Kimm.: Kimmeridgian; Tith.: Tithonian. Small dotscorrespond to geodic calcites from Oxfordian limestones (HTM102 drillhole). *: Rocks fields are indicated using data from previous studies (Buschaert et al., 2001; Demars, 1994).*

7.5.1 Calcite from tension gashes

In borehole HTM 102, calcite veins hosted by the Oxfordian and the Bathonian limestones present distinct $\delta^{13}C$ values, respectively (Fig. 7.5): in the Middle-Upper Oxfordian, $\delta^{13}C$ values range from 2.60 to 3.20 ‰, while in the Bathonian, they are 1.65 ± 0.15 ‰. These two ranges are those of the host limestones (fields indicated in Fig. 7.5, using data from previous studies (Buschaert et al., 2001; Demars, 1994; Worden et al., 1999). The situation is opposite for oxygen: $\delta^{18}O$ values are similar in the Oxfordian and the Bathonian-hosted fracture calcites (from 20.05 to 21.10 ‰, mean = 20.5 ‰), and they are distinctly different from those of the host limestones which have $\delta^{18}O$ values in between 26 and 27 ‰ (Table 7.1, values in brackets).

Thus, $\delta^{18}O$ values display a significant difference (*c.* - 6‰) between vein calcites and host rocks.

$\delta^{18}O$ values of the Oxfordian and the Bathonian regional fracture samples (Fig. 7.5) are comparable: 18.5 to 22.2 ‰ (mean= 20.7 ‰). More precisely, O isotopic signatures of fractures calcite in the Oxfordian to Tithonian range between 20.6 and 22.2 ‰ (mean: 21.4 ‰) and between 18.5 and 21.4 ‰ (mean: 20.2 ‰) in the Bathonian. These O isotopic compositions are comparable with those of the borehole fractures. Moreover, $\delta^{13}C$ values reflect those of the host lithologies (Fig. 7.5): in the Bathonian, calcites infillings and their host limestones are found around 1.5 ‰, while in the Oxfordian, both are found in the 2.5 to 3 ‰ range. As for the geodic cavities of boreholes HTM 102 and HTM 103 (Buschaert et al., 2001) we observe on a regional scale that the C isotopic composition of fracture infillings is controled by the host limestones, while their O isotopic ratios are homogeneously lighter. The observation that fractures, geodic cavities and microporosities in limestones are locally connected and share similar O isotopic compositions argues that all these calcite infillings had a common origin. It is worth noting here that calcite cavities and carbonate cements with similar oxygen isotopic signatures (19 to 22 ‰) have been found in the Dogger limestones (Fig. 7.6) occurring at greater depths in the central part of Paris Basin (Demars, 1994; Matray et al., 1994; Worden et al., 1999).

7.5.2 Main fault zones

The infillings for different strike directions of fractures from the regional Gondrecourt fault zone provide an interesting exception to the data described above. The three successive calcite generations from the same fault (AB7) which, in that sampling location, crosscuts Kimmeridgian formations, display different $\delta^{13}C$ values: 1.1, 1.82 and 2.65 ‰. This encompasses the whole range of $\delta^{13}C$ values recorded in Bathonian to Oxfordian (Kimmeridgian) series (Fig. 7.5).

7.6 Interpretation of fluid origin

7.6.1 Carbon source

As in the case of the geodic calcite in boreholes HTM 102 and EST103 (Buschaert et al., 2001) the C isotopic composition of fractures infillings is controlled by a proximal source, the host limestones. In other words, C was transferred from the adjacent limestone into fracture without isotopic fractionation. The most likely explanation requires that: i) the fluid filling the local medium (fracture, cavity and rock pore space) was not a significant reservoir of externally derived carbon and, ii) the effects of carbon isotopic fractionation related to dissolution were cancelled by a reverse one during crystallization.

The calcitic material crystallized in major faults (Gondrecourt) cannot be explained in such a way. The variations of C isotopic compositions reflect i) either isotopic fractionations during the fluid/rock interaction, or ii) different sources of carbon or iii) both. For example, fluids equilibrated with Bathonian-type and Oxfordian-type lithologies may have carried successively these two types of carbon up to the Kimmerigian-hosted fault infillings (which would imply in that case an upward fluid

migration along the fault system). In any case, these data indicate that the large fault behave in open system as concerns the C redistributed in fractures.

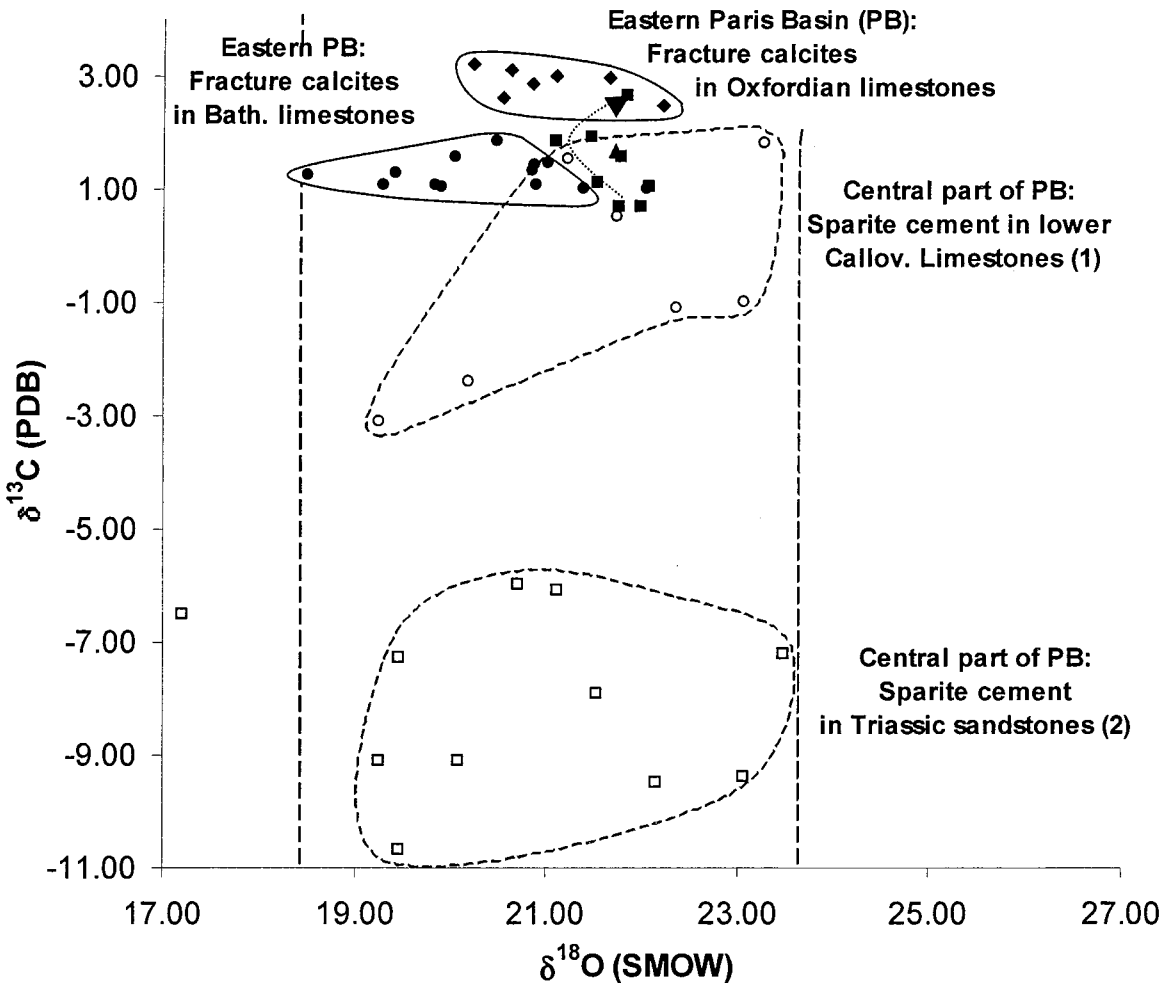

Fig. 7.6. $\delta^{13}C$ (PDB) versus $\delta^{18}O$ (SMOW) diagram for diagenetic calcites from the Paris Basin: i) data from this study (regional and HTM102 borehole sampling: black dots), and ii) from previous studies of sparite cements from central part of Paris Basin: (1) calcite cements from lower Callovian limestones at depths ranging from 1600 to 1850 m (Demars, 1994), (2) carbonate cements from Triassic sandstones (Worden et al., 1999).

7.6.2 Source of calcite-forming fluid

The homogeneity of O isotopic signatures in all the calcite infillings found from regional fault systems down to small fractures ($\delta^{18}O$ values *c.* 20-21 ‰) strongly argues for the circulation of a common type of fluid at similar temperatures throughout the area. Estimates of the temperatures prevailing during calcite crystallization is not possible using the thickness of the sediment pile because the degree of erosion is not well constrained in that area and above all, and because the infilling epoch is not determined independently. Fluid inclusions studies performed on the scarce primary fluid inclusions found in calcite from fractures in the Bathonian to Tithonian limestones (boreholes HTM 102-EST103) indicate that the fluid salinity was

rather low (2.6 % wt. eq. NaCl), that calcite crystallized at temperatures lower than 40 to 45°C (Buschaert et al., 2001), probably close to 37°C on account of the biomarkers typology in organic matter (Landais and Elie, 1999) and the clay mineralogy (Ruck-Mosser et al., 1999).

The distribution of the fluids $\delta^{18}O$ values are computed by using temperatures estimated to be 35 and 45°C for the crystallization of fracture calcite, using the isotopic fractionation coefficients of (Kim and O'Neil 1997). Fluid present during the crystallization of calcite infillings had $\delta^{18}O$ values between -7.6 ‰ and –2.5 ‰ (means –6.0 ‰ and –4.0 ‰) for respective crystallization temperatures of 35°C and 45°C. It is worth noting that these are limit values corresponding to a fluid acting as an infinite isotopic reservoir. If that was not the case, the fluid isotopic composition could have been lighter. Thus, on the basis of such isotopic estimates, those fluids were meteoric water or mixtures between marine and meteoritic waters. Mixing of diagenetic seawater with early (i.e., Cretaceous) infiltrated continental water is unlikely because the relatively high salinity (2.6% wt. eq. NaCl) found in fluid inclusion would require the continental pole to have had quite low $\delta^{18}O$ values in the -15 / -22‰ range which is incompatible with the warm Cretaceous climate. The problem is similar if we admit that the diagenetic sea-water-derived component was a brine with much higher salinities, because such brines possess positive $\delta^{18}O$ values (e.g., Sofer and Gat, 1975). Mixing with continental water during younger, cold climatic episodes is less difficult to envision but is also unlikely. Indeed, climatic conditions much colder than today and able to produce strongly ^{18}O-depleted continental water existed only since the late Pliocene/Quaternary (≤ 2.4 Ma.). By analogy with the well-known last glacial episode, such cold epochs were also presumably dry (periglacial loess deposition) with a probable presence of permafrost, conditions that are not favorable to deep fluid infiltration. Therefore, we rule out this type of explanation.

Thus we conclude that the salinity of our fluids was the result of salt dissolution. Two levels in the Paris Basin contain salts of marine derivation: the first one is located at the bottom of the sedimentary pile (Keuper). Salted fluids of complex derivation, involving a meteoric water component mixed with a seawater or a groundwater component that has dissolved Triassic halite (Keuper) are well documented in the lower sections of the Paris Basin. They have isotopic compositions similar to those discussed in the present case (e.g., Fontes and Matray, 1993). These fluids dissolving salts are also evoked in the Carnian-Rhetian level (Worden et al., 1999) in the central part of Paris basin at present day depth around 2600 m, as well as occasionally in the Dogger (Demars, 1994; Fontes and Matray, 1993; Matray et al., 1994; Worden and Matray, 1995; Bril et al., 1994). In such a case, the migration of fluids responsible for calcite crystallization is globally vertical, in relation with compaction or tectonic activity. On the other hand, the Callovo-Oxfordian argillitic layer does not show fracturation, which is consistent with the low competence and low permeability of this layer. Thus, the most likely way for salted fluids of deep origin (Keuper) to reach the upper part of the series is to travel through the by-pass structures, which are the regional fault systems. The similarity of isotope data on calcite infillings of geodic cavities and on recrystallized sparitic cements of the Oxfordian & Kimmeridgian limestones (Buschaert et al., 2001) argues that the considerable reduction of the limestones porosity was achieved by a fluid with the

same isotopic and thermal characteristics. This suggests that these fluids were laterally outpouring from the faults above the low permeability argillitic layer.

The second salted levels in the Paris Basin are located within the Oxfordian (horizons characterised by anhydrite nodules typical of emerged supratidal zones) and above the Oxfordian-Kimmeridgian limestones. Paleogeographical reconstructions of the eastern Paris Basin at different periods indicate that during the Lower Cretaceous, two sedimentation gaps related to emersion exist, one being reknown for the discovery near St Dizier, west of the studied zone, of terrestrial faunas including a dinosaur skeleton (*Iguanodon*). Formations (Purbeckian - Lower Berriasian) located at the basis of the first emersion event contain salt deposits (Guillocheau et al., 2000). In that case, the salinity is disconnected from the isotopic composition and the meteoric fluid flow occurred downward, through fractures and the whole macro and micro-porosity. Groundwater with the isotopic composition estimated above may correspond to many periods with relatively temperate climate after sediment deposition (present-day $\delta^{18}O$ values in the studied area are not precisely recorded but in the nearby area in Chalons sur Marne, surface waters have a mean $\delta^{18}O$ value of *c.* -7.3‰; (Dever et al., 1990). We favour the groundwater explanation because a preliminary D/H measurement performed directly on fluid inclusions in calcite infillings of one geodic cavity (□D = -50-60‰) is consistent, within errors, with the O isotopic composition calculated above (Buschaert and France-Lanord, work in progress). In any case, this event, of unknown age, is necessarily younger than Tithonian, and probably occurred during the Tertiary compressive period.

7.7 Summary and conclusions

All the fracture calcite sampled in the Eastern Paris Basin display similar $\delta^{18}O$ values around 20-21 ‰. The mean calculated fluids $\delta^{18}O$ signatures are in the -6‰ to -4 ‰ range for the crystallization temperatures (35°C to 45°C) inferred for that type of calcite. Early diagenesis involving seawater-derived fluids is ruled out and these infillings appears to be related to younger episodes of fluid flow involving a meteoric water component.

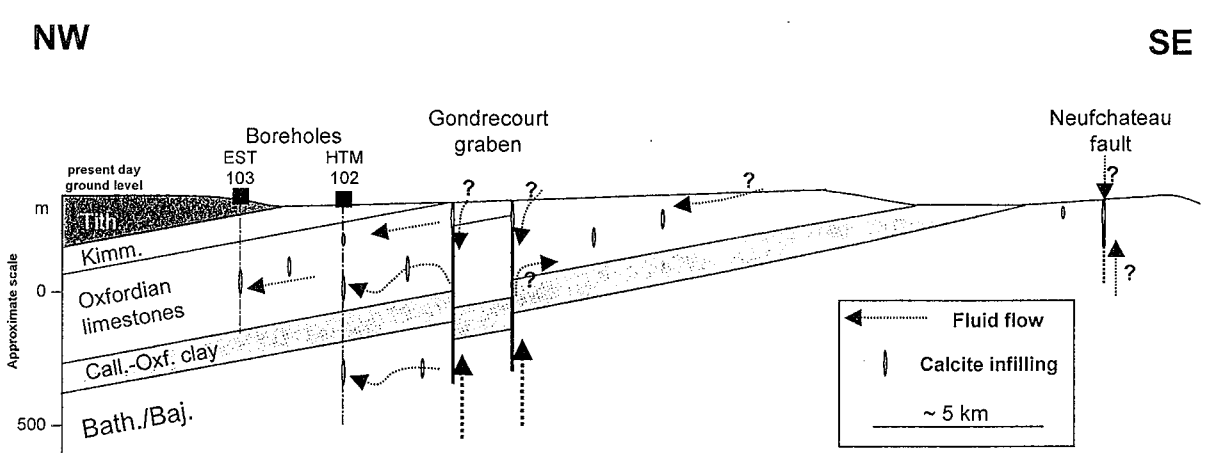

Fig. 7.7. Schematic drawing of fluid circulation along major faults and in microporosity (pores & microfractures) of the limestones.

Taking into acount the data obtained on calcite cements from limestones (especially in the Oxfordian), it appears that the fluid circulation was also pervasive and induced a considerable recrystallization of cements in the limestones. Thus, the distinct result of that fluid event was to reduce both the macro- and the microporosity of the limestone series.

In the present stage of knowledge, it is difficult to locate this fluid flow event in the geological time scale. Nevertheless, these fluid circulations were certainly tectonically controlled whatever the direction of fluid flow (either upward or downward, Fig. 7.7) and therefore, must be younger than Tithonian. The most likely periods are situated between the Oligocene and recent times, when the Paris Basin was experiencing successive compressive tectonics during the Tertiary (Guillocheau et al., 2000; Mégnien, 1980a; Mégnien, 1980b).

ACKNOWLEDGEMENTS

This study was financially supported by CNRS and Andra (French Nuclear Waste Management Company) through the GdR FORPRO - Action 98-III and corresponds to the GdR FORPRO contribution number 2001/14 A. Andra is acknowledged for the facilities and permission of sampling the drill cores. Stéphane Buschaert benefitted from a grant by Andra for completion of his PhD.

REFERENCES

Andra, 1999. Referentiel géologique du site de Meuse/Haute-Marne. Synthesis activity report. A RP ADS 99-005.

Blyth, A., Frape, S., Blomqvist, R. and Nissinen, P., 2000. Assessing the past thermal and chemical history of fluids in crystalline rock by conbining fluid inclusion and isotopic investigations of fracture calcite. Appl. Geochem., 15: 1417-1437.

Bril, H., Velde, B., Meunier, A. and Iqdari, A., 1994. Effects of the 'Pays de Bray' fault on fluid paleocirculations in the Paris Basin Dogger Reservoir, France. Geothermics, 23(3): 305-315.

Buschaert, S., Fourcade, S., Cathelineau M., Deloule E., Martineau F., Ayt Ougougdal M., Trouiller A., 2001. Widespread cementation induced by inflow of continental water in the eastern part of the Paris basin: O and C isotopic study of carbonate cements. Submitted to App. Geochem.

Demars, C., 1994. Evolution diagénétique, paléofluides et paléothermicité dans les réservoirs du Keuper et du Dogger du bassin de Paris. PhD Thesis, INPL.

Dever, L., Marlin, C. and Vachier, P., 1990. Teneurs en ^{2}H, ^{18}O, ^{3}H et en chlorures des pluies dans le Nord-Est de la France (Châlons-sur-Marne): relation avec la température et l'origine des masses d'air. Geodynamica acta, 4: 133-140.

Fontes, J.C. and Matray, J.M., 1993. Geochemistry and origin of formation brines from the Paris basin, France. 2. Saline solutions associated with oil fields. Chem. Geol., 109: 177-200.

Guillocheau, F., 1991. Mise en évidence de grands cycles transgression-régression d'origine tectonique dans les sédiments mésozoïques du Bassin de Paris. C. R. Acad. Sci. Paris, 312: 1587-1593.

Guillocheau, F. et al., 2000. Meso-cenozoic geodynamic evolution of the Paris Basin: 3D stratigraphic constraints. Geodyn. Acta, 13-4, 189-246.

Kim, S.T. and O'Neil, J.R., 1997. Equilibrium and nonequilibrium oxygen isotope effects in synthetic carbonates. Geochim. Cosmochim. Acta, 61: 3461-3475.

Lamiraux, C. and Mascle, A., 1998. Petroleum exploration and production in France. First break, 16(4): 109-117.

Landais, P. and Elie, M., 1999. Utilisation de la géochimie organique pour la détermination du paléoenvironnement et de la paléothermicité dans le Callovo-Oxfordien du site de l'Est de la France, Etude de l'Est du Bassin Parisien. Actes de Journées Scientifiques CNRS/Andra, Bar-le Duc, 20 et 21 oc. 1997. EDP Sciences, pp. 35-58.

Matray, J.M., Lambert, M. and Fontes, J.C., 1994. Stable isotope conservation and origin of saline waters from the Middle Jurassic aquifer of the Paris Basin, France. Appl. Geochem., 9: 297-309.

Maurin, J.-C. and Nivière, B., 2000. Extensional forced folding and decollement of the pre-rift series along the Rhine graben and their influence on the geometry of the syn-rift sequences. In: J.W.A. Cosgrove, M.S., eds. (Editor), Forced folds and fractures. Geol. Soc. London Spec. Pub., pp. 73-86.

McCrea, J.M., 1950. On the isotopic of carbonates and paleotemperature scale. J. Chem. Phys., 18: 849-857.

Mégnien, C., 1980a. Synthèse géologique du Bassin de Paris.Stratigraphie et Paleogeographie. 101.

Mégnien, C., 1980b. Tectogenèse du Bassin de Paris: étapes de l'évolution du bassin. Bull. Soc. Géol. Fr., 22: 669-680.

Pommerol, C., 1989. L'évolution du Bassin Parisien. In: ASF (Editor), Dynamique et méthodes d'étude des bassins sédimentaires. Editions Technip, Paris, pp. 165-178.

Ruck-Mosser, R. et al., 1999. Pétrographie, géochimie et cristallochimie détaillée d'échantillons représentatifs des argilites de la Haute-Marne : Synthèse des données et implications géochimiques sur la diagénèse des sédiments.

Sofer, Z. and Gat, J.R., 1975. The isotope composition of evaporating brines: effect of the isotopic activity ratio in saline solutions. Earth Planet. Sci. Letters, 26: 179-186.

Worden, R.H., Coleman, M.L. and Matray, J.-M., 1999. Basin scale evolution of formation waters: a diagenetic and formation water study of the Triassic Chaunoy Formation, Paris Basin. Geochim. Cosmochim Acta, 63(17): 2513-28.

Worden, R.H. and Matray, J.-M., 1995. Cross formational flow in the Paris Basin. Basin Res., 7: 53-66.

CONCLUSIONS GENERALES

CONCLUSIONS GENERALES

Les études pétrographiques, minéralogiques et isotopiques des cristallisations dans les fractures des sites Andra de la Vienne, du Gard et de l'Est du bassin de Paris permettent de proposer une histoire des circulations fluides dans des contextes géologiques variés, ayant tous en commun de présenter un système de fractures (ou de cavités) colmatées par des remplissages minéraux, le plus souvent des carbonates.

Le but était d'identifier et de comprendre les paléo -circulations et -transferts à la fois dans les milieux granitiques et les bassins sédimentaires étudiés (séries mésozoïques des bassins de Paris et du Sud-Est). La compréhension de la paléo-hydrologie d'un système géologique est une des bases essentielles à la caractérisation et à la modélisation du comportement hydrogéologique et hydrogéochimique, ancien à actuel, des formations semi-perméables à imperméables et des aquifères fracturés les encadrant.

L'évolution dans le temps et l'espace des principaux événements de percolations, et l'origine de la circulation des fluides anciens à récents peuvent être recherchées par l'étude des générations de colmatages déposés dans les fractures et cavités associées.

Les circulations fluides dans le massif granitique de la Vienne

Reconnaissance pétrographique des stades de colmatages

Trois types d'événements principaux ont été reconnus dans la Vienne, dont les deux premiers sont attribuables à deux épisodes géodynamiques majeurs :

Stade 1 : Le métamorphisme rétrograde tardi-Hercynien produit différentes générations successives de fluides associés aux flux de chaleur magmatiques. La paragenèse d'altération typique associée à ces circulations est constituée par la séquence suivante : épidote / prehnite / quartz / chlorite / hématite ± carbonates (dolomite, calcite) ± adulaire ± laumontite et par les colmatages veines à (quartz) / chlorite / phengite / muscovite / quartz / sulfures / illite. Ces fluides appartiennent aux systèmes CO_2-N_2, H_2O-CO_2, et H_2O-sels, et sont piégés dans une gamme P-T étendue : 130° à 450°C, 0,5 à 3,5 kb.

Stade 2 : Les saumures mésozoïques chaudes (environ 100-110°C, caractérisées par des salinités de plusieurs centaines de g/l) ont colmaté les fractures du socle par une association paragénétique prédominante (par rapport aux autres stades) et constante à hématite / adulaire / dolomite / quartz / fluorite / barytine ± sulfures (Cu, Zn) / calcite.

Stade 3 : Les remplissages fissuraux tardifs, peu abondants, du stade 3 sont représentés par la séquence suivante à (kaolinite) / calcite / oxy-hydroxydes de fer. Ils se sont formés à partir de fluides de basse température (<50°C), en relation avec des épisodes mineurs de circulation. Des calcites de même type ont par ailleurs été identifiées dans des géodes dans la couverture.

Historique des fluides

Pendant l'Hercynien tardi-magmatique (stade I_A), il est montré par le couplage du domaine de stabilité de l'épidote avec la barométrie de l'hornblende et les données des inclusions fluides que le refroidissement du complexe plutonique débute à environ 4 kbar. Il se poursuit durant l'uplift du massif jusqu'à des températures de 200 à 280°C et sous des pressions de 2 à 3 kbar jusqu'à l'assemblage prehnite-pumpellyite. Ensuite, les circulations hydrothermales de haute température (HT, 400-450°C) associées à l'intrusion du leucogranite induisent la formation de minéralisations de type greisen. Cependant, l'uplift se poursuivant, les greisens sont altérés en un assemblage à chlorite-phengite- dolomite associé aux circulations à des fluides de HT contenant de l'azote. Les fluides aquo-carboniques associés à ces altérations sont typiquement des eaux magmatiques et/ou métamorphiques aux températures de circulations considérées. Ils correspondent à des fluides ayant profondément interagi avec les plutonites à haute température.

Plus tardivement dans l'Hercynien (stade I_B), la diminution de la température aux environs de 150° à 250°C et de la pression à une valeur proche de 0.5 kbar, lors de l'uplift du massif, produit une nouvelle altération représentée par la paragenèse quartz / dolomite / illite / chlorite. Le fluide associé présente une composante isotopique météorique en accord avec les faibles salinités des fluides piégés dans les carbonates et les quartz. Par ailleurs, ces fluides Hercyniens ont nettement percolé les plutonites comme le montrent les valeurs isotopiques des carbonates disséminés qui présentent des $\delta^{18}O$ intermédiaires entre les carbonates de fractures du stade I_A et I_B.

La séquence paragenétique suivante (Stade II) laissée par l'événement à saumures à la fois dans le socle et dans la partie inférieure de la couverture (Infra-Toarcien) est systématiquement représentée par : hématite - adulaire/ quartz / dolomite (±fluorite ±barytine ± sulfates de Cu, Zn, Fe)/ calcite. Les analyses des fluides piégés dans les inclusions de cette paragenèse témoignent d'une saumure à H_2O-NaCl-KCl-$CaCl_2$-($MgCl_2$) de salinité de l'ordre de 16 à 23 eq. wt. % NaCl. Les fluides, qui présentent des rapports Na/K de 5 à 40, Na/Li de 20 à 350 et Cl/Br de 200 à 1000, sont donc typiques d'eaux de bassins profonds. Les températures de circulations du fluide sont autour de 90 ±25°C et les eaux ont pour composition isotopique reconstituée un $\delta^{18}O$ de 6 ± 2‰ SMOW et un δD de -30 ± 10‰. Ces fluides, ayant percolé également fortement les plutonites de manière pervasive, sont interprétés comme des saumures chaudes de type bassin sédimentaire profond, circulant à l'interface socle/couverture, et pénétrant profondément le socle. Ces saumures ont probablement été expulsées lors du maximum de subsidence du bassin Aquitain pendant l'ouverture de l'océan Atlantique et du golfe de Gascogne. Cependant, les distances de migration de ces fluides sont encore mal contraintes.

Les fluides plus tardifs du stade III sont des fluides de basse température (T<50-55°C), d'âge compris post-Toarcien, présentant une signature marine à diagenétique. Les calcites déposées sont trouvées à la fois dans le socle et dans la couverture calcaire. Par contre, les valeurs en carbone sont nettement influencées par l'encaissant immédiat. (*voir source du carbone ci-dessous).*

Problème de l'âge des circulations

L'âge des circulations est le problème majeur pour contraindre dans le temps les paléo- circulations. Les carbonates étant difficilement datables (faible concentration en U), nous avons donc focalisé notre étude sur les fractures argileuses (ou gouges). Celles ci se sont créées très précocement dans l'histoire du massif et sont toujours actuellement le lieu de circulations fluides. L'objectif était de tester sur les phyllosilicates, probablement Hercyniens, l'influence des circulations ultérieures. Les argiles échantillonnées ont été séparées en différentes sous-fractions, puis analysées en ^{18}O et datées en K/Ar. Les argiles des gouges sont essentiellement dominées par la présence d'illite et d'interstratifiés à prépondérance illitique. Les argiles analysées globalement (<2 μm) et les sous-fractions granulométriques réalisées entre 0 et 2 μm présentent des $\delta^{18}O$ compris entre 8 et 18‰ SMOW corrélés respectivement avec les âges K/Ar qui vont de 290 à 188 ± 5 Ma. On observe ainsi un rééquilibrage des fractions fines (<0.2 μm) des argiles lors d'un événement de circulation d'âge inférieur à 188 Ma. La partie néorfomée cristallise à partir d'un fluide recalculé ayant pour $\delta^{18}O$ une valeur de l'ordre de 5 ± 2 ‰ SMOW, donnée en accord avec celles obtenues sur les autres remplissages (carbonates et quartz) de cette même génération. Cependant, cet âge n'est certainement pas le pôle représentant strictement l'enregistrement des circulations mésozoïques, car cette fraction est aussi en partie un mélange entre argiles hercyniennes et mésozoïques. L'événement mésozoïque majeur, interprété comme lié aux épisodes distensifs associés au rifting de l'océan Atlantique et/ou du golfe de Gascogne, est estimé avoir eu lieu dans la période 190 – 110 Ma avec deux périodes généralement invoquées autour de 180 Ma et 115 Ma (rifting de l'Atlantique puis du Golfe de Gascogne ; Brunet, 1983 ; Curnelle et Dubois, 1986). Ces âges sont aussi identifiés sur minéralisation uranifère (Lancelot et Vella, 1989 ; Le Guen et al., 1991).

Source du carbone

Les valeurs en carbone mesurées pour les différentes générations de carbonates de la Vienne sont très similaires au cours du temps. Ce stock carbone a été introduit précocement lors du métamorphisme précoce rétrograde Hercynien. Cette valeur particulière du $\delta^{13}C$ entre -9 et -11‰ pourrait correspondre à un mélange entre une source crustale locale et une source externe de carbone réduit et sédimentaire amenée par des fluides de surface s'équilibrant avec les plutonites. Malgré l'existence de fluides successifs de signature très différente en oxygène, le carbone est systématiquement remobilisé et réutilisé dans les carbonates successifs de l'Hercynien tardif, des saumures Mésozoïques. Une seule disparité est à signaler pour les calcites tardives du stade III situées peu profondément sous l'interface du socle. Celles-ci présentent des valeurs intermédiaires, car elles sont influencées à la fois par le carbone des calcaires de la couverture et le stock carbone du socle. Par contre, les calcites 'III' plus profondes ont utilisé le stock carbone du socle.

Perspectives

Il serait intéressant de contraindre à l'échelle de l'Ouest de la Chaine Varisque en France les percolations de saumures mésozoïques afin de préciser l'extension latérale et verticale des percolations et les distances de migration de ces fluides. Les percolations ont lieu à l'interface socle-couverture liasique, et cela quel que soit la nature des fluides invoqués (eaux de mer ou de bassin, saumures interagissant avec les horizons inférieurs des séries du Lias ou du Trias). En effet, sur le massif central et sur la Bretagne se pose toujours le problème de l'extension réelle des transgressions mésozoïques.

Enfin, il reste à étudier le rôle du matériel de fracture ancien sur les caractéristiques chimiques des eaux actuelles, notamment l'origine des eaux salines.

Les circulations fluides dans les ensembles sédimentaires du Gard et de l'Est

Reconnaissance pétrographique des stades de colmatages

Dans le Gard, la cimentation précoce des roches a induit une forte diminution de la perméabilité, ce qui a favorisé la formation de fissures dans ces niveaux compétents. L'analyse de la séquence diagenétique a permis de mettre en évidence les stades suivants de cimentation des lits gréseux :

i) formation de grains de glauconite soit en néoformation, soit en épigénie (pellets fécales, épigénie de minéraux ferro-magnésiens comme des chlorites ou des biotites), probablement très précoces car entièrement cimentés par les stades suivants,

ii) néoformation de cristaux automorphes de calcite (I) englobant les grains de quartz détritiques dans les lits gréseux, puis de cristaux automorphes de dolomite, notamment à l'interface entre les lits silteux et gréseux, stade suivi d'une cristallisation épitaxique d'une frange d'ankérite sur la dolomite. La sidérite est rencontrée exceptionnellement dans certaines fissures; les bioclastes sont épigénisés en calcite II. Des interstratifiés illite/smectite sont observés en intime association avec la calcite II, en remplissage des loges de foraminifères ou de gastéropodes et sont interprétés comme néoformés à ce stade.

iii) formation d'un ciment de calcite III xénomorphe remplissant toute la porosité résiduelle de la roche, ceci expliquant la très faible perméabilité des siltites.

Les échantillons de la couche silteuse sont constitués par des alternances de lits argileux (siltite gréseuse) constitués de minéraux détritiques phyllosilicatés et de lits grèseux à ciment carbonaté riches en bioclastes. Les siltites sont également cimentées, à un moindre degré que les grès, par de la calcite.

La cimentation précoce a favorisé la fissuration des niveaux compétents lors de l'enfouissement et lors des phases tectoniques pyrénéennes (Eocène) et Oligocène.

Ces fractures ont alors été colmatées par des phénomènes plus syn à post Oligocène, amenant à la très faible perméabilité actuelle du site.

Dans l'Est, bien que des ciments précoces aient été conservés par endroit, notamment dans les niveaux de type mudstone, les calcaires Oxfordiens ont été fortement recristallisé par une calcite sparitique étudié par analyses isotopiques ponctuelles en oxygène. Ces sparites sont également retrouvées dans les fractures et les géodes. Bien qu'elles montrent des similitudes pétrographiques et minéralogiques, leur comparaison isotopique était essentielle.

Caractéristiques des fluides

Dans le Gard, dans l'intervalle Aptien-Albien, les calcites des fractures montrent des $\delta^{18}O$ très variables allant de 17 à 27 ‰ SMOW (Fig. 8.1), ce qui correspond également aux valeurs globales des ciments analysés dans les roches adjacentes (18 à 29 ‰). Dans les formations sous jacentes, les calcaires montrent des valeurs marines ($\delta^{18}O$ de 25.5 à 29 ‰), alors que les calcites de fractures présentent des $\delta^{18}O$ inférieurs à 21 ‰.

La cimentation de la porosité apparaît comme relativement précoce sous l'effet de fluides diagénétiques, sous des conditions de diagenèse très modérée (température faible < 50°C), ce qui explique la préservation des argiles néoformées (I/S riches en smectite) et des matières organiques (totale immaturité thermique attestée par l'étude des biomarqueurs, Fleck, 2000).

Le colmatage des fractures créées lors des phases tectoniques plus tardives a lieu en fonction des niveaux lithologiques, soit en système clos avec redistribution locale de matière, l'identité en C étant conservée entre les calcites de fracture et l'encaissant (carbonates diagénétiques précoces de la porosité) suivant le niveau stratigraphique, soit en système plus ouvert avec introduction de C et O par des sources externes (Fig. 8.1 et 8.2). En effet, la participation d'eaux météoriques mélangées aux eaux d'origine marine dans le colmatage des fissures ou des macropores des sédiments est cependant suspectée pour certaines fractures du Gard, notamment dans les niveaux aquifères calcaires et gréseux. Ces processus tardifs ont globalement contribué aux faibles perméabilités actuelles du site par le colmatage du réseau de fractures.

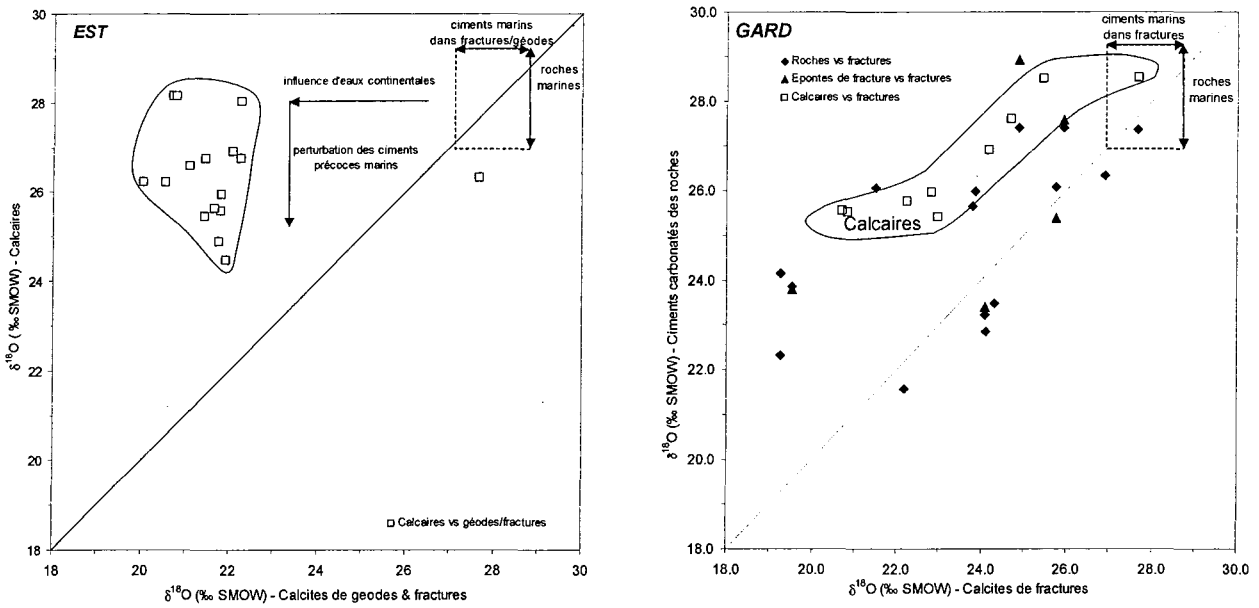

Fig. 8.1. $\delta^{18}O$ (SMOW) des roches encaissantes en fonction du $\delta^{18}O$ (SMOW)des calcites de fractures (et geode) pour les sites de l'Est et du Gard.

Les figures 8.1 et 8.2 illustrent les variations de compositions isotopiques des roches encaissantes en fonction de celles des calcites tardives de fractures et/ou géodes. i) Les droites de pentes 1 représentent les paires roches/(fractures-géodes) montrant des signatures équivalentes en C ou en O. ii) Le découplage des calcites tardives par rapport aux roches apparaît selon une direction horizontale si la roche conserve sa signature marine initiale. iii) Par contre, l'influence des ciments calcitiques tardifs sur les caractéristiques des roches sera représentée par une tendance verticale.

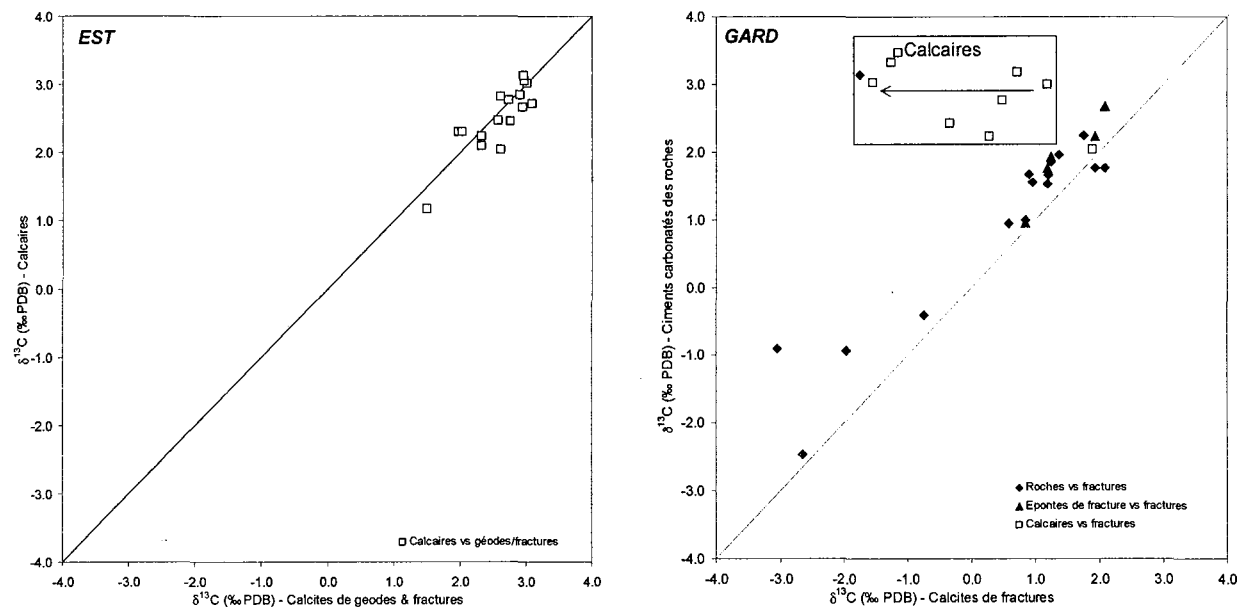

Fig. 8.2. $\delta^{13}C$ (PDB) des roches encaissantes en fonction du $\delta^{13}C$ (PDB) des calcites de fractures (et geode) pour les sites de l'Est et du Gard.

Dans l'Est, sur les forages étudiés, la fraction carbonatée globale des calcaires et argilites présente des valeurs de $\delta^{18}O$ relativement proches de celles qui sont attendues au cours d'une sédimentation en milieu marin (28-29 ‰ SMOW), bien qu'un peu plus faible (25 à 27 ‰ SMOW). Par contre, les données sur les calcites de géodes et fractures ($\delta^{18}O$ de 21±1 ‰ SMOW, Fig. 8.1) sont très différentes des roches encaissantes (caractéristique a priori non prévisible à l'étude pétrographique), bien que le carbone utilisé soit local (Fig. 8.2). Les valeurs en oxygène permettent de calculer, pour une température de précipitation de 35 à 40°C déterminée par l'étude des inclusions fluides, un $\delta^{18}O$ d'environ -4 à - 6 ‰ SMOW pour l'eau correspondante. Ce fluide est interprété comme un fluide d'origine continentale avec une composante météorique.

Les résultats isotopiques ponctuels obtenus sur la sonde 1270 du CRPG montrent que les éléments calcaires présentent des valeurs en $\delta^{18}O$ comprises entre 24 et 28 ‰ (SMOW), ce qui était attendu par rapport aux analyses globales des calcaires (de 25 à 28.5 ‰). Les premiers ciments calcitiques, rarement conservés, qui se présentent par une fine frange accolée aux éléments calcaires, ont des valeurs similaires allant de 24.5 à 27 ‰. Ceci confirme leur origine phréatique marine précoce.

Par contre, les ciments de type sparitique qui obturent la porosité, présentent des valeurs (20 à 21.5 ‰) tout à fait comparables à celles obtenues sur les ciments carbonatés des géodes et des fractures par analyses ponctuelles (19 à 23 ‰) et globales (21 ‰). Ces données confirment le caractère continental des eaux à l'origine des derniers ciments aussi bien au niveau des pores que dans les fractures.

Les échantillons étudiés de fractures/géodes de l'Est sont liés à un épisode relativement tardif de percolation des fluides d'origine continentale d'âge indéterminé sous un régime de températures relativement faibles. Ce fluide a aussi recristallisé la porosité de la plupart des calcaires. Cependant, il ne semble pas avoir eu d'influence notable sur les caractéristiques isotopiques des ciments des argilites, étant plus imperméables que les calcaires.

L'origine de la recharge a été envisagée par l'échantillonnage des calcites de fractures et fentes de tension régionales. Les résultats en $\delta^{18}O$ sur ces calcites (20-21 ‰ SMOW) sont similaires aux résultats donnés précédemment sur les calcites géodiques et de fractures des forages, et cela quelle que soit l'orientation des fractures ou fentes. Aux températures de cristallisations considérées (T<45°C), le fluide calculé pour ces calcites régionales a une valeur moyenne autour de -5 ‰, soit une valeur comparable au fluide reconstitué au niveau des forages. Ceci montre que l'origine des calcites dans les géodes, fractures et pores des ensembles sédimentaires du site est bien liée à la présence de grands fossés distensifs (Gondrecourt, Neufchateau), généralement interprétés comme d'âge Oligocène (en liaison avec l'ouverture du fossé Rhénan). De plus, les valeurs isotopiques en C tendent à indiquer que ces fluides ont remonté le long de ces accidents.

La percolation de ce fluide continental dans les roches mésozoïques du site de l'Est, latéralement à ces accidents, est à l'origine de la cimentation / recristallisation intense des calcaires oolitiques à grande porosité initiale (cavités dans les

biohermes, pores dans les calcaires oolitiques et oncholitiques) et a contribué aux faibles valeurs de perméabilités actuelles.

Problème de l'âge des circulations

Dans le Gard, les circulations des fluides diagenétiques à tendance marine, parfois influencés par une source plus météorique.

Par contre, *dans l'Est*, un seul type de fluide a percolé la série. Ce fluide continental de basse température a circulé par les accidents régionaux, puis infiltré les calcaires. Cependant, même si la tectonique nous renseigne quant aux périodes favorables de circulation, notamment durant le Tertiaire, il n'y a pas de contrainte forte sur l'âge et sur la durée du phénomène.

Perspectives

Dans l'Est, il reste essentiel de dater plus précisément cet épisode de circulation tardif. Cependant, les calcites et sont hors limite de la méthode U/Pb. La méthodologie proposée à l'avenir est de tenter de contraindre un intervalle, dont la borne inférieure pourrait être contrainte par les méthodes de datations des carbonates récents. En effet, bien que probablement hors limite U/Th (âge < 450 000 ans) et ^{14}C (< 50 000 ans), il est proposé de tenter ces méthodes de datations afin de réduire éventuellement la limite inférieure de l'intervalle. Des essais sont actuellement en cours. La borne supérieure de l'âge possible des calcites pourrait être mieux contrainte par l'amélioration de l'extension régionale du fluide, initiée dans ce travail en s'intéressant aux autres failles régionales, telles que celle de la Marne ou encore celles situées en Champagne, où des brèches hydrauliques à remplissage calcitique ont également été décrites. Ceci implique aussi un meilleur contrôle en temps de la tectonique cassante. Des études tentent actuellement de préciser cela.

Par ailleurs, il serait intéressant d'étudier, pour comparaison, les calcites trouvées dans les paléo-karts de Poissons dans le Barrois (Tithonien). En effet, elles présentent des similitudes morphologiques avec celles échantillonnées dans les fractures. Seul leur caractérisation géochimique pourra permettre de mettre en évidence ou non une quelconque relation. Sachant que ces calcites 'karstiques' se sont développées postérieurement aux karsts, leur âge est contraint entre -3 MA (développement du karst) et -500 000 ans (hors méthode U/Th) (Jaillet, 2000).

Enfin, un problème non traité ici est l'origine des dolomites observées soit de façon dispersée à la fois dans les argillites, dans les stylolites des calcaires soit en accumulation dans certains niveaux calcaires. Quelques mesures isotopiques ponctuelles en O effectuées sur des dolomites ont montré des valeurs comparables aux sparites tardives étudiées ici. Des études plus systématiques restent nécessaires pour identifier l'origine des dolomites.

Conclusions méthodologiques

Cette étude a montré que les épisodes de circulations et leurs caractéristiques ne sont pas forcément ceux attendus préalablement par le seul examen pétrographique et macroscopique des témoignages cristallins. Par exemple, dans le cas de l'Est du bassin parisien, des études préliminaires (Moretto et Mettraux, 1997) avaient conclues à une diagenèse précoce des calcaires. Bien qu'une diagenèse précoce y soit reconnue et conservée par endroit, la majeure partie des colmatages (sparites) observés sont à relier à un phénomène tardif de circulation, même ceux se trouvant dans les cavités formées précocement. Seul l'examen pétrographique couplé à une étude isotopique fine en C et O peut donc permettre de conclure quant aux sources des fluides. Cependant, d'un point de vue méthodologique, la composition isotopique en C doit être employée avec précaution pour le traçage des fluides dans l'éventualité d'une (re)cristallisation polyphasée de carbonates, car le C initial des minéraux peut être remobilisé lors de circulations fluides plus tardives. Par contre, le traçage isotopique en C et O par méthode conventionnelle et *in situ* des minéraux remplissant les discontinuités ou porosités, couplé aux études pétrographiques, minéralogiques et thermiques obtenues sur les inclusions fluides, les matières organiques et les argiles, constitue un outil puissant pour reconstituer les conditions paléo-hydrogéologiques, quel que soit le contexte.

Ces données, notamment isotopiques, ont permis d'étayer des modèles conceptuels de circulations fluides, malgré les difficultés inhérentes aux matériaux étudiés (peu d'inclusions fluides, calcite très pure, aucun minéral accompagnateur, etc.). Malgré cela, ces minéraux sont les seuls éléments significatifs du point de vue de l'ouverture des systèmes et des transferts. En effet, même si les fluides sont présents à tout moment, seules quelques crises majeures de percolation ont été (et seront à l'avenir) enregistrées par les minéraux.

L'efficacité du colmatage lors de ces événements a des conséquences très importantes sur :

i) les caractéristiques actuelles des sites, notamment leurs perméabilités et le stock élémentaire dans les zones susceptibles d'être percolées actuellement.

ii) les caractéristiques actuelles des fluides (peu abondants) qui seront dominées par les systèmes colmatages/encaissants altérés, notamment dans la disponibilité du Cl, Sr, CO_3^{2-}, SO_4^{2-}, Ca, Mg. Il sera donc difficile d'approfondir la caractérisation des fluides récents dans des systèmes à rapport liquide/roche faible à l'exception de propriétés isotopiques telles que $\delta^{18}O$, δH, ^{36}Cl, $^{234}U/^{238}U$ et ^{14}C pour estimer et tester les hypothèses quant aux âges des processus de circulations.

REFERENCES GENERALES

REFERENCES GENERALES

Alexandrov, P., 2000. Geochronologie U-Pb et 40Ar/39Ar de deux segments de la chaine varisque: le Haut Limousin et les Pyrénées orientales. Unpubl. PhD thesis, Nancy, 186p.

Amedro, F., Robaszynski, F., 1997. Datations précises en forages à l'aide des ammonites. J. Sci. Andra, 20-21 oct. 97, Bagnols/Cèze, p.7-8.

Andra, 1999. Referentiel géologique du site de Meuse/Haute-Marne. Synthesis activity report. A RP ADS 99-005.

André, A.S., Lespinasse, M., Cathelineau, M., Boiron, M.C., Cuney, M., Leroy, J.L., 1999. Percolation de fluides tardi-hercyniens dans le granite de Saint Sylvestre (Nord-Ouest du Massif Central Français): données des inclusions fluides sur un profil Razès-Saint-Pardoux. Compte Rendus de l'Académie des Sciences, Paris, 329, 23-30.

Azaroual, M., Fouillac, C., 1999. Thermodynamic modelling of modern basinal brines from the Paris Basin: Implication for MVT ore genesis. In Mineral Deposits, Process to Processing, Stanley et al., Eds, Balkema, vol. 2, 809-812.

Bakker, R. J., 1997. Clathrates: Computer programs to calculate fluid inclusion V-X properties using clathrate melting temperatures. Computers & Geosciences, 23, 1-18.

Bakker, R.J., 1999. Adaptation of the Bowers and Helgeson (1983) equation of state to the H2O-CO2-CH4-N2-NaCl system. Chemical Geology, 154, 225-236.

Balderer, W., Fontes, J.-Ch., Michelot, J-L., and Elmore, D., 1987. Isotopic investigations of the water-rock system in the deep crystalline rock of northern Switzerland. In "Saline water and gasses in crystalline rocks" (Fritz P., and Frape, S.K., eds.), GAC Spec. paper n°33, 175-195.

Banks, D.A. Giuliani, G., Yardley, B.W.D., Cheilletz, A. 2000. Emerald mineralisation in Colombia: Fluid chemistry and the role of brine mixing. Mineral. Deposita 35, 699-713.

Banks, D.A., Davies, G.R., Yardley, B.W.D., McCaig, A.M., Grant, N.T., 1991. The chemistry of brines from an Alpine thrust system in the Central Pyrenees: An application of fluid inclusion analysis to the study of fluid behaviour in orogenesis. Geochim. Cosmochim. Acta 55, 1021-1030.

Baranyl I., Lippolt H.J., Todt W. (1976)- Kalium Argon Altersbestimmunen an tertiären vulkaniten des Oberrheingraben-Gebietes : II die Alterstraverse vom Hegau nach Lothringen. Oberrhein geol. Abh. Karsruhe, 25.

Baudrimont, A.F., Dubois, P., 1977. Un bassin mésogéen du domaine péri-alpin : le Sud-Est de la France. Bulletin du Centre de Recherche d'Exploitation et Production d'Elf Aquitaine, 1, 1, 261-308.

Beaudoin, B., 1997. Stratigraphie de l'Albien et calibrage temps de la série de Marcoule. Proceedings of the Andra Sci. Meeting Bagnols-sur-Cèze, EDP Sciences Publ.,

Beaudouin, B., Accarie, H., Berger, E., Brulhet, J., Cojan, I., Haccard, D., Mercier, D., and Mouroux, B., 1997. Les enseignements de la crise " fini-messinienne ". Proceedings of the Andra Sci. Meeting Bagnols-sur-Cèze, EDP Sciences Publ., 115--135.

Berner, R.A., 1980. Early diagenesis - a theoritical approach. Princeton Univ. Press, 237 pp.

Bertrand, J.M., Leterrier, J. and Delaperrière, E., 1996. Géochronologie U-Pb de granitoïdes du Confolentais, de Vendée et des forages de Charroux-Civray. 17ème Réunion des Sciences de la Terre, Brest, Soc. Géol. Fr., p. 74 (Abstract).

Bertrand, J.M., Leterrier, J., Delaperrière, E., Brouand, M., Cuney, M., Stussi, J.M., Virlogeux, D., 2000. Géochronologie U-Pb sur zircon de granitoides du Confolentais, du massif de Charroux-Civray (seuil du Poitou) et de Vendée. Bull. Soc. Geol. Fr. in press.

Blyth, A., Frape, S., Blomqvist, R. and Nissinen, P., 2000. Assessing the past thermal and chemical history of fluids in crystalline rock by conbining fluid inclusion and isotopic investigations of fracture calcite. Appl. Geochem., 15: 1417-1437.

Bodnar, R. J., 1993. Revised equation and table for determining the freezing point depression of H_2O-NaCl solutions. Geochim. Cosmochim. Acta 57, 683-684.

Bohlke, J.K., Irwin, J.J., 1992. Laser microprobe analyses of noble gas isotopes and halogens in fluid inclusions: Analyses of microstandards and synthetic inclusions in quartz. Geochim. Cosmochim. Acta 56, 187-201.

Boiron, M.C., Cathelineau M., Banks D.A., Buschaert S., Fourcade S., Coulibaly Y., Michelot J.L., Boyce A., Nitjchoua R., 2001. Penetration of brines into a crystalline basement during extensional tectonics: role on fracture sealing, and mass transfer. Submitted.

Boiron, M.C., Essarraj S., Sellier E., Cathelineau M., Lespinasse M., Poty B., 1992. Identification of fluid inclusions in relation with their host microstructural domains in quartz by cathodoluminescence. Geochimica Cosmochimica Acta, 56, 175-185.

Boiron, M.C., Cathelineau, M., Banks, D., Vallance, J., Fourcade, S. and Marignac, Ch., 2000. Behaviour of fluids in Variscan crust during the late carboniferous uplifting and fluid mixing, and their consequences on metal transfer and deposition. In " Orogenic gold deposits in Europe ", Geode-GeoFrance 3D workshop (Bouchot, V. and Moritz, R., eds.), Doc. BRGM 297, ext. abstr., 56-57.

Boiron, M.C., Cathelineau, M., Trescases, J.J., 1989. Conditions of gold-bearing arsenopyrite crystallization in the Villeranges basin, Marche-Combrailles shear zone, France. A mineralogical and fluid inclusion study. Econ. Geol., 84, 1340-1362.

Bonhomme, M.G., 1982, Age triasique et jurassique des argiles associées aux minéralisations filoniennes et des phénomènes diagénétiques tardifs en Europe de l'Ouest - Contexte géodynamique et implications génétiques. C.R. Acad. Sci. 294, 521-524.

Bowers, TS, Helgeson H.C., 1983. Calculation of the thermodynamic and geochimical consequences of non-ideal mixing in the system H_2O-CO_2–NaCl on phase relations in geologic system: metamorphic equilibria at high pressures and temperatures. American Mineralogist, 68, 1059-1075.

Bricker, O.P., 1971. Carbonate cements, 19. John Hopkins Univ. Studies in Geology, 376 pp.

Bril, H., Velde, B., Meunier, A. and Iqdari, A., 1994. Effects of the 'Pays de Bray' fault on fluid paleocirculations in the Paris Basin Dogger Reservoir, France. Geothermics, 23(3): 305-315.

Brunet, M.F., 1983. La subsidence du bassin d'Aquitaine au Mésozoïque et au Cénozoïque. C.R. Acad. Sci. Paris, 297, 599-602.

Burke, W.H., Denison R.E., Hetherington E.A., Koepnick R.B., Nelson N.F. and Otto J.B., 1982. Variation of seawater $^{87}Sr/^{86}Sr$ throughout phanerozoic time. Geology, 10, 516-519.

Buschaert, S., Fourcade, S., Cathelineau M., Deloule E., Martineau F., Ayt Ougougdal M., Trouiller A., 2001. Widespread cementation induced by inflow of continental water in the eastern part of the Paris basin: O and C isotopic study of carbonate cements. Submitted to App. Geochem.

Capdevila, R. 1997. Les suites plutoniques metalumineuses recoupées par les forages Andra de la Vienne: caractérisation, mode de mise en place et discussion du contexte géodynamique. Andra Sci. Meeting, Poitiers, Posters Atlas, p. 13.

Capdevila, R., 1998. Les suites orogéniques dévoniennes du batholite de Charroux-Civray (Vienne) et leur contexte géodynamique. 17ème Réunion des Sciences de la Terre, Brest, Soc. Géol. Fr., p. 86 (Abstract).

Carpenter, A.B., Trout, M.L., Pickett, E.E., 1974. Preliminary report on the origin and chemical evolution of lead- and zinc-rich oil field brines in central Mississippi. Econ. Geol. 69, 1191-1206.

Casanova, J., Negrel, P., Kloppmann, W., Aranyossy, J.F., 2001, Origin of deep saline groundwaters in the Vienne granitic rocks (France): constraints inferred from boron and strontium isotopes. Geofluids, 1, 91-102.

Cathelineau M., 1988. Cation site occupancy in chlorites and illites as a function of temperature. Clay Minerals, 23, 471-485.

Cathelineau M., Cuney M., Boiron M.C., Coulibaly Y., Ayt Ougougdal M., 1999. Paléopercolations et paléo-interactions fluides - roches dans les plutonites de Charroux-Civray. Actes des Journées Scientifiques 1997 CNRS- Andra, Etude du massif de Charroux - Civray, EDP Sciences 159-179.

Cathelineau M., Marignac C., Boiron M.C., Gianelli G., Puxeddu M., 1994. Evidence of Li-rich brines and early magmatic water-rock interaction in a geothermal field: the fluid inclusion data from the Larderello field. Geochimica Cosmochimica Acta, 58, 1083-1099.

Cathelineau, M., Ayt Ougougdal, M., Elie, M. and Ruck, R., 1997. Mise en évidence d'une diagenèse de basse température dans les séries mésozoïques du site Est: une étude des inclusions fluides, des argiles et de la matière organique, J. Scientif. Andra, Bar-le Duc, Abstract EG8.

Cathelineau, M., Fourcade, S., Clauer, N., Buschaert, S., Rousset, D., Boiron, M.C., Martineau, F., Meunier, A., Javoy, M., Nitjchoua, R., 2001. Multistage paleofluid percolations in granites: A stable isotope and K-Ar study of fracture illite from Vienne plutonites (N.W. of the french Massif Central). Clay Min., submitted.

Cheilletz A., Cuney, M., Coulibaly, Y., Brouand M., Cathelineau, M., Stussi J.M., 1997. L'adularisation à l'interface socle-couverture dans la région de Charroux-Civray. Actes des Journées Scientifiques CNRS/Andra, Poitiers 13 et 14 octobre 1997, abstract VG12, p16.

Clauer N., 1981. 87Sr/86Sr ratios of the Barremian and early Aptian seas. In : thiede J., Vallier T.L. et al., initial reports of the deep sea drilling project. U.S. Government Printing Office, 62, 781-783.

Clauer N., 1981. Rb-Sr and K-Ar dating of precambrian clays and glauconies. Precambrian Research, 15, 331-352.

Clauer N., Chaudhuri S., Subramanium R., 1989. Strontium isotopes as indicators of diagenetic recrystallization scales with carbonate rocks. Chem. Geol., 80, 27-34.

Clauer, N., Frape, S.K., and Fritz, B., 1989. Calcite veins in the Stripa granite (Sweden) as records of the origin of ground waters and their interactions with the granitic body. Geochim. Cosmochim. Acta 53,1777-1782.

Clauzon, G;, Suc, J.-P., Gautier, F., Berger, A. and Loutre, M.-F., 1996. Alternate interpretation of the Messinian salinity crisis: controversy resolved ? Geology, 24, 4, 363-366.

Clayton R.N., Mayeda T.K.1963. The use of bromine pentafluoride in the extraction of oxygen from oxides and silicates for isotopic analyses. Geochimica Cosmochimica Acta, 27, 2075-2092.

Combes, Ph., Carbon, D., 1997. Néotectonique et sismicité du Gard Rhodanien. Proceedings of the Andra Sci. Meeting Bagnos-sur-Cèze, EDP Sciences Publ., 93-114.

Coulibaly Y., 1998. Recherche des traces de circulation récentes en milieu cristallin : Une approche analytique sur les cristallisations dans les fractures et les paléofluides, PhD Thesis, INPL Nancy.

Crawford M.L., 1981. Phase equilibria in aqueous fluid inclusions. In MAC short course on fluid inclusions, Mineral. Assoc. Can., Hollister and Crawford Eds, 75-100.

Cuney, M., Brouand, M., Stussi, J.M., Gagny, C. 1999. Le massif de Charroux-Civray (Vienne): un exemple caractéristique des premières manifestations plutoniques de la chaîne hercynienne - Etude du Massif de Charroux-Civray. Actes des Journées Scientifiques CNRS/Andra, EDP Sciences, Poitiers, 63-104.

Curnelle R., Dubois P., 1986. Evolution mésozoïque des grands bassins sédimentaires français, bassin de Paris, d'Aquitaine et du Sud-Est. Bull. Soc. Géol. Fr., 8, 529-546.

Curnelle, R., 1983. Evolution structuro-sédimentaire du Trias et de l'infra-lias d'Aquitaine. Bull. Cent. Rech. Explor. Prod. Elf Aquitaine 7-1, 69-99.

Curnelle, R., Dubois, P., 1986. Evolution mésozoïque des grands bassins sédimentaires français, bassin de Paris, d'Aquitaine et du Sud-Est. Bull. Soc. Géol. Fr. 8, 529-546.

Demars, C., 1994. Evolution diagénétique, paléofluides et paléothermicité dans les réservoirs du Keuper et du Dogger du bassin de Paris. PhD Thesis, INPL Nancy, France, 394 pp.

Dever, L., Marlin, C. and Vachier, P., 1990. Teneurs en ^{2}H, ^{18}O, ^{3}H et en chlorures des pluies dans le Nord-Est de la France (Châlons-sur-Marne): relation avec la température et l'origine des masses d'air. Geodynamica acta, 4: 133-140.

Drits V.A., Lindgreen H., Sakharov B.A., Salyn A.S., 1997, Sequence structure transformation of illite-smectite-vermiculite during diagenesis of Upper Jurassic shales, North sea. Clay Minerals, 33, 351-371.

Dubessy J., Poty B., Ramboz C., 1989. Advances in the C-O-H-N-S fluid geochemistry based on micro-Raman spectroscopic analysis of fluid inclusions. European Journal of Mineralogy, 1, 517-534.

Dubessy, J., 1984. Simulation des équilibres chimiques dans le système C-O-H. Conséquences méthodologiques pour les inclusions fluides. Bulletin Mineralogique, 107, 155-168.

Durlet, C. and Loreau, J.P., 1996. Séquence diagénétique intrinsèque des surfaces durcies : mise en évidence de surface d'emersion et de leur ablation marine. exemple de la plate-forme bourguignonne, Bajocien (France). C. R. Acad. Sci. Paris, 323(5): 389-396.

Durlet, C., 1996. Apports de la diagenèse des discontinuités à l'interprétation paléo-environnementale et séquentielle d'une plate-forme carbonatée. Exemple des "calcaires à entroques" du Seuil de Bourgogne (Aalénien-Bajocien), PhD Thesis, Univ. of Bourgogne, 444 pp.

Duthou J.L., Cantagrel J.M., Didier J., Vialette Y., 1984. Paleozoic granitoids from the French Massif Central: age and origin studied by 87Rb-87Sr system. Physical Earth and Planetary Sciences International, 35, 131-144.

Essarraj S., Boiron M.C., Cathelineau M., Fourcade S., 2001. Multistage deformation of Au-quartz veins : Evidence for late gold introduction from microstructural, Isotopic and fluid inclusion studies. Tectonophysiscs, in press.

Fallick, A.E., Jocelyn, J., Hamilton, P.J., 1987. Oxygen and hydrogen stable isotope systematics in Brazilian agates. In: Rodriguez Clemente, E. (Ed.), Geochemistry of the Earth Surface and Processes of Mineral Formation, 99-117.

Ferry, S., 1999. Apport des forages Andra à la connaissance de la marge crétacée rhodanienne. Proceedings of the Andra Sci. Meeting Bagnols-sur-Cèze, EDP Sciences Publ., 63-91.

Fleck S., 2001. Corrélation entre géochimie organique, sédimentologie et stratigraphie séquentielle pour la caractérisation des environnements de dépôt. PhD Thesis Univ. Nancy I, France.

Fontes, J.C., Matray, J.M., 1993. Geochemistry and origin of formation brines from Paris Basin, France. 1. Brines associated with triassic salts. Chem. Geol. 109, 149-175.

Fontes, J.C. Matray, J.M., 1993. Geochemistry and origin of formation brines from the Paris basin, France. 2. Saline solutions associated with oil fields. Chem. Geol., 109: 177-200.

Fouillac, C., Michard, G., 1981. Sodium/lithium ratio in water applied to geothermometry of geothermal reservoirs. Geothermics 10, 55-70.

Fourcade, S., Boiron, M.C., Cathelineau, M., Guerrot, C., Lerouge, C., Marignac, C., Martineau, F. and Vallance, J., 2000. Fluids and late carboniferous Variscan gold mineralizations in the French Massif Central. The bearing of stable isotopes. In " Orogenic gold deposits in Europe ", Geode-GeoFrance 3D workshop (Bouchot, V. and Moritz, R., eds.), Doc. BRGM 297, ext. abstr., 58-59.

Fourcade, S., Martineau, F., 2000. Composition isotopique de l'oxygène et de l'hydrogène dans les fractions argileuses des sites de Mont-Terri et de Tournemire. Rapport Final Action 99-I (eaux intersticielles), Forpro-Andra, 11p.

Fourcade, S., Michelot, J.L., Buschaert, S., Cathelineau, M., Freiberger, R., Coulibaly, Y., Nitjchoua, R., 2001. Early introduction of carbon in plutonic rocks and its successive remobilizations during subsurface fluid-rock interactions : the case study of the Vienne granitoids (France). Submitted to Chemical Geology.

Fournier, R.O., 1979. A revised equation for Na/K geothermometer. Geotherm. Res. Counc. Trans., 3, 221-224.

Franck, T.D. and Lohmann, K.C., 1996. Diagenesis of fibrous magnesian calcite marine cement: implications for the interpretation of $\delta^{18}O$ and $\delta^{13}C$ values of ancient equivalents. Geochim. Cosmochim. Acta 60, 2427-2436.

Frape, S.K., Fritz, P., 1987, Geochemical trends from groundwaters from the Canadian Shield. In: Saline waters and gases in crystalline rocks. Fritz, P and Frape, S.K. Eds. Geol. Assoc. Canada Spec. Paper, 33, 19-38.

Freiberger R., 2000. P-T-X conditions of the late magmatic to early postmagmatic crystallization history of intermediate to basic plutonites: The Hercynian granitoid complex of Charroux-Civray, NW border of the Massif Central, France. Unpubl. PhD thesis, Lehrstuhl für Angewandte Mineralogie und Geochemie, TU München, Hieronymus-Verlag, 204 p.

Freiberger R., Cuney M., 1999. Magmatic anhydrite in plutonic rocks: Occurrence from the Hercynian calcalkaline batholith of Charroux-Civray (NW' Massif Central, France). In: The origin of granites and related rocks - Fourth Hutton Symposium, Clermont-Ferrand (ed Barbarin B). Editions BRGM, 290, 209.

Freiberger, R., Boiron, M.C., Cathelineau, M., Cuney, M., Buschaert, S., 2001. Retrograde P-T evolution and high temperature – low pressure fluid circulation in relation to late Hercynian intrusions: a mineralogical and fluid inclusion study of the Charroux-Civray granitoids (NW Massif Central, France). Submitted to Geofluid.

Freiberger, R., Hecht, L., Cuney, M. and Morteani, G., 2001. Secondary Ca-Al-silicates from Mid-European Hercynian granitoids: Implications for the cooling history of granitic plutons. Contributions to Mineralogy and Petrology (in press).

Frey, M., de Capitani, C. and Liou, J.G., 1991. A new petrogenetic grid for low-grade metabasites. J. of Metamorphic Geology 9, 497-509.

Friedman, I. and O'Neil, J.R., 1977. Compilation of stable isotope fractionation factors of geochemical interest. In " Data of Geochemistry, 6th ed. (Fleischer, M., ed.), U.S. Gov. Printing Office, Washington, D.C.

Goldstein, R.H. and Reynolds, T.J., 1994. Systematics of fluid inclusions in diagenetic minerals. SEPM short course 31, 212 pp.

Grelet B., 1997. Analyse de la fracturation en forages. Proceedings of the Andra Sci. Meeting Bagnols-sur-Cèze, Abstract GG17.

Guillocheau, F. et al., 2000. Meso-cenozoic geodynamic evolution of the Paris Basin: 3D stratigraphic constraints. Geodyn. Acta, 14-4, 189-246.

Guillocheau, F., 1991. Mise en évidence de grands cycles transgression-régression d'origine tectonique dans les sédiments mésozoïques du Bassin de Paris. C. R. Acad. Sci. Paris, 312: 1587-1593.

Horita, J., Friedman, T.J., Lazar, B., Holland, H.R., 1991. The composition of Permian seawater. Geochim. Cosmochim. Acta 55, 417-432.

Huault, V., 1994. Recherches palynologiques dans le Dogger de la bordure Sud-Est du bassin de Paris. Palynostratigraphie, analyse de l'évolution des assemblages microfloristiques et confrontation avec les variations du niveau marin relatif, PhD Thesis, Univ. of Bourgogne, 253 pp.

Illies J.H., Fuchs K. (1974) - Approach to taphrogenesis. Proc. Int. Rift Symp. Karlsruhe 1972. Int Union Commission on Geodynamics Scientif Report n°8. Schweizerbatt ed. Stuttgart, 460p.

Irwin, H., Curtis, C. and Coleman, M., 1977. Isotopic evidence for source of diagenetic carbonates formed during burial of organic-rich sediments. Nature 269, 209-213.

Jaillet S., 2000., Un karst couvert de bas-plateau : le Barrois : structure, fonctionnement, évolution. PhD Thesis, Univ. Bordeaux 3.

Javoy, M. and Pineau, F., 1991. The volatiles record of a " popping " rock from the Mid-Atlantic Ridge at 14°N: chemical and isotopic composition of the gas trapped in the vesicles. Earth Planet. Sci. Letters 107, 598-611.

Jendrzejewski, N., Javoy, M., and Trull, T., 1996. Mesure quantitative de carbone et d'eau dans les verres basaltiques naturels par spectroscopie infrarouge. Partie I : Le carbone, C. R. Acad. Sci., Paris 322, série IIa, 645-652.

Keller, J., 1999. Primary magmas in the tift valley volcanism of the upper Rhinegraben province. EUG 10, J. of Conf. Abst., Cambridge Pubs. 4, 1, 322.

Kerrich R., 1987. Stable isotope studies of fluids in the crust. In: Short course in stable isotope geochemistry in low-temperature fluids (ed Kyser TK). Mineralogical Association of Canada, Saskatoon, 13, 258-286.

Kesler, S.E., Martini, A.M., Appold, M.S., Walter, L.M., Huston, T.J., Furman, F.C., 1996. Na-Cl-Br systematics of fluid inclusions from Mississippi Valley-type deposits, Appalachian

basin: Constraints on solute origin and migration paths. Geochim. Cosmochim. Acta 60, 225-233.

Kharaka, Y.K., Maest, A.E., Carothers, W.W, Law, L.M., Lamothe, P.J., Fries, T.L., 1987. Geochemistry of metal-rich brines from central Mississippi Salt dome Basin, USA. Applied Geoch., 2, 543-561.

Kim, S.T., O' Neil, J.R., 1997. Equilibrium and non-equilibrium oxygen isotope effects in synthetic carbonates. Geochim. Cosmochim. Acta 61, 3461-3475.

Knauth, L.P., Beeunas, M.A., 1986. Isotope geochemistry of fluid inclusions in Permian halite with implications for the isotopic history of ocean water and the origin of saline formation waters. Geochim. Cosmochim. Acta 50, 419-433.

Komor, S.C., 1995. Chemistry and petrography of calcite in the KTB pilot borehole, Bavarian Oberpfalz, Germany. Chem. Geol. 124, 199-215.

Kyser, T.K., Kerrich, R., 1990. Geochemistry of fluids in tectonically active crustal regions. In " Short Course on Fluids in Tectonically Active Regimes of the Continental Crust ", Min. Assoc. Canada, Vancouver, Nesbitt, B.E., ed,.18, 133-230.

Lamiraux, C. and Mascle, A., 1998. Petroleum exploration and production in France. First break, 16(4): 109-117.

Lancelot J., Leclerc, S., Verdoux P., and Aranyossy J.F. 1999. A strontium and lead isotopic study of the Marcoule silty-clay layer (Gard, France) and implications for charcaterization of water-rock intercations in low permeability argillaceous media. OCDE Proc. NEA/ EC Workshop "Fluid flow through faults and fractures in argillaceous formations" Berne, 223-242.

Lancelot, J., 1997. Discussion de l'évolution des isotopes radiogéniques dans la couche silteuse de Marcoule en domaines non fracturés et fracturés. Proceedings of the Andra Sci. Meeting Bagnols-sur-Cèze, EDP Sciences Publ., 139--166.

Lancelot, J., Vella, V., 1989. Datation U-Pb liasique de la pechblende de Rabajac - Mise en évidence d'une préconcentration uranifère permienne dans le bassin de Lodève (Hérault). Bull. Soc. Géol. Fr. 8, 309-315.

Landais, P. and Elie, M., 1999. Utilisation de la géochimie organique pour la détermination du paléoenvironnement et de la paléothermicité dans le Callovo-Oxfordien du site de l'Est de la France, Actes de Journées Scientifiques CNRS/Andra, Bar-le Duc, 20 et 21 oc. 1997. EDP Sciences, Paris, pp. 35-58.

Lanson B., 1990. Mise en évidence des mécanismes de transformation des interstratifiés illite/smectite au cours de la diagénèse.Thèse de l'Université Paris 6-Jussieu, 366 p

Le Guen M., Orgeval J.J. and Lancelot J., 1991. Lead isotope behaviour in a polyphase Pb-Zn ore deposit : Les malines (Cevennes, France). Mineral. Deposita 26, 180-188.

Lebon P., 1997. La couche silteuse de Marcoule : des propriétés exceptionnelles. Proceedings of the Andra Sci. Meeting Bagnols-sur-Cèze, EDP Sciences Publ., 3-12.

Leclerc, S., 1999. Contribution de la méthode Rb/ Sr à la démontsration de la qualité de confinement de la couche silteuse de marcoule (Gard Rhodanien). Thesis, Montpellier Univ., 208.

Lehmann B., 1990. Metallogeny of tin. In: Lecture Notes in Earth Sciences (eds. Bhattacharji S, Friedman GM, Neugebauer HJ, Seilacher A). Springer-Verlag, 32, 211 p.

Lespinasse M., Cathelineau M., 1990. Fluid percolations in a fault zone: a study of fluid inclusions planes in the St Sylvestre granite, North-West Massif Central, France. Tectonophysics, 184, 173-187.

Leveque M.H., Lancelot J.R., George E., 1988. The Bertholène uranium deposit-mineralogical characteristics and U-Pb dating of primary U mineralization and its subsequent remobilization: consequences for the evolution of the U-deposits of the Massif Central, France. Chem. Geol., 69, 147-163.

Lhomme, T., Dubessy, J., Rull, F., 1999. Determination of chlorinity in aqueous fluids using Raman spectroscopy at room temperature. GeoRaman'99, Valladolid, Spain, 93-94.

Li, L., Barry, D.A., Stagnitti, F. and Parlange, J.-Y., 1999. Submarine groundwater discharge and associated chemical input to a coastal area. Water Res., 35: 3253-3259.

Lippolt H.J., Todt W. and Horn P (1974) - Apparent Potassium-Argon Ages of lower Tertiary Rhine Graben volcanics in (Illies J.H. and Fuchs K.) Proc. Int. Rift Symp. Karlsruhe 1972. Int Union Commission on Geodynamics Scientif Report n°8. Schweizerbatt ed. Stuttgart, 460p.

Lyman, J. and Fleming, R.H., 1940. The composition of seawater. J. Marine Res., 3: 134-146.

Lynn Ingram, L.B., Conrad, M.E. and Ingle, J.C., 1996. Stable isotope and salinity systematics in estuarine waters and carbonates: San Francisco Bay. Geochim. Cosmochim. Acta, 60(3): 455-467.

Macpherson, C.G., Hilton, D.R., Newman, S. and Mattey, D.V., 1999. CO_2, $^{13}C/^{12}C$ and H_2O variability in natural basaltic glasses: A study comparing steeped heating and FTIR spectroscopic techniques. Geochim. Cosmochim. Acta 63, 1805-1813.

Maes, P., 2001, Signification des signatures isotopiques en Sr des eaux porales et des paléofluides sur discontinuités des formations argileuses très imperméables (Mt Terri, Tournemire, Bure), Actes des Journées Andra des doctorants, Paris, 21 juin 2001, résumé pp. 31-33

Marignac, C., Cathelineau, M., Boiron, M.C., Fourcade, S., Vallance, J. and Souhassou, M., 2000. The Q-Au lodes of W Europe: towards the definition of a Variscan-type of shear-zone hosted gold deposits. In " Orogenic gold deposits in Europe ", Geode-GeoFrance 3D workshop (Bouchot, V. and Moritz, R., eds.), Doc. BRGM 297, ext. abstr., 82-85.

Marumo, K., Nagasawa, K., Kuroda, Y., 1980. Mineralogy and hydrogen isotope geochemistry of clay minerals in the ohnuma geothermal area, northeast Japan. Earth Planet. Sci. Letters, 47, 255-262.

Matray, J.M., Lambert, M., Fontes, J.C., 1994. Stable isotope conservation and origin of saline waters from the Middle Jurassic aquifer of the Paris Basin, France. Appl. Geochem., 9: 297-309.

Maurin, J.-C., Nivière, B., 2000. Extensional forced folding and decollement of the pre-rift series along the Rhine graben and their influence on the geometry of the syn-rift sequences. In: J.W.A. Cosgrove, M.S., eds. (Editor), Forced folds and fractures. Geol. Soc. London Spec. Pub., pp. 73-86.

Maury, R.C. and Varet, J., 1980. Le volcanisme tertiaire et quaternaire en France. In: Autran, A. and Dercourt, J (Eds), "Evolutions géologiques de la France", Mem. BRGM 107, pp.137-159.

McCrea, J.M., 1950. On the isotope chemistry of carbonates and a paleotemperature scale. J. Chem. Phys. 18, 849-857.

Mégnien, C., 1980a. Synthèse géologique du Bassin de Paris. Stratigraphie et Paleogeographie. . Mém. BRGM 101.

Mégnien, C., 1980b. Tectogenèse du Bassin de Paris: étapes de l'évolution du bassin. Bull. Soc. Géol. Fr., 22: 669-680.

Meyers, W.J., 1991. Calcite cement stratigraphy: An Overview, *In:* Luminescence Microscopy: Quantitative and Qualitative Aspects. SEPM Short Course n°25, pp. 133-147.

Michelot, J.L., 1999, Les eaux du système granitique de la Vienne: reconnaissance hydrogéochimique et isotopique, In: Etude du Massif de Charroux-Civray, Actes des journées scientifiques Andra, Poitiers, EDP Sciences. 181-199.

Milliman, J.D., 1975. Recent Sedimentary Carbonates 1, Marine Carbonates. Springer-Verlag, Berlin, 375 pp.

Moore, W.S., 1996. Large groundwater inputs to coastal waters revealed by ^{226}Ra enrichments. Nature, 380, 612-614.

Moretto, R., Mettraux, M., 1997. Diagenèse précoce dans les carbonates de l'Oxfordien moyen/supérieur (forages HTM102 et MSE101) : incidence sur la porosité. J. Scientif. Andra, Bar-le Duc, poster EG9.

Mouroux B., 1999. La démarche scientifique de l'Andra. Actes des Journées Scientifiques 1997 CNRS- Andra, Etude du massif de Charroux - Civray, EDP Sciences 1-33.

Mouroux, B., Brulhet, J., 1999, La démarche scientifique de l'Andra : site du Gard. Proceedings of the Andra Sci. Meeting Bagnols-sur-Cèze, EDP Sciences Publ., 13-33.

Muchez, P., Sintubin, M. and Swennen, R., 2000. Origin and migration pattern of palaeofluids during orogeny: discussion on the Variscides of Belgium and northern France. Journal of Geochemical Exploration, 69-70: 47-51.

Munoz M.,. Boyce A. J, Courjault-Rade P., Fallick A. E., Tollon F., 1999. Continental basinal origin of ore fluids from southwestern Massif Central fluorite veins (Albigeois, France): evidence from fluid inclusion and stable isotope analyses, Appl. Geochem. 14, 447-458

Munoz, M., Boyce, A.J., Courjault-Rade, P., Fallick, A.E., Tollon, F., 1995. Multi-stage fluid incursion in the Palaeozoic basement-hosted Saint-Salvy ore deposit (NW Montagne Noire, southern France), International Journal of Rock Mechanics and Mining Science & Geomechanics Abstracts, 32, 5, 202A .

O'Neil, J.R., 1987. Preservation of H, C, and O isotopic ratios in the low temperature environment. In " Stable isotope geochemistry of low temperature fluids ", Vol. 13 (Kyser, T.K., ed.), Saskatoon, Min. Assoc. of Canada, 85-128.

O'Neil, J.R., Clayton, R.N. and Mayeda, T.K., 1969. Oxygen isotope exchange in divalent metal carbonates. J. Chem. Phys. 51, 5547-58.

Ohmoto, H., 1972. Systematics of sulfur and carbon isotopes in hydrothermal ore deposits. Econ. Geol., 67, 551-579.

Ohmoto, H.; and Rye, R.O. 1979. Isotopes of sulfur and carbon; In H.L. Barnes (Ed.) Geochemistry of hydrothermal ore deposits. John Whiley & Sons. 509-561.

Okulitch, A.V., 1999. Geological time scale, 1999. Geol. Surv. of Canada, Open file 3040 (National Earth Sci. Ser., Geol. Atlas).

Orberger, B. & Pagel, M., 2000. Diagenetic evolution of Cretaceous siltstones from drill hole MAR 501 (South-Eastern France). Journal of Geochemical Exploration, 69-70, 115-118.

Peiffer, M.-T., 1986. La signification de la ligne tonalitique du Limousin. Son implication dans la structuration varisque du Massif Central français. C.R. Acad. Sci. Paris 303, sér. II, 305-310.

Pellenard, P., Deconinck, J. F., Marchand D., Thierry J., Fortwengler, D, Vigneron, G., 1999. Eustatic and volcanic influence during Middle Callovian to Middle Oxfordian clay

sedimentation in the eastern part of the Paris Basin. C. R. Acad. Sci. Paris, 328(12): 807-813.

Philip J., 1984. Tectonique méso-crétacée en Provence « Synthèse géologique du Sud-Est de la France ». Edité par Debrand-Passard et al. Mém. BRGM, n° 125, pp. 384-386.

Pierre, C., 1989. Sedimentation and diagenesis in restricted marine basins. In " Handbook of Environmental Isotope Geochemistry, 3. The Marine Environment ", Fritz, P. and Fontes, J.C., eds, Elsevier, Amsterdam, 257-315.

Pierre, C., Ortlieb L., Person A., 1984. Supratidal evaporitic dolomite at Ojo de Liebre lagoon: mineralogical and isotopic arguments for primary crystallization. J. Sedimen. Petrol. 54, 1049-1061.

Pineau, F. and Javoy, M., 1994. Strong degassing at ridge crests: The behaviour of dissolved carbon and water in basaltic glasses at 14°N, Mid-Atlantic Ridge, Earth and Planet. Sci. Letters 123, 179-198.

Pommerol, C., 1989. L'évolution du Bassin Parisien. In: ASF (Editor), Dynamique et méthodes d'étude des bassins sédimentaires. Editions Technip, Paris, pp. 165-178.

Poty, B., Leroy, J., Jachimovicz L., 1976. Un nouvel appareil pour la mesure des températures sous le microscope: l'installation de la microthermométrie Chaixmeca. Bull. Soc. Fr. Minéral. Cristallogr., 99, 182-186.

Reeder, R.J., Valley, J.W., Grahamm, C.M., Eiler, J.M. 1997. Ion microprobe study of oxygen isotope compositions of structurally nonequivalent growth surface on synthetic calcite. Geochim. Cosmochim Acta 61(23), 5057-63.

Respault, .J. P., Cathelineau M., Lancelot J.R., 1991, Multistage evolution of the Pierres plantées uranium ore deposit (Margeride, France) : evidence >from mineralogy and U-Pb systematics. Eur.J. Mineral., 3, 85-103.

Reynolds, R.C., Hower J., 1970. The nature of interlayering in mixed-layer illite-montmorillonite. Clays and Clay Minerals, 18, 25-36.

Robaszynski, F., Amedro F., Devalque C.,1997. Positionnement de la limite stratigraphique entre les étages cénomanien et turonien dans les sondages de Marcoule. J. Sci. Andra, 20-21 oct. 97, Bagnols/Cèze, p. 9.

Roedder, E., 1984. Fluid inclusions. Reviews in mineralogy, 12, Mineralogical Society of America, 644 p.

Rolin, P., Colchen, M., 1995. Le socle cristallin du confolentais le long de la vallée de la Vienne. Andra Report # OUTPT 95001, 91p.

Rollion-Bard, C. 2001. Mesures isotopiques (B, C et O) par sonde ionique sur marqueurs paléoenvironnementaux. PhD Thesis, INPL Nancy, France

Roubeuf, V., 2000. Interactions entre fluides et sédiments argileux naturels : Étude expérimentale dans des conditions simulant un stockage souterrain de déchets radioactifs. Thesis Univ. Nancy I.

Roure, F. and Colletta, B., 1996. Cenozoic inversion structures in the foreland of the Pyrénées and the Alps. In: "Peri-tethys Memoir 2: Structure and aspects of Alpine basins and forelands " (Ziegler, P.A. and Horvàth, F., eds.), Mém. Mus. Hist. Nat., 170, 173-209.

Ruck-Mosser, R., Cathelineau, M., Elie, M., Landais, P., Boiron, M.C., Roubeuf, V., 1999.Pétrographie, géochimie et cristallochimie détaillée d'échantillons représentatifs des argilites de la Haute-Marne: Synthèse des données et implications géochimiques sur la diagénèse des sédiments, Report Andra..

Rye, D.M., and Williams, N., 1981. Studies of the base metal sulfide deposits at McArthur River, Northern Territory, Australia: III. The stable isotope geochemistry of the H.Y.C., Ridge, and Cooley deposits. Econ. Geol. 76, 1, 1-26.

Sacchi, E. and Michelot, J.L., 1996. Etude des cristallisations dans les fractures. Applications au site Andra Vienne-Sud. Int. Report Andra n° 315747 AO, 34 p.

Sakai, H. and Tsutsumi, M., 1978. D/H fractionation factors between serpentine and water at 100°C to 500°C and 2000 bar water pressure. Earth Planet. Sci. Letters, 40, 231-242.

Savin, S.M., Lee, M., 1988. Isotopic studies of hydrous phyllosilicates. In " Hydrous Phyllosilicates (exclusive of micas) " (Bailey, S.W., ed.), Rev. of Mineralogy, Vol. 19, Min. Soc. America, 189-233.

Scaillet S., Cheilletz A., Cuney M., Farrar E., Archibald D., 1996. Cooling patterns and mineralization history of the Saint Sylvestre and Western Marche leucogranite plutons, French Massif Central. I. 40Ar/39Ar isotopic constraints. Geochimica Cosmochimica Acta, 60, 23, 4653-4671.

Séranne, M., 1999. The Gulf of Lion continental margin (NW Mediterranean) revisited by IBS: an overview. In: " The Mediterranean Basins: Tertiary Extension within the Alpine Orogen " (Durand, B., Jolivet, L., Horvàth, F and Séranne, M., eds.), Geol. Soc. London Spec. Publ. 156, 15-36.

Shaw, A., Downes H., Thirlwall M.F., 1993. The quartz diorites of Limousin: elemental and isotopic evidence for Devono-Carboniferous subduction in the Hercynian belt of the French Massif Central. Chem. Geol. 107, 1-18.

Sheppard, S.M.F., 1984. Stable isotopes studies of formation waters and associated Pb-Zn hydrothermal ore deposits. In: Thermal phenomena in sedimentary basins. Ed. Technip 301-317.

Sheppard, S.M.F., 1986. Characterization and isotopic variations in natural waters. In "Stable isotopes in high temperature geological processes", Reviews in Mineralogy Min. Soc. Am., Valley, J.W., Taylor, H.P., Jr., O'Neil, J., eds, 16, 165-183.

Sheppard, S.M.F., Charef, A., 1986. Eau organique: caractérisation isotopique et évidence de son rôle dans le gisement Pb-Zn de Fedj-el-Adoum, Tunisie. C.R. Acad. Sci. 302-II, 1189-1192.

Sheppard, S.M.F., Schwarcz, H.P., 1970. Fractionation of C and O isotopes and magnesium between coexisting metamorphic calcite and dolomite. Contrib. Mineral. Petrol. 26, 161-198.

Sofer, Z., Gat, J.R., 1975. The isotope composition of evaporating brines: effect of the isotopic activity ratio in saline solutions. Earth Planet. Sci. Letters, 26: 179-186.

Steiger RH, Jäger, E., 1977. Subcomission on Geochronology: Convetion on the use of decay constants in geo-and cosmogeochronology. Earth PlanetSci. Lett., 36:359-362.

Suchy, V., Heijlen, W., Sykorova, I., Muchez, P., Dobes, P., Hladikova, J., Jackova, I., Safanda, J., Zeman, A., 2000. Geochemical study of calcite veins in the Silurian and Devonian of the Barrandian Basin, (Czech Republic): evidence for widespread post-Variscan fluid flow in the central part of the Bohemian Massif. Sed. Geol. 131, 3-4, 201-219.

Taylor, B.E., 1987. Stable isotope geochemistry of ore-forming fluids. In " Short Course in Stable Isotope Geochemistry of Low Temperature Fluids ", Min. Assoc. Canada, Saskatoon, Kyser, T.K., ed., 13, 337-345.

Thiéry R., Vidal J., Dubessy J., 1994. Phase equilibria modelling applied to fluid inclusions liquid-vapor equilibria and calculation of the molar volume in the CO2-CH4-N2 system. Geochimica Cosmochimica Acta, 58, 1073-1082.

Trave, A., Calvet, F., Sans, M., Verges, J., Thirlwall, M., 2000. Fluid history related to the Alpine compression at the margin of the south-Pyrenean Foreland basin: the El Guix anticline. Tectonophysics, 321(1): 73-102.

Trouiller, A. and Lebon, P., 1999. La démarche scientifique de l'Andra dans l'Est de la France., Actes de Journées Scientifiques CNRS/Andra, Bar-le Duc, 20 et 21 oc. 1997. EDP Sciences, Paris, pp. 3-26.

Turpin L,. Cuney M., Friedrich M., Bouchez J.L., Aubertin M., 1990. Meta-igneous origin of Hercynian peraluminous granites in NW French Massif Central: Implications for crustal history reconstitutions. Contribution to Mineralogy and Petrology, 104, 163-172.

Vallance, J, M.C. Boiron, M. Cathelineau, S. Fourcade and C. Marignac. (submitted to Mineralium Deposita). High T-low P fluid rock interaction and early As introduction in the granite hosted Au deposit of Moulin de Cheni (St Yrieix District, french massif central).

Valley, J.W., Komor, S.C., Baker, K., Jeffrey, A.W.A., Kaplan, I.R., and Raheim, A., 1988. Calcite crack cements in granite from the Siljan Ring, Sweden: stable isotope results. In " Deep drilling in crystalline bedrock ", (Bode, A. and Erikkson, K.G., eds.), Vol. 1, Springer, Berlin, 156-179.

Velde B., 1977. Clays and clay minerals in natural and synthetic systems. in: Developments in Sedimentology, 21.

Verdoux P., 1997.Contribution des systèmes Rb/Sr et U/Pb à la charactérisation des circulations et des paléocirculations de fluides en domaine continental entre 0 et 2000 m de profondeur. Conséquences sur les ressources en eaux et le stockage des déchets radioactifs en profondeur. Ph.D Thesis, Univ. de Montpellier, France, 342 pp.

Verma, S., Santoyo, E., 1997. New improved equations for Na/K, Na/Li and SiO_2 geothermometers by outlier detection and rejection. J. Volcanol. Geotherm. Res. 79, 9-23.

Virlogeux, D., Roux, J, Guillemot, D., 1999. Apports de la géophysique à la connaissance géologique du massif de Civray-Charroux et du socle poitevin. Proceedings of the Andra Sci. Meeting Poitiers, EDP Sciences Publ., 33-61.

Wallin, B., Peterman, Z., 1999. Calcite fractures as indicators of paleohydrology at Laxemar at the Äspö Hard Rock Laboratory, southern Sweden. Applied Geochem. 14, 953-962.

Wenner, D.B., Taylor, H.P., Jr., 1971. Temperatures of serpentinzation of ultramafic rocks based on $^{18}O/^{16}O$ fractionation between coexisting serpentine and magnetite. Contrib. Mineral. Petrol., 32, 165-185.

White, A.F., Bullen, T.D., Vivit, D.V., Schulz, M., Clow, D.W., 1999. The role of disseminated calcite in the chemical weathering of granitoid rocks. Geochim. Cosmochim. Acta 63, 1939-1953.

Winter, B.L., Valley, J.W., Simo, J.A., Nadon, G.C., Johnson, C.M., 1995. Hydraulic seals and their origins: evidence from the stable isotope geochemistry of dolomites in the Middle Ordovician St. Peter Sandstone, Michigan Basin. Am. Ass. Petrol. Geol. Bull. 79, 1, 30-48.

Worden, R.H., Coleman, M.L., Matray, J.-M., 1999. Basin scale evolution of formation waters: a diagenetic and formation water study of the Triassic Chaunoy Formation, Paris Basin. Geochim. Cosmochim Acta, 63(17): 2513-28.

Worden, R.H., Matray, J.-M., 1995. Cross formational flow in the Paris Basin. Basin Res., 7: 53-66.

Yeh, H.W., 1980. D/H ratios and late-stage dehydration od shales during burial. Geochim. Cosmochim. Acta, 44, 341-352.

Zhang, Y. G., Frantz, J. D., 1987. Determination of the homogenization temperatures and densities of supercritical fluids in the system NaCl-KCl-$CaCl_2$-H_2O using synthetic fluid inclusions. Chem. Geol. 64, 335-350.

Zheng, Y.F., 1993. Calculation of oxygen isotope fractionation in anhydrous silicate minerals. Geochim. Cosmochim. Acta 56, 1079-1091.

Zheng, Y.F., 1993. Calculation of oxygen isotope fractionation in hydroxyl-bearing silicates. Earth Planet. Sci. Letters, 120, 247-263.

Ziserman A., 1980. Le gisement de Chaillac (Indre): la barytine des Redoutières, la fluorine du Rossignol. Association d'un gite stratiforme de couverture et d'un gite filonien du socle . 26° CGI, Gisements français, Fascicule E3.

S.C.D. - U.H.P. NANCY 1
BIBLIOTHÈQUE DES SCIENCES
BOULEVARD DES AIGUILLETTES
54506 VANDŒUVRE-LES-NANCY Cedex

Monsieur **BUSCHAERT Stéphane**

DOCTORAT de l'UNIVERSITE HENRI POINCARE, NANCY-I

en SCIENCES DE L'UNIVERS

VU, APPROUVÉ ET PERMIS D'IMPRIMER

Nancy, le 15 octobre 2001 n° 582

Le Président de l'Université

UNIVERSITÉ HENRI POINCARÉ, NANCY
LE PRÉSIDENT
J.M. URLET

Université Henri Poincaré, Nancy-I
24-30 rue Lionnois - B.P. 3069 - 54013 NANCY CEDEX
Tél. : 03 83 85 48 00 - Fax : 03 83 85 48 48

Résumé
Abstract

L'étude des colmatages minéraux déposés dans les discontinuités et porosités lors des circulations de fluides, anciennes à récentes, est l'unique moyen c reconstituer les comportements paléo-hydrologique et -hydrogéochimique des milieux granitiques ou sédimentaires. Le couplage d'outils pétrographiques, min ralogiques, isotopiques (C, O, H), et géochimiques (K/Ar) a permis de déterminer la source et la nature des fluides à l'origine des colmatages (carbonates silicates), ainsi que les processus physico-chimiques mis en jeu. Cette étude a été ciblée sur trois contextes distincts dans le cadre des recherches menée par l'Andra pour l'implantation d'un laboratoire géologique souterrain :

- Dans les plutonites sous couverture sédimentaire de Charroux-Civray (Vienne), trois événements principaux de percolations fluides (fluides hercynien saumures mésozoïques et eaux diagénétiques) ont été identifiés au cours de l'histoire du massif. Les carbonates déposés dans les fractures ou di séminés dans les plutonites lors des épisodes de circulations se sont formés à partir d'une source unique en C (d13C entre -9 et -14 ‰) introduit précocement lors du métamorphisme rétrograde hercynien, et remobilisée par les différents fluides successifs, donnant à ces plutonites riches en Ca un capacité d'auto-colmatage efficace face aux circulations fluides.
- Dans les siltites et les encaissants gréso-calcaires Crétacés de Marcoule (Gard Rhodanien), le colmatage calcitique des fractures, elles-mêmes créées lor de compressions éocènes et/ou lors des extensions oligocènes a lieu sous gradient thermique modéré (T<50-55°C). Les sources en C et O des calcite des fractures diffèrent en fonction du niveau stratigraphique, et leur colmatage a lieu : i) en système clos avec redistribution locale de matière, répercutar ainsi, dans les fractures, l'identité des carbonates diagénétiques plus précoces de la porosité, ou ii) dans les niveaux initialement plus poreux, en systèm ouvert avec participation d'eaux météoriques et introduction de C et O d'origine externe. Ces processus tardifs ont globalement contribué aux faible perméabilités actuelles du site par le colmatage du réseau de fractures.
- Dans l'Est du bassin de Paris, durant le Tertiaire, des circulations de fluides météoriques ont été identifiées à l'échelle régionale dans les fractures ainsi qu dans la porosité des ensembles calcaires Bathoniens et Kimméridgiens encadrant les argilites Callovo-Oxfordiennes. Les valeurs isotopiques en C des ca cites déposées montrent que ces fluides ont circulé de façon ascendante le long des accidents distensifs régionaux. La précipitation des calcites dans l porosité des calcaires a été induite par l'infiltration de ces fluides latéralement aux failles. Ceci explique les faibles valeurs de perméabilités actuelles de calcaires. Cependant, ces fluides ne semblent pas avoir eu d'influence notable sur les caractéristiques isotopiques des ciments des argilites.

D'un point de vue méthodologique, la composition isotopique en C doit être employée avec précaution pour le traçage des fluides dans l'éventualité d'un (re)cristallisation polyphasée de carbonates, car le carbone des minéraux initiaux peut être remobilisé lors de circulations fluides plus tardives. Ce travail montré que le traçage isotopique en C et O des minéraux remplissant les discontinuités ou porosités, couplé aux études pétrographiques, minéralogiques, e thermiques obtenues sur les inclusions fluides, sur les matières organiques et sur les argiles, constitue un outil puissant pour reconstituer les condition paléo-hydrogéologiques, quel que soit le contexte. ■

The study of minerals sealing the discontinuities and the cavities by past to recent fluid circulations is the only method to assess the paleo -hydrological an -hydrogeochemical behavior of both sedimentary or granitic systems. Petrographic, mineralogic, isotopic (C, O, H) and geochemical (K/Ar) tools provide th opportunity: i) to identify the source and the nature of sealing (carbonates and quartz) -forming waters and ii) to precise the physical and chemical mechanism occurring during fluid circulations. This study is focused on 3 sites selected in the framework of a survey managed by Andra for the feasibility of an undergroun laboratory:

- *In the covered plutonites of Charroux Civray (Vienne), 3 major fluid circulations (Hercynian fluids, Mesozoic brines, diagenetic waters) have been identifiec The carbonates deposited in discontinuities or pervasively inside the granitic rocks have been formed from an unique C source (d13C ranging from -9 and 14 ‰). C stock has been early introduced during retrograde metamorphism, and afterwards, remobilized by successive fluid inputs. This confers on the Ca rich plutonic rocks an efficient self-sealing capacity during later fracturing and fluid flow.*
- *In Cretaceous siltites and surrounding limestones and sandstones of Marcoule (South-eastern Basin), calcites from fracture formed during Eocen compression and/or Oligocene extension have been deposited under low temperature conditions (T<50-55°C). C and O sources of fracture calcites differ a a function of stratigraphical levels. Fracture sealing occurs: i) either in close system, by redistribution of the nearby host-rock cements, or ii) in open syster with introduction of C and O from external sources. These late events have contributed to reduce the global permeability of the rocks trough the sealing c the fractures.*
- *In the Eastern part of the Paris basin, circulations of meteoric fluids have occurred at a regional scale during Tertiary, both in the fractures, cavities an in the porosity of the Bathonian and Oxfordian limestone series surrounding the Callovian-Oxfordian argillites. Carbon isotopic values of deposited calcite indicate that fluid circulations occurred upwards along the distensive regional faults. Fluids have also infiltrated limestones and sealed the porosity b crystallizing late sparite, resulting in the low present-day permeability values. However, these fluids have not influenced the isotopic characteristics c argillites cements.*

The carbon isotopic composition must be exercised with caution to unravel the fluid origins in the event of poly-cyclic carbonate redistribution, as carbon of earl minerals could be easily redistributed by the later fluid flows. Our methodology, based on the combined use of C-O isotopic tracers, petrographic, mineralogica and thermal (fluid inclusion, organic matter, clay typology) studies, is a promising powerful tool to assess the paleo-hydrogeologic behavior in geologica systems. ■

Mots - clefs / Keywords :

Fracture • Colmatage • Isotopes stables • Paleo-circulation • Interaction fluide-roche • Redistribution du carbone • Plutonites de la Vienne • Séries Mesozoïques • Est du bassin Parisien • basin du Sud-Est.

Discontinuity sealing • Stable isotopes • Paleo-circulation • Fluid-rock interaction • Carbon remobilization • Vienne plutonites • Mesozoic series • Eastern Paris basin • South Eastern basin.

ANDRA

Agence nationale
pour la gestion des déchets radioactifs

Parc de la Croix Blanche - 1/7, rue Jean Monnet - 92298 Châtenay-Malabry Cedex - Tél.: 01 46 11 80 00 - www.andra.fr